Synthesis, Structure and Properties of a Novel "Frustrated" Benzoxaborole and the Role of Boron in Bioconjugation

by

Jasmine Bhangu

A thesis submitted in partial fulfillment of the requirements for the degree of

Master of Science

Department of Chemistry

University of Alberta

Abstract

Chapter 2 describes an optimized 7-step successful synthesis of a first of its kind permanently open-form ortho-hydroxyalkyl arylboronic acid, otherwise known as a "frustrated benzoxaborole", with a columnless purification and complete structure elucidation. This novel compound is completely water soluble due to its pKa of 7.5, which is unexpectedly low for a non-deactivated boronic acid. The rationale behind this low pKa is due to the ortho hydroxy involvement in stabilizing the trihydroxyboronate conjugate base by H-bonding to one of the boronate oxygens. Conjugation of this new compound with biological amino and thiol groups was comparable with current methods involving ortho formyl and acetyl phenylboronic acid.

Chapter 3 summarizes collaborative work with the National Research Council in Halifax for the development of a boronic acid polymer gel column "catch-and-release" system of diol containing marine neurotoxins. Such a system would provide pre-purification of toxins to eliminate background noise for easier detection in analytical methods. A survey of 22 boronic acids was conducted for efficient boronate ester formation and acid hydrolysis utilizing tetrodotoxin as a model. 2-(Trifluoromethyl)phenylboronic acid proved to be the ideal compound and was redesigned and synthesized with a conjugatable carboxylic acid for installation on a polymer gel.

Chapter 4 highlights work done in collaboration with Prof. Brudno at the University of North Carolina for the *in vivo* imaging of a boronate/thiosemicarbazone systems developed by the Hall Group. The previously published synthesis of the precursors was improved in terms of yield, purity and reproducibility, as well as derivatized for detection by fluorescence microscopy. The imaging in live mice was shown to be promising and future work will be planned to optimize the system.

Preface

Parts of Chapter 2 of this thesis were written with the assistance of Prof. D. G. Hall for the purposes of a manuscript for eventual publication in an academic scientific journal. I was actively involved with the project design and execution. I was responsible for the synthesis and optimization of all compounds, as well the spectroscopic structure elucidation and bioconjugation studies with amines and amino acids. The lysozyme binding studies were experimentally performed by myself, then submitted to Dr. R. Whittal who performed the identification of boronic acid bound lysozyme and produced the mass spectra.

The LC-MS experiments described in Chapter 3 were entirely done by myself at the metrology department at the National Research Council in Halifax. The LC-MS method used for all runs was developed with the assistance of Dr. Christopher Miles. I was responsible for making all solutions, setting up LC-MS runs and collecting and analyzing the data at the various pH for the conjugation of tetrodotoxin with boronic acids. I performed the kinetics studies of acid hydrolysis of all formed conjugates. I performed the synthesis of the final compound at the University of Alberta for eventual solid support conjugation to be planned at Halifax.

Most of synthesis work described in Chapter 4 is previously published work and I was responsible for the improvement of several synthetic steps and derivatization of the final compounds for a collaboration with Prof. Y. Brudno at the University of North Carolina. I performed the re-synthesis and derivatization of required precursors requested by Prof. Brudno. The HPLC purification of the NIR-797 nopol diol fluorophore was accomplished with the assistance of Ed Fu. The final compounds were then shipped to Prof. Brudno, where they were imaged in live mice by their fluorescence microscope. The *in vivo* results presented in this thesis were collected and graphed by the Brudno Group and sent to Prof. D. G. Hall and myself.

Acknowledgments

I am extremely grateful for the supervision and support of Prof. D. G. Hall during my graduate studies. His constant passion, drive and positive outlook on science gave me the inspiration to continue during the most trying of times. Prof. Hall provided the push I needed to meet and exceed the potential I never knew I had as a scientist, as well as being an exceptional role model to help me navigate through my own growing career and ever-changing life. I would also like to thank Dr. Christopher Miles at the NRC Halifax for his leadership during my stay and his inspirational imparted wisdom through our many talks about life.

I would like to express my sincerest gratitude to the exceptional Hall Group members both past and present. I could not have had such a successful time without the friendship of Carl Estrada and Hannah Hackney, both of whom were always available for emotional support as we went through this journey together from the start. I would also like to thank Dr. Timothy Morgan for his patience in training me, and all other Hall group members that provided invaluable support in one way or another: Hwee Ting Ang, Di Wu, Marco Paladino, Helen Clement, Jason Rygus, Rory McDonald, Xiangyu Li, Burcin Akgun, Michele Boghi, Mohamed Estaitie and Kevin Nguyen. A special mention Ed Fu for his assistance in purification and also to the technical staff at the University of Alberta for always providing help whenever needed: Mark Miskolzie (NMR), Béla Reiz (MS), Randy Whittal (MS).

Lastly, I would like to thank my parents and brother for always believing in me with their unconditional love and support no matter where I've ended up in the world over the years. Most importantly, I would like to thank Kyle Doke for his unwavering love and patience during the past 2.5 years. He became my home in an unfamiliar city and always provided me with strength and warmth to continue to grow as a person.

Table of Contents

List of Tables

List of Figures

List of Schemes

List of Abbreviations

2-APBA	2-acetylphenylboronic acid
2-FPBA	2-formylphenylboronic acid
AcCl	acetyl chloride
ACN	acetonitrile
AcOH	acetic acid
app t	apparent triplet
BA	boronic acid
B_2pin_2	bis(pinacolato)diboron
BAG	boric acid gel
calcd	calculated
comp m	complex multiplet
CPME	cyclopentyl methyl ether
CRM	certified reference material
d	doublet
DCC	*N*,*N*′-dicyclohexylcarbodiimide
DCM	dichloromethane
DCU	dicyclohexylurea
dd	doublet of doublet
ddd	doublet of doublets of doublets
dddd	doublet of doublet of doublet of doublets
DFT	density functional theory
DIPEA	*N*,*N*-diisopropylethylamine

DMF	dimethylformamide
DMSO	dimethylsulfoxide
dppf	1,1'-bis(diphenylphosphino)ferrocene
E. Coli	Escherichia Coli
EI	electron impact
ESI	electrospray ionization
ESI-FT ICR-MS	electrospray ionization - Fourier transform ion cyclotron resonance - mass spectrometry
ESI-MS	electrospray ionization - mass spectrometry
Et_3N	triethylamine
EtOAc	ethyl acetate
EtOH	ethanol
eV	electron volts
FDA	food and drug administration
g	grams
h	hours
HATU	hexafluorophosphate azabenzotriazole tetramethyl uranium
HPLC	high performance liquid chromatography
HRMS	high-resolution mass spectrometry
Hz	hertz
IR	infrared
K. pneumoniae	Klebsiella pneumoniae
Keq	equilibrium constant

LC-MS	liquid chromatography-mass spectrometry
LDA	lithium diisopropylamine
M	molar
m	multiplet
m/z	mass-to-charge ratio
Me-THF	2-methyltetrahydrofuran
MeOH	methanol
mg	miligrams
MHz	megahertz
MIBA	5-methoxy-2-iodophenylboronic acid
min	minutes
mL	millilitres
mmol	millimole
n-BuLi	n-butyllithium
NBS	*N*-bromosuccinimide
NMO	*N*-methylmorpholine N-oxide
NMR	nuclear magnetic resonance
NRC	National Research Council
PBA	phenylboronic acid
PBS	phosphate buffered saline
PEG	polyethylene glycol
$PhNTf_2$	*N*-phenyl-bis(trifluoromethanesulfonimide)
*p*TSA•H_2O	para-toluenesulfonic acid mono hydrate

q	quartet
RNase A	ribonuclease A
s	singlet
S. aureus	Staphylococcus aureus
SPE	solid phase extraction
sulfo-NHS	*N*-hydroxysulfosuccinimide sodium salt
t	triplet
TBDMSCl	tert-butyldimethylsilyl chloride
td	triplet of doublet
Tf	trifluoromethanesulfonate
TFA	trifluoroacetic acid
THF	tetrahydrofuran
TLC	thin layer chromatography
TM	transition metal
TMSCl	trimethylsilyl chloride
TTX	tetrodotoxin
TzB	thiazolidino
UNC	University of North Carolina
µL	microlitre
µM	micromolar
µmol	micromole

Chapter One

Properties and Structure of Boron Compounds and their Applications in Biological Systems

1.1 Introduction to Boron

The role of boron in biomolecules and catalysis has grown recently due to the nature of boron itself being a mild and biocompatible metalloid, with properties distinct from both organic and metallic elements.[1] Boron containing compounds are found to exist in varying structures containing anywhere from zero to three B–O bonds, shown in Figure 1–1.[2]

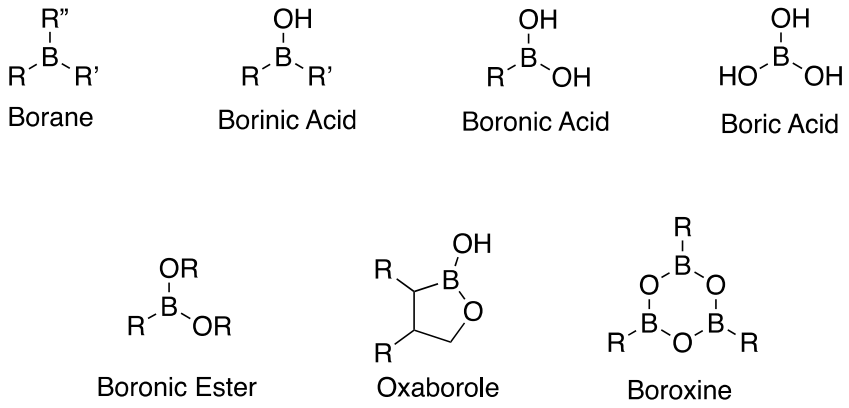

Figure 1–1. Commonly found boron compound structures.

Boron containing compounds have emerged as new targets for drug discovery due to the new and interesting properties they hold relative to established pharmacophores. The first FDA approved drug to contain boron, bortezomib, sold as Velcade®, was a major breakthrough for the treatment of multiple myeloma by a novel mechanism of multistep action.[3] This movement of boron in therapeutics is further highlighted by the recent approval of the new drugs, vaborbactam,

tavaborole and crisaborole (Figure 1–2), which were marketed for treatment towards antibiotic resistance, onychomycosis and psoriasis, respectively, along with other derivatives that have shown potential towards a range of health issues.[2,4,5]

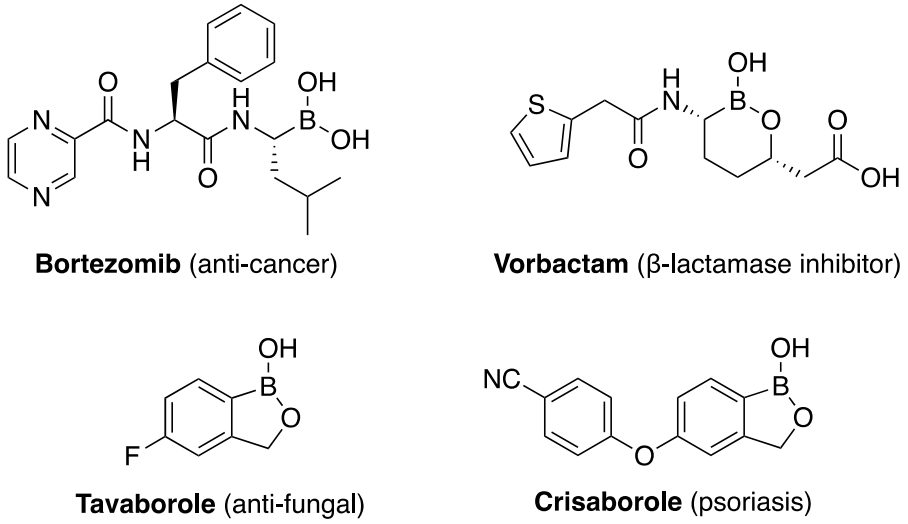

Figure 1–2. Boron in commercial pharmaceutical drugs.

Due to the ever-growing relevance of boron in the world of chemistry, the physical properties of boron compounds, the synthesis behind some of these important structures and the role of boron in biological systems, will be discussed. The first section will focus on the Lewis acidity and pKa of boron containing compounds in different types of structures, and the relevance of these structures in terms of reactions and biocompatibility. The next section will look at the most common synthetic routes to prepare common boron compounds. Lastly, the current state applications of boron in biological systems with regards to bioconjugation will be explored. The chapter will conclude with a statement of objectives for this thesis.

1.1.1 Properties of Boron Compounds

Boron is a versatile element that is studied in many fields of chemistry from synthesis and therapeutics to materials. The versatility of boron is the result of several advantageous properties that boron containing compounds hold relative to other organic substances. These physical properties of boron, and their implications in bonding and reactivity, will be discussed.

1.1.1.1 Lewis Acidity and pKa of Boron Compounds

All trivalent boron compounds have six valence electrons with a sp^2 boron atom containing a vacant p-orbital. This p-orbital lies orthogonal to the rest of the planar structure and is capable of accepting a lone-pair of electrons. Despite having two hydroxy groups, boronic acids, with a few exceptions, do not behave as Brønsted-Lowry acids; instead they are widely found to be Lewis acids.[1] In an aqueous solution at an appropriate pH, boron undergoes nucleophilic attack by the oxygen of water, thus releasing a proton, which is picked up by another water molecule (Figure 1–3).[1,6,7]

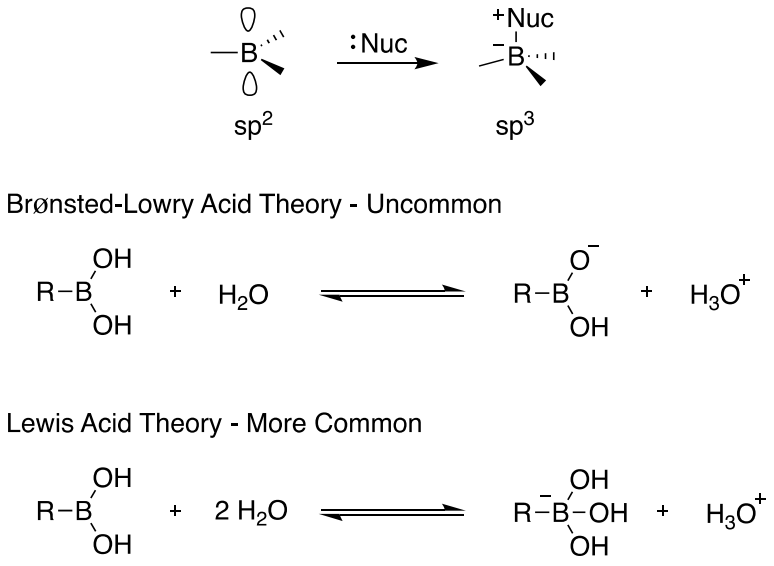

Figure 1–3. Brønsted-Lowry acidity vs Lewis acidity of boronic acids.

Most arylboronic acids normally have a pKa of around eight to nine, but many factors can affect that pKa. Benzoxaborole, first obtained by Torssell in 1957, for example, has ring strain associated with the internal 5-membered ring.[8] The pKa of benzoxaboroles is lower than boronic acids because the formation of a tetrahedral hydroxy adduct, from the attack of water, causes a release of ring strain (Figure 1–4a).[6,7] If an arylboronic acid has a strongly electron withdrawing group, the boron atom can better stabilize the boronate anion's negative charge; thus it will have a lower pKa, e.g. 4-nitrophenylboronic acid, which has a pKa of 7.1.[9] On the other hand, if that same substituent is placed next to the boronic acid, i.e. 2-nitrophenylboronic acid, the pKa will increase due to prevention of boronate anion formation from sterics/congestion (Figure 1–4b).[10] Ortho-(*N*,*N* dimethylaminomethyl)phenylboronic acid, shown in Figure 1–4c, has a pKa of 5.2 due to the lone-pair contribution from nitrogen into the empty p-orbital of boron, and has a second pKa value greater than 12, from the boronate anion formation.[11–14] As mentioned previously, there are a few suspected examples Brønsted-Lowry boronic acids where the formation of a tetrahedral boronate is highly unfavorable because it would break the partial aromatic character of the central ring, so instead, the hydroxy proton is removed (Figure 1–4d), although this is highly controversial.[15]

a) pKa affected by ring strain

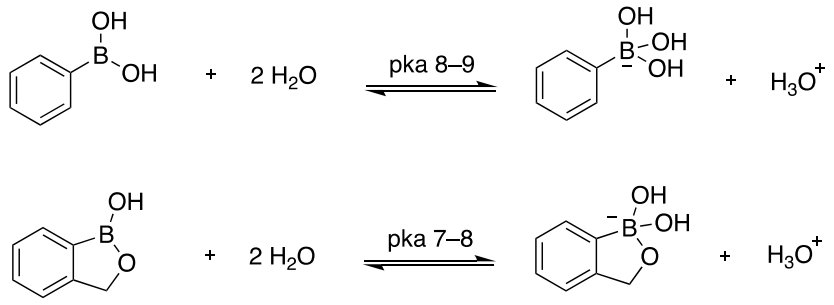

b) pKa affected by proximal sterics

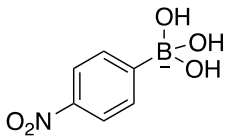

Exists at pH > 7.1
Negative charge stablized by electron withdrawing NO_2

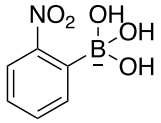

Exists at pH > 9.2
Ortho NO_2 group introduces donation of lone-pairs into boron, preventing OH from binding at lower pH

c) pKa affected by anchimeric participation

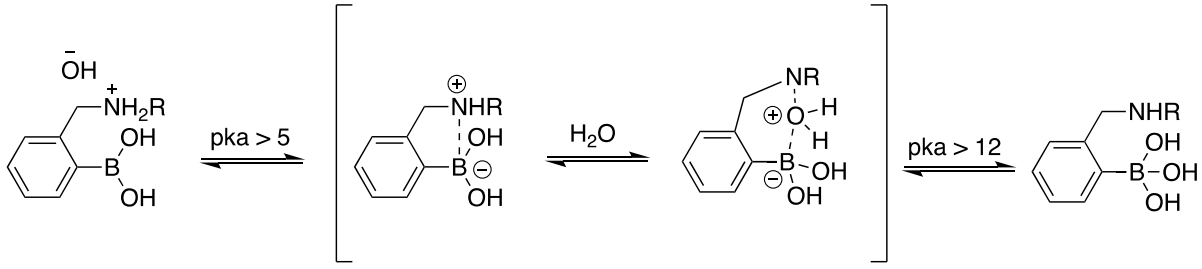

d) pKa based on Brønsted-Lowry acids

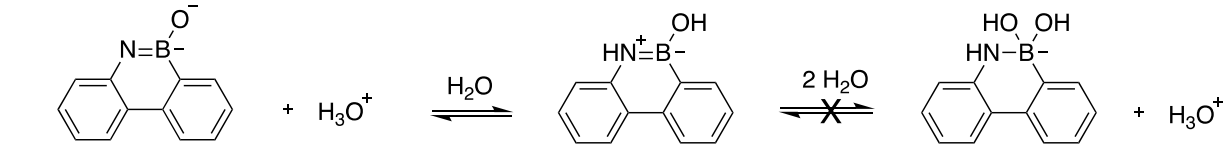

Brønsted-Lowry Acid
Partial aromaticity of central ring intact

Lewis Acid
Partial aromaticity of central ring broken

Figure 1–4. Effect of structure on pKa of boron compounds.

1.1.1.2 Bonding and Structure

The bonding and structure of boron will be analyzed in four different forms: boronic acid, boronic ester, benzoxaborole and boroxine. X-ray crystallographic analysis has shown that benzoxaborole crystalizes exclusively as a dimer whereas other boronic acids possess intermolecular hydrogen bonds (Figure 1–5a and b) to allow for a multiple boronic acid units to form a larger structure.[16,17] In anhydrous organic solvents such as chloroform, boronic acids are known to spontaneously condense and lose three water molecules to form cyclic anhydride structures known as boroxines (Figure 1–5c).[18–20] Boroxine formation usually does not interfere with reactions such as cross-coupling or Miyaura borylation, but it can cause complications in the analysis, quantification and characterization of boronic acids.[1] Due to this spontaneous condensation effect of boronic acids, boronic esters have become a preferred option in synthetic applications, as they can be later hydrolyzed to give the free boronic acid.[1]

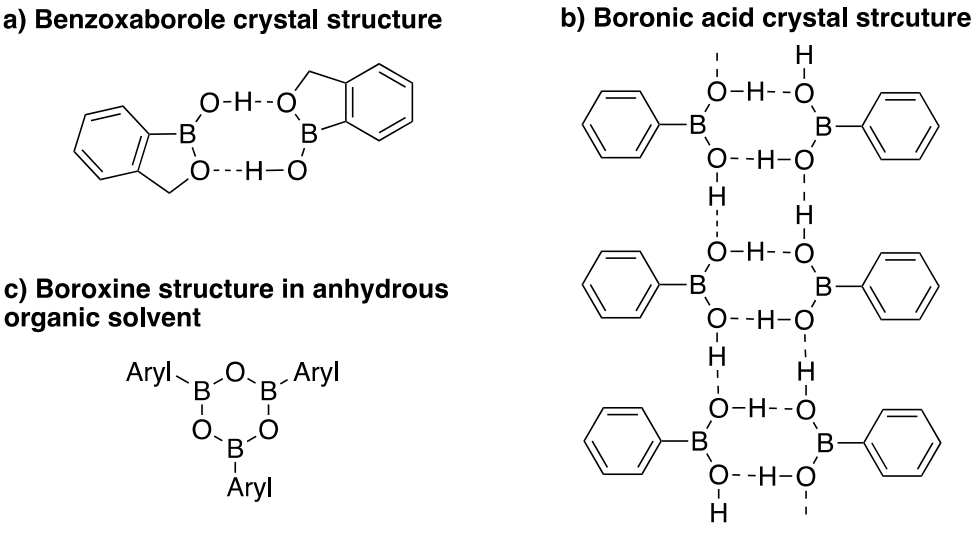

Figure 1–5. Bonding of various boron structures.

1.1.2 Traditional Synthesis of Boron Compounds

Ethylboronic acid was the first boronic acid synthesized, in 1860, by treating diethylzinc with triethylborate, to produce triethylborane, which was oxidized by air.[21,22] The synthesis of boronic acids was relatively slow until about 1995, when it exploded due to the ever-growing applications of these unique compounds.

1.1.2.1 Synthesis of Aryl Boronic Acids and Esters

Arylboronic acids and esters are the most commonly used boron containing compounds in pharmaceutical chemistry, especially for their use in the cross-coupling of aryl units. This important cross-coupling reaction was highlighted in the Nobel Prize awarded to Suzuki, Heck and Negishi, and the need to synthesize boronic acids/esters became more apparent with the growing popularity of this reaction.[23] One common method to synthesize arylboronic acids is the conversion of an aryl halide to a hard organometallic, by metal-halogen exchange, followed by trapping of the negatively charged species with a borate ester and subsequent hydrolysis.[24,25] The other well-known method is the transition metal-catalyzed coupling of aryl halides/triflates with diboron reagents, for example, in the Miyaura borylation using a palladium catalyst and bis(pinacolato)diboron.[23] Direct borylation of aryl C–H bonds can also be accomplished by transition metal (TM) catalysis.[26,27] These main preparative methods are summarized in Scheme 1–1.

a) Metal-halogen exhange of aryl halides and trapping with borates

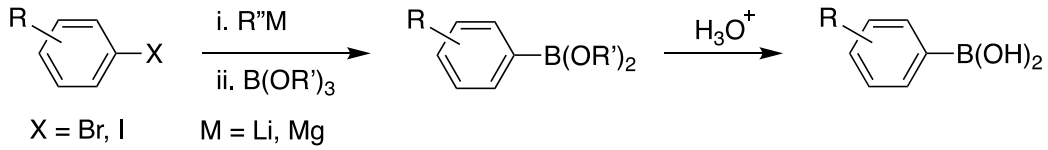

b) Transition metal catalyzed coupling of aryl halide with boronate

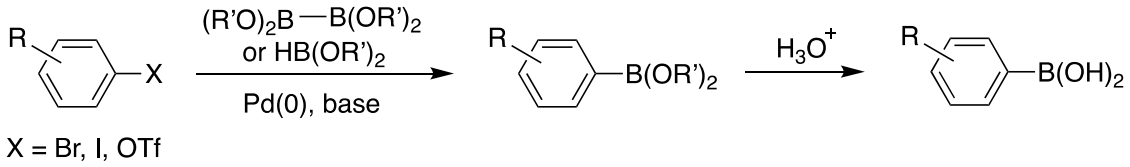

c) Transition metal catalyzed C–H borylation

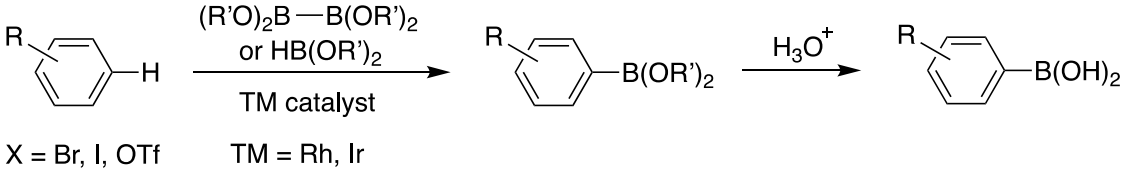

Scheme 1–1. Common methods to synthesize arylboronic esters and acids.

1.1.2.2 Synthesis of Oxaborole Compounds

Oxaboroles, the most popular of which are benzoxaboroles, are considered fundamentally different than boronic acids because of their cycle structure caused by internal ring formation with one of the two hydroxyl groups on a boronic acid. Some of the notable differences from boronic acids include benzoxaborole having a more stable B–C bond that is less susceptible to oxidation and superior stability in water due to lower pKa.[6,28] For these reasons, benzoxaborole structures have become a recognized chemotype in drug discovery, and the synthesis of these types of structures has become more relevant.[29] The starting point for the two most commonly used methods to synthesize these compounds can start with an aryl halide with either an ortho methyl, or an ortho formyl group.[30] The former method involves first the bromination of the methyl group, followed by conversion to a protected alcohol, after which the halide is converted to a boronic

ester by one of the aforementioned methods, and finally a double deprotection, which will induce cyclization to form the benzoxaborole core (Scheme 1–2a). The second method introduces a boronic ester to the halide position first, followed by aldehyde reduction to the alcohol, with concomitant deprotection of the boron moiety, which induces cyclization to form benzoxaborole (Scheme 1–2b).

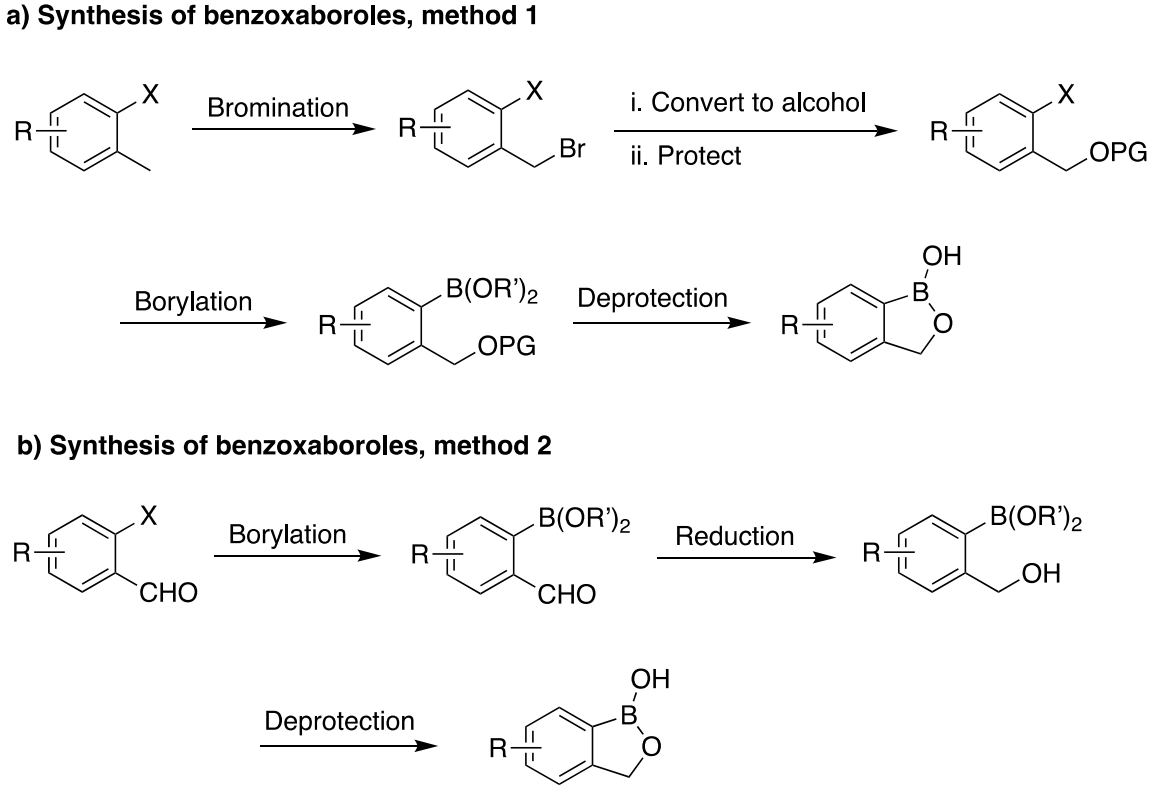

Scheme 1–2. Common methods to synthesize benzoxaborole-type structures.

From these well-established synthetic methods, benzoxaboroles have become an achievable moiety to introduce to pharmaceuticals synthetically, and study the effects they have in biological systems.[31]

1.2 Boron in Bioconjugation

Bioorthogonal chemistry is a term used to describe a chemical reaction in a biological system that does not affect biochemical processes that otherwise naturally occur.[32] This is important when studying the effects of a certain labelling or modification technique as the chemical reaction being introduced has to be site specific and not be toxic to the cell. A vast number of bioorthogonal reactions exist to target biomolecules such as glycans, proteins and lipids.[32,33] Many bioorthogonal reactions require prior modification of a native structure in order to achieve the desired transformation, but many times the existing functionality of a biomolecule can be utilized directly. The most popular native functionalities targeted are the amino groups on peptides, thiol groups on cysteines and diol groups on sugars and carbohydrates.[32] As shown in Scheme 1–3, boron chemistry has emerged as a significant tool in the design of bioorthogonal reactions as it has several attractive properties that can be leveraged for bioconjugation.[34]

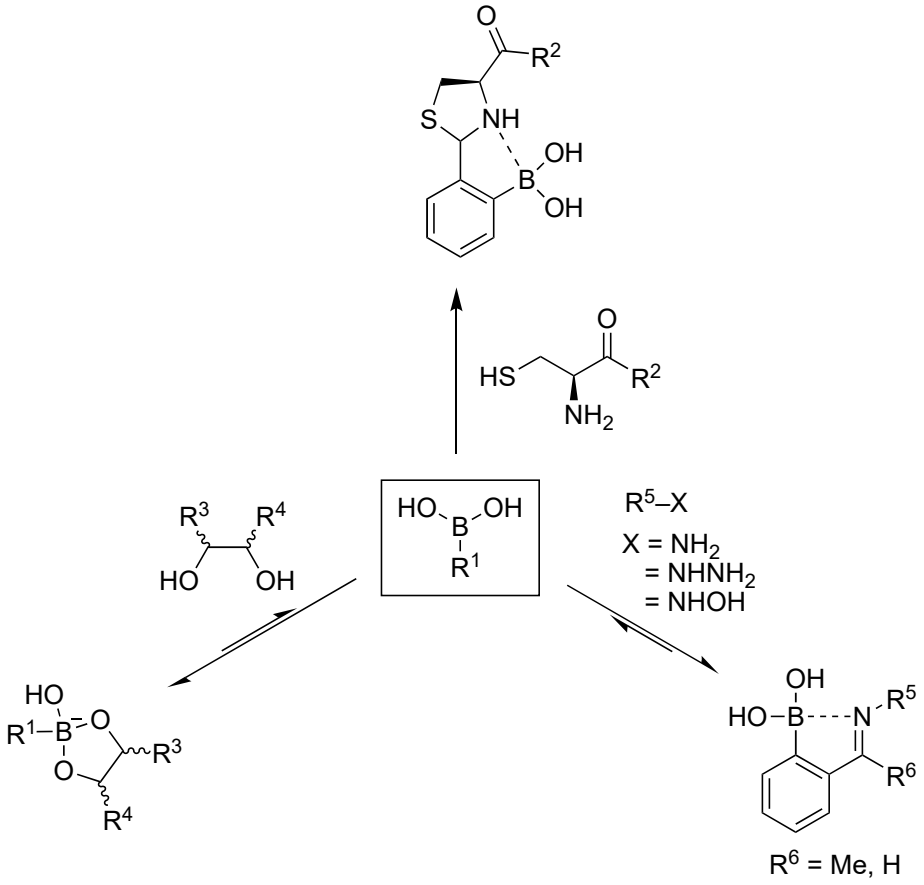

Scheme 1–3. Boronic acid bioconjugation of native functionalities found in biological systems.

1.2.1 Iminoboronate Chemistry

Imine formation is a simple bioconjugation method that uses the amino functionality on the N-terminal of a protein, or on a lysine residue, to condense with a carbonyl unit, usually an aldehyde.[32,34] Imine formation, however, is reversible in aqueous media giving back the amine and aldehyde, therefore imines usually need to be reduced to an amine to achieve permanent conjugation. In order to form a more stable imine bond, Gois and coworkers introduced a boronic acid group close to the site of imine formation, through the utilization of 2-formylphenylboronic acid (2-FPBA) and 2-acetylphenylboronic acid (2-APBA).[35] Conjugation of 2-FPBA and 2-APBA with butylamine to form iminoboronate structures leads to moderate conversion up to 52% and

88% respectively (Scheme 1–3).[35] The boron atom increases stability through a dative B–N bond that shows extensive bioorthogonal binding with lysine, along with several other proteins such as somatostatin, lysozyme and myoglobin. To test the reversibility of these iminoboronates, competing biomolecules, such as fructose, dopamine and glutathione, were introduced and were found to replace the previously bound compounds indicating the imine formation is reversible.[35] Gois and coworkers functionalized iminoboronates with further bioorthogonal handles such as azides, alkynes and polyethylene glycol (PEG) chains to assemble cancer-cell-targeting drug conjugates, and also to enable these structures with fluorescent probes for imaging cancer cells.[36,37] Yatsimirsky and coworkers also reported iminoboronate formation around the same time, except with a focus on binding of amino sugars instead of lysine residues.[38] DFT studies of iminoboronates conducted by Gois and coworkers showed that iminoboronate products with a B–N dative bond are about 7.4 kcal/mol more favorable in energy compared to amine structures lacking this bond.[35] This work was further expanded upon by Gillingham and coworkers by introducing boron assisted oxime formation with the use of 2-FPBA and hydroxyamines, indicating large rate constants of 10^4 $M^{-1}s^{-1}$, which were attributed to the involvement of boron's dynamic coordination chemistry in many steps of the oxime condensation (Scheme 1–4a).[39]

a) Mechanism of iminoboronate formation

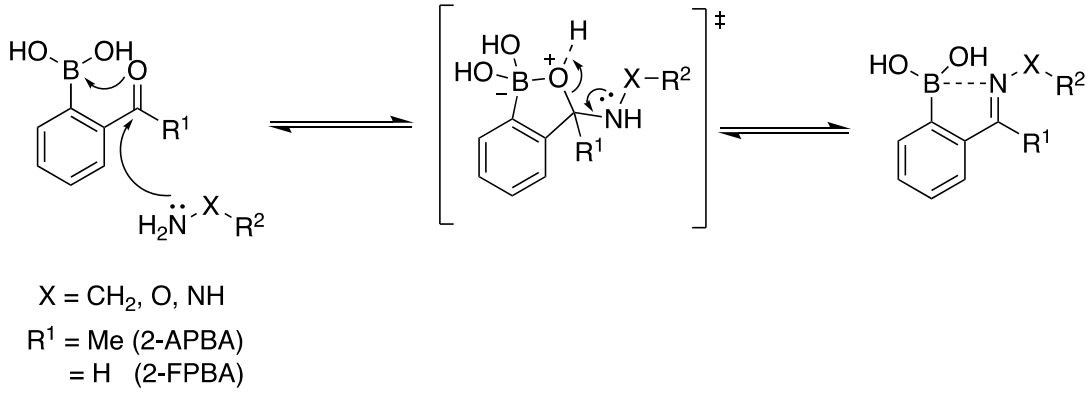

X = CH_2, O, NH

R^1 = Me (2-APBA)
= H (2-FPBA)

b) Imine stablization with formyl- and acetyl-iminoboronates

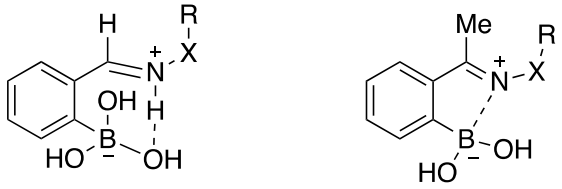

Scheme 1–4. Mechanism of iminoboronate formation.

In order to study the mechanism behind iminoboronate reactions, Gao and coworkers used a combination of spectroscopic measures for the formation of these structures.[40] The authors proposed a mechanism where the initial B–O bond with the carbonyl plays a key role for the nucleophilic attack of the amine, and also in the dehydration step by a favorable boronate elimination.[35,40] Further work done by Gillingham and coworkers agreed with the above mechanism and further indicated that 2-FPBA iminoboronates are the more favorable and stable conjugate.[41] In the case of 2-FPBA, it is thought that hydrogen bonding and coulombic interactions play a part in ground state stabilization, and in the case of 2-APBA, Lewis acid/base interaction is the primary stabilizing force (Scheme 1–4b).[41]

Although iminoboronates are shown to be efficient for bioconjugation, they are known to be reversible, which can be undesirable if the objective is long term labelling studies. To tackle

this issue of reversibility, Bane and coworkers tested the conjugation between 2-FPBA and 4-hydrazinylbenzoic acid and they made two key observations: a) hydrazine nucleophiles in fact form benzodiazaborine structures, not simply iminoboronate structures as previously thought, and b) the added carboxylic acid functionality makes this process irreversible (Scheme 1–5a).[42,43] Gao and coworkers argued that the use of phenylhydrazine is cytotoxic, and therefore used semicarbazides to form similar benzodiazaborine structures.[44] These reagents proved to be more biocompatible and, with the addition of a fluorescent probe, showed to be useful in the imaging of bacterial cell walls due to a fast and irreversible conjugation, with minimal interreference from other biomolecules (Scheme 1–5b).[44]

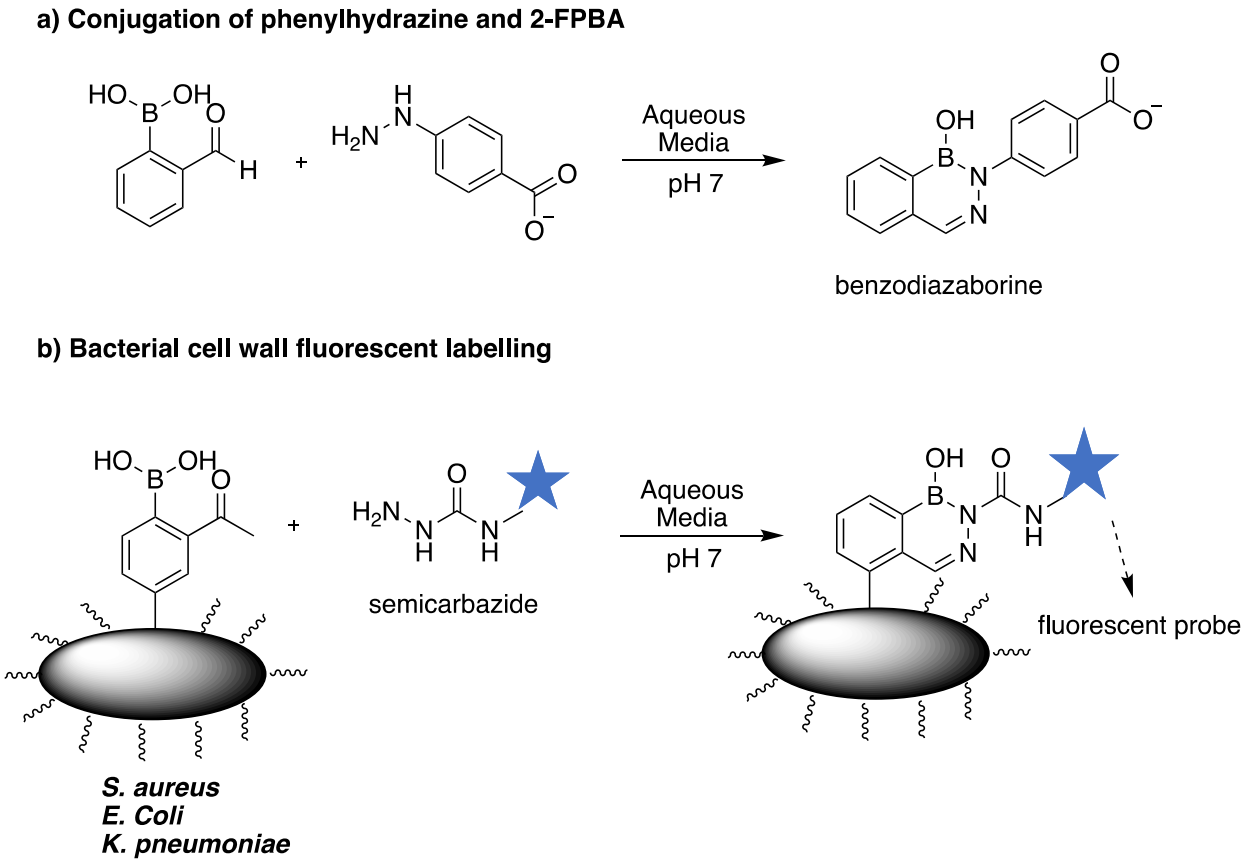

Scheme 1–5. Irreversible benzodiazaborine formation.

1.2.2 Thiazolidine/Cysteine Conjugation

Another popular bioconjugation method recently explored involves the N-terminal cysteine on a protein.[44–46] N-terminal cysteines are known to conjugate with aldehydes to form thiazolidines; however, it is a slow process that requires slightly acidic conditions.[47] Gao and coworkers, and Gois and coworkers, simultaneously reported that N-terminal cysteine conjugation with 2-FPBA forms a thiazolidino boronate (TzB) structure.[45,46] TzB demonstrates superior stability and faster conjugation, at a rate of 10^3 $M^{-1}s^{-1}$, than thiazolidines alone, due to the dative B–N bond (Scheme 1–6).[45,46] Furthermore, the TzB structure was not affected by a range of competing biomolecules such as those found to interfere with other iminoboronate structures: fructose, lysine and glutathione.[45] The TzB formation tolerates many amino acid residues next to the N-terminal cysteine, however, it is reversible in mildly acidic and mildly basic conditions.[46]

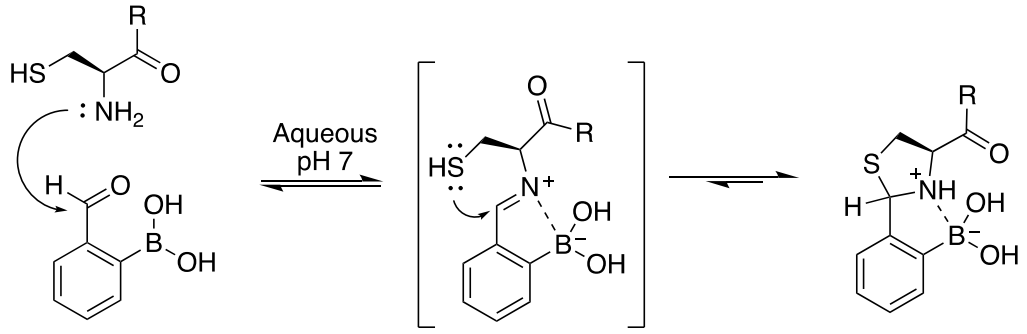

Scheme 1–6. Conjugation of N-terminal cysteine with 2-FPBA.

1.2.3 Boronic Acid Conjugation with Diols

1.2.3.1 Reversible Boronate Formation

A major attribute of boronic acids, other than their Lewis acidity, is their ability to form esters with diols. The most common example of this feature in bioconjugation is the ability of boronic acids to form boronate esters with cis-diols on glycols, sugars and glycoproteins.[48–50] Boronic acids have been used for recognition of carbohydrates, however, a major limitation was the inability to bind to non-reducing sugars and glycosides, which are a largely found on cell surfaces.[48] "Wulff-type" ortho-dialkylaminomethyl arylboronic acids were used for conjugation with simple reducing sugars, and later derivatized using anthracene for visual labeling of diols on cancer cells (Scheme 1-7a).[51,52] Unfortunately, these types of structures can have poor solubility in aqueous solutions.[53] In 2006, Hall and coworkers showed that benzoxaborole-type structures bind to biological glycosides significantly better than the "Wulff-type" boronic acids, and do so under relevant aqueous physiological conditions without solubility issues (Scheme 1–7b).[48] Raines and coworkers expanded on this work to show that benzoxaborole binds with high affinity to glycopyranosides, which are highly abundant in the glycocalyx of cancer cells.[49,50] They conjugated cytotoxic bovine pancreatic ribonuclease (RNase A) to benzoxaborole, and then subjected it to human erythroleukemia cells, which effectively inhibited proliferation.[49] With this knowledge, they further created a novel drug delivery system by linking a protein amine group via a "trimethyl lock" to benzoxaborole. The latter conjugates with the diol groups on carbohydrates, and the protein is released intracellularly through cleavage by cellular esterases (Scheme 1-7c).[50]

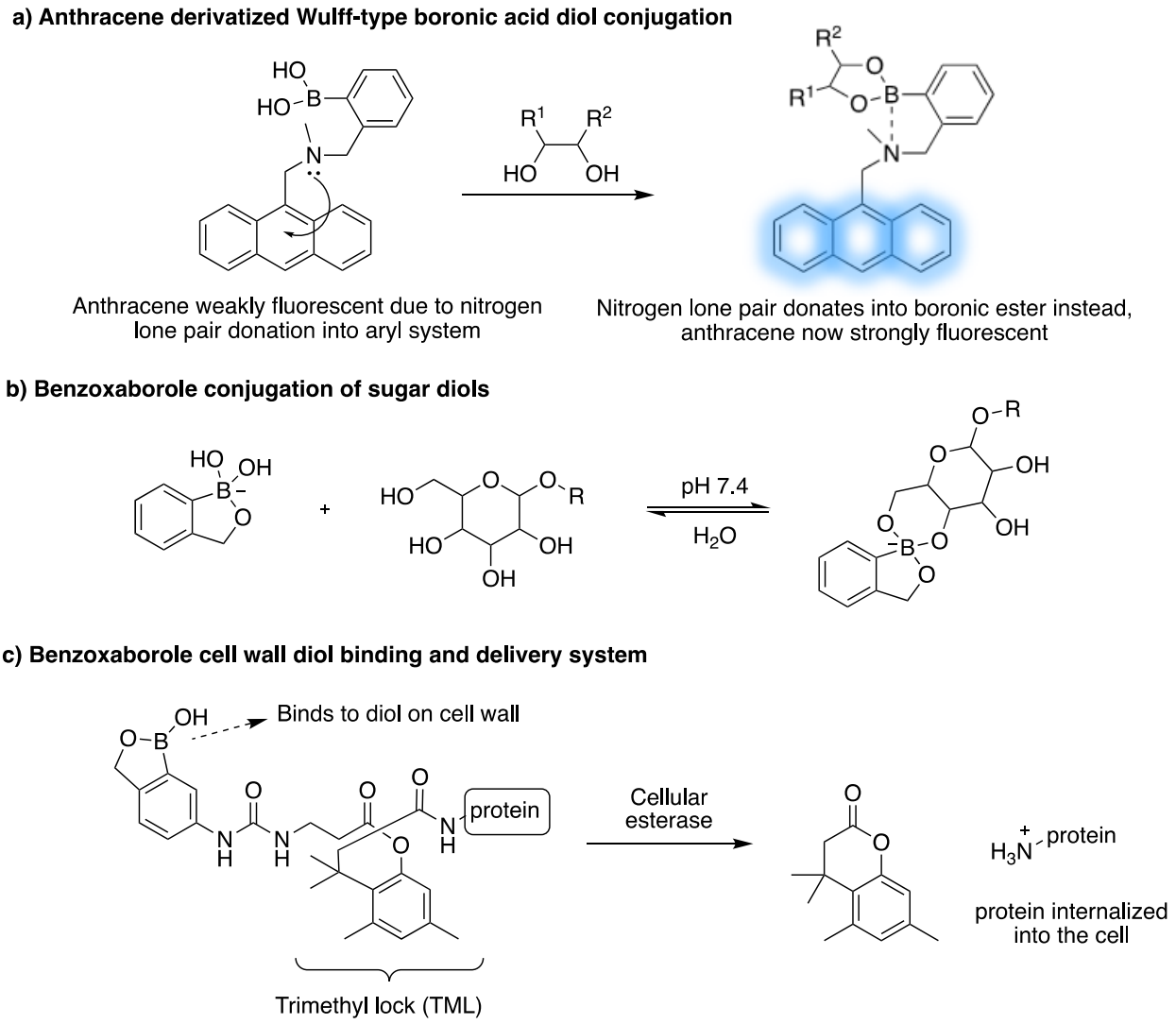

Scheme 1–7. Various boronic acid and benzoxaborole diol binding agents.

The use of boronate diol conjugation has also been used for cell imaging.[54–56] In one example, Hall and coworkers developed a fast, tight and reversible boronate conjugation with a nopoldiol derivative, modified with a hydroxy handle capable of conjugation with a fluorescent tag for imaging.[54] This conjugation displayed a fast ligation rate at 340 $M^{-1}s^{-1}$ and also has a good equilibrium constant (K_{eq}) of 10^5–10^6 M^{-1} favoring the boronate conjugate (Scheme 1–8a).[54]

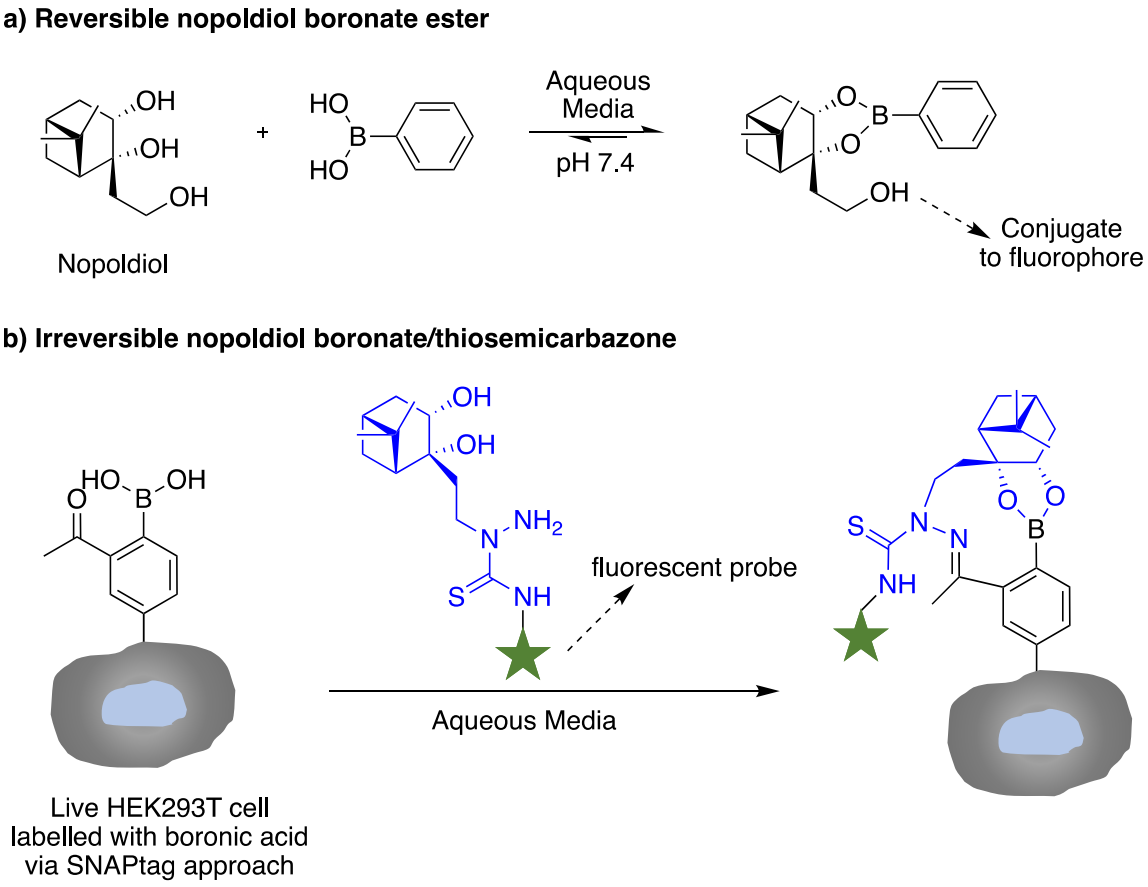

Scheme 1–8. Boronic acid and nopoldiol reversible (a) and irreversible (b) bioconjugation for cell imaging.

1.2.3.2 Irreversible Boronate Formation

To develop a new and irreversible system with diols, Anslyn and coworkers designed a two 3-component systems involving boronate ester formation with an iminoboronate.[57,58] The first of these systems uses 2-FPBA, hydroxylamine and catechol in aqueous media to form an irreversible assembly (Scheme 1–9a).[57] The second system again uses 2-FPBA and catechol, but this time substitutes the hydroxylamine for an amine, forming a similar 3- component assembly however with the insertion of methanol (Scheme 1–9b).[58] These systems are both irreversible between strongly basic (pH 13) and acidic (pH 1) solutions, as well as temperatures up to 50 ºC.

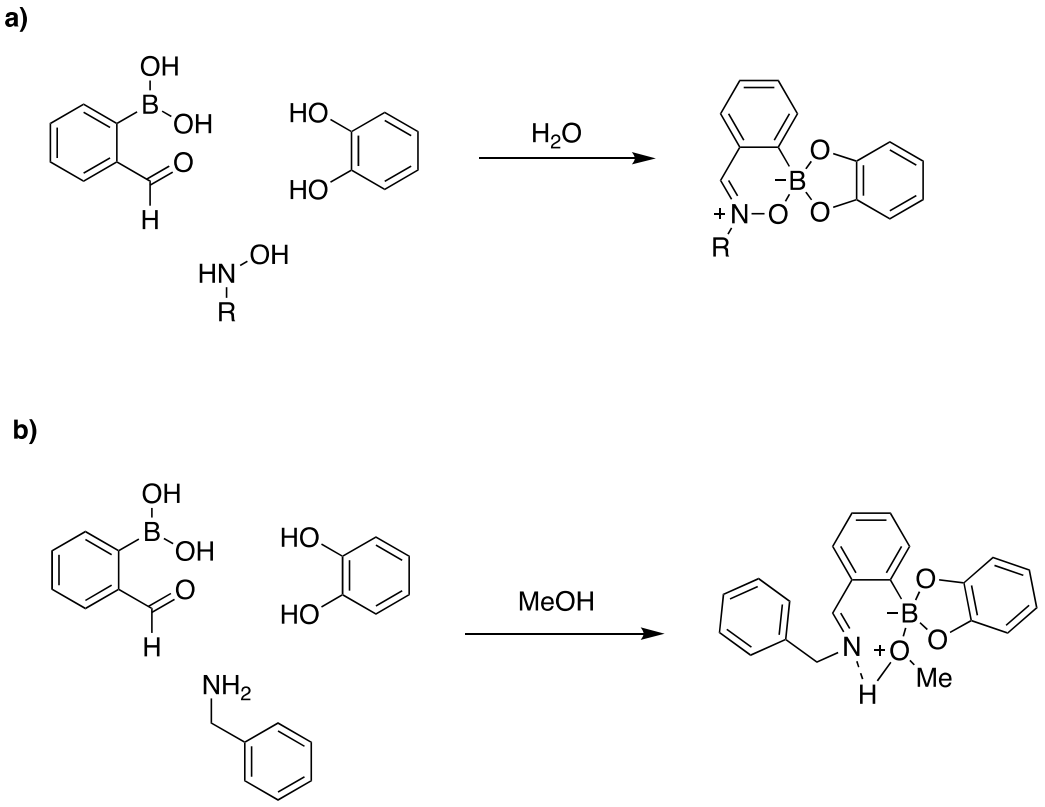

Scheme 1–9. Three component irreversible diol conjugate systems.

Hall and coworkers also modified their original nopoldiol boronate chemistry into an irreversible one by introducing a thiosemicarbazide-functionalized nopoldiol to condense with 2-APBA.[55] The thiosemicarbazide condenses with the acetyl group to form an adjacent imine that stabilizes the boronate ester. This system was applied in live cells using a SNAP-tag approach to first install the boronic acid construct to beta-2 adrenergic receptor in HEK293T cells, followed by incubation with the fluorescently labelled thiosemicarbazide-functionalized nopoldiol, which resulted in visible fluorescence via microscope at a low reagent concentration of 10 μM. The bifunctional system is fast and irreversible in biological conditions, and also stable to other biocompetitors (Scheme 1–8b).

1.3 Thesis Objectives

As seen in Section 1.1, boron containing compounds have potential to be applicable to many aspects of chemistry, and the synthesis of new types of boron compounds is desirable to find use in a wide range of applications. Hall and coworkers recently demonstrated, through spectroscopic NMR evidence, that benzoxaborole largely exists in the closed form in water, and yet can undergo rapid and reversible hydrolysis to the open form.[59] Currently no examples of permanently open benzoxaborole derivatives exist. The question therefore becomes, what unique properties does a predominantly open form of benzoxaborale have and how can these properties be utilized for applications towards chemical reactions and biological systems. This idea of a frustrated benzoxaborole brings the boronic acid moiety and a nucleophilic alkylhydroxy group in close proximity without actually closing on one another, leaving two open sites for reactivity.

Chapter 2 describes the efforts made in the development and synthesis of a novel, water soluble, "frustrated" benzoxaborole. The synthetic roadblocks to installing an ortho hydroxy group next to a boronic acid proved to be challenging and required modified literature procedures to adequately obtain the final product. The absolute structure of this novel compound was established using various spectroscopic means, and its unique properties, such as its bonding behavior and pKa in aqueous systems, was explored. The bioconjugation ability of this novel compound was tested against various compounds containing amino groups, and also with lysine residues on lysozyme as a model protein.

Chapter 3 highlights the work done during a collaboration of the Hall group and the National Research Council (NRC) in Halifax. Here a large survey of mostly ortho substituted boronic acids was examined for the binding of a potent neurotoxin called tetrodotoxin (TTX). The importance of pKa and Lewis acidity of these boronic acids were explored in these assays as the

binding affinity of boronic acids to TTX was affected by change in pH of the solution. The kinetics behind the formation of boronic acid/TTX structures was also examined and analyzed by LC-MS. Finally, Chapter 4 is on the collaboration efforts with Prof. Brudno's group at the University of North Carolina (UNC). Here, the work previously mentioned in Section 1.2.3.2 by Hall and coworkers was attempted to be performed in live mice.[55] The synthesis of the boronic acid tag was improved upon, and a different fluorescent tag was utilized for the nopol diol derivative for fluorescence detection.

1.4 References

(1) Hall, D. G. *Boronic Acids. Preparation and Applications in Organic Synthesis, Medicine and Materials*, 2nd Completely Revised ed.; Hall, D. G., Ed.; Wiley-VCH: Weinheim, Germany, 2011.

(2) Baker, S. J.; Zhang, Y.-K.; Akama, T.; Lau, A.; Zhou, H.; Hernandez, V.; Mao, W.; Alley, M. R. K.; Sanders, V.; Plattner, J. J. *J. Med. Chem.* **2006**, *49* (15), 4447.

(3) Field-Smith, A.; Morgan, G. J.; Davies, F. E. *Ther. Clin. Risk Manag.* **2006**, *2* (3), 271.

(4) Lomovskaya, O.; Sun, D.; Rubio-Aparicio, D.; Nelson, K.; Tsivkovski, R.; Griffith, D. C.; Dudley, M. N. *Antimicrob. Agents Chemother.* **2017**, *61* (11), e01443.

(5) Akama, T.; Baker, S. J.; Zhang, Y.-K.; Hernandez, V.; Zhou, H.; Sanders, V.; Freund, Y.; Kimura, R.; Maples, K. R.; Plattner, J. J. *Bioorg. Med. Chem. Lett.* **2009**, *19* (8), 2129.

(6) Adamczyk-Woźniak, A.; Borys, K. M.; Sporzyński, A. *Chem. Rev.* **2015**, *115* (11), 5224.

(7) Adamczyk-Woźniak, A.; Cyrański, M. K.; Żubrowska, A.; Sporzyński, A. *J. Organomet. Chem.* **2009**, *694* (22), 3533.

(8) Torssell, K. *Ark. Kemi.* **1957**, *10*, 507.

(9) Settepani, J. A.; Stokes, J. B.; Borkovec, A. B. *J. Med. Chem.* **1970**, *13* (1), 128.

(10) Torssell, K.; McClendon, J. H.; Somers, G. F. *Acta Chem. Scand.* **1958**, *12* (7), 1373.

(11) Wiskur, S. L.; Lavigne, J. J.; Ait-Haddou, H.; Lynch, V.; Chiu, Y. H.; Canary, J. W.; Anslyn, E. V. *Org. Lett.* **2001**, *3* (9), 1311.

(12) Ni, W.; Kaur, G.; Springsteen, G.; Wang, B.; Franzen, S. *Bioorganic Chem.* **2004**, *32* (6), 571.

(13) Zhu, L.; Shabbir, S. H.; Gray, M.; Lynch, V. M.; Sorey, S.; Anslyn, E. V. *J. Am. Chem. Soc.* **2006**, *128* (4), 1222.

(14) Collins, B. E.; Sorey, S.; Hargrove, A. E.; Shabbir, S. H.; Lynch, V. M.; Anslyn, E. V. *J. Org. Chem.* **2009**, *74* (11), 4055.

(15) Dewar, M. J. S.; Jones, Richard. *J. Am. Chem. Soc.* **1967**, *89* (10), 2408.

(16) Allen, F. H. *Acta Crystallogr. Sect. B* **2002**, *58* (3 Part 1), 380.

(17) Cyrański, M. K.; Jezierska, A.; Klimentowska, P.; Panek, J. J.; Sporzyński, A. *J. Phys. Org. Chem.* **2008**, *21* (6), 472.

(18) Korich, A. L.; Iovine, P. M. *Dalton Trans* **2010**, *39* (6), 1423.

(19) Bhat, K. L.; Markham, G. D.; Larkin, J. D.; Bock, C. W. *J. Phys. Chem. A* **2011**, *115* (26), 7785.

(20) Adamczyk-Woźniak, A.; Kaczorowska, E.; Kredátusova, J.; Madura, I.; Marek, P. H.; Matuszewska, A.; Sporzyński, A.; Uchman, M. *Eur. J. Inorg. Chem.* **2018**, *2018* (13), 1492.

(21) Frankland, E.; Duppa, B. F. *Ann. Chem. Pharm.* **1860**, *115* (3), 319.

(22) Frankland, E.; Duppa, B. F. *Proc. R. Soc. Lond.* **1860**, *10*, 568.

(23) Miyaura, N.; Suzuki, A. *Chem. Rev.* **1995**, *95* (7), 2457.

(24) Gilman, H.; Santucci, L.; Swayampati, D. R.; Ranck, R. O. *J. Am. Chem. Soc.* **1957**, *79* (12), 3077.

(25) Evans, D. A.; Katz, J. L.; Peterson, G. S.; Hintermann, T. *J. Am. Chem. Soc.* **2001**, *123* (49), 12411.

(26) Ishiyama, T.; Takagi, J.; Ishida, K.; Miyaura, N.; Anastasi, N. R.; Hartwig, J. F. *J. Am. Chem. Soc.* **2002**, *124* (3), 390.

(27) Chotana, G. A.; Rak, M. A.; Smith, M. R. *J. Am. Chem. Soc.* **2005**, *127* (30), 10539.

(28) Tomsho, J. W.; Pal, A.; Hall, D. G.; Benkovic, S. J. *ACS Med. Chem. Lett.* **2012**, *3* (1), 48.

(29) Nocentini, A.; Supuran, C. T.; Winum, J.-Y. *Expert Opin. Ther. Pat.* **2018**, *28* (6), 493.

(30) Zhang, J.; Zhu, M.; Lin, Y.; Zhou, H. *Sci. China Chem.* **2013**, *56* (10), 1372.

(31) Fernandes, G. F. S.; Denny, W. A.; Dos Santos, J. L. *Eur. J. Med. Chem.* **2019**, *179*, 791.

(32) Sletten, E. M.; Bertozzi, C. R. *Angew. Chem. Int. Ed.* **2009**, *48* (38), 6974.

(33) Ramil, C. P.; Lin, Q. *Chem. Commun.* **2013**, *49* (94), 11007.

(34) Akgun, B.; Hall, D. G. *Angew. Chem. Int. Ed.* **2018**, *57* (40), 13028.

(35) Cal, P. M. S. D.; Vicente, J. B.; Pires, E.; Coelho, A. V.; Veiros, L. F.; Cordeiro, C.; Gois, P. M. P. *J. Am. Chem. Soc.* **2012**, *134* (24), 10299.

(36) Cal, P. M. S. D.; Frade, R. F. M.; Cordeiro, C.; Gois, P. M. P. *Chem. - Eur. J.* **2015**, *21* (22), 8182.

(37) Cal, P. M. S. D.; Frade, R. F. M.; Chudasama, V.; Cordeiro, C.; Caddick, S.; Gois, P. M. P. *Chem. Commun.* **2014**, *50* (40), 5261.

(38) Gutiérrez-Moreno, N. J.; Medrano, F.; Yatsimirsky, A. K. *Org. Biomol. Chem.* **2012**, *10* (34), 6960.

(39) Schmidt, P.; Stress, C.; Gillingham, D. *Chem. Sci.* **2015**, *6* (6), 3329.
(40) Bandyopadhyay, A.; Gao, J. *Chem. - Eur. J.* **2015**, *21* (42), 14748.
(41) Gillingham, D. *Org. Biomol. Chem.* **2016**, *14* (32), 7606.
(42) Dilek, O.; Lei, Z.; Mukherjee, K.; Bane, S. *Chem. Commun.* **2015**, *51* (95), 16992.
(43) Gu, H.; Chio, T. I.; Lei, Z.; Staples, R. J.; Hirschi, J. S.; Bane, S. *Org. Biomol. Chem.* **2017**, *15* (36), 7543.
(44) Bandyopadhyay, A.; Cambray, S.; Gao, J. *J. Am. Chem. Soc.* **2017**, *139* (2), 871.
(45) Bandyopadhyay, A.; Cambray, S.; Gao, J. *Chem. Sci.* **2016**, *7* (7), 4589.
(46) Faustino, H.; Silva, M. J. S. A.; Veiros, L. F.; Bernardes, G. J. L.; Gois, P. M. P. *Chem. Sci.* **2016**, *7* (8), 5052.
(47) Botti, P.; Pallin, T. D.; Tam, J. P. *J. Am. Chem. Soc.* **1996**, *118* (42), 10018.
(48) Dowlut, M.; Hall, D. G. *J. Am. Chem. Soc.* **2006**, *128* (13), 4226.
(49) Ellis, G. A.; Palte, M. J.; Raines, R. T. *J. Am. Chem. Soc.* **2012**, *134* (8), 3631.
(50) Andersen, K. A.; Smith, T. P.; Lomax, J. E.; Raines, R. T. *ACS Chem. Biol.* **2016**, *11* (2), 319.
(51) Wulff, G. *Pure Appl. Chem.* **1982**, *54* (11), 2093.
(52) Yang, W.; Fan, H.; Gao, X.; Gao, S.; Karnati, V. V. R.; Ni, W.; Hooks, W. B.; Carson, J.; Weston, B.; Wang, B. *Chem. Biol.* **2004**, *11* (4), 439.
(53) Hoeg-Jensen, T. *QSAR Comb. Sci.* **2004**, *23* (5), 344.
(54) Akgun, B.; Hall, D. G. *Angew. Chem. Int. Ed.* **2016**, *55* (12), 3909.
(55) Akgun, B.; Li, C.; Hao, Y.; Lambkin, G.; Derda, R.; Hall, D. G. *J. Am. Chem. Soc.* **2017**, *139* (40), 14285.
(56) Halo, T. L.; Appelbaum, J.; Hobert, E. M.; Balkin, D. M.; Schepartz, A. *J. Am. Chem. Soc.* **2009**, *131* (2), 438.
(57) Meadows, M. K.; Roesner, E. K.; Lynch, V. M.; James, T. D.; Anslyn, E. V. *Org. Lett.* **2017**, *19* (12), 3179.
(58) Chapin, B. M.; Metola, P.; Lynch, V. M.; Stanton, J. F.; James, T. D.; Anslyn, E. V. *J. Org. Chem.* **2016**, *81* (18), 8319.
(59) Vshyvenko, S.; Clapson, M. L.; Suzuki, I.; Hall, D. G. *ACS Med. Chem. Lett.* **2016**, *7* (12), 1097.

Chapter Two

Design, Synthesis and Structure of a "Frustrated Benzoxaborole" and its Applications in the Complexation of Amino Groups

2.1 Introduction

Boronic acids and their cyclic hemiboronic acid derivatives have recently emerged as new and unconventional pharmacophores in drug discovery efforts. These compounds offer unprecedented properties as mild Lewis acids, with the unique ability to undergo reversible exchange with alcohol and carboxylate functional groups on target biomolecules. As described in Chapter 1, benzoxaboroles are a class of stable cyclic 5-membered hemiboronic acids that have received significant attention owing to the recent approval of two new drugs, tavaborole and crisaborole, which are marketed for the treatment of onychomycosis and psoriasis, respectively.[1,2] Other benzoxaborole derivatives have shown potential to treat a range of health issues,[3] along with significant success and further promise in other applications such as carbohydrate recognition, catalysis, and as biomaterials.[4] To fully exploit the potential of benzoxaboroles, complementary studies must be conducted to understand their structural and physicochemical properties. In this regard, Hall and coworkers recently demonstrated, through NMR spectroscopic evidence, that benzoxaborole exists largely in its closed form in aqueous medium, yet it can undergo rapid and reversible hydrolysis to the open form (Figure 2–1a).[5] This new structural information can help provide a better understanding of the pharmacokinetic and pharmacodynamic behavior of benzoxaborole drugs.

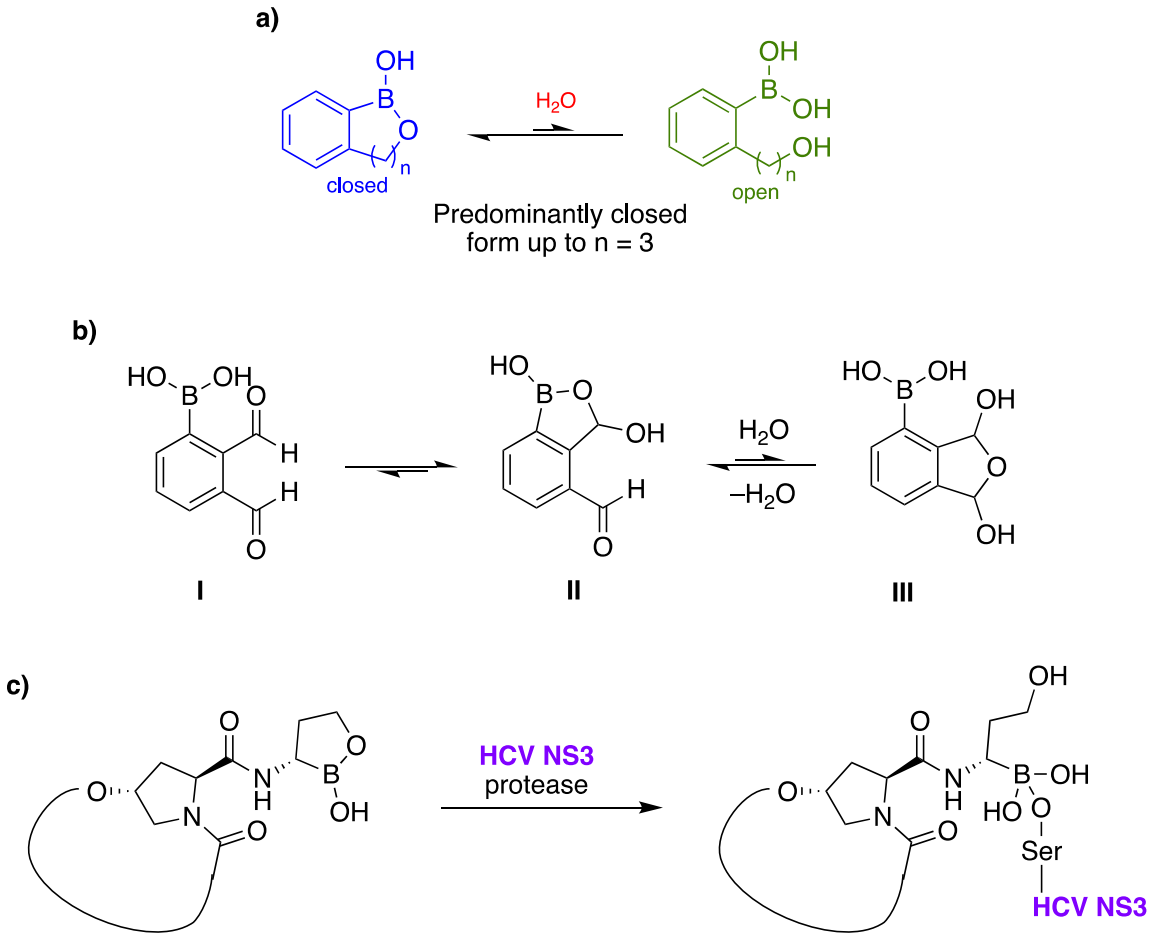

Figure 2–1. Examples of open and closed benzoxaborole compounds.

Remarkably, there appears to be no example of a permanently open benzoxaborole derivative. Lulinski and Serwatowski studied the ortho-phthalaldehyde derivative **I**, which was found to exist predominantly in its closed benzoxaborole form **II** in wet organic solvent, with **III**, an open benzoxaborole, as only a minor form (Figure 2–1b).[6] The only other reported instance of a temporary open member of this class of benzoxaboroles is an aliphatic α-amino oxaborole bound to the NS3 serine protease (Figure 2–1c).[7] The question therefore becomes, what unique properties would a predominantly and permanently open benzoxaborole possess, and how can these properties be exploited for applications in chemical biology and catalysis.

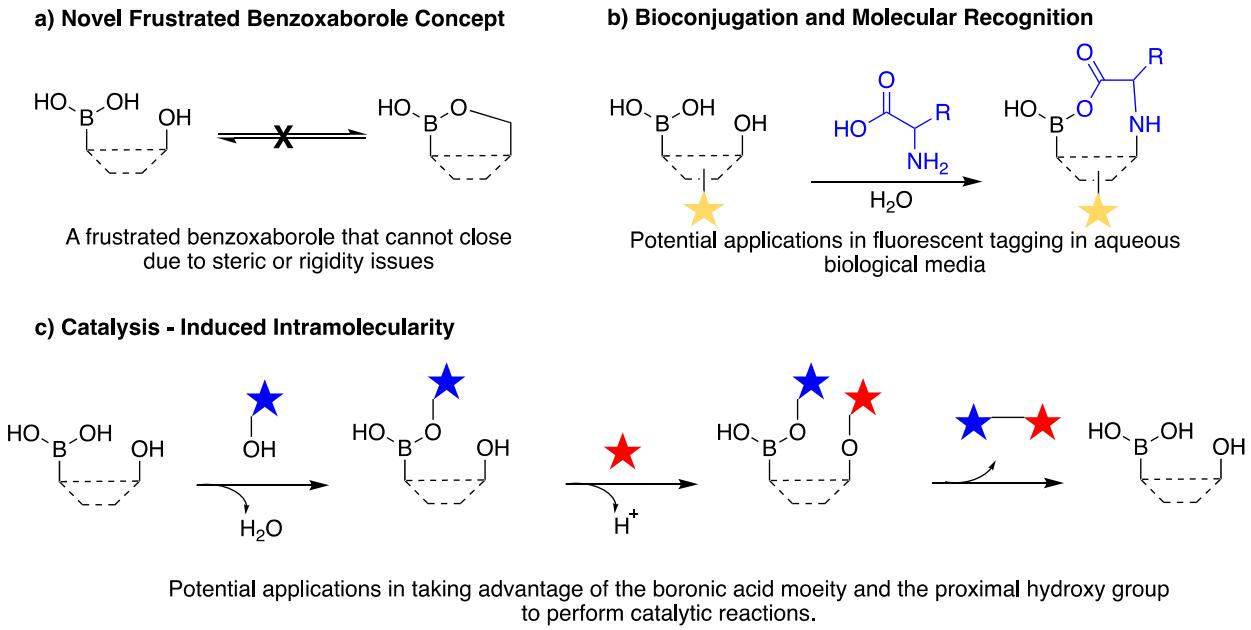

Figure 2–2. New concept of a "frustrated benzoxaborole" (a) and its potential applications in biology (b) and catalysis (c).

Figure 2–2a shows the general structural concept of an open benzoxaborole, which can be used for potential dual binding of biomolecules (Figure 2–2b) and the utility of a boronic acid with an adjacent hydroxy group to bring chemical components in close proximity for reactivity in catalysis (Figure 2–2c).

2.2 Objectives

With this work, the goal is to successfully synthesize and study a permanently open benzoxaborole by the installation of a hydroxy group next to an aryl boronic acid on a rigid organic framework (Figure 2–1a). In order to achieve an open structure, the hydroxy arm must be held rigid and be placed at an adequate distance from the boronic acid to avoid isomerization of the benzoxaborole structure. The inspiration for this new design came from the work shown in Figure 2–1b. The goal is to modify the synthesis to keep the equilibrium significantly favoring the ortho-

hydroxy boronic acid **III**. This design would be the first permanently open ortho-hydroxy boronic acid, or "frustrated benzoxaborole", leaving both the boronic acid and hydroxy group open for reactivity. The properties of this new structure, such as solubility, pKa and bonding, are to be studied and compared to that of traditional boronic acids and benzoxaboroles. This novel compound is expected to have superior iminoboronate binding properties to that of 2-formylphenylboronic acid (2-FPBA) and 2-acetylphenylboronic acid (2-APBA), as mentioned in Section 1.2.1 and 1.2.2 (Chapter 1), which are known to be reversible in even slightly acidic and basic conditions. Furthermore, the bioconjugation of this novel compound with amino groups, including the lysine residue on lysozyme, amino alcohols and *N*-terminal cysteines, are to be studied and compared to known literature systems.

2.3 Results and Discussion

2.3.1. Design and Synthesis

In Figure 2–1a, compound **I** was successfully synthesized by Luliński and coworkers, which showed a dynamic equilibrium of isomers via NMR analysis.[6] Boronic acid isomerization with the ortho-formyl group is exceptionally favorable to form a relatively stable benzoxaborole **II**, which is the major isomer seen. The authors also observed the condensation of the two ortho and meta formyl groups to form hemiacetal compound **III**, which was present in an exceptionally minor amount. In order to make this type of hemiacetal structure more permanent, we envisioned a hydroxymethyl arm at the meta position of compound **I** (**2-1I** in Figure 2–3a)**.** With this modification, it is believed that the isomerization of the very nucleophilic and proximal hydroxy arm with formyl group to form **2-1II** is far more energetically favorable than the isomerization of the boronic acid by hydration of the formyl group to form a benzoxaborole-like **2-1III** (Figure 2–

3a). It is possible, however, that **2-1II** can dehydrate and form a benzoxaborole-like compound **2-1IV**. The equilibrium of such a system has not been reported, so it is unknown where its position may lie.

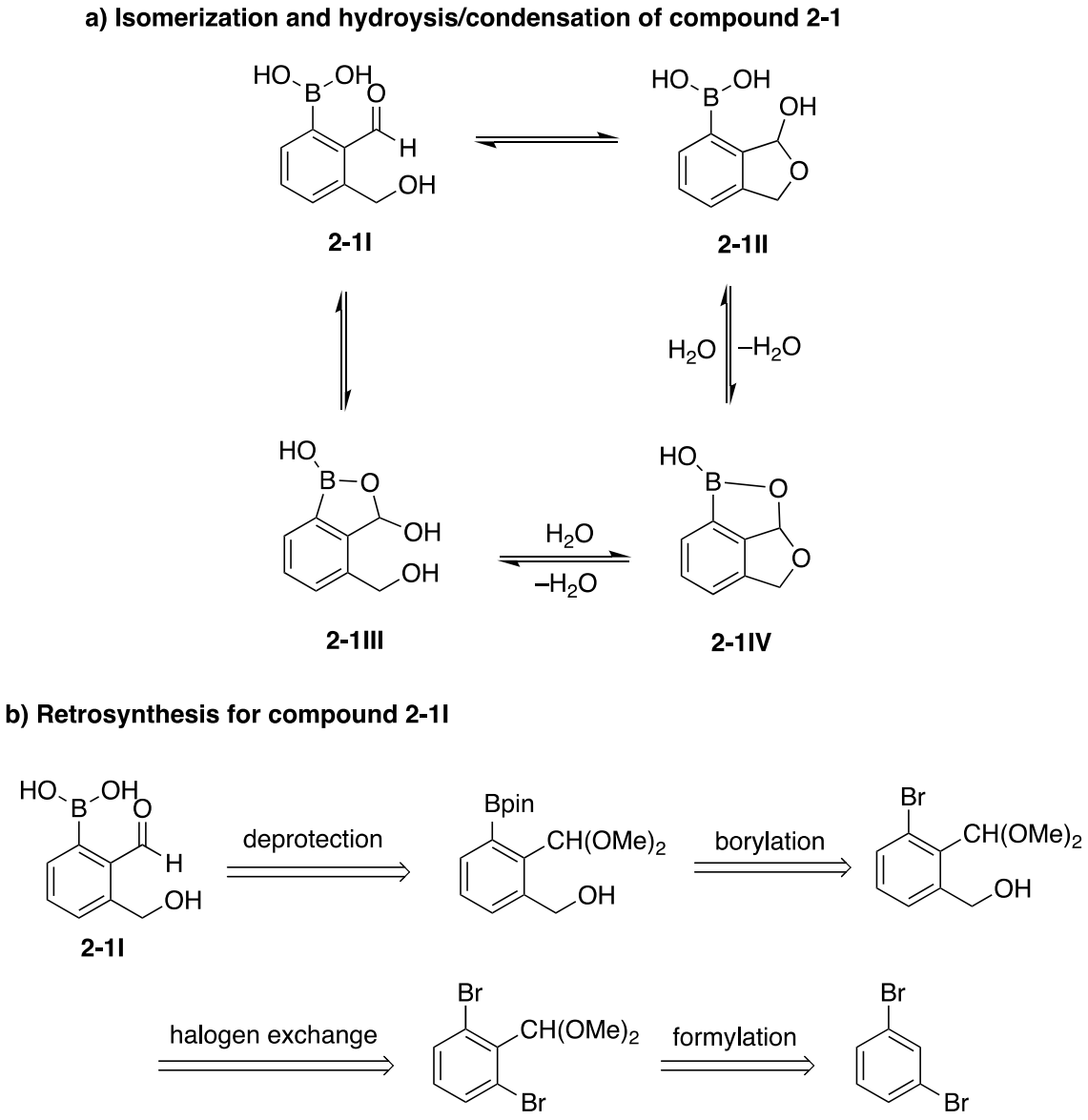

Figure 2–3. Design and retrosynthesis of a novel "frustrated benzoxaborole".

The retrosynthetic route to compound **2-1I** is shown in Figure 2–3b. 1,3-Dibromobenzene was selected as a starting point as it can be selectively deprotonated at the acidic 2-position, and

the two halogen sites can exchange relatively easily with metals, followed by electrophile trapping at all these positions to install the desired functionalities.

The first few steps towards the synthesis of compound **2-1I** were known in the literature, up to compound **2-5**, shown in Scheme 2–1.[6] Thus, the known compound 1,3-dibromobenzene **2-2** was selectively deprotonated by LDA, followed by formylation and acetal protection to give dibromide **2-4**. The latter underwent a single lithium-halogen exchange, followed by formylation with DMF, then a reduction to give alcohol **2-7**, which fully isomerizes to **2-8**, as seen by the lack of an aldehyde peak and a diastereotopic pair of methylene protons in NMR.

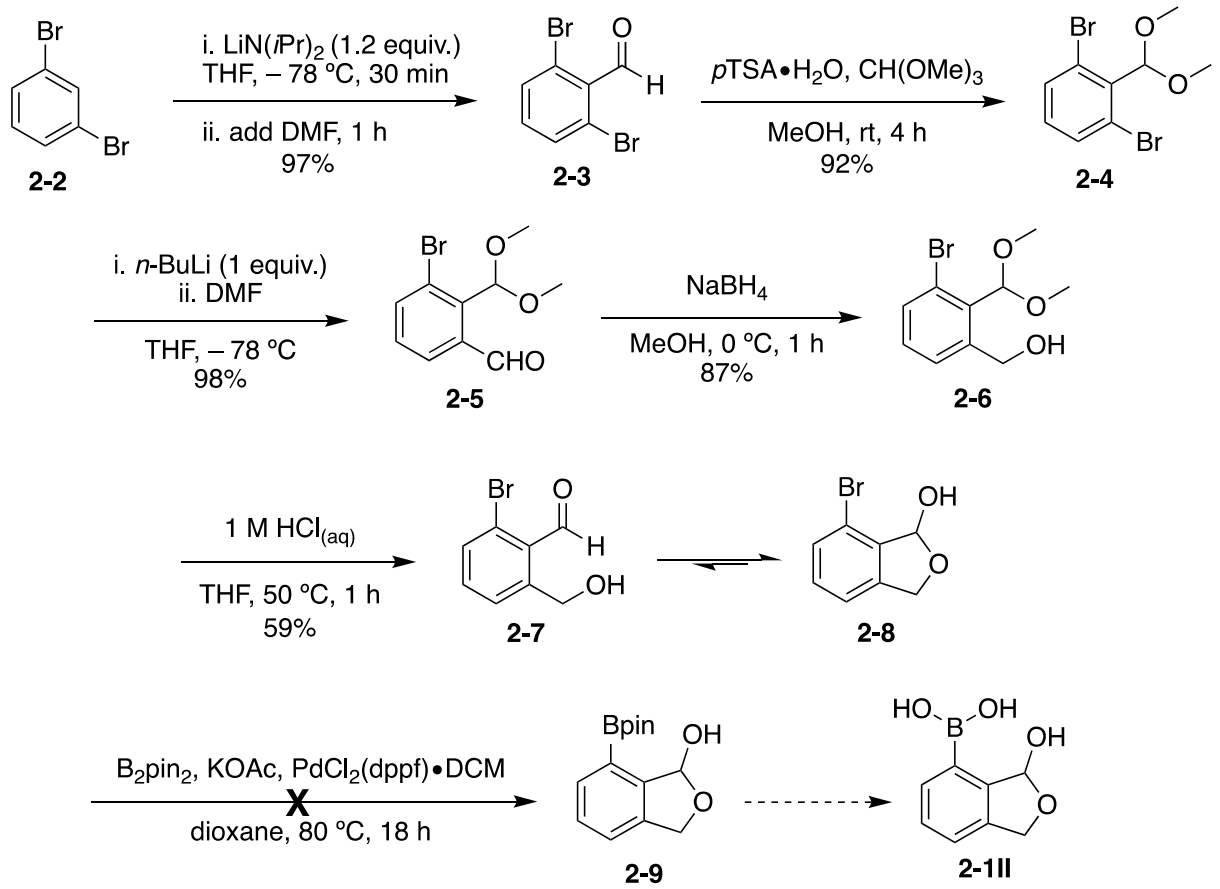

Scheme 2–1. First attempt at the synthesis of **2–1.**

However, issues arose when a classical Miyaura borylation was attempted with **2-8**, which resulted in only starting material and degradation.[8] This failed attempt came as a surprise, and it was rationalized by the proposal that the adjacent hydroxy group was interfering in some way, possibly either by steric or electronic effects from the oxygen lone-pair. In order to try to suppress the nucleophilicity of the hydroxy group, a silyl protection was attempted, but the subsequent borylation still failed (Scheme 2–2a). Further attempts were made to directly add a boronic acid to compound **2-8**, instead of a boronate ester. Both direct lithium halogen exchange followed by borate trapping and hydrolysis, and a Molander borylation[9] were attempted, but neither resulted in the desired transformation (Scheme, 2–2b).

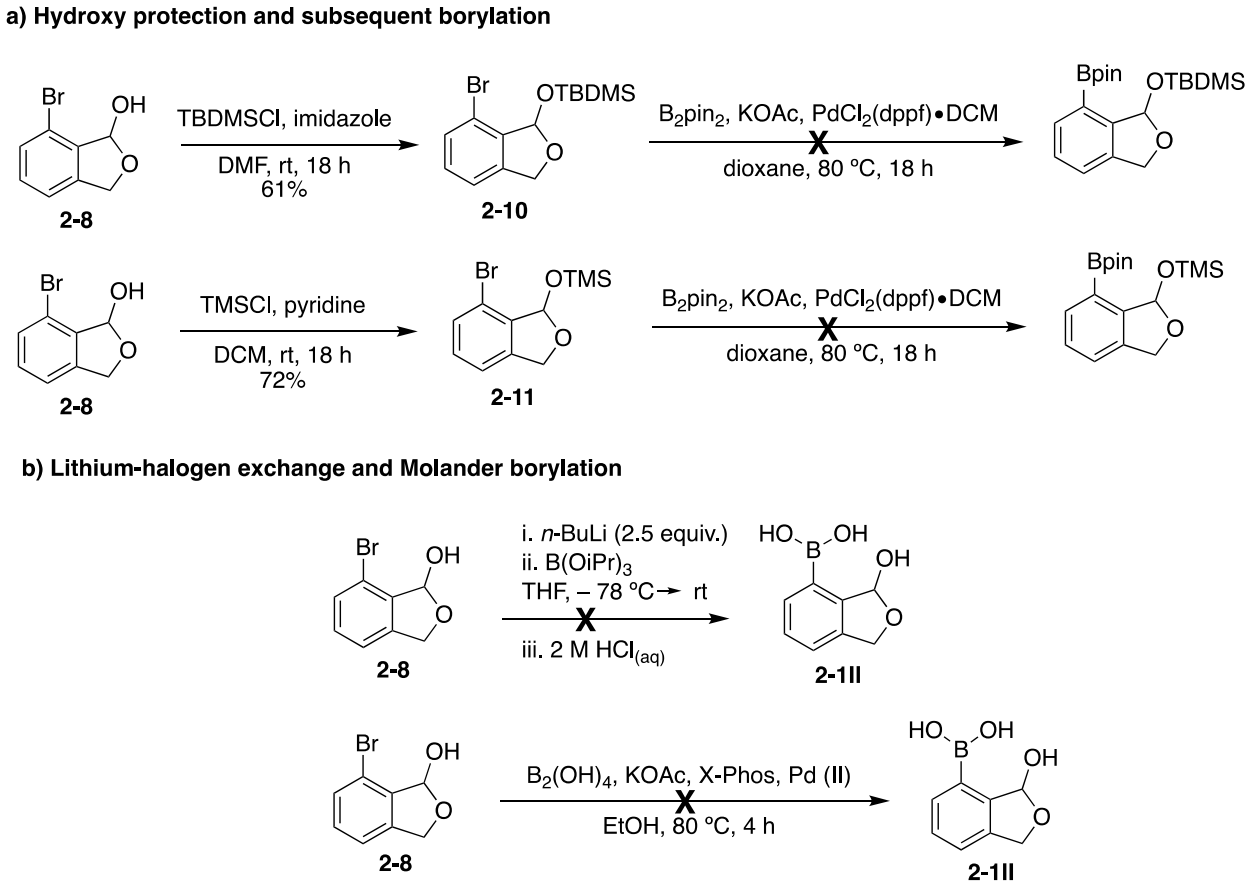

Scheme 2–2. Further borylation attempts with compound **2-8**.

After these failed attempts, it was ultimately decided to perform the borylation step earlier in the reaction sequence, with compound **2-5**, which gratifyingly provided boronic ester **2-12** in a 54% yield (Scheme 2–3). Compound **2-12** was then reduced to alcohol **2-13**, but the acetal hydrolysis with aqueous HCl proved to be difficult and only resulted in starting material degradation, even when utilizing a weaker acid such as *p*TSA. (Scheme 2–3).

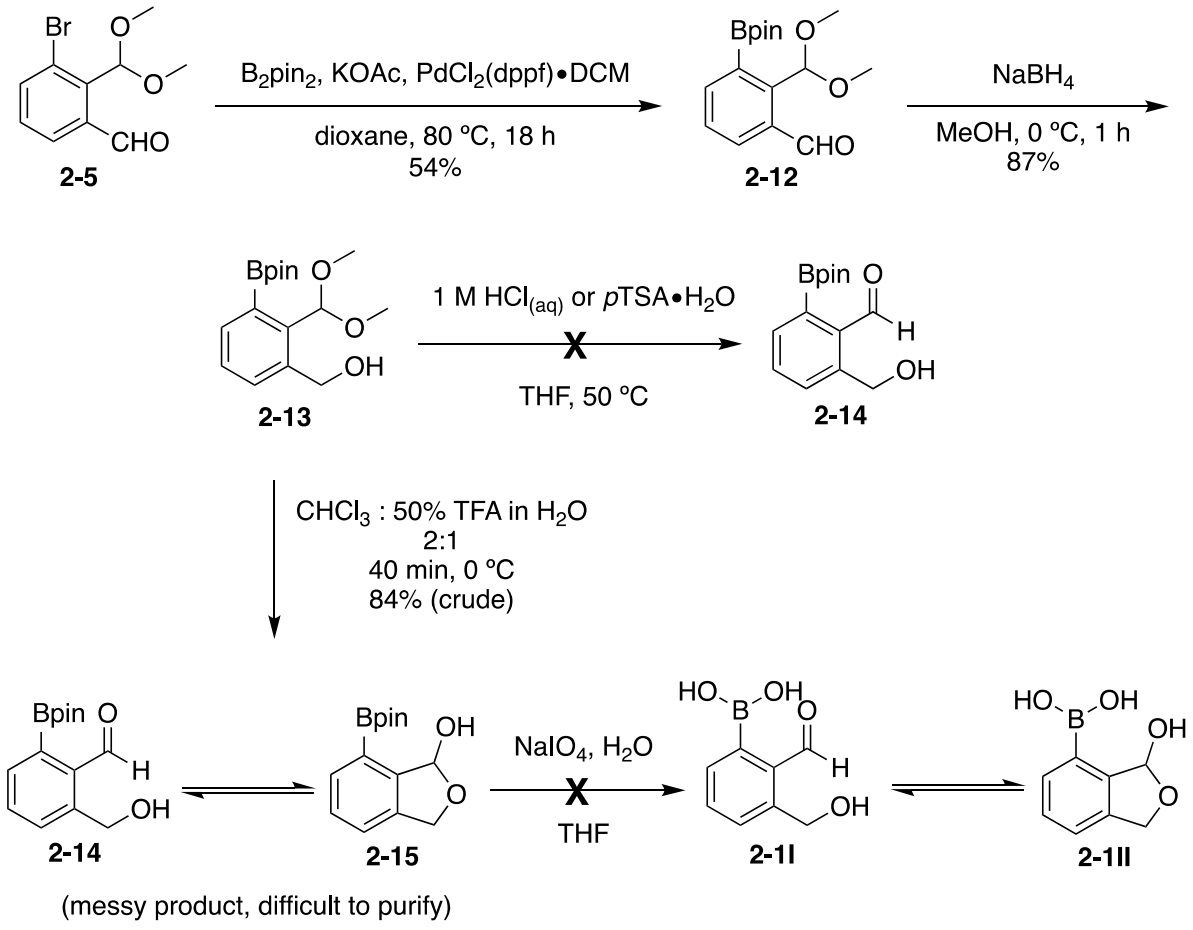

Scheme 2–3. Continued attempts to synthesis compound **2-1**.

The conditions that eventually worked for the acetal deprotection of **2-13** involved using a solution of TFA in water and chloroform; however, deprotection resulted in a somewhat messy product, which was difficult to purify by either silica gel flash chromatography or recrystallization (Scheme 2–3). The subsequent attempt at the pinacol group deprotection to obtain the free boronic acid once

again resulted in degraded material. To tackle the issue of poor acetal deprotection and a resulting impure product, compound **2-13** was converted into the corresponding trifluoroborate salt effectively using aqueous KHF_2. This reaction releases HF in the reaction medium, which in turn cleaves the acetal *in situ* to yield **2-16**, which isomerizes to **2-17**, as a readily isolable precipitate (Scheme 2–5).[10] The literature work-up for this step involves solvent removal *in vacuo*, leaving the trifluoroborate **2-17** and potassium fluoride salts remaining in the flask. To separate this mixture, hot acetone was added to dissolve the desired product and separate the potassium fluoride salts by filtration. Using this literature work-up proved less than ideal for compound **2-17** as it has low solubility even in hot acetone. To overcome this isolation issue, a hot solution of 8% methanol in acetone was instead used to increase the solubility of **2-17** and isolate it in a good yield, while potassium fluoride salts remain undissolved, and easily filtered out. The final step of trifluoroborate hydrolysis in this synthesis proved to be tricky as it was predicted that target compound **2-1** would be highly water-soluble and therefore difficult to isolate and purify. This problem was tackled by using a strong, solid fluorophile, in this case silica gel, a procedure developed by Molander and co-workers to extract the fluorides from boron without any contamination of either the organic or aqueous phase.[11] When initially attempted, the silica gel was filtered, and the reaction diluted with EtOAc and water and the phases separated. However, compound **2-1** was mostly found in the aqueous phase, but a considerable amount was also found in the organic phase along with major impurities. In addition, silica gel is partially soluble in water, so the clean product from the aqueous phase was contaminated with a small amount of silica gel at all times. To fix this issue, the reaction is instead diluted with acetone, then silica gel is easily separated by filtration and the filtrate concentrated *in vacuo*. For purification, the white crude solid was dissolved in water, and any intractable organic impurities are separated by filtration and

product **2-1** is obtained in good yield with minor impurities after a simple evaporation (Scheme 2–4).

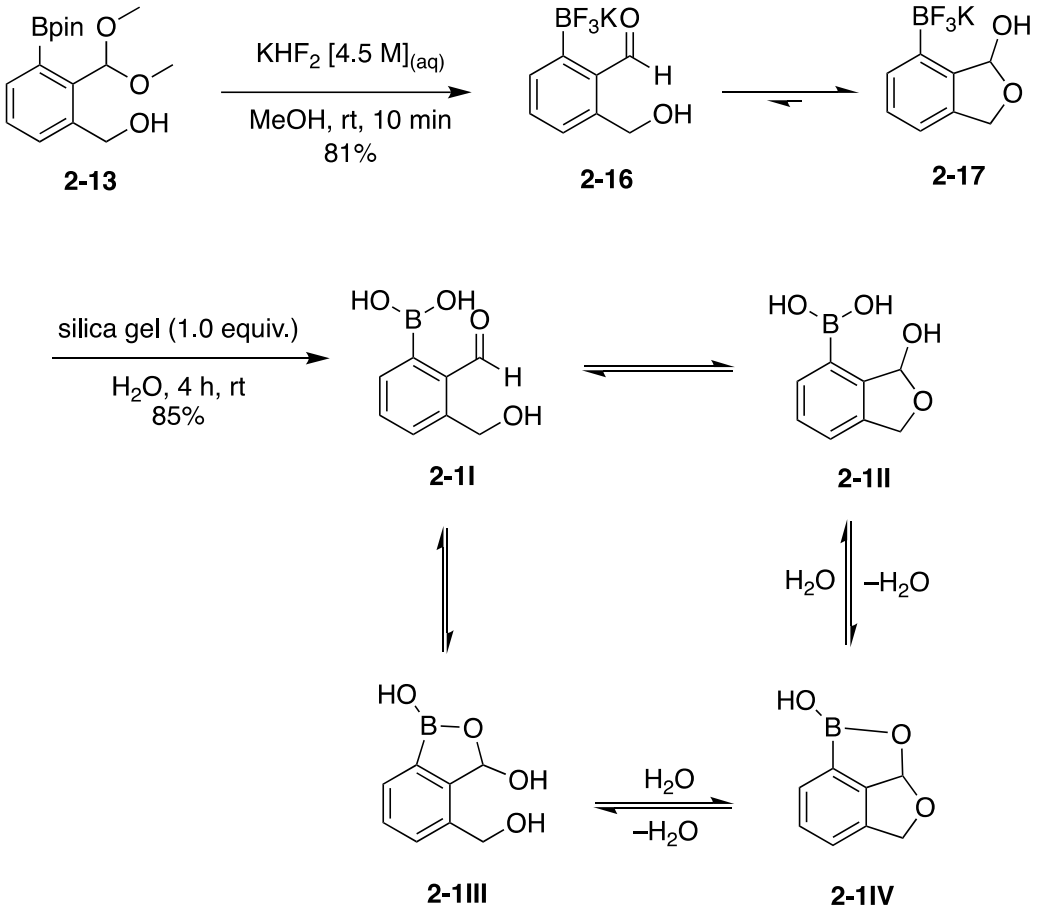

Scheme 2–4. Successful completion of synthesis of compound **2-1**.

The ^{1}H NMR spectrum of compound **2-1** was obtained in acetone with a drop of D_2O to suppress boroxine formation. The aldehyde peak for isomer **2-1I** was not seen by ^{1}H NMR analysis, indicating that this isomer is not present to any major degree. The methylene hydrogens are diastereotopic, suggesting that the hydroxy arm closes onto the formyl group, which rules out the possibility of benzoxaborole isomer **2-1III**. Due to exchange of hydroxy protons with deuterium in NMR solution, it was exceptionally difficult at this stage to conclusively state if compound **2-1**

exists as the open structure **2-1II,** or the closed benzoxaborole structure **2-1IV**, or if there is an appreciable equilibrium between these two forms. More studies are required, and which are described in the next section.

2.3.2. Complete Structure Elucidation

2.3.2.1 NMR Spectroscopy Studies

With the synthesis of **2-1** complete, the next task was to conclusively prove the equilibrium position of **2-1II** and **2-1IV** (cf. Scheme 2–4). Compound **2-1** was dissolved in very dry deuterated DMSO and immediately analyzed by ^{1}H NMR, which initially revealed extensive boroxine formation (Figure 2–4a).

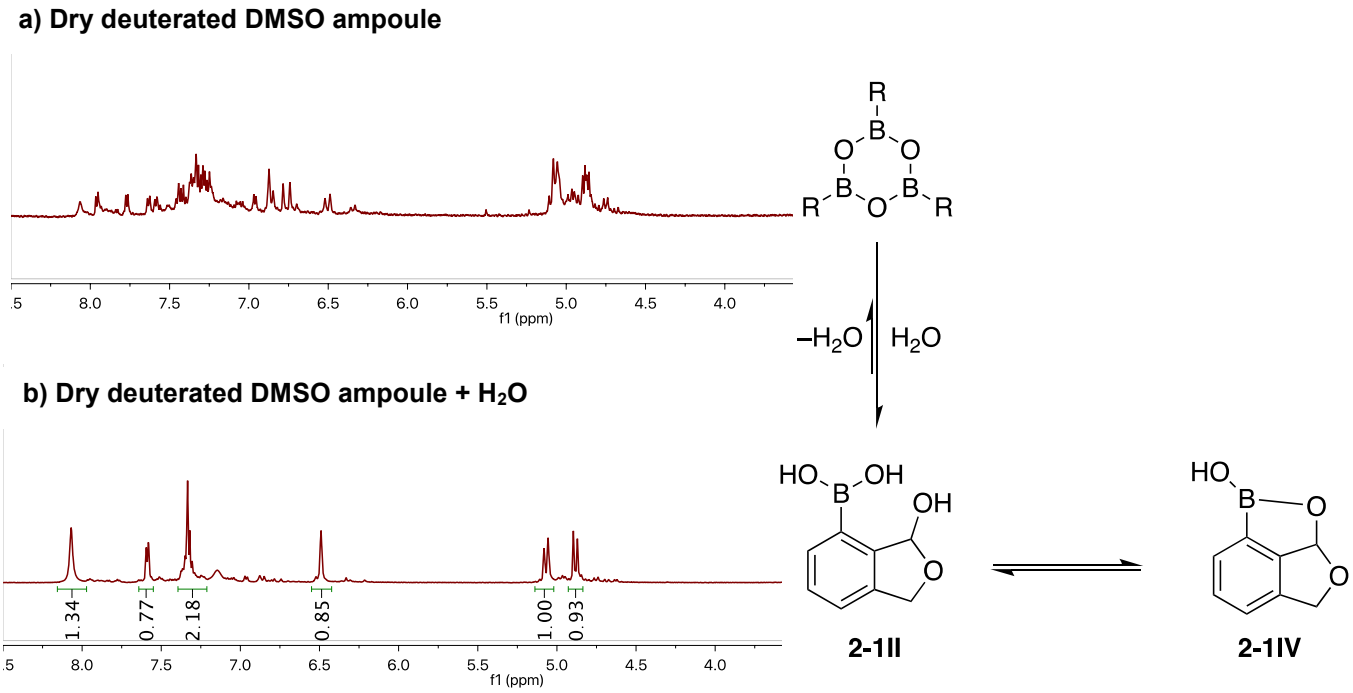

Figure 2–4. Compound **2–1** in dry (a) and wet (b) DMSO.

In an attempt to hydrolyze boroxine without deuterium exchange of hydroxy protons, H_2O was slowly added to the NMR tube (Figure 2–4b). The proton signals at about 8 ppm are attributed to the hydroxy groups attached to boron and integrate to 1.3, a value that lies quite confusingly between that of structures **2-1II** and **2-1IV**, which should have had two or one protons respectively.

For further evidence of a concrete structure of compound **1**, the ^{1}H and ^{11}B shifts of **1** were compared to other boron containing compounds (Figure 2–5). The NMR experiments were performed in DMSO-d_6 with a drop of H_2O to suppress boroxine formation. Benzoxaborole **2-18** has a ^{11}B chemical shift of 32.3 ppm versus 29.5 ppm for blocked *ortho*-hydroxymethyl arylboronic acid **2-19**. The adjacent oxygen of **2-19** is incapable of closing onto the boronic acid. Compound **2-20**, the methoxy derivative of compound **2-1II**, also incapable of ring-closing, shows a ^{11}B shift at 28.7 ppm. In the event, compound **2-1**, has a ^{11}B chemical shift of 30.3 ppm, indicating it is closer in structure to the open boronic acid form than the benzoxaborole form. The ^{1}H shift of the protons on the B(OH) moiety are also diagnostic as benzoxaborole **2-18** shows the chemical shift to be at 9.15 ppm while the other B(OH) ^{1}H shifts on open boronic acid compounds, **2-19, 2-20** and **2-1**, show up at around 8.0 ppm.

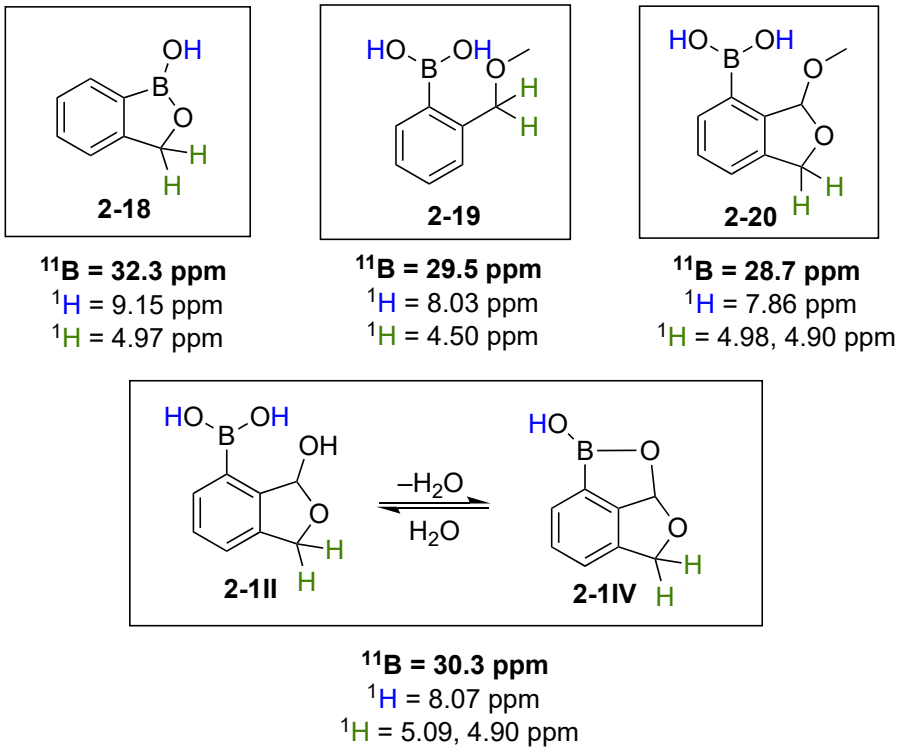

Figure 2–5. Comparison of NMR chemical shifts of various boron containing compounds in DMSO-d_6 + one drop H_2O.

Although all NMR experiments mentioned above point in the direction of compound **2-1** existing the open boronic acid form **2-1II**, the most concrete data would consist in ultimately have all of the hydroxy protons visible and integrate correctly in the NMR spectrum. Thus, the ^{1}H NMR spectrum of **2-1** was run in alternative solvents. The spectrum in acetone with water prevents the dimerization and oligomerization of B–OH groups and was very informative (Figure 2–6). Under these conditions, the hydroxy protons were found to exchange with the solvent at a rate slower than the spectrometer time scale, and are thus observable as distinct, sharp peaks. The singlet at 7.6 ppm, with an integration of 2H, was attributed to the boronic acid resonances, and the doublet at 6.6 ppm was tentatively assigned to the hemiacetal OH group. These assignments were confirmed by a deuterium-exchange experiment; not only did these peaks disappear, the quartet

proton H_a at 6.55 ppm became a doublet (the residual small coupling of 2.4 Hz originates through a W coupling with one of $H_{c/d}$), thus confirming this resonance belongs to the hemiacetal methine. Altogether, these NMR spectroscopic studies in wet polar solvent provide overwhelming evidence that compound **2-1** exists exclusively in its open form, **2-1II**, not in the closed benzoxaborole form **2-1IV**.

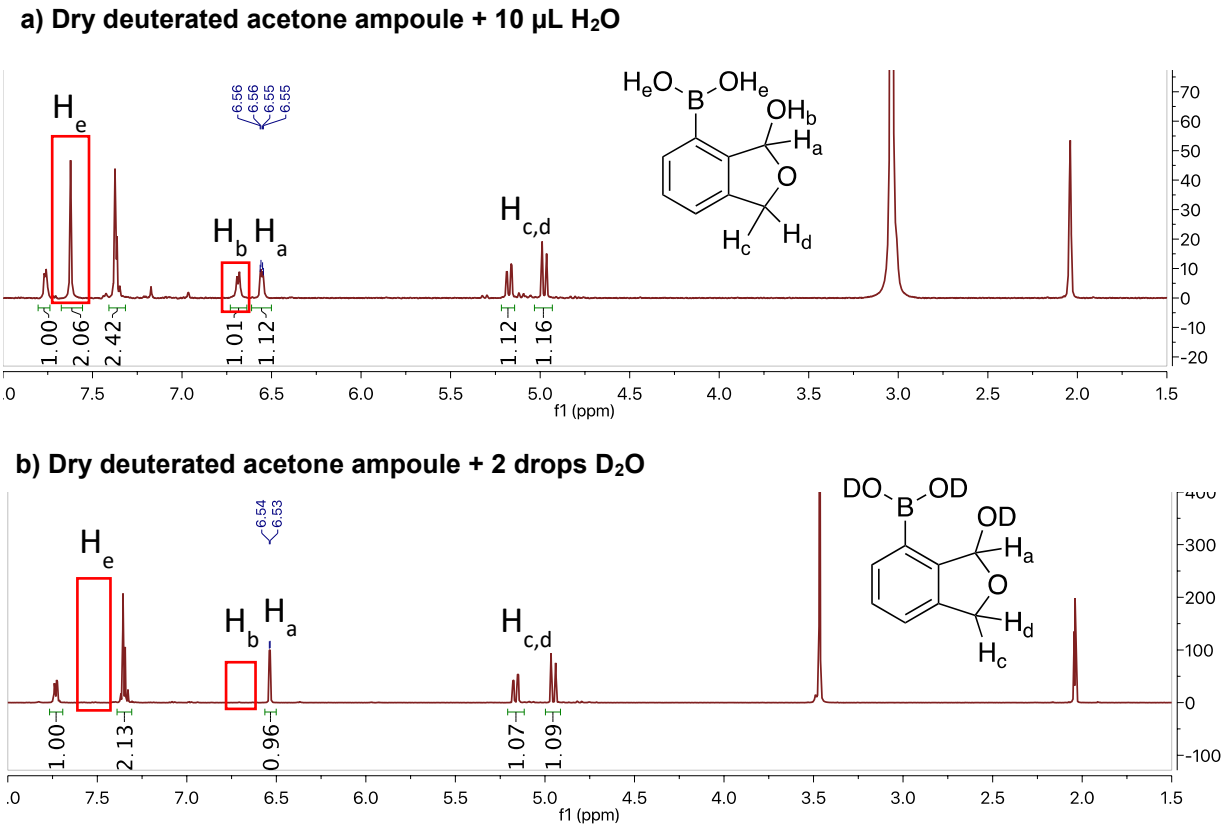

Figure 2–6. Complete ^{1}H NMR spectrum of structure **2-1II** (a) and deuterium exchange of hydroxy protons (b).

With strong evidence in hand for the hemiacetal structure of **2-1II**, the pKa of compound **2-1** was studied via NMR and compared to that of benzoxaborole **2-18** by following the ^{11}B chemical shift at various pH, shown in Figure 2–7.[12]

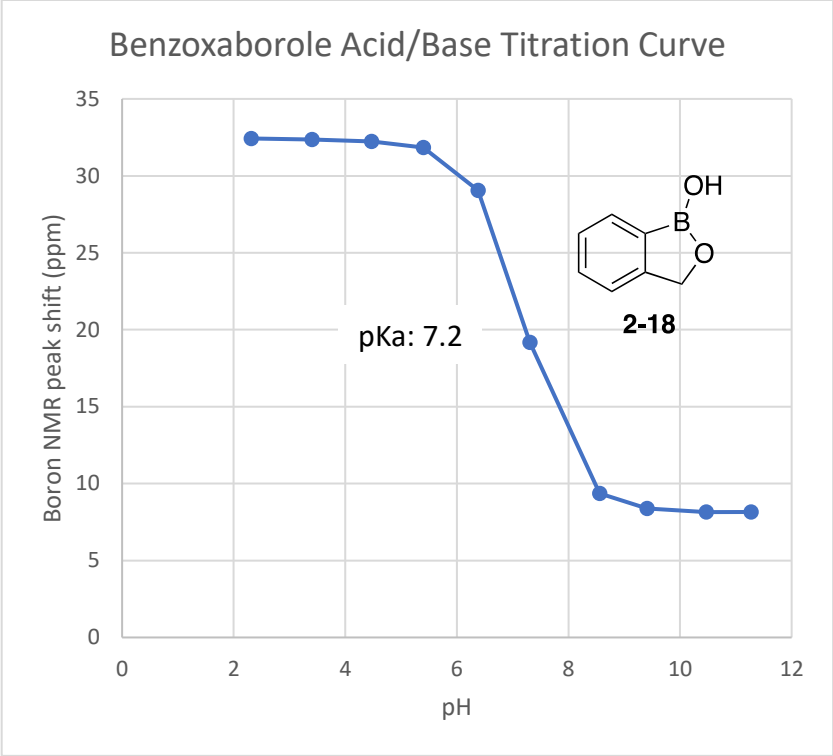

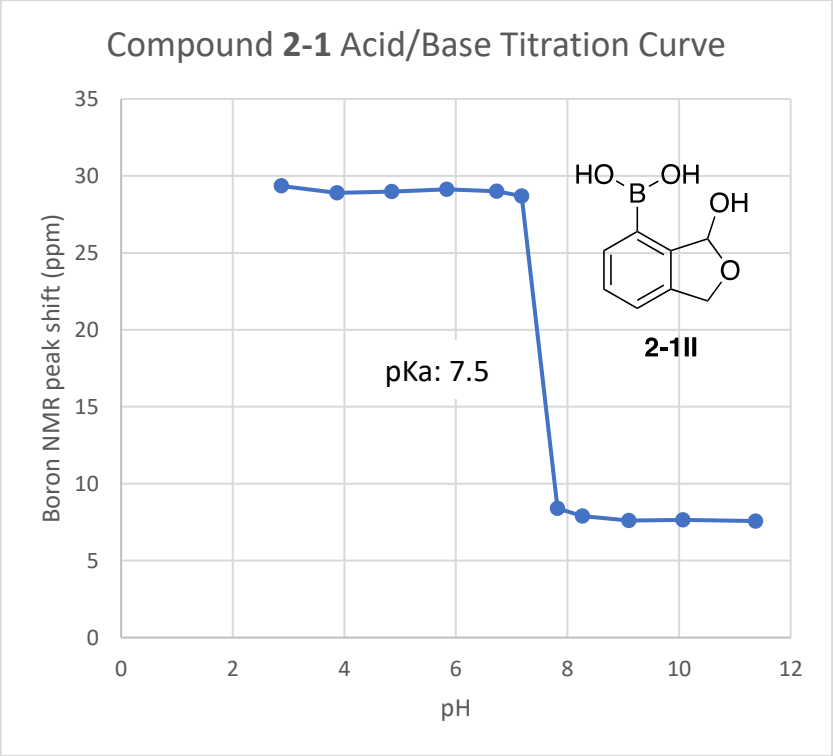

Figure 2–7. pKa titration curves of compounds **2-1** and **2-18**.

As mentioned in Section 1.1.1.1 in Chapter 1, benzoxaboroles generally display a pKa approximately one to two units lower than the corresponding arylboronic acids. For example, the reported pKa of 7.2 for benzoxaborole is 1.7 units lower than that of phenylboronic acid (8.9).[4] Herein, we measured the pKa of compound **2-1** through a ^{11}B NMR titration method (Figure 2–7).[12] To our surprise, the resulting pKa of 7.5 is closer to that of benzoxaborole (reproducibly measured to be 7.2 in our hands) than that of a normal boronic acid. Another noteworthy observation of the graphs in Figure 2–7 is the pH range difference of the titration curve between the two plateaus. For compound **2-18**, the titration curve is broad, spanning about 4 pH units, but for compound **2-1**, this curve is quite steep, with less than one pH difference from the first plateau to the second. This difference in curvature indicates that compounds **2-1** and **2-18** possibly have different mechanisms of capturing hydroxy ions from an increasing pH solution, highlighted in Figure 2–8. Whereas benzoxaborole **2-18** has a low pKa, likely due to favorable ring strain release upon hydroxy coordination, it is thought that the lower than expected pKa of compound **2-1** is due to assisted hydroxy anion coordination to boron, from the adjacent secondary alcohol, through hydrogen bonding. This type of hydrogen bond assistance is seen in "Wulff" type *ortho* methylamine boronic acids as well, which have pKa's closer to 5, also shown in Figure 2–8.[13] This lower pKa for compound **2-1** means it exists largely exist as a charged species at biological pH, as do benzoxaborole-type structures. This behavior results in increased solubility in water compared to boronic acids, which suggests utility in medicinal chemistry.

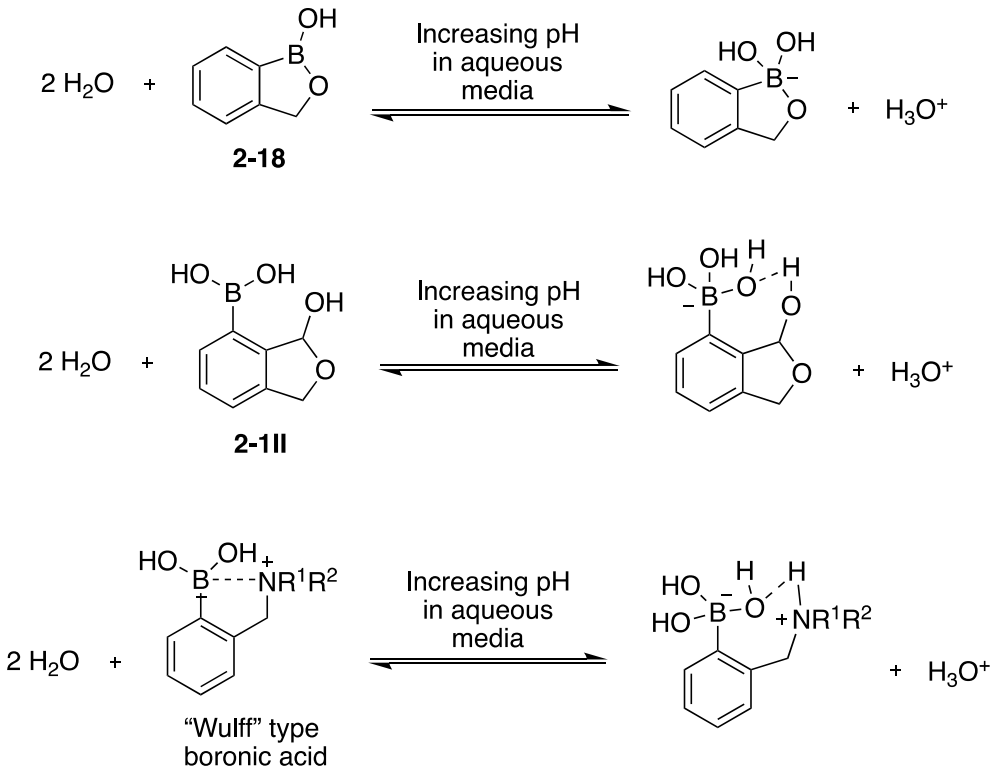

Figure 2–8. Addition mechanism of hydroxy groups with various boron compounds.

2.3.2.2 Mass Spectrometric Studies

A key feature of a free boronic acid moiety is the ability to dehydrate to form anhydride species under dry solvent conditions or in the gas phase. The behavior of compound **2-1** was examined by high-resolution ESI-MS. The trimeric boroxine or dimeric anhydride was not observed for compound **2-1**. Instead, compound **2-1** displays the loss of only two molecules of water to form the putative dimer, which can only originate through the involvement of the alcohol unit in the open form **2-1II** (Figure 2–9). Such a doubly dehydrated dimer does not occur with either benzoxaborole **2-18** or the blocked ortho-hydroxymethyl arylboronic acid **2-19**. Therefore, mass spectrometric analysis corroborates the above NMR evidence in support of the open, "frustrated benzoxaborole" form (**2-1II**) of compound **2-1**.

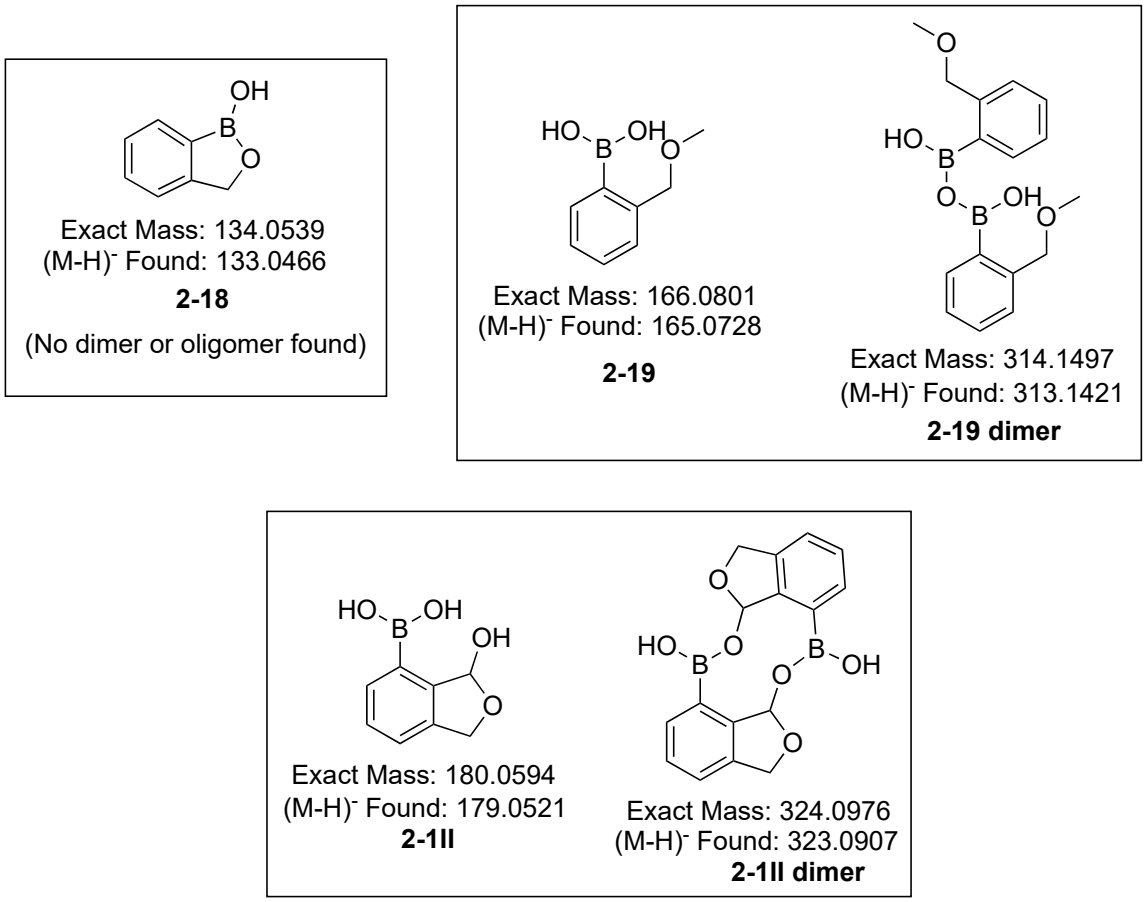

Figure 2–9. ESI-MS species found for compounds **2-1II**, **2-18** and **2-19**.

2.3.3. Bioconjugation Studies

Having convincingly demonstrated that compound **2-1** exists predominantly in its open "frustrated benzoxaborole" form **2-1II**, we turned towards a preliminary examination of the reactivity of this unique molecule. As mentioned in Section 1.2.1 (Chapter 1), the carbonyl groups of 2-FPBA and 2-APBA are known to condense with amines to form imines, which are further stabilized by a dative B–N bond with the adjacent boronic acid.[14] These types of structures were termed "iminoboronates", shown in Figure 2–10a, Since imine formation is known to be reversible in mildly acidic or basic aqueous solutions, imines often need to be reduced in order to afford irreversible conjugates.

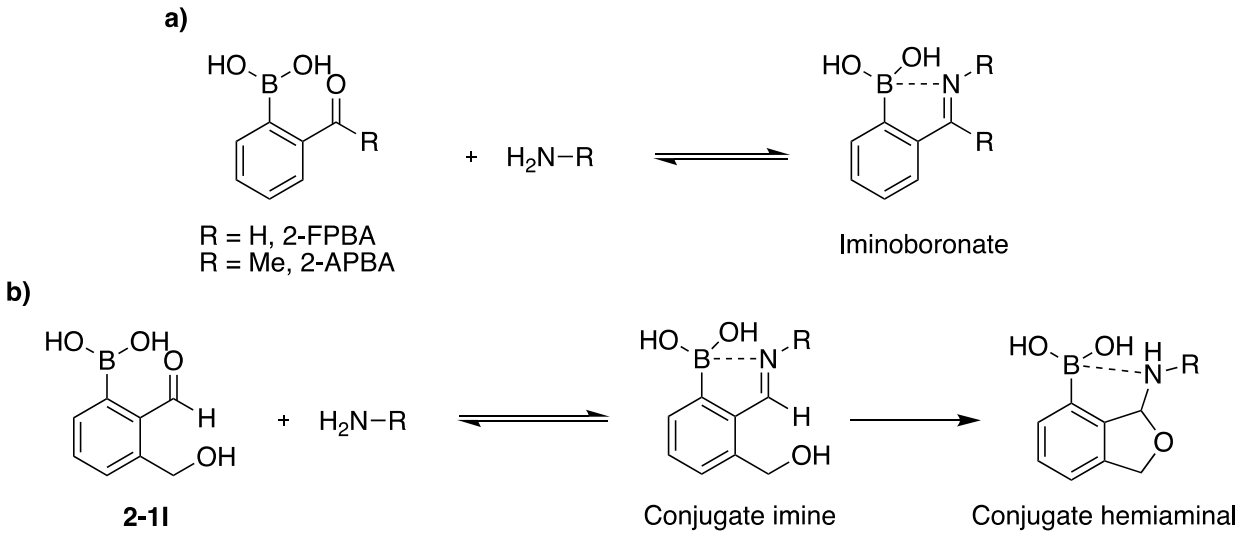

Figure 2–10. Amine conjugate formation with 2-FPBA, 2-APBA and compound **2-1**.

It was hypothesized that if an equilibrium between isomers **2-1I** and **2-1II** does in fact exist, even to a minor degree, then compound **2-1** would also be able to bind to amines in a similar fashion to 2-FPBA and 2-APBA. The dynamic nature of the hydroxy arm on compound **2-1** however, could potentially result in a more stable, possibly irreversible, hemiaminal structure, which could be favored over the imine structure (Figure 2–10b).

2.3.3.1 Amino Group Conjugation

Initial studies conducted to study the binding of **1** with benzylamine were performed in acetone and studied via NMR and LC-MS analysis to note any signs of conjugation. Shown in Figure 2-11 is compound **2-1** in deuterated acetone, followed by the addition of one equivalent of benzylamine. The most important change in the ^{1}H NMR spectrum is the upfield shift of the hemiacetal proton H_a, from 6.54 ppm in the unbound compound **2-1**, to 6.05 ppm when benzylamine is added (Figure 2–11). It is also notable that one of the two diastereotopic methylene protons, presumably the one on the same side as hydroxy/amino group, has shifted from 4.93 ppm

to 5.04 ppm and shows extra coupling with the N-H proton with upon addition of benzylamine. Both these differences indicate that the hemiacetal hydroxy group on compound **2-1** has been replaced by benzylamine. This result provides strong evidence that the ring-opened isomer **2-1I** exists long enough to form an imine with benzylamine. Subsequent ring closing of the hydroxy group on the imine gives a 5-membered hemiaminal structure.

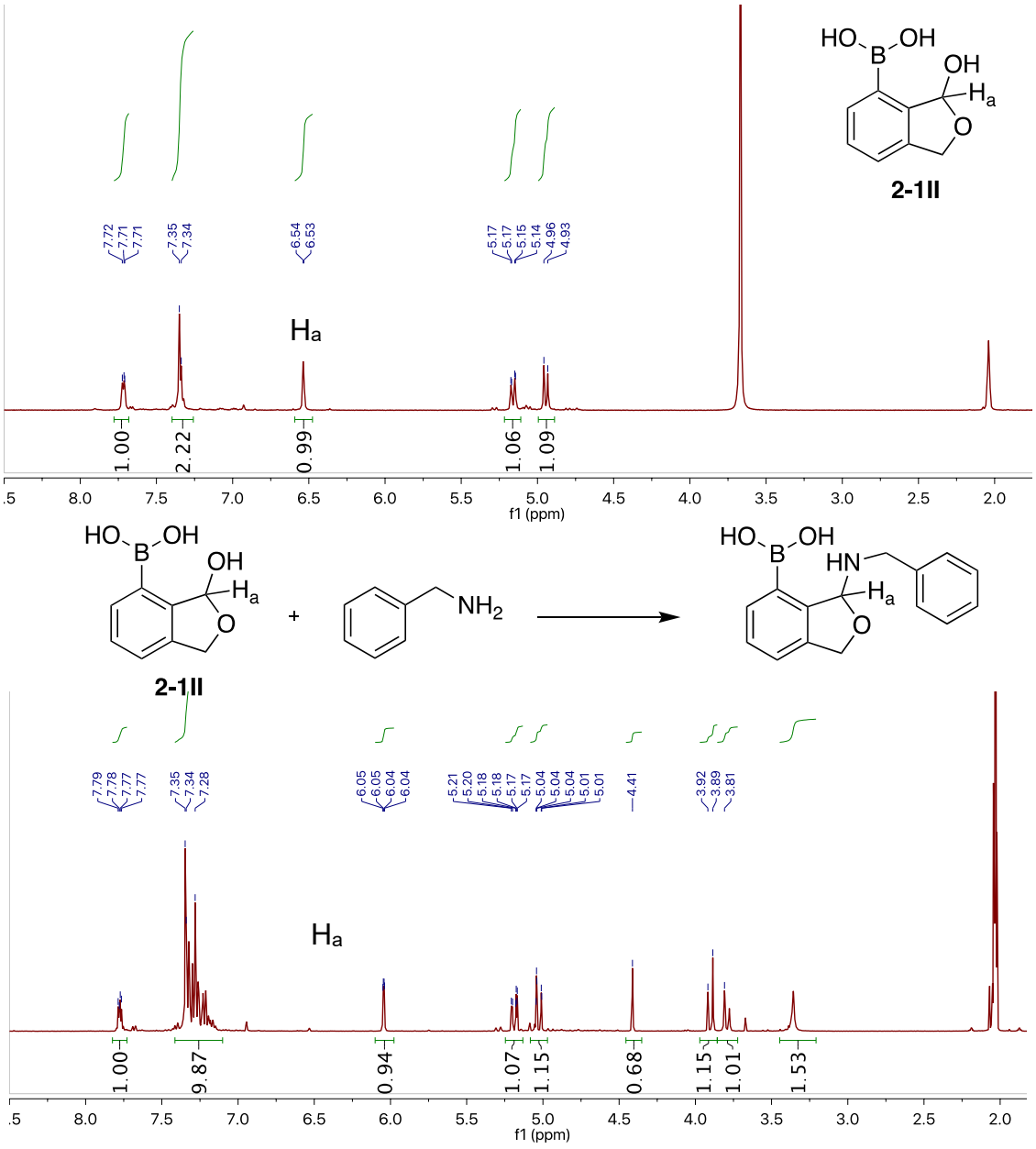

Figure 2-11. ^{1}H NMR spectrum of conjugate of compound **2-1** with benzylamine in acetone-d_6.

Furthermore, the LC-MS chromatogram of the benzylamine addition product after 30 mins shows majority hemiaminal product, with a small amount of leftover starting material (Figure 2–12).

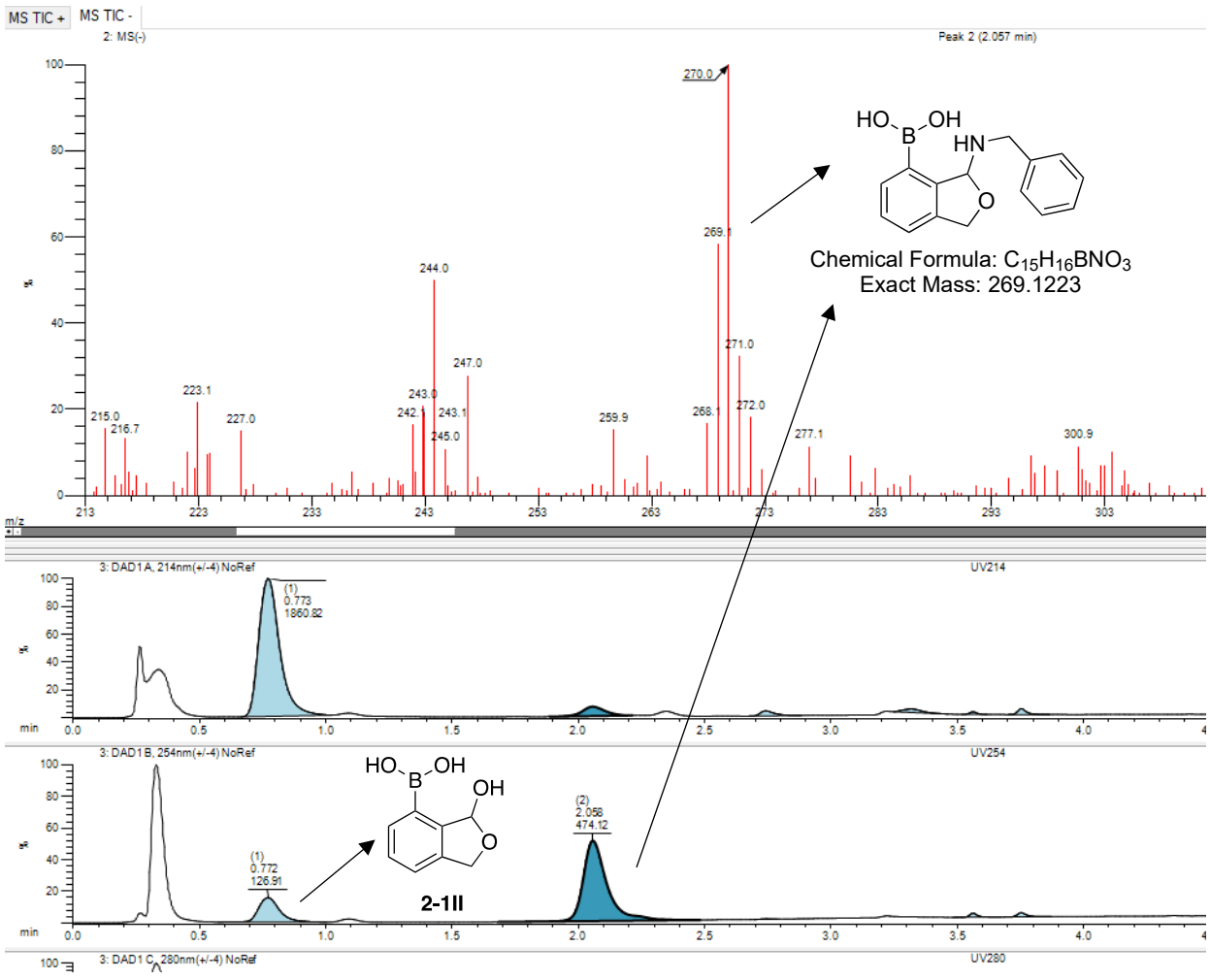

Figure 2-12. LC-MS of the conjugate of compound **2-1** with benzylamine.

After concluding that benzylamine binds effectively to compound **2-1**, we were interested to see if the adjacent boronic acid could achieve more than simply provide stability through a B–N dative bond. Compound **2-1** was mixed with 2-(aminomethyl)phenol and the reaction was analyzed once again by NMR and LC-MS analysis. A similar upfield shift of proton H_a was again observed by NMR spectrum as was seen with benzylamine, but the LC-MS result provided more insight as to the exact nature of the bonding of the phenol unit. The LC-MS mass spectrum in

Figure 2–13 suggests that the mass of the conjugated species of compound **1** and 2-(aminomethyl)phenol results in a structure where the ortho hydroxy group on the reagent does bind with the adjacent boron with a loss of one water molecule. Therefore, compound **2-1** seems to act as a bifunctional reagent with amino alcohols, binding with both the amine and hydroxy moieties.

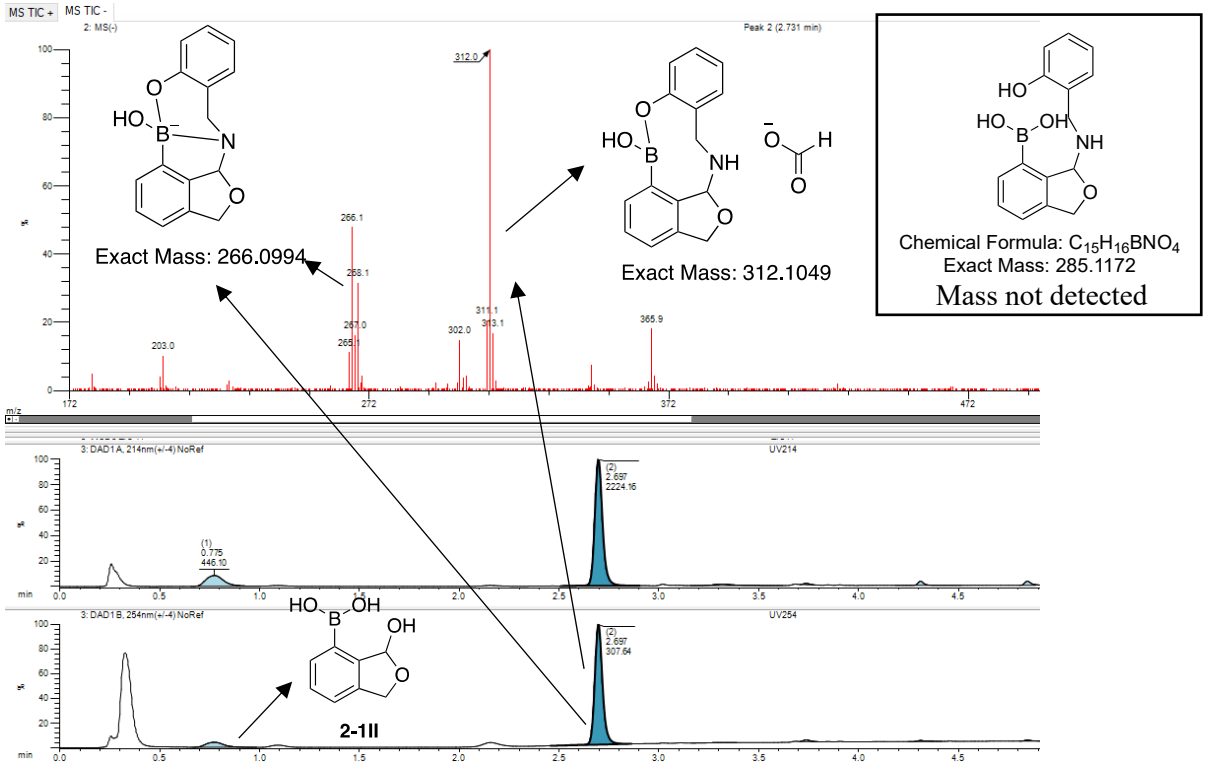

Figure 2–13. LC-MS of compound **2-1** conjugate with 2-(aminomethyl)phenol.

2.3.3.2 Lysozyme Binding

To determine the conjugation applicability of compound **2-1** in biologically relevant systems, binding assays with the amino groups of the six lysine residues on lysozyme were conducted and analyzed using ESI-Fourier transform ion cyclotron resonance (FTICR)-MS. The conjugate formation of compound **2-1** with lysozyme was compared to that of 2-FPBA and 2-APBA (Figure 2–13, left) after stirring for 30 min in 50 mM ammonium acetate buffer at room

temperature. Although all three compounds show up to six modifications of the lysozyme peak, 2-FPBA shows the least amount of free lysozyme (mass peak of 1789), indicating superior binding, whereas compound **2-1** shows the highest level of free lysozyme. It should be noted that the decreased signal strength seen with increasing binding may be due to decreased ionization of the lysozyme conjugate as more lysine residues are bound. To test the reversibility of the boronic acid/lysozyme conjugates, fructose was added as a biomolecular competitor and the change in the free lysozyme peak was monitored (Figure 2–13, right). With the addition of fructose, 2-FPBA showed almost complete reversibility with a much stronger free lysozyme peak with most other peaks in the spectra belonging to fructose bound lysozyme. Compound **2-1II**, which opens to the *ortho*-formyl structure **2-1I** to bind amines, shows no reversibility whatsoever, as shown by no change in the spectrum after fructose addition. Here, it is hypothesized, that once **2-1I** forms the initial imine structure, the hydroxy arm quickly closes, to form a hemiaminal, which is evidently more stable to competing biomolecules such as fructose (cf. Figure 2–10). 2-APBA also showed no change in the spectra after the addition of fructose, so it is also considered to be irreversible and forms a considerably more stable iminoboronate structure than 2-FPBA. Despite their good binding, 2-FPBA and 2-APBA do have minor drawbacks. 2-FPBA was clearly seen to be reversible, and, moreover, an aldehyde functionality may not be considered bioorthogonal as it is highly reactive and would react with other molecules in biological media. 2-APBA displays tight binding and is considered to be irreversible, however, it was observed that 2-APBA has poorer solubility in water than 2-FPBA and compound **2-1**. In this regard compound **2-1** is thought to be favored over both 2-FPBA and 2-APBA.

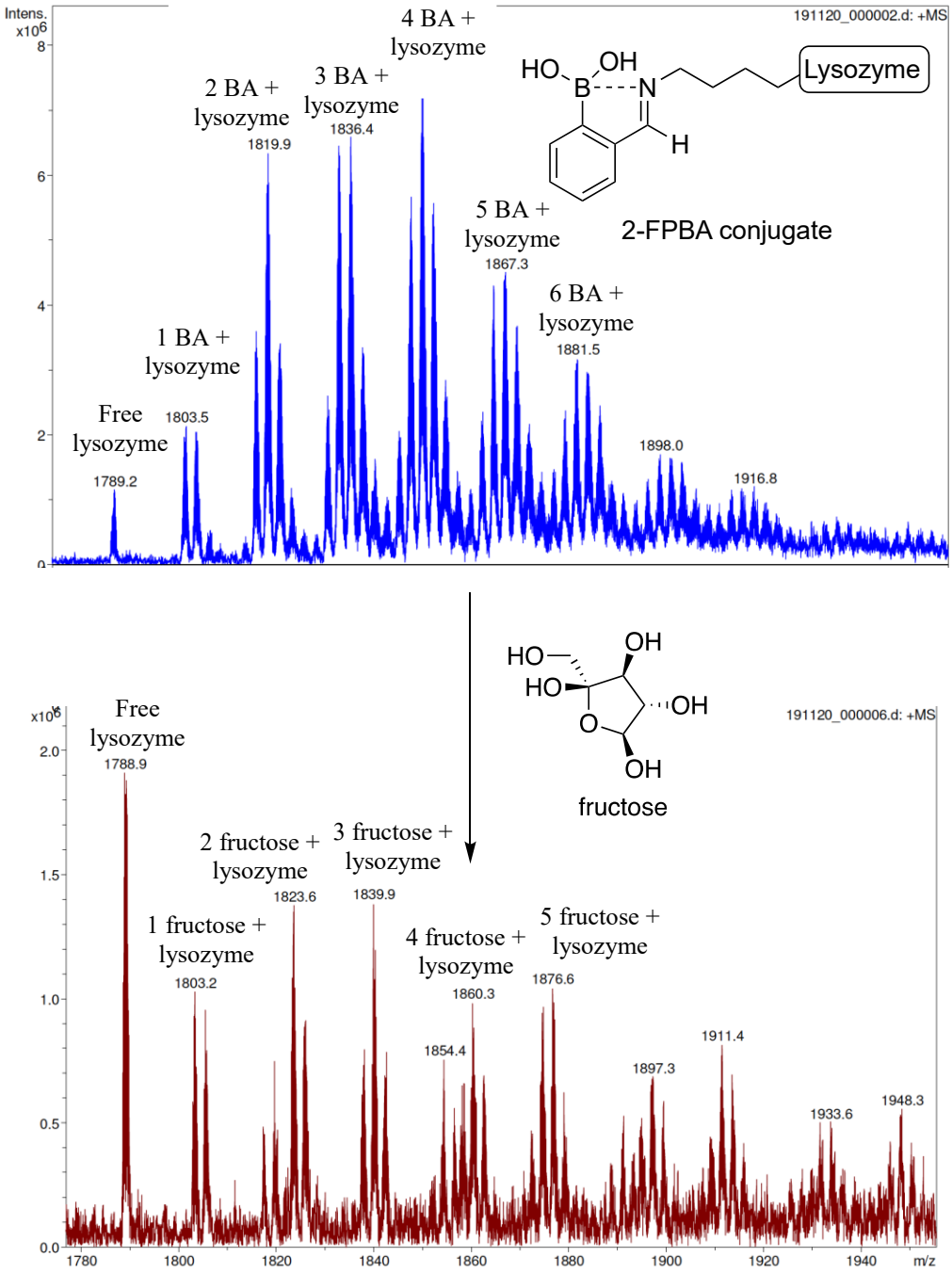

Figure 2–14. ESI-FTICR-MS lysozyme binding assays with 2-FPBA (top) and competition studies with fructose (bottom). BA = Boronic acid used in assay.

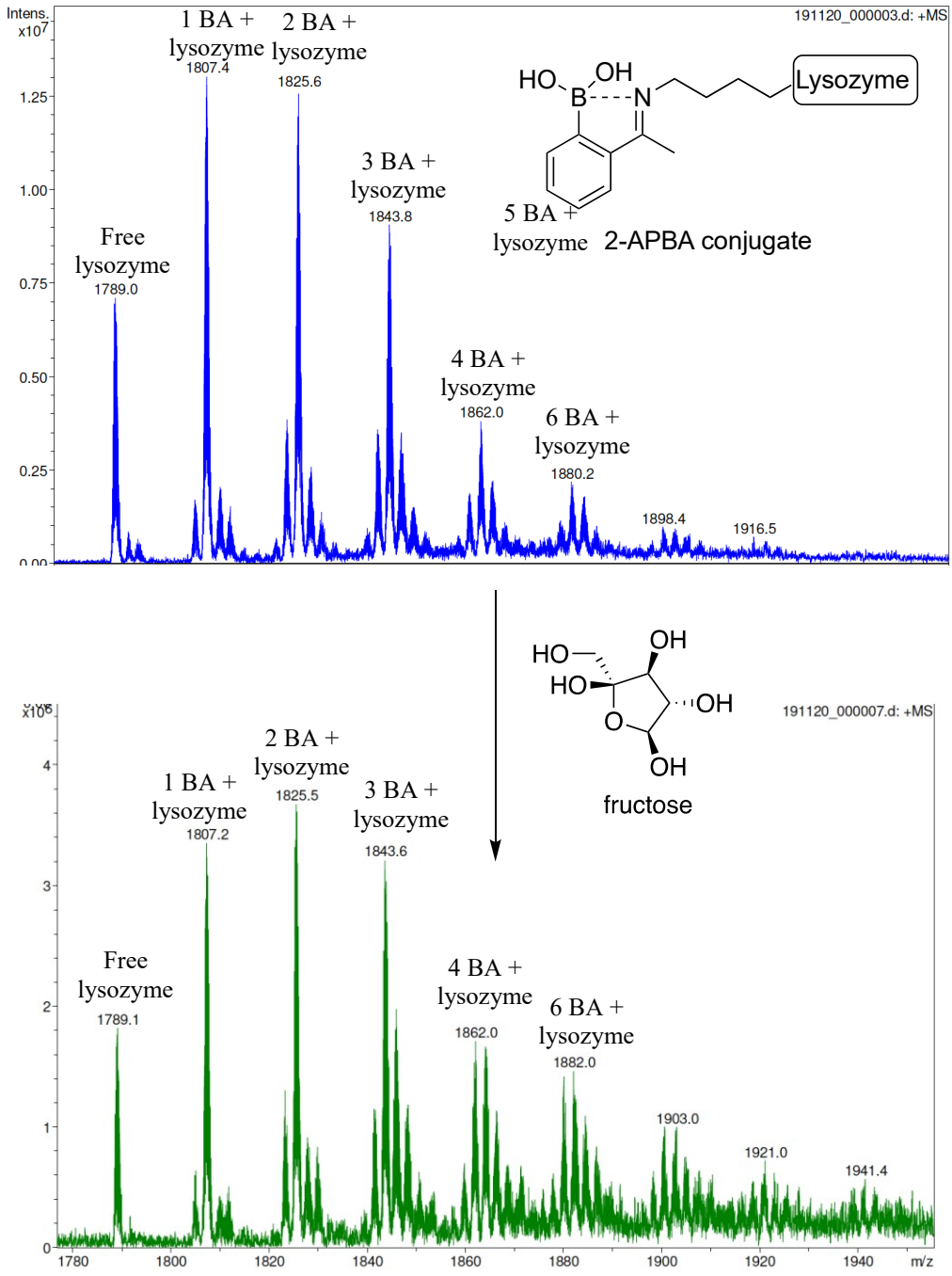

Figure 2–15. ESI-FTICR-MS lysozyme binding assays with 2-APBA (top) and competition studies with fructose (bottom). BA = Boronic acid used in assay.

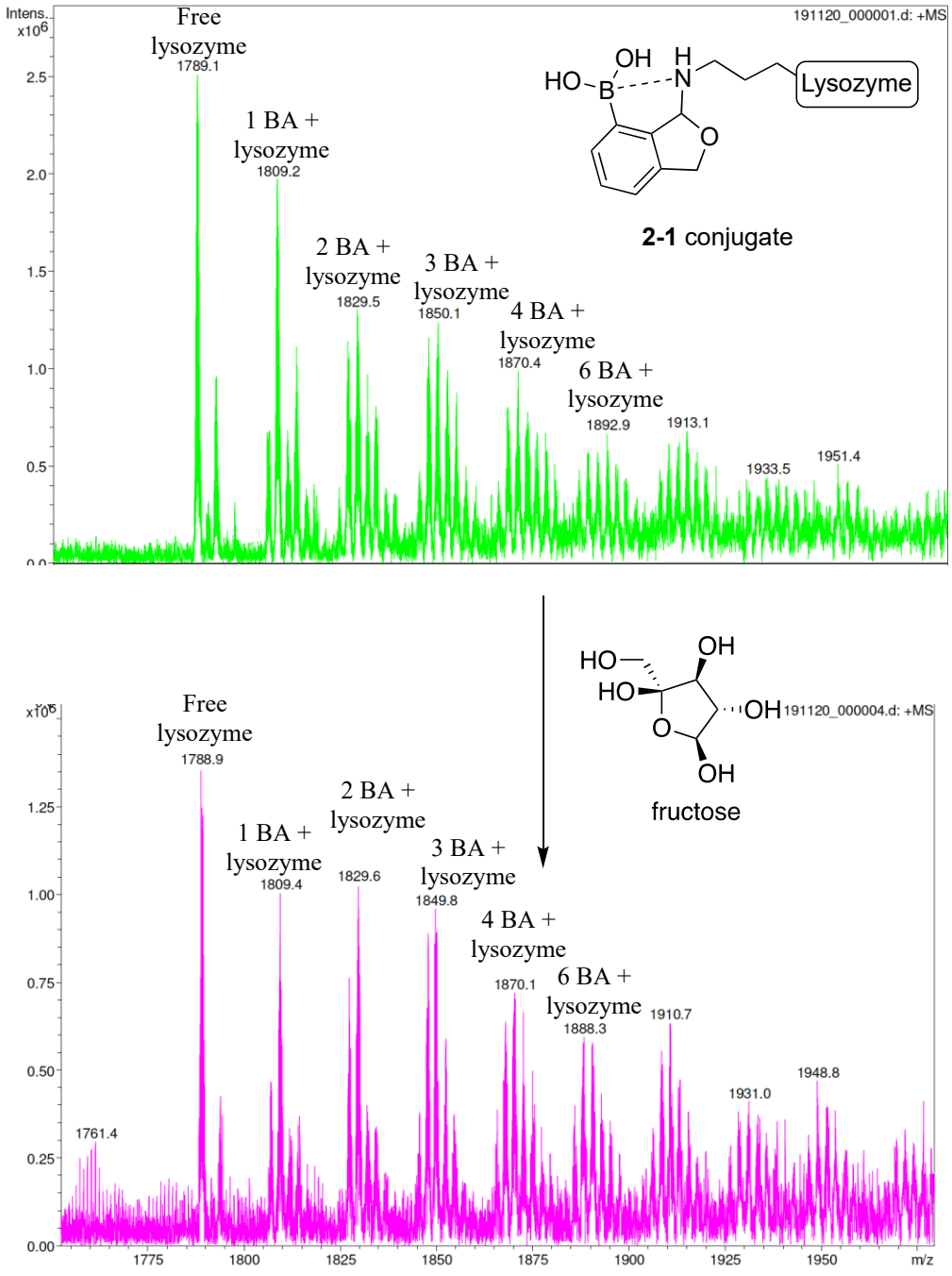

Figure 2–16. ESI-FTICR-MS lysozyme binding assays with **2-1** (top) and competition studies with fructose (bottom). BA = Boronic acid used in assay.

2.3.3.3 Amino Acid Conjugation

As mentioned in Section 1.2.2, 2-FPBA and 2-APBA are also known to bind to *N*-terminal cysteines and form a thiazolidino boronate (TzB) structure (Figure 2–17a).[15,16] TzB structures, unlike iminoboronates, are stable to competing biomolecules present in solution, although they are also known to be reversible in slightly acidic or basic solutions. It was proposed that compound **2-1** would form a similar type of structure, but instead have enhanced stability due to the additional adjacent hydroxy arm that would form an additional ring on the conjugate structure. Therefore, binding with compound **2-1** could potentially form a fused 3-membered ring conjugate that would be more stable and irreversible (Figure 2–17b).

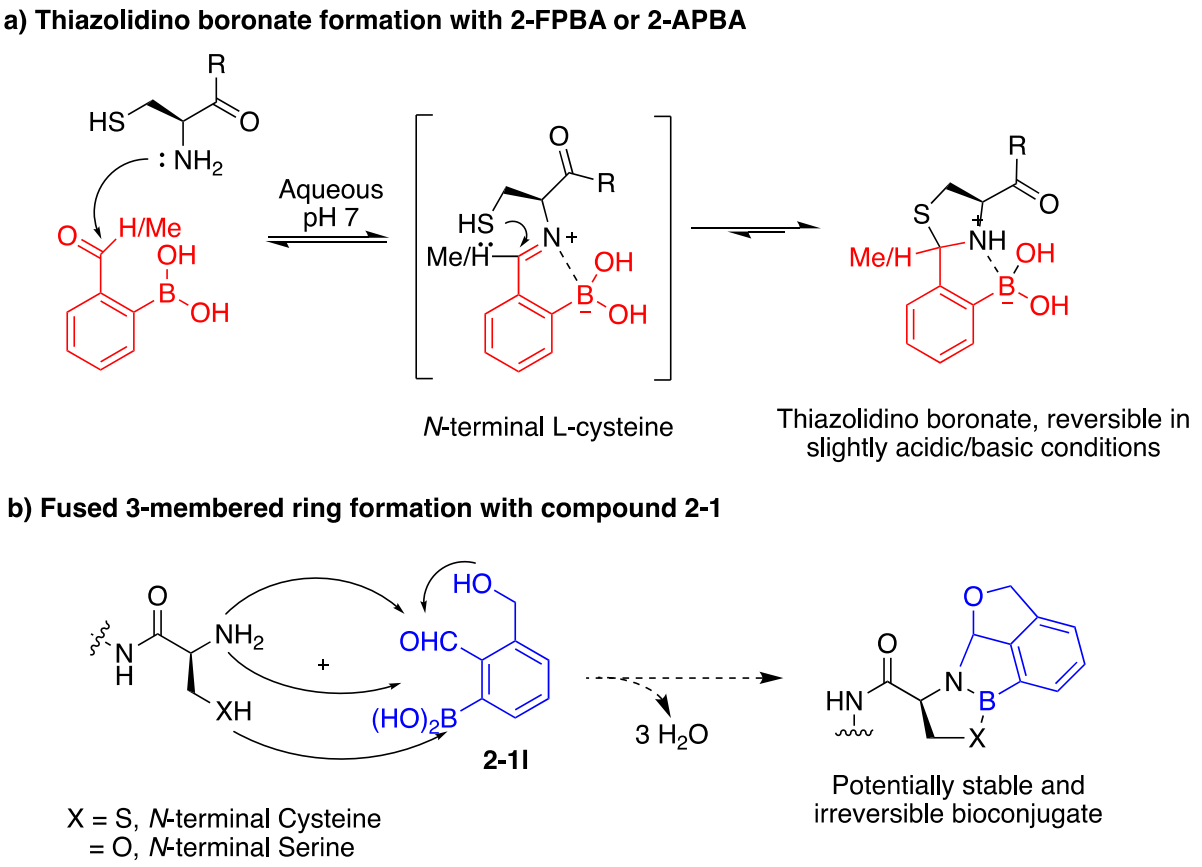

Figure 2–17. *N*-Terminal amino acid conjugation with 2-FPBA, 2-APBA and compound **2-1**.

To evaluate cysteine and serine conjugation, compound **2-1** was dissolved in ammonium acetate buffered aqueous solution with one equivalent of each amino acid and left to stir at room temperature. In the case of cysteine, a white solid material crashed out of solution within 5 minutes. This material was collected by filtration and analyzed by NMR, the results of which are shown in Figure 2–18.

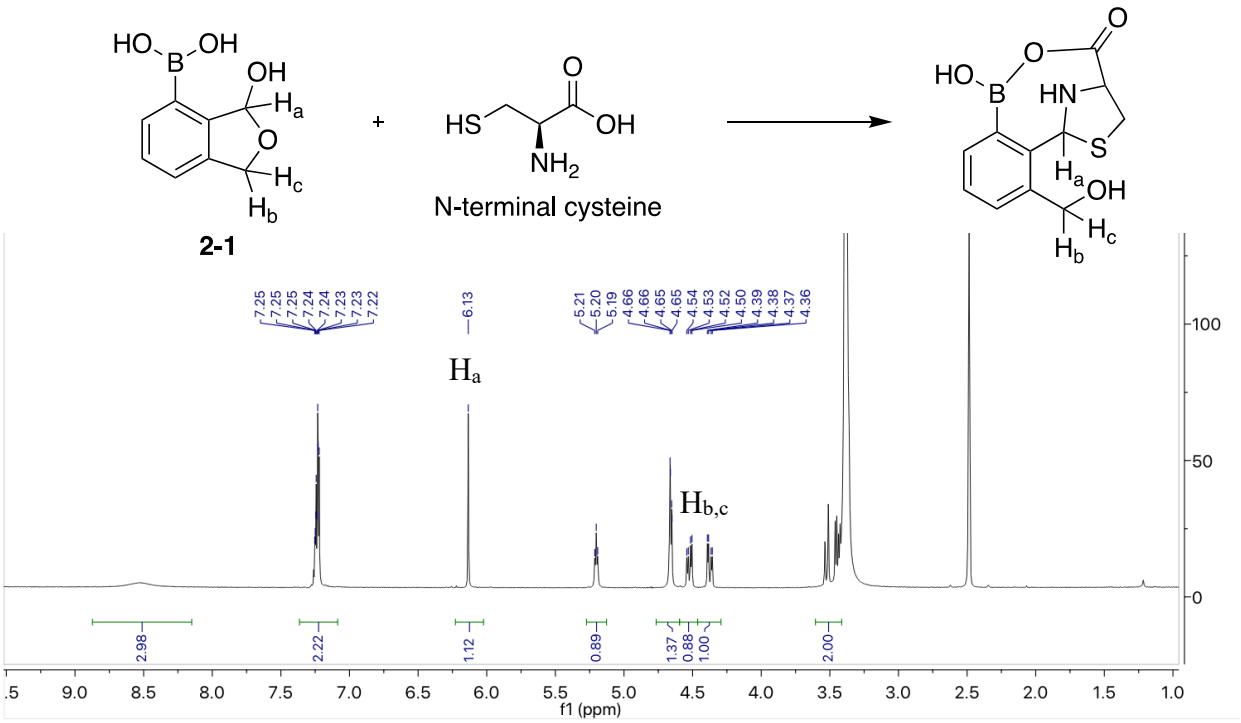

Figure 2–18. NMR spectrum of the conjugate of cysteine and compound **2-1** in acetone-d_6.

There are a few notable details in the ^{1}H NMR spectrum in Figure 2–18. Firstly, the hemiacetal proton H_a has once again shifted upfield from 6.5 to about 6.3 ppm, similar to amine binding in Section 2.3.3.1. This is less of a shift than when compound **2-1** formed a conjugate with amines, but still a significant change. Secondly, the methylene protons H_c and H_d have shifted vastly from 5.0 ppm to 4.5 ppm. This large shift most likely indicates that the environment of the hydroxy arm has changed significantly, and these methylene protons have a closer chemical shift to those of compound **2-13**, where the hydroxy arm is still open, and the peak of which are seen at 4.75 ppm

(cf. Scheme 2–4). This information strongly suggests that the conjugate of *N*-terminal cysteine with compound **2-1** is a structure with an open hydroxy methylene arm. Attempts at conjugate formation between compound **2-1** and serine was met with minimal success (Figure 2–19). After stirring at room temperature for 24 hours, mostly starting material was observed with very minor other peaks present, circled in red, that indicate there may be some conjugation occurring. It is believed that the hydroxy group in serine is not as nucleophilic, and hence less reactive, than the thiol group in cysteine.

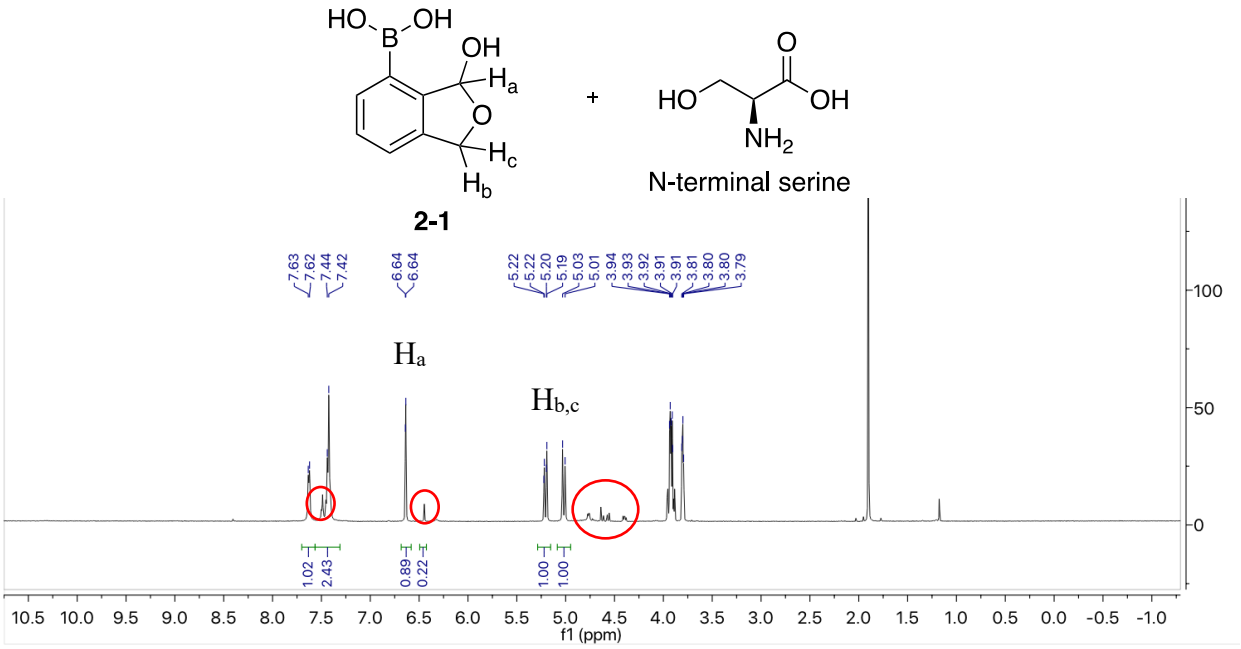

Figure 2–19. NMR of *N*-terminal serine conjugation attempts with compound **2-1** in acetone-d_6.

To mimic a terminal peptide, L-cysteine ethyl ester was reacted with **2-1** under the same conditions. Surprisingly, a white solid material crashed out of solution within 5 minutes again. The proton signals from the ethyl group of protected L-cysteine are not found in the NMR spectrum of the resulting white solid. Therefore, during the reaction, the ethyl ester was cleaved, and an

ethoxide group was lost. The high-resolution mass spectrum of the white solid material confirmed the loss of ethoxide, to once again give the open methylene hydroxy arm structure (Figure 2-20).

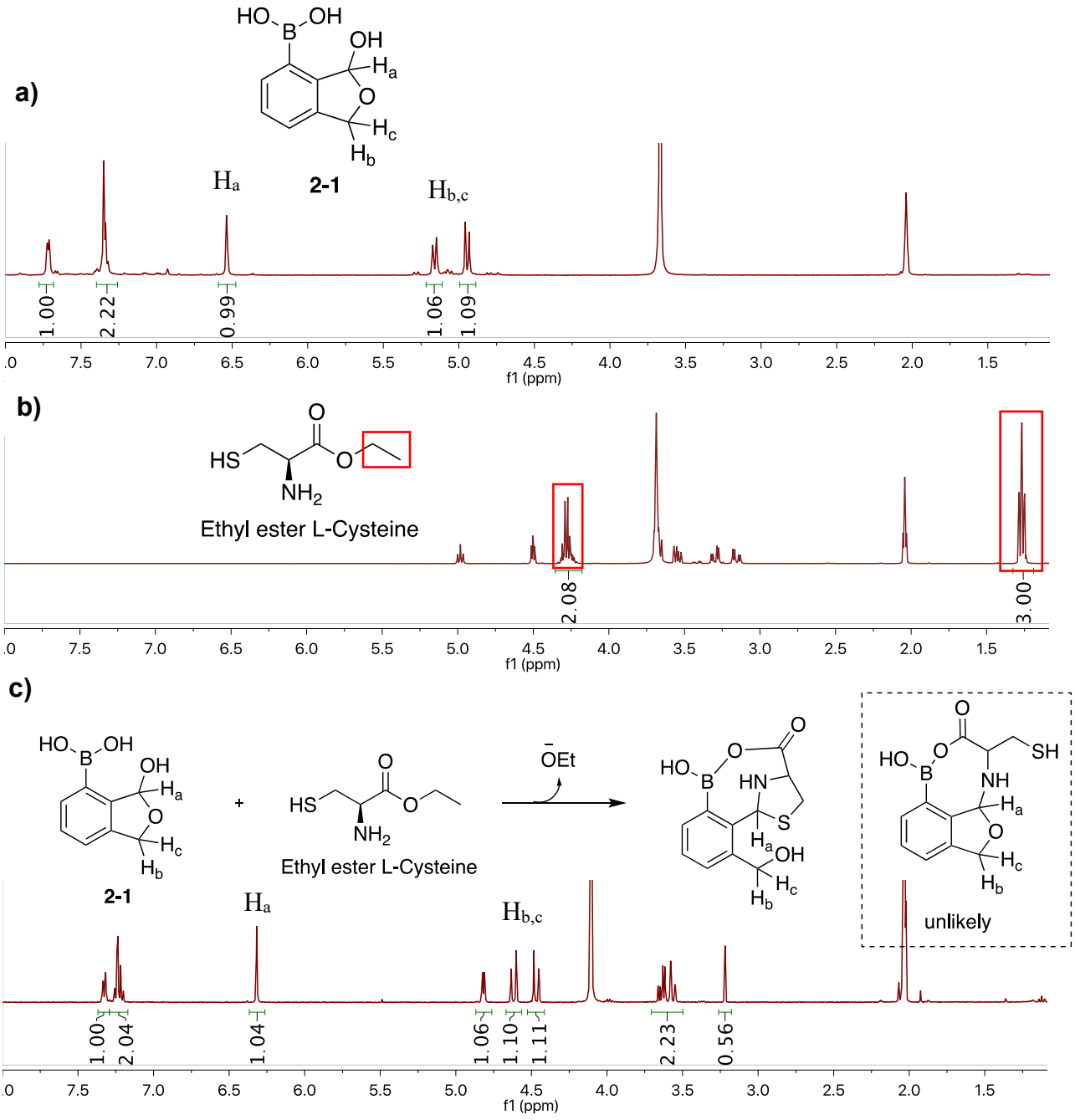

Figure 2–20. NMR of Ethyl ester cysteine conjugate with compound **2-1** in acetone-d_6.

2.3.4. Amidation Catalyst Studies

Amide bonds are found abundantly in peptides, proteins and natural products, as well as an estimated 25% of all pharmaceuticals.[17] There have been elegant stoichiometric reagents developed for the coupling of amines and carboxylic acids to form amide bonds, including carbodiimides, phosphonium salts and uronium salts.[18,19] Although these methods are efficient, many of these reagents are toxic and give wasteful by-products. As a means to be more atomically efficient, Yamamoto and coworkers first introduced catalyzed amidation reactions using 3,4,5-trifluorophenylboronic acid, followed by others using (diisopropyl-aminomethyl)phenylboronic acid and boric acid; however these reactions tend to need high temperatures to occur.[20–22] In 2012, Hall and coworkers introduced a new boronic acid catalyst, 5-methoxy-2-iodophenylboronic acid (MIBA), which could perform amidation reactions at room temperature when using activated molecular sieves.[23] All the boronic acid catalysts mentioned so far have one thing in common: they activate the carboxylic acid in the reaction only. From the amine conjugation mentioned in Section 2.3.3.1, it was hypothesized that compound **2-1** could bring the amine and carboxylic acid group in close proximity for a dehydrative amidation reaction to occur (Scheme 2-5).

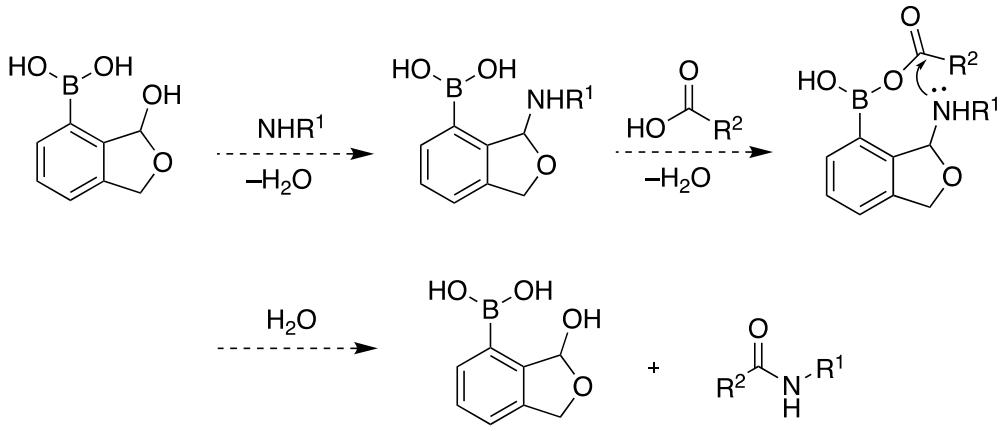

Scheme 2-5. Mechanism of compound **2-1** for amidation reaction.

Following the procedure outlined for the MIBA catalyst using benzylamine and phenylacetic acid[23], the amidation in Scheme 2-5 was attempted in many different conditions and monitored for product by LC-MS (Table 2–1).

Table 2–1. Amidation attempts with various conditions using compound **2-1** as a catalyst.

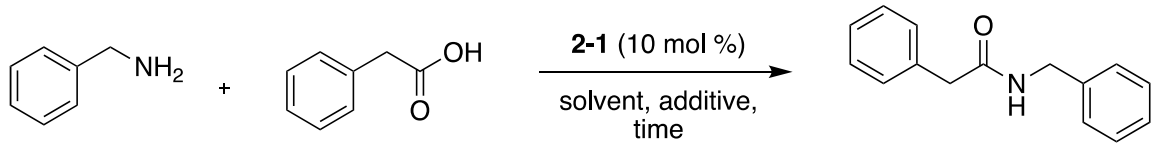

Entry	Solvent	Time	Additive	Product
1	DCM	1 h	Activated molecular sieves	None
2	DCM	18 h	Activated molecular sieves	None
3	CPME	18 h	Activated molecular sieves	None
4	CPME	18 h	None	None
5	Me-THF	18 h	Activated molecular sieves	Trace
6	Me-THF	18 h	None	None

The optimal solvent for MIBA amidation was DCM, and although compound **2-1** does not dissolve in DCM, the amidation reaction was still attempted but it failed to give the product. The next best solvents for MIBA were CPME and Me-THF in which compound **2-1** does dissolve easily. Although entry 6 showed some according to LC-MS (Figure 2–21), no product could be isolated from the reaction.

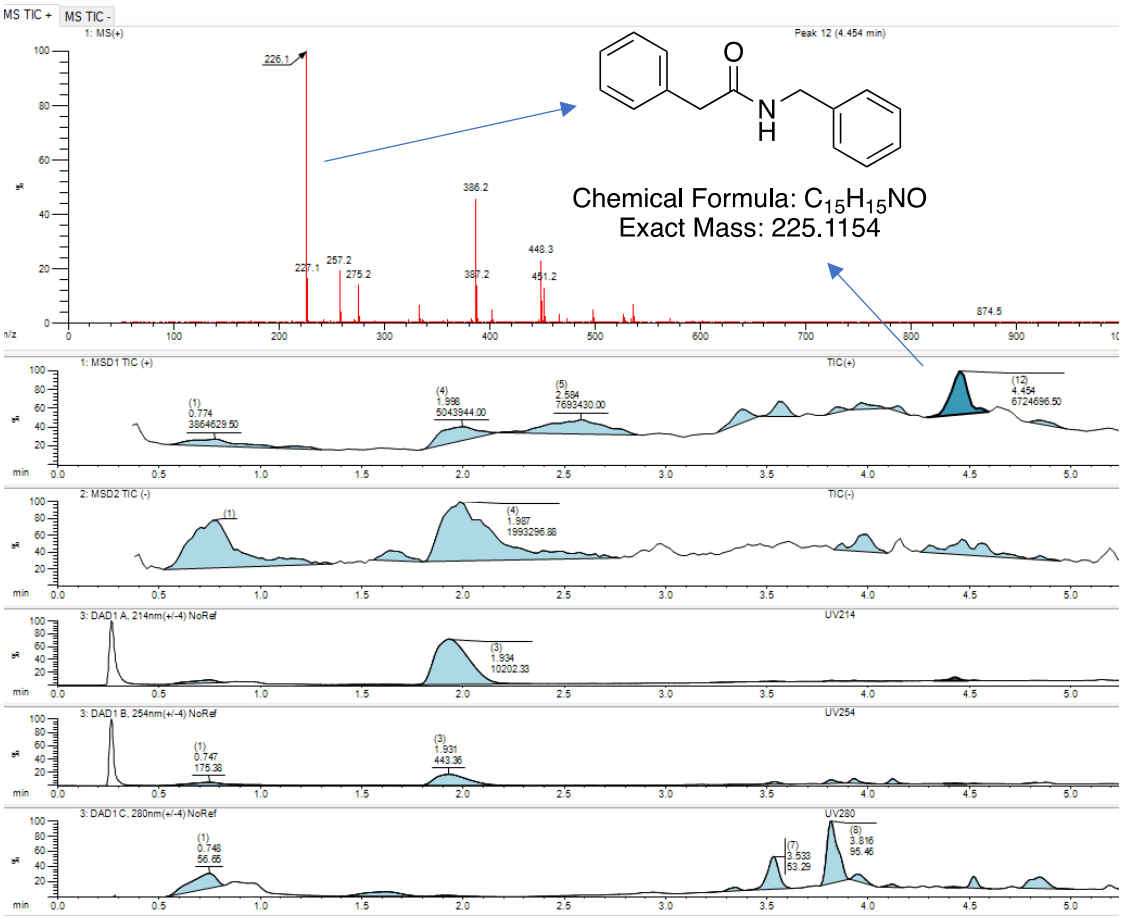

Figure 2-21. LC-MS result of amidation catalyzed by compound **2-1** from entry 6 in Table 2–1.

2.4 Conclusions

Chapter 2 describes the efforts made in the development and synthesis of a novel, water soluble, "frustrated benzoxaborole" compound **2-1** and explored its applications in bioconjugation. An efficient and high yielding seven step synthesis was optimized and exploited the high polarity of the new compound with simple purification without the need for chromatography. Through several NMR experiments, compound **2-1** was found to exist in the open ortho hemiacetal arylboronic acid structure **2-1II** as the major form. Compound **2-1** was found to have a similar pKa to that of benzoxaboroles of 7.5, which is significantly lower than traditional boronic acids. The relatively low pKa of compound **2-1** is proposed to be the result of stabilization of the

trihydroxyborate conjugate base by the hydrogen-bonding effect of the ortho hydroxyalkyl unit. This low pKa allows full solubility in water, which increases the potential which for the use of compound **2-1** in aqueous biological systems. In this regard, compound **2-1** showed extensive conjugation to form hemiaminal structures with amino groups, including highly effective binding with lysozyme. Additionally, binding with cysteines was also explored which surprisingly induces formation of the open structure containing a free hydroxy arm, as the amino and thiol group bind preferentially on the formyl group. As more novel boron containing drugs and bioconjugate compound are explored, a first of its kind permanently open "frustrated benzoxaborole" compound **2-1** with its unique properties can be further explored to meet ever growing needs and applications.

2.5 Experimental

2.5.1 General Information

Unless otherwise indicated, all reactions were performed under a nitrogen atmosphere using glassware that was washed thoroughly prior to use. All reagents were purchased from Sigma-Aldrich, Combi-Blocks or Alfa Aesar and used as received except diisopropylamine and benzylamine, which were distilled over calcium hydride prior to use. DMF and THF were used directly from an MBraun Solvent Purification System. Thin layer chromatography (TLC) was performed on Merck Silica Gel 60 F254 plates, and visualized with UV light and *p*-anisaldehyde stain. Flash chromatography was performed on ultra-pure silica gel 230-400 mesh. Nuclear magnetic resonance (NMR) spectra were recorded on Agilent/Varian INOVA-400 and INOVA-500 MHz instruments. The residual solvent protons (^{1}H) of $CDCl_3$ (7.26 ppm), Acetone-d_6 (2.05 ppm), DMSO-d_6 (2.50 ppm), and D_2O (4.79 ppm) were used as internal standards, and the carbons signal (^{13}C) of $CDCl_3$ (77.06 ppm), DMSO-d_6 (39.51) and acetone-d_6 (29.84 and 206.26 ppm) were

used as an internal standard. MestReNova software was used to analyze all of the NMR data. The following abbreviations are used in reporting NMR data: s, singlet; d, doublet; t, triplet; app t, apparent triplet; q, quartet; dd, doublet of doublets; ddd, doublet of doublet of doublets; dddd, doublet of doublet of doublet of doublets; dhept, doublet of heptlet; td, triplet of doublet; m, multiplet; comp m, complex multiplet. In ^{13}C NMR spectroscopy, the quaternary carbon bound to the boron atom is often missing due to the quadrupolar relaxation of boron. This effect was observed in each boronic acid or boronate ester compound. Infrared spectra (performed on a Nicolet Magna-IR 750 instrument equipped with a Nic-Plan microscope) were recorded by the University of Alberta Analytical and Instrumentation Laboratory. High-resolution mass spectra were recorded by the University of Alberta mass spectrometry services laboratory using either electron impact (EI) or electrospray ionization (ESI) techniques. High-resolution mass spectra (HRMS) using electrospray ionization (ESI), and LC-MS mass spectra were recorded by the University of Alberta Mass Spectrometry Services Laboratory. ESI-FTICR-MS was performed on Bruker Daltonics 9.4T Apex-Qe FTICR MS with Apollo II Dual source. Positive ion electrospray was used and the instrument was tuned to maximize sensitivity over the *m/z* range 900 to 2500. The instrument was calibrated with Agilent low concentration tuning mix.

2.5.2 Chemical Synthesis and Analytical Data

Synthesis of compound **2-8** (Scheme 2–1)

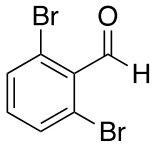

2-3

2,6-dibromobenzaldehyde (**2-3**): To a flame-dried 250 mL round bottom flask under nitrogen was added dry THF (50.0 mL) and diisopropylamine (1.30 mL, 9.28 mmol) and cooled to – 78 °C. To the solution was added *n*-BuLi (3.80 mL, 9.50 mmol) dropwise and the reaction was stirred for 15 min. 1,3-dibromobenzene **2–2** (0.96 mL, 7.94 mmol) was added dropwise at a rate of ~1 drop per second and the solution was allowed to stir for 30 min before DMF (1.20 mL, 15.5 mmol) was added. The reaction was allowed to warm to room temperature and stopped by addition of 2 M H_2SO_4 (10 mL), diluted with EtOAc (20 mL) and the layers separated. The aqueous layer was extracted with EtOAc (2 × 10 mL) and the combined organic extracts were washed with brine, dried over Na_2SO_4, filtered and concentrated *in vacuo* to afford the title compound as a pale-yellow solid (1.90 g, 91%) without any further purification. All spectral data matched the literature.[6]

^{1}H NMR (498 MHz, $CDCl_3$) δ 10.26 (s, 1H), 7.64 (d, J = 8.0 Hz, 2H), 7.22 (t, J = 8.0 Hz, 1H).

^{13}C NMR (126 MHz, $CDCl_3$) δ 191.3, 134.1, 133.8, 133.1, 125.0.

IR (cast film, cm^{-1}): 3386, 3360, 3139, 3084, 2889, 2774, 1701, 1661, 1571, 1551, 1429, 1400, 1270, 1204, 1184, 1070, 1059.

HRMS (EI) for $C_7H_4O^{81}Br_2$: *calcd.*: 265.8588; *found*: 265.8585.

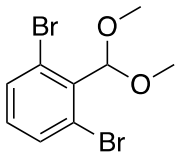

2-4

1,3-dibromo-2-(dimethoxymethyl)benzene (**2-4**): To a 250 mL round bottom flask was added **2-3** (1.90 g, 7.20 mmol), *p*TSA•H_2O (164 mg, 0.864 mmol) and trimethyl orthoformate (4.05 mL, 36.9 mmol) and MeOH (60 mL). The reaction was stirred at room temperature for 18 h under nitrogen then stopped by addition of $NaHCO_3$ and diluted with water. The layers were separated and the aqueous layer was extracted with EtOAc (2 × 10 mL) and the combined organic extracts washed with brine, dried over Na_2SO_4, filtered and concentrated *in vacuo* to afford the title compound as a yellow solid (1.93 g, 86%) without any further purification. All spectral data matched the literature.[6]

^{1}H NMR (498 MHz, $CDCl_3$) δ 7.56 (d, *J* = 8.0 Hz, 2H), 7.01 (t, *J* = 8.0 Hz, 1H), 5.83 (s, 1H), 3.48 (s, 6H).

^{13}C NMR (126 MHz, $CDCl_3$) δ 135.2, 133.7, 130.8, 124.1, 107.0, 56.0.

IR (cast film, cm^{-1}): 3073, 3001, 2933, 2903, 2834, 1570, 1553, 1444, 1380, 1363, 1215, 1207, 1188, 1148, 1105, 1075.

HRMS (EI) for $C_9H_{10}O_2{}^{79}Br^{81}Br$: *calcd*.: 309.9027; *found*: 309.9028.

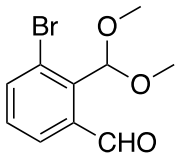

2-5

3-bromo-2-(dimethoxymethyl)benzaldehyde (**2-5**): To a flame-dried 50 mL round bottom flask under nitrogen was added **2-4** (1.85 g, 5.97 mmol) and dissolved in dry THF (10 mL) and cooled to – 78 °C before *n*-BuLi (2.39 mL, 5.97 mmol) was added drop-wise and the reaction was stirred for 15 min. To the reaction was added DMF (600 μL, 7.76 mmol) and stirred for 30 min. The reaction was allowed to warm to room temperature and stopped with addition of 1 M HCl (3 mL), diluted with EtOAc (20 mL) and the layers separated. The aqueous layer was extracted with EtOAc (3 × 10 mL) and the combined organic extracts washed with brine, dried over Na_2SO_4, filtered and concentrated *in vacuo*. The crude material was purified by flash chromatography (5:1 Hexanes:EtOAc) to afford the title compound as a yellow crystalline solid (1.42 g, 92%). All spectral data matched the literature.[6]

^{1}H NMR (498 MHz, $CDCl_3$) δ 10.69 (d, *J* = 0.9 Hz, 1H), 7.89 (dd, *J* = 7.7, 1.3 Hz, 1H), 7.73 (dd, *J* = 8.0, 1.3 Hz, 1H), 7.29 (td, *J* = 7.8, 0.9 Hz, 1H), 5.86 (s, 1H), 3.51 (s, 6H).

^{13}C NMR (126 MHz, $CDCl_3$) δ 192.6, 139.4, 137.8, 137.2, 130.4, 128.0, 123.5, 107.1, 56.3.

IR (cast film, cm^{-1}): 3072, 2998, 2934, 2912, 2832, 1692, 1586, 1566, 1447, 1376, 1241, 1211, 1121, 1104, 1065.

HRMS (EI) for $C_{10}H_{11}O_3{}^{81}Br$: *calcd*.: 259.9871; *found*: 259.9859.

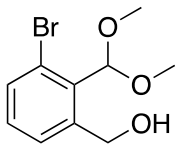

2-6

(3-bromo-2-(dimethoxymethyl)phenyl)methanol (2-6): To a 50 mL round bottom flask under nitrogen was added **2-5** (1.36 g, 5.24 mmol) and dissolved in MeOH (8 mL) and cooled to 0 °C before $NaBH_4$ (297 mg, 7.86 mmol) was added portion-wise and the reaction stirred for 1 h. The reaction was stopped with addition of 5 mL water and about half of the MeOH was removed *in vacuo*. The solution was diluted with EtOAc, the phases separated and the aqueous phase extracted with EtOAc (3 × 15 mL). The combined organic extracts were washed with brine, dried over Na_2SO_4, filtered and concentrated *in vacuo* to afford the title compound as a yellow oil (1.12 g, 87%) without any further purification.

^{1}H NMR (498 MHz, $CDCl_3$) δ 7.50 (dd, *J* = 8.0, 1.3 Hz, 1H), 7.36 (dd, *J* = 7.6, 1.3 Hz, 1H), 7.23 – 7.12 (m, 1H), 5.89 (s, 1H), 4.81 (d, *J* = 5.5 Hz, 2H), 3.51 (s, 6H).

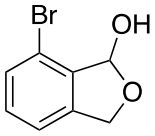

2-8

7-bromo-1,3-dihydroisobenzofuran-1-ol (2-8): To a 25 mL round bottom flask was added **2-6** (200 mg, 0.766 mmol) and dissolved in THF (5 mL). To this solution was added 1 M HCl (0.383 mL, 0.383 mmol) and the reaction stirred at 60 °C for 1 h before being brought down to room temperature. The reaction was stopped with addition of a saturated aqueous solution of $NaHCO_3$ and phases separated. The aqueous phase was extracted with EtOAc (3 × 15 mL). The combined organic extracts were washed with brine, dried over Na_2SO_4, filtered and concentrated *in vacuo*.

The crude solid material was recrystalized in a solution of 4:1 Hexanes: EtOAc, filtered and dried to afford the title compound as a yellow solid (96.0 mg, 59%).

^{1}H NMR (498 MHz, $CDCl_3$) δ 7.47 (dq, *J* = 7.6, 0.9 Hz, 1H), 7.28 – 7.20 (m, 3H), 6.49 (dd, *J* = 6.9, 2.1 Hz, 1H), 5.39 – 5.31 (m, 1H), 5.06 (dt, *J* = 13.0, 0.8 Hz, 1H).

Synthesis of compounds **2-10** and **2-11** (Scheme 2–3)

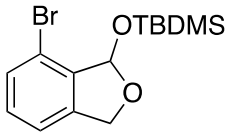

2-10

((7-bromo-1,3-dihydroisobenzofuran-1-yl)oxy)(tert-butyl)dimethylsilane (**2-10**): To a 25 mL round bottom flask was added **2-8** (33.2 mg, 0.154 mmol), 1H-imidazole (26.2 mg, 0.385 mmol), and TBDMSCl (27.9 mg, 0.185 mmol) to 5 mL of dry DMF and the reaction stirred overnight at room temperature. The solution was diluted with EtOAc and H_2O and the phases separated. The aqueous phase was extracted with EtOAc (3 × 10 mL) and the combined organic extracts were washed with brine, dried over Na_2SO_4, filtered and concentrated *in vacuo*. The crude oil was purified by flash chromatography (4:1 DCM:EtOAc) to afford the title compound as a yellow oil (31.0 mg, 61%).

^{1}H NMR (498 MHz, $CDCl_3$) δ 7.45 – 7.39 (m, 1H), 7.23 – 7.15 (m, 2H), 6.45 (d, *J* = 1.9 Hz, 1H), 5.31 – 5.20 (m, 1H), 4.99 (dt, *J* = 12.8, 1.9, 0.7 Hz, 1H), 0.94 (s, 9H), 0.22 (s, 3H), 0.19 (s, 3H).

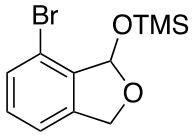

2-11

((7-bromo-1,3-dihydroisobenzofuran-1-yl)oxy)trimethylsilane (**2-11**): To a flame-dried 25 mL round bottom flask with 5 mL dry DCM was dissolved **2-8** (60.0 mg, 0.279 mmol). To the solution was added via syringe TMSCl (42.5 μL, 0.335 mmol) and pyridine (56.4 μL, 0.698 mmol) and the reaction stirred at room temp for 2 h. The reaction was washed with H_2O (5 × 10 mL) and the organic phase was dried over Na_2SO_4, filtered and concentrated *in vacuo*. The crude oil was purified by flash chromatography (5:1 DCM:EtOAc) to afford the title compound as a yellow oil (58.0 mg, 72%).

^{1}H NMR (498 MHz, $CDCl_3$) δ 7.45 – 7.39 (m, 1H), 7.23 – 7.15 (m, 2H), 6.45 (d, *J* = 1.9 Hz, 1H), 5.31 – 5.20 (m, 1H), 4.99 (dt, *J* = 12.8, 0.7 Hz, 1H), 0.20 (s, 3H).

Synthesis of compound **2-15** (Scheme 2–4)

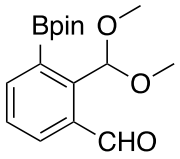

2-12

2-(dimethoxymethyl)-3-(4,4,5,5-tetramethyl-1,3,2-dioxaborolan-2-yl)benzaldehyde (**2-12**): To a flame-dried 250 mL round bottom flask under argon was added **2-5** (1.58 g, 6.11 mmol), B_2pin_2 (3.10 g, 12.2 mmol), KOAc (1.80 g, 18.3 mmol) and Pd(dppf)Cl_2•DCM (500 mg, 0.611 mmol) and freshly distilled dioxane (60 mL). The solution was degassed with argon for 10 mins then heated to 80 °C and stirred for 18 h. The reaction was brought to room temperature and filtered through Celite and the filtrate collected and washed with a saturated aqueous solution of

ammonium chloride. The organic extracts were concentrated in vacuo and purified by flash chromatography (40:1 DCM:EtOAc) to afford the title compound as a yellow solid (1.00 g, 53%).

^{1}H NMR (498 MHz, $CDCl_3$) δ 10.64 (s, 1H), 7.98 (dd, *J* = 7.7, 1.5 Hz, 1H), 7.85 (dd, *J* = 7.4, 1.5 Hz, 1H), 7.44 (td, *J* = 7.6, 0.8 Hz, 1H), 6.12 (s, 1H), 3.43 (s, 6H), 1.38 (s, 12H). Excess B_2pin_2 seen at around 1.25 ppm in spectra.

^{13}C NMR (126 MHz, $CDCl_3$) δ 193.9, 145.5, 139.2, 135.0, 131.1, 128.3, 104.4, 84.3, 83.7, 55.3, 25.2, 25.1.

^{11}B NMR (160 MHz, $CDCl_3$) δ 30.7.

IR (cast film, cm^{-1}): 2979, 2932, 2832, 1688, 1578, 1473, 1380, 1373, 1350, 1127, 1069.

HRMS (EI) for $C_{16}H_{22}O_5{}^{11}B$ $(M + H)^+$: *calcd*.: 305.1560; *found*: 305.1561.

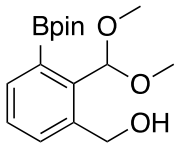

2-13

(2-(dimethoxymethyl)-3-(4,4,5,5-tetramethyl-1,3,2-dioxaborolan-2-yl)phenyl)methanol (**2-13**): To a 50 mL round bottom flask under nitrogen was added **2-12** (1.00 g, 3.86 mmol) and dissolved in MeOH (12 mL) and cooled to 0 °C before $NaBH_4$ (219 mg, 5.79 mmol) was added portion-wise and the reaction stirred for 1 h. The reaction was stopped with addition of 5 mL water and about half of the MeOH was removed *in vacuo*. The solution was diluted with EtOAc, the phases separated and the aqueous phase extracted with EtOAc (3 × 15 mL). The combined organic extracts were washed with brine, dried over Na_2SO_4, filtered and concentrated *in vacuo*. The crude material was purified by flash chromatography (3:1 Hexanes:EtOAc) to afford the title compound as colourless oil (857 mg, 84%).

^{1}H NMR (498 MHz, $CDCl_3$) δ 7.59 (dd, *J* = 7.4, 1.5 Hz, 1H), 7.42 (dd, *J* = 7.5, 1.5 Hz, 1H), 7.32 (t, *J* = 7.5 Hz, 1H), 5.96 (s, 1H), 4.75 (d, *J* = 6.7 Hz, 2H), 3.43 (s, 6H), 1.37 (s, 12H).

^{13}C NMR (126 MHz, $CDCl_3$) δ 140.9, 139.4, 133. 8, 133.0, 128.5, 105.1, 83.8, 64.2, 55.0, 25.1.

^{11}B NMR (160 MHz, $CDCl_3$) δ 30.7.

IR (cast film, cm^{-1}): 3450, 3063, 2933, 2832,1591, 1474, 1444, 1371, 1346, 1292, 1170, 1148, 1131.

HRMS (ESI-TOF): for $C_{16}H_{25}BO_5Na$ $(M + Na)^+$: *calcd*.: 331.1687; *found*: 331.1690.

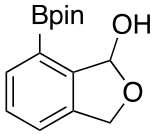

2-15

7-(4,4,5,5-tetramethyl-1,3,2-dioxaborolan-2-yl)-1,3-dihydroisobenzofuran-1-ol (**2-15**): To a 25 mL round bottom flask was added **2-13** (200 mg, 0.649 mmol) and dissolved in chloroform (4 mL) and cooled to 0 °C before 50% TFA in H_2O (1 mL) was added and the reaction stirred for 1 h. The reaction was stopped with addition of a saturated aqueous solution of $NaHCO_3$ and phases separated. The aqueous phase extracted with chloroform (3 × 15 mL). The combined organic extracts were washed with brine, dried over Na_2SO_4, filtered and concentrated *in vacuo* to afford the title compound as a yellow oil (142 mg, 84%) without any further purification.

^{1}H NMR (498 MHz, $CDCl_3$) δ 7.77 – 7.67 (m, 1H), 7.34 (q, *J* = 3.8, 3.2 Hz, 2H), 6.31 (d, *J* = 1.9 Hz, 1H), 5.19 (dd, *J* = 12.6, 1.9 Hz, 1H), 5.03 – 4.91 (m, 1H), 3.55 (s, 2H), 1.45 – 1.28 (m, 12H).

Synthesis of compound **2-1** (Scheme 2–5)

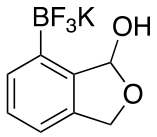

2-17

Potassium trifluoro(3-hydroxy-1,3-dihydroisobenzofuran-4-yl)borate (2-17): To a 25 mL round bottom flask was added **2-13** (423 mg, 1.37 mmol) and dissolved in MeOH (4.15 mL) followed by the addition of 4.5 M aqueous KHF_2 (1.67 mL, 7.54 mmol). The reaction was stirred for 10 min then immediately concentrated *in vacuo*. The solid white material was filtered through Celite using a solution of hot 8% MeOH in acetone and the filtrate collected and concentrated *in vacuo*. The crude material was dissolved in a minimal amount of hot acetone and recrystalized with diethyl ether to afford the title compound as a white solid (209 mg, 63%) without any further purification.

compound as colourless oil (857 mg, 84%).

^{1}H NMR (498 MHz, D_2O) δ 7.56 (d, *J* = 7.3 Hz, 1H), 7.44 (t, *J* = 7.4 Hz, 1H), 7.34 (d, *J* = 7.5 Hz, 1H), 6.65 (s, 1H), 5.27 (d, *J* = 12.5 Hz, 1H), 5.02 (d, *J* = 12.7 Hz, 1H).

^{13}C NMR (126 MHz, D_2O) δ 141.3, 138.6, 132.2, 132.2, 129.6, 121.1, 102.1, 71.8.

^{11}B NMR (160 MHz, D_2O) δ 3.32.

IR (cast film, cm^{-1}): 3524, 3053, 3017, 2947, 2903, 2859, 1434, 1413, 1244, 1231, 1069, 1044, 1010, 977.

HRMS (ESI-TOF): for $C_8H_7F_3BO_5$ $(M)^-$: *calcd*.: 203.0491; *found*: 203.0492.

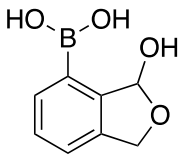

2-1ll

(3-hydroxy-1,3-dihydroisobenzofuran-4-yl)boronic acid (**2-1**): To a 10 mL round bottom flask was added **2-17** (80 mg, 0.331 mmol) and silica gel (20.0 mg, 0.331 mmol) and water (1.10 mL) and the reaction was stirred for 4 h at rt. The reaction was diluted with acetone (8 mL) and the silica gel filtered off and the filtrate concentrated *in vacuo*. The solid white material was dissolved in water and any intractable organic solids were filtered. The filtrate was collected and concentrated *in vacuo* to afford the title compound as a white solid (60.3 mg, 85%) without any further purification.

^{1}H NMR (498 MHz, Acetone-d_6) δ 7.77 (dd, *J* = 5.7, 2.8 Hz, 1H), 7.63 (s, 2H), 7.38 (d, *J* = 5.7 Hz, 2H), 6.70 (d, *J* = 7.1 Hz, 1H), 6.56 (dd, *J* = 7.1, 2.4 Hz, 1H), 5.18 (dd, *J* = 12.7, 2.4 Hz, 1H), 4.99 (d, *J* = 12.7 Hz, 1H).

^{13}C NMR (126 MHz, Acetone-d_6) δ 208.6, 144.6, 139.4, 134.8, 129.1, 123.8, 102.4, 72.5.

^{11}B NMR (160 MHz, Acetone-d_6) δ 28.93.

IR (cast film, cm^{-1}): 3389, 3295, 3206, 2936, 2885, 1603, 1449, 1382, 1361, 1080, 1038, 1009.

HRMS (ESI-TOF): for $C_{25}H_{33}N_6O_5$ $(M + H)^+$: *calcd*.: 179.0521; *found*: 179.0521.

2.5.3 NMR pKa Data

The pKa of benzoxaborole **2-18** and compound **2-1** was determined as follows[12]:

A phosphate buffer solution was prepared by dissolving 690 mg $NaHPO_3$ in 5 mL D_2O and ~30 mL H_2O in a 50 mL volumetric flask, then diluting to 50 mL total volume. In a second 25 mL volumetric, 0.5 mmol of the either **2-18** or **2-1** was dissolved in a minimum amount of deuterated

DMSO, then diluted to 25 mL total volume with the phosphate buffer solution. A volume of ~1.0 mL of the solution was added to 12 separate vials, and the pH of each was adjusted with NaOH (0.1% and 1%) and HCl (0.3%) so that a range of pH's between ~2 and ~11 was achieved. The various solutions were transferred to NMR tubes and their ^{11}B NMR spectra were recorded. The ^{11}B chemical shift was plotted against the pH and from this the pKa of the boron containing compound was determined. NMR lock was done on D_2O.

The results of the NMR ^{11}B shifts at various pH's are shown below:

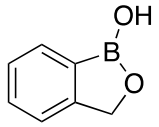

2-18

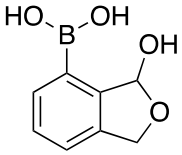

2-1II

*Benzoxaborole **2-18***	
pH	Boron Shift (ppm)
2.31	32.428
3.4	32.369
4.47	32.236
5.4	31.838
6.38	29.048
7.31	19.178
8.56	9.367
9.41	8.384
10.47	8.146
11.27	8.160

*Compound **2-1***	
pH	Boron Shift (ppm)
2.87	29.350
3.87	28.893
4.85	28.984
5.84	29.126
6.73	28.998
7.18	28.691
7.82	8.393
8.27	7.904
9.1	7.602
10.07	7.643
11.37	7.574

2.5.3 Amino Group, Amino Acid and Lysozyme Conjugation

Conjugation experiments of compound **2-1** with amino group containing small molecules were performed in deuterated acetone at a concentration of 0.05 mM in a 1:1 ratio. Each reaction was stirred at room temperature for 30 min then immediately submitted for analysis by ^{1}H NMR spectroscopy. A small aliquot of each reaction was also diluted in ACN and submitted for LC-MS and the data analyzed using mass hunter software.

Amino acid conjugation was performed in 50 mM ammonium acetate buffered D_2O at a concentration of 0.05 mM of both compound **2-1** and either cysteine, ethyl ester *O*-protected cysteine or serine. In the case of cysteine and ethyl ester *O*-protected cysteine conjugation, the solid white material that crashed out of solution was collected by filtration, dried in vacuo, then dissolved in deuterated acetone for ^{1}H NMR analysis. A small amount of material was also submitted to HRMS. Serine conjugation produced no such precipitate and was therefore allowed to stir for 24 hours before being analyzed by ^{1}H NMR.

Lysozyme conjugate studies were performed by mixing 10 μM lysozyme with 10 mM 2-FPBA, 2-APBA or compound **2-1** in 2 mL of 50 mM ammonium acetate buffer and allowed to stir at room temperature for 30 mins. A 100 μL aliquot of each reaction was diluted with 100 μL ACN and subjected to ESI-FTICR-MS. For fructose competition studies, 10 mM of fructose was added to the 2 mL conjugation mixtures, stirred for 5 mins, followed by another 100 μL aliquot removed and diluted with 100 μL ACN and analyzed by ESI-FTICR-MS.

2.6 References

(1) Akama, T.; Baker, S. J.; Zhang, Y.-K.; Hernandez, V.; Zhou, H.; Sanders, V.; Freund, Y.; Kimura, R.; Maples, K. R.; Plattner, J. J. *Bioorg. Med. Chem. Lett.* **2009**, *19* (8), 2129.

(2) Baker, S. J.; Zhang, Y.-K.; Akama, T.; Lau, A.; Zhou, H.; Hernandez, V.; Mao, W.; Alley, M. R. K.; Sanders, V.; Plattner, J. J. *J. Med. Chem.* **2006**, *49* (15), 4447.

(3) Nocentini, A.; Supuran, C. T.; Winum, J.-Y. *Expert Opin. Ther. Pat.* **2018**, *28* (6), 493.

(4) Adamczyk-Woźniak, A.; Cyrański, M. K.; Żubrowska, A.; Sporzyński, A. *Journal of Organometallic Chemistry* **2009**, *694* (22), 3533.

(5) Vshyvenko, S.; Clapson, M. L.; Suzuki, I.; Hall, D. G. *ACS Med. Chem. Lett.* **2016**, *7* (12), 1097.

(6) Luliński, S.; Serwatowski, J. *J. Organomet. Chem.* **2007**, *692* (14), 2924.

(7) Li, X.; Zhang, Y.-K.; Liu, Y.; Ding, C. Z.; Zhou, Y.; Li, Q.; Plattner, J. J.; Baker, S. J.; Zhang, S.; Kazmierski, W. M.; Wright, L. L.; Smith, G. K.; Grimes, R. M.; Crosby, R. M.; Creech, K. L.; Carballo, L. H.; Slater, M. J.; Jarvest, R. L.; Thommes, P.; Hubbard, J. A.; Convery, M. A.; Nassau, P. M.; McDowell, W.; Skarzynski, T. J.; Qian, X.; Fan, D.; Liao, L.; Ni, Z.-J.; Pennicott, L. E.; Zou, W.; Wright, J. *Bioorg. Med. Chem. Lett.* **2010**, *20* (19), 5695.

(8) Miyaura, N.; Suzuki, A. *Chem. Rev.* **1995**, *95* (7), 2457.

(9) Molander, G. A.; Trice, S. L. J.; Kennedy, S. M.; Dreher, S. D.; Tudge, M. T. *J. Am. Chem. Soc.* **2012**, *134* (28), 11667.

(10) Yuen, A. K. L.; Hutton, C. A. *Tetrahedron Lett.* **2005**, *46* (46), 7899.

(11) Molander, G. A.; Cavalcanti, L. N.; Canturk, B.; Pan, P.-S.; Kennedy, L. E. *J. Org. Chem.* **2009**, *74* (19), 7364.

(12) Ricardo, C. L.; Mo, X.; McCubbin, J. A.; Hall, D. G. *Chem. Eur. J.* **2015**, *21* (11), 4218.

(13) Zhu, L.; Shabbir, S. H.; Gray, M.; Lynch, V. M.; Sorey, S.; Anslyn, E. V. *J. Am. Chem. Soc.* **2006**, *128* (4), 1222.

(14) Cal, P. M. S. D.; Vicente, J. B.; Pires, E.; Coelho, A. V.; Veiros, L. F.; Cordeiro, C.; Gois, P. M. P. *J. Am. Chem. Soc.* **2012**, *134* (24), 10299.

(15) Faustino, H.; Silva, M. J. S. A.; Veiros, L. F.; Bernardes, G. J. L.; Gois, P. M. P. *Chem. Sci.* **2016**, *7* (8), 5052.

(16) Bandyopadhyay, A.; Cambray, S.; Gao, J. *Chem. Sci.* **2016**, *7* (7), 4589.
(17) Roughley, S. D.; Jordan, A. M. *J. Med. Chem.* **2011**, *54* (10), 3451.
(18) Valeur, E.; Bradley, M. *Chem. Soc. Rev.* **2009**, *38* (2), 606.
(19) Montalbetti, C. A. G. N.; Falque, V. *Tetrahedron* **2005**, *61* (46), 10827.
(20) Ishihara, K.; Ohara, S.; Yamamoto, H. *J. Org. Chem.* **1996**, *61* (13), 4196.
(21) Arnold, K.; Batsanov, A. S.; Davies, B.; Whiting, A. *Green Chem.* **2008**, *10* (1), 124.
(22) Starkov, P.; Sheppard, T. D. *Org. Biomol. Chem.* **2011**, *9* (5), 1320.
(23) Gernigon, N.; Al-Zoubi, R. M.; Hall, D. G. *J. Org. Chem.* **2012**, *77* (19), 8386.

Chapter Three

The Development of a Boronic Acid Catch-and-Release System for Diol Containing Marine Neurotoxins

3.1 Introduction

One of the most common applications of boronic acids in bioconjugation is their ability to bind to *cis*-diols on glycols, sugars and glycoproteins.[1–7] The reversible formation of boronic esters is useful for the labelling and recognition of these molecules in biological systems. A major area where diols are abundantly present, but under explored in terms of boron conjugation, is marine neurotoxins.[8] The mechanism of toxicity of these compounds involves blocking the passage of sodium, potassium and calcium ions by binding to the respective ion channels, ultimately causing paralytic effects that can be potentially fatal to an organism.[9] The detection of these toxins in collected shellfish samples is usually done by mass spectrometry, but is often difficult due to their low concentration relative to other species present in the matrix.[10] Moreover, these other species can cause ion suppression of toxins during detection, arginine being a major contributor to this effect. One method to remove signals from the matrix is to use solid phase extraction (SPE) to bind toxins of interest and wash away the analytes.[9,11,12] In this regard, Miles and coworkers, at the National Research Council (NRC) department of Metrology in Halifax, sought to utilize the diols present in marine toxins for pre-analysis purification using boronic acid SPE.[13] They were able to successfully use boric acid gel (BAG), containing the parent structure phenylboronic acid, to bind azaspiracids, a known class of marine neurotoxins, via boronic ester formation (Figure 3–

1).[13] Once the toxin was bound, the extract was washed away, and the toxin cleaved from BAG with aqueous formic acid to obtain a pure sample for better cleaner analysis by mass spectrometry.

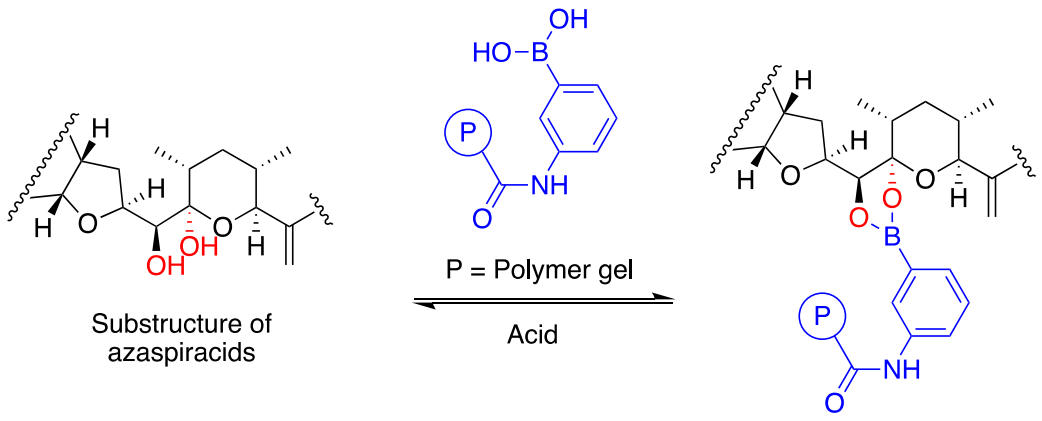

Figure 3–1. Solid phase extraction (SPE) of diol containing marine toxins using polymer bound boric acid gel (BAG).

Another well-known neurotoxin, tetrodotoxin (TTX), has the highest fatality rate of all known marine toxins, most commonly occurring from the ingestion of contaminated puffer fish, which is a culinary delicacy in Japan known as fugu.[10,14] Figure 3–2 shows TTX situated in a sodium ion channel, blocking passage of sodium ions.[15] Carbons 6 and 11 are highlighted to show potentially strong binding of the diols at these sites in the channel. TTX has no known antidotes to date. Miles and coworkers attempted the purification of TTX with BAG as before with azaspiracids, but quickly realized that once TTX was bound, acid cleavage proved to be futile, resulting in low recovery of purified TTX at around 30%. To address regioselectivity, control studies of TTX analogs, without the vicinal diol at carbons 6 and 11, were also ran on the BAG column, but they were not retained. Furthermore, LC-MS/MS studies of boronic acid/TTX conjugates showed boron containing fragments were found on the hydroxy groups on carbons 6 and 11 only. The rationale behind exceptionally tight binding of TTX to BAG is currently unknown.

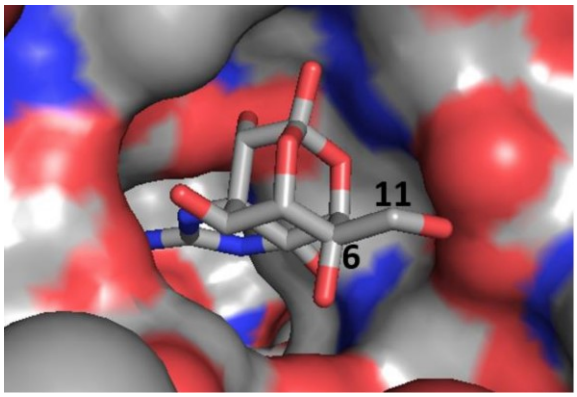

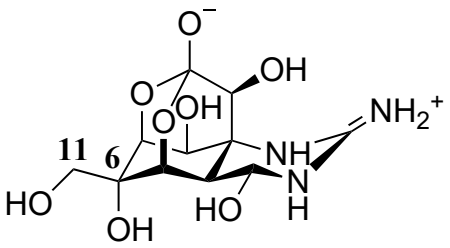

Tetrodotoxin (TTX)

Figure 3–2. Cryo-electron microscopy of TTX bound to Na^+ channel (left, Shen et. al., 2018). TTX structure (right).

3.1.1 Boronate-Diol Chemistry

The strength of boronic ester formation and cleavage between boronic acids and diols can be affected by many factors including pKa of the boronic acid, pH of the solution, dihedral angle of the diol, and steric hindrance. The process is an equilibrium, with the formation of boronate favored with rigid cyclic *cis*-diols under dehydrating conditions.[16] A key factor that affects the complexation equilibrium is the pH of the solution and the pKa of the boronic acid. Lorand and Edwards showed that boronic ester formation was favored in a solution of high pH where the boronic acid predominantly exists as a trihydroxyborate, over neutral pH (Figure 3–3).[17]

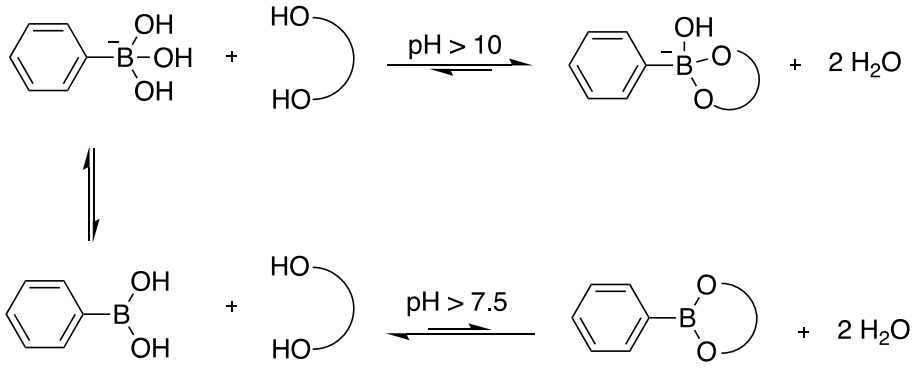

Figure 3–3. Equilibrium of boronate ester formation with diols at high and neutral pH.

Another strategy to favor trihydroxyborate formation is to introduce an electron withdrawing group to the aryl group, which lowers the pKa of the boronic acid. Furthermore, the study also revealed that free boronic acids have a higher pKa than when they are bound to a diol. The authors state that the hydroxy complexation of diol bound boronate esters is favorable as it causes ring strain release from the rehybridization of the boron from sp^2 to sp^3.[17] Based on this research it is hypothesized that boronic acids with electron-withdrawing groups will have more trihydroxy boronate structure at neutral pH, thus a more favorable complexation with diols. The hydrolysis of all acyclic boronic esters is very rapid and favorable, however, with hindered cyclic esters, this hydrolysis is significantly slowed down. The conversion back to a free boronic acid with these cyclic boronic esters can be exceptionally difficult and mostly ineffective with simple aqueous acid conditions.

3.2 Objectives

As mentioned in Section 3.1, TTX binds to BAG exceptionally well and the strength of this binding prevents straightforward hydrolysis with an aqueous acid. To tackle this issue of irreversibility, it was hypothesized that the arylboronic acid component of BAG could be modified in terms of pKa, sterics and/or electronics for both the efficient binding of and cleavage from diol containing toxins. In this regard, a collaboration with the NRC-Halifax and the Hall Group at the University of Alberta sought to identify an arylboronic acid that could potentially achieve this goal. If such an arylboronic acid exists, it could be coupled to a polymer gel to develop a new boronic acid bound polymer gel for the use in columns for pre-purification of many neurotoxins (Figure 3–4). This product can result in a selective extraction method of diol containing toxins and can simplify toxin analysis of real environmental samples to reduce background signals from the

matrix. This research will lead to a better understanding of the chemical interactions of boronic acid complexation to toxins, which can be exploited to develop improved boron-based analysis and purification methods.

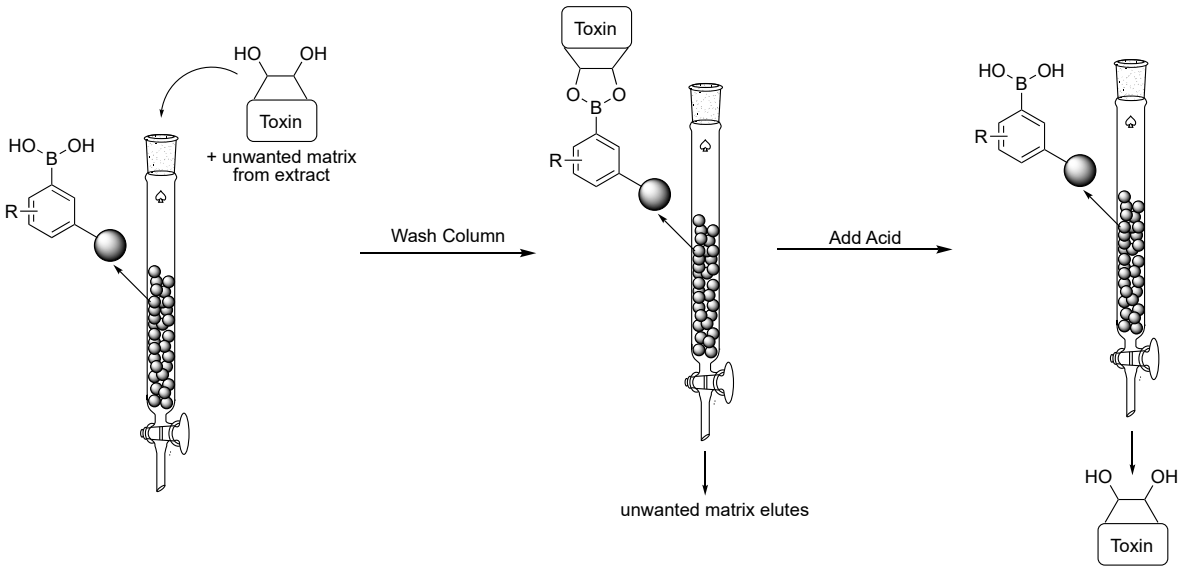

Figure 3–4. Solid phase extraction (SPE) of diol containing marine toxins using polymer bound modified boronic acid gel.

3.2 Results and Discussion

3.2.1 Boronic Acid/TTX Binding Survey

A total of 22 arylboronic acids were chosen for TTX binding evaluation from the Hall Group inventory. Most of these boronic acids are known or commercially available, and some are not yet reported in the literature from on-going student projects (Figure 3–5). The boronic acids were selected based on varied ortho functionality in terms of electron donating and withdrawing ability, neutral alkyl groups as well as some heterocyclic aryl rings. For the purpose of this study, standard solutions of the boronic acids were made in 1:1 H_2O:ACN, in which compounds **3-10** and **3-18** were unable to dissolve, and therefore excluded. Phenylboronic acid (PBA) was also

studied as a control compound. An aliquot of each respective boronic acid, and TTX (obtained from NRC-Halifax inventory) were mixed in ammonium acetate buffer, stored in a fridge overnight and run on a LC-high resolution mass spectrometer (HRMS).

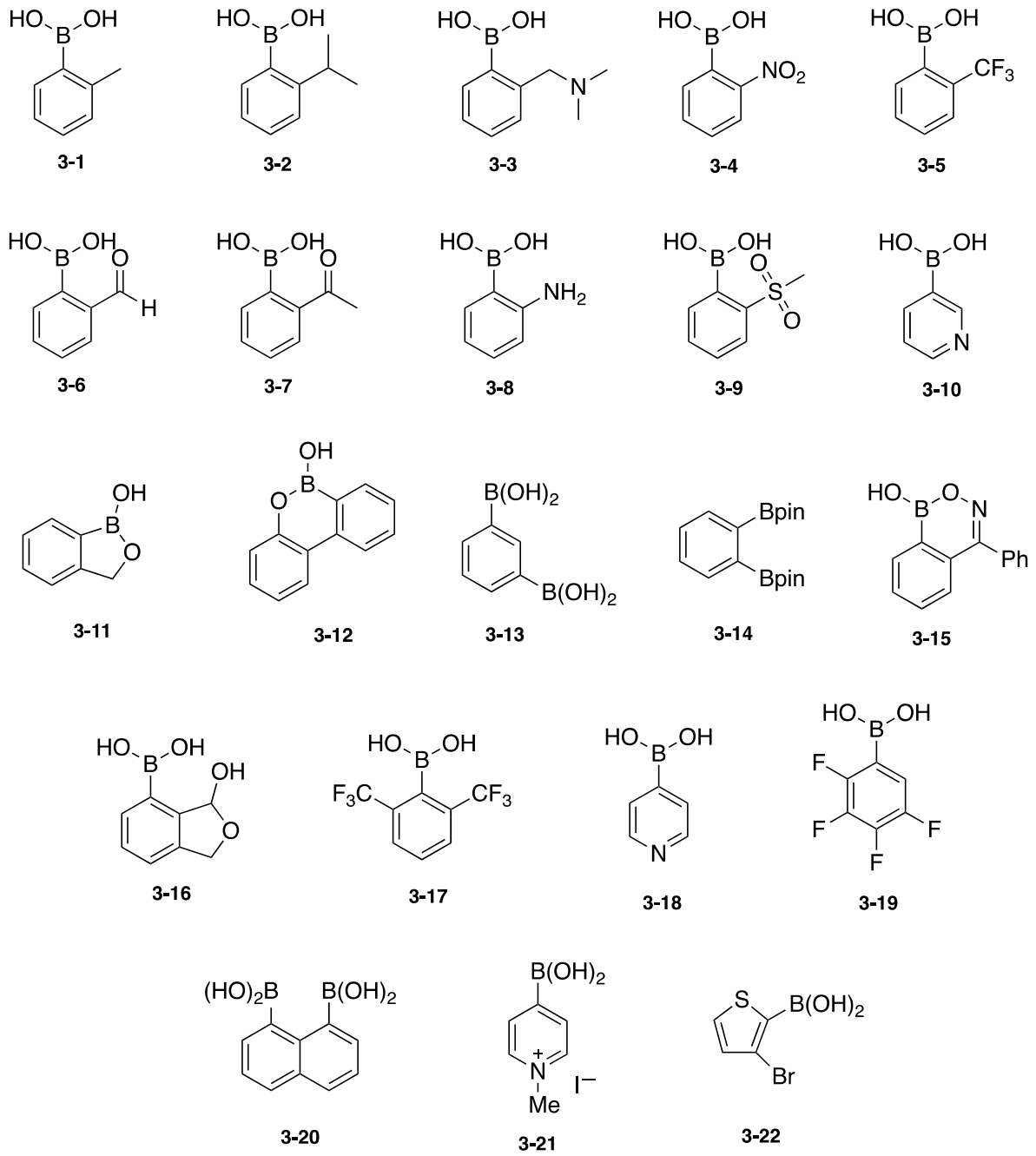

Figure 3–5. Selection of boronic acids to test for TTX binding.

The resulting LC-HRMS data of the TTX and boronic acid solution was analyzed in two ways. First, the peak area of free unbound TTX in each assay was found and compared to that of a control sample of TTX in buffer at the same concentration (Table 3–1 and Figure 3–6). Monitoring the percent of free TTX remaining in solution was a means to consistently compare binding in all the assays. It was assumed the ionization of free TTX in each analysis would be relatively the same, unlike that of the boronate conjugates, which could differ considerably as they are all of different structures. Second, the LC-HRMS data was searched for possible TTX boronate conjugates peaks, the area of which is reported (Table 3–2 and Figure 3–7). All reported TTX boronate conjugates were found in positive mode corresponding to structure **3-F**, with the exception of compounds **3-11** and **3-21**, which were found in the structures **3-F11** and **3-F21** (Figure 3–8). Compound **3–15** gave inexplicable results that prevented its inclusion in the data set.

In Figure 3–6, it can be seen that PBA binds to TTX very well, as there is a very small amount of free TTX remaining in solution. This result is consistent with the favorable TTX BAG binding studies mentioned in Section 3.1. Compounds **3-3**, **3-19**, **3-21** and **3-22** show superior binding, with almost zero free TTX in solution, as well as the respective corresponding TTX boronate conjugate in Figure 3–7. Here, it can be seen that compound **3-19** gives the best result, there is almost no free TTX remaining and the TTX boronate conjugate affords an exceptionally strong signal. In some cases, the pH trends seen in Figure 3–6 and 3–7 agree with the discussion in Section 3.1.1 where it was stated that boronic acids bind cis-diols better when they are in their anionic trihydroxy boronate form over their neutral form. For example, boronic acids **3-1**, **3-2** and **3-4** all have a known high pKa, and all three show the best results, i.e. low free TTX and high boronate TTX complexation, in a higher pH solution than at neutral or low pH.

Table 3–1. Percentage of free TTX remaining in each reaction relative to standard TTX solution as seen by LC-HRMS at various pH.

pKa of Boronic Acid	*Boronic Acid*	*pH 5.7*	*pH 6.8*	*pH 8.2*
8.8	**PBA**	7.2	0.0	4.5
9.7	**3-1**	28.1	14.3	0.0
9	**3-2**	47.3	36.1	0.0
5.5	**3-3**	0.0	0.0	0.0
9.2	**3-4**	29.0	16.3	0.0
unknown	**3-5**	34.9	32.8	0.0
7	**3-6**	5.6	4.2	0.0
7	**3-7**	51.7	50.6	53.7
unknown	**3-8**	1.4	3.4	0.0
unknown	**3-9**	38.9	36.0	7.7
7.2	**3-11**	40.2	39.1	145.1
7.2	**3-12**	50.9	73.2	106.7
unknown	**3-13**	3.7	0.0	0.0
unknown	**3-14**	3.7	138.0	95.2
7.5	**3-16**	59.8	65.7	70.1
unknown	**3-17**	35.9	10.4	0.0
6	**3-19**	0.0	0.0	0.0
unknown	**3-20**	64.7	92.0	155.3
4.5	**3-21**	0.0	0.0	0.0
unknown	**3-22**	0.0	0.0	0.0

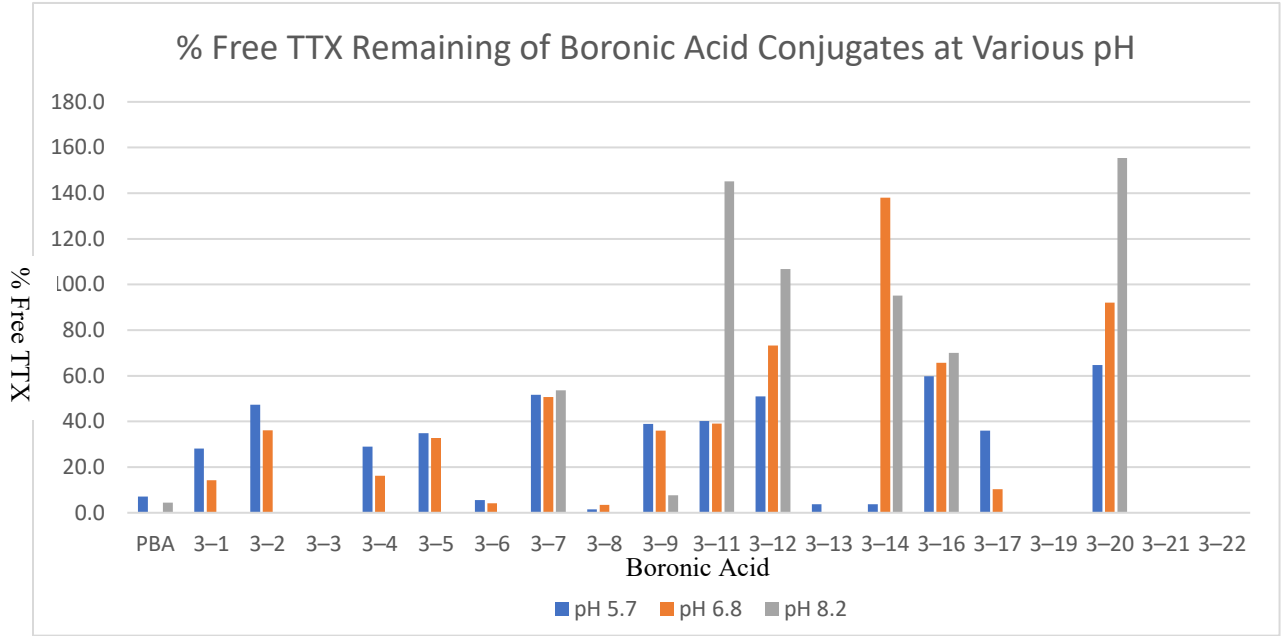

Figure 3–6. Percentage of free TTX remaining in boronic acid assays at various pH.

Table 3–2. Peak area of boronic acid/TTX conjugate as seen by LC-HRMS at various pH.

pKa of Boronic Acid	*Boronic Acid*	*pH 5.7*	*pH 6.8*	*pH 8.2*
8.8	**PBA**	13777453	16497315	16763431
9.7	**3-1**	7270067	14163323	20212548
9	**3-2**	4266015	13776796	31768499
5.5	**3-3**	0	11001107	7711650
9.2	**3-4**	4016962	10261568	16616408
unknown	**3-5**	6395992	23867445	66844200
7	**3-6**	14602056	17252889	17622027
7	**3-7**	0	0	3187162
unknown	**3-8**	478973	668723	524806
unknown	**3-9**	0	502511	512246
7.2	**3-11**	1466719	2737652	8719803
7.2	**3-12**	0	0	0
unknown	**3-13**	4040169	3997184	4081344
unknown	**3-14**	0	0	0
7.5	**3-16**	0	0	0
unknown	**3-17**	0	85093737	89817629
6	**3-19**	39549023	67911383	63288419
unknown	**3-20**	0	0	0
4.5	**3-21**	15038417	14320735	15512938
unknown	**3-22**	6720055	3242073	7850165

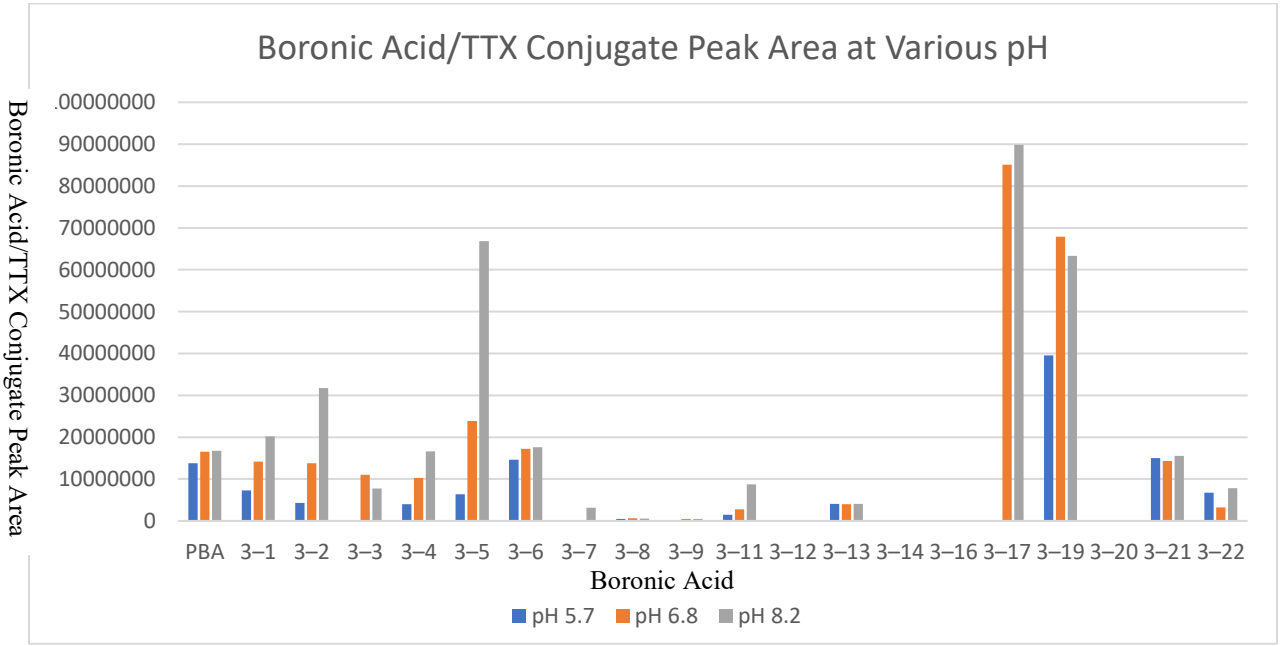

Figure 3–7. Boronic acid/TTX conjugate peak area at various pH.

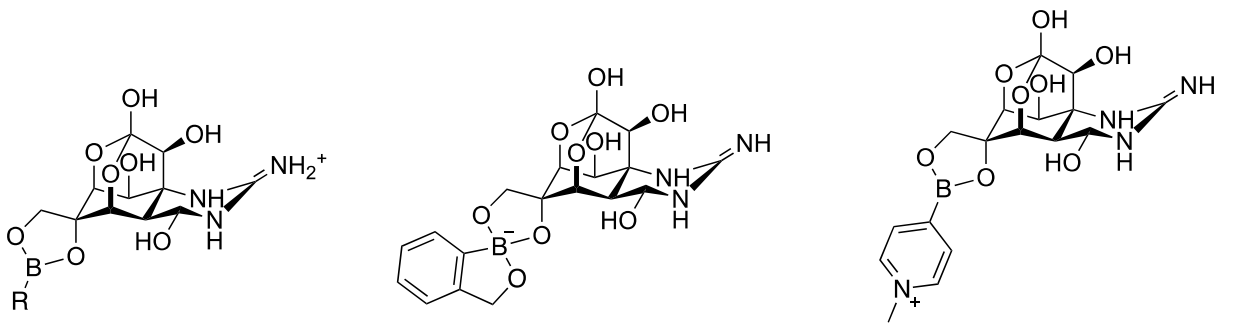

Figure 3–8. Structure of boronic acid/TTX found in LC-HRMS.

In contrast, compound **3-21**, with a known low pKa of 4.5, is mostly in the anionic trihydroxy form at all times, even at the low pH of 5.7, and shows consistent boronate TTX conjugate at every pH tested. In fact, in Figure 3-7, for almost every TTX boronate conjugate studied, the samples in low pH had the smallest peak area of conjugate formed, where boronic acids would less likely be in their anionic trihydroxy form. There are notable contradictions in this data however. In Figure 3–6, compounds **3-11**, **3-12** and **3-20** clearly show greater free TTX in higher pH solutions; the opposite trend expected for boronic acids. It is interesting to note that compounds **3-11** and **3-12** are both benzoxaborole structures, and their conjugates should be found in negative mode, as shown in Figure 3–8 as structure **3-F11**, but very little conjugate is seen. It is possible that these conjugates form a zwitter ion with a negative charge around boron and a positive charge on the guanidium moiety of TTX and thus are silent by HRMS. Compound **3-8** showed minimal amount of free TTX, but unfortunately the conjugate could not be identified or found in the data.

3.2.2 TTX Boronate Conjugate Acid Hydrolysis

Compounds that showed moderate to good TTX boronate conjugate peak area were then analyzed for hydrolysis with acid. To 50 µL aliquots from each conjugation assay was added 30

μL 0.1 M AcOH and left to stir for at least 6 hours before being analyzed by LC-HRMS. The data was then searched for peaks of TTX boronate conjugate and free TTX (retention time at about 9 mins) and compared to that of the original spectrum (Figure 3–9).

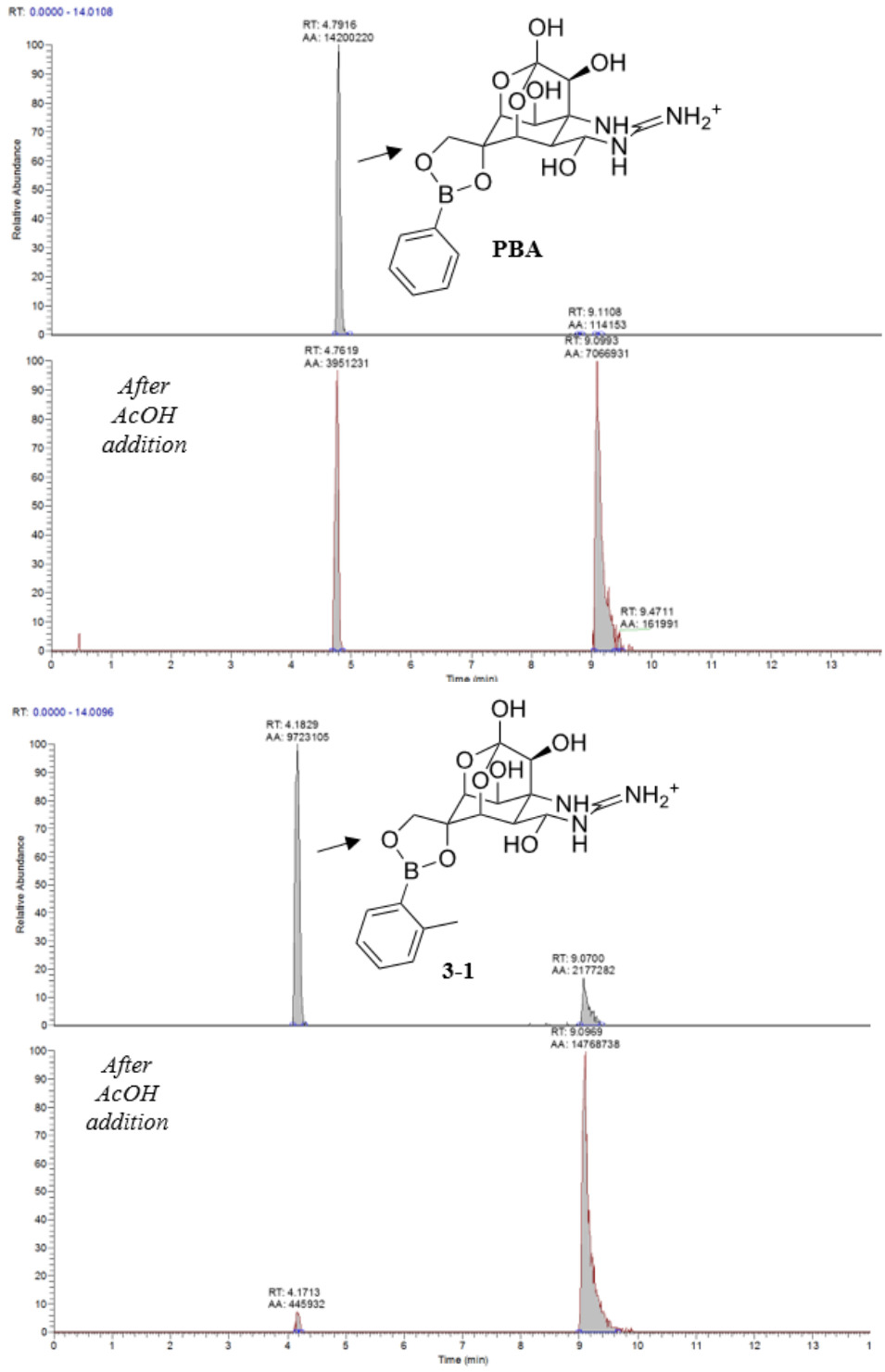

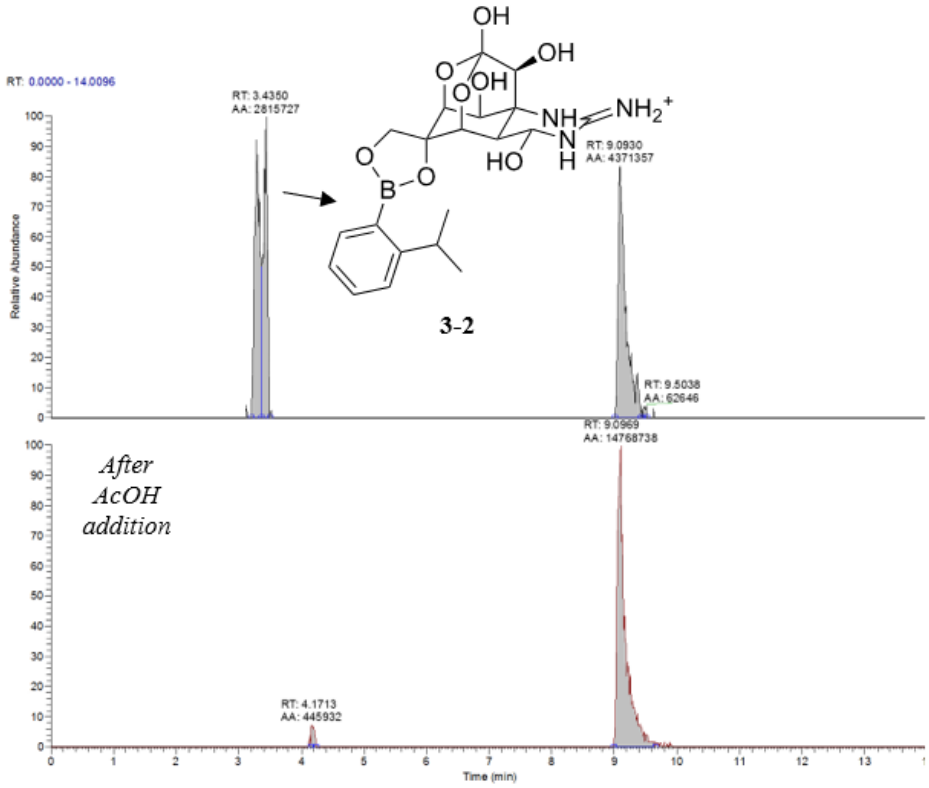
RT: 0.0000 - 14.0096
RT: 3.4350
AA: 2815727
RT: 9.0930
AA: 4371357
RT: 9.5038
AA: 62646
RT: 9.0969
AA: 14768738
RT: 4.1713
AA: 445932
Relative Abundance
Time (min)
After AcOH addition
3-2

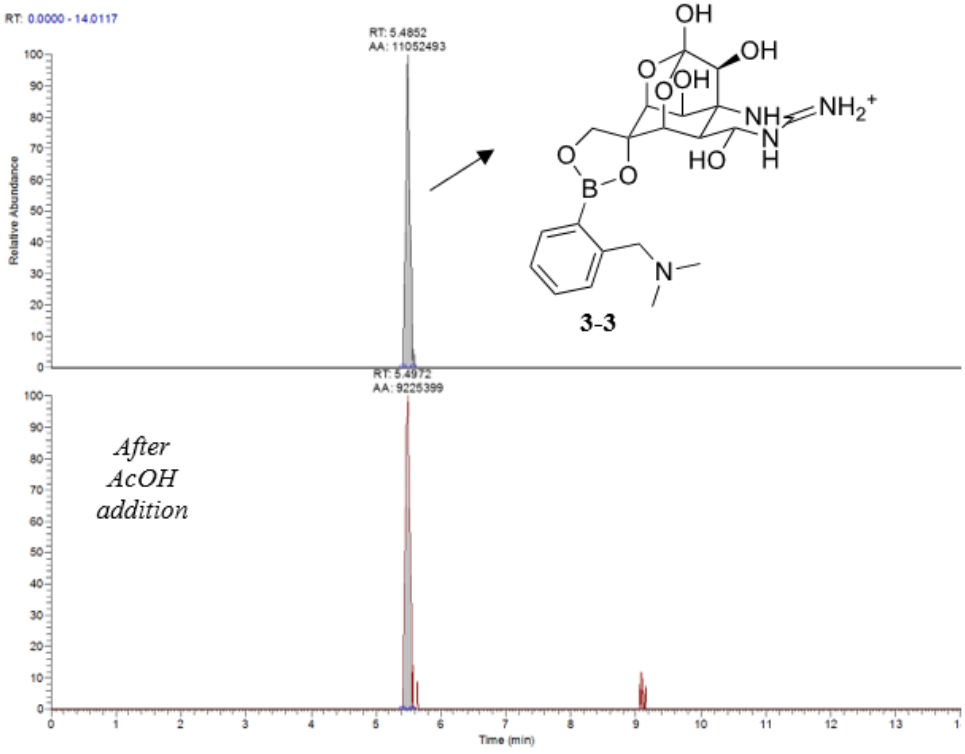
RT: 0.0000 - 14.0117
RT: 5.4852
AA: 11052493
RT: 5.4972
AA: 9225399
Relative Abundance
Time (min)
After AcOH addition
3-3

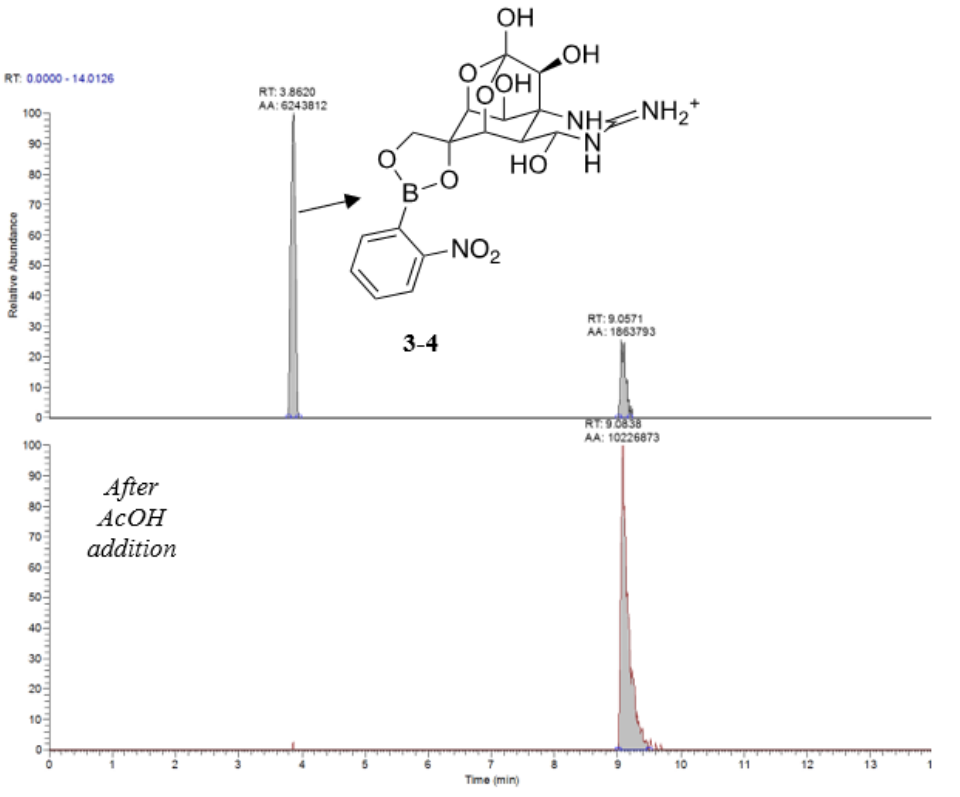
RT: 0.0000 - 14.0126
RT: 3.8620
AA: 6243812
RT: 9.0571
AA: 1863793
RT: 9.0838
AA: 10226873
Relative Abundance
Time (min)
After
AcOH
addition
3-4

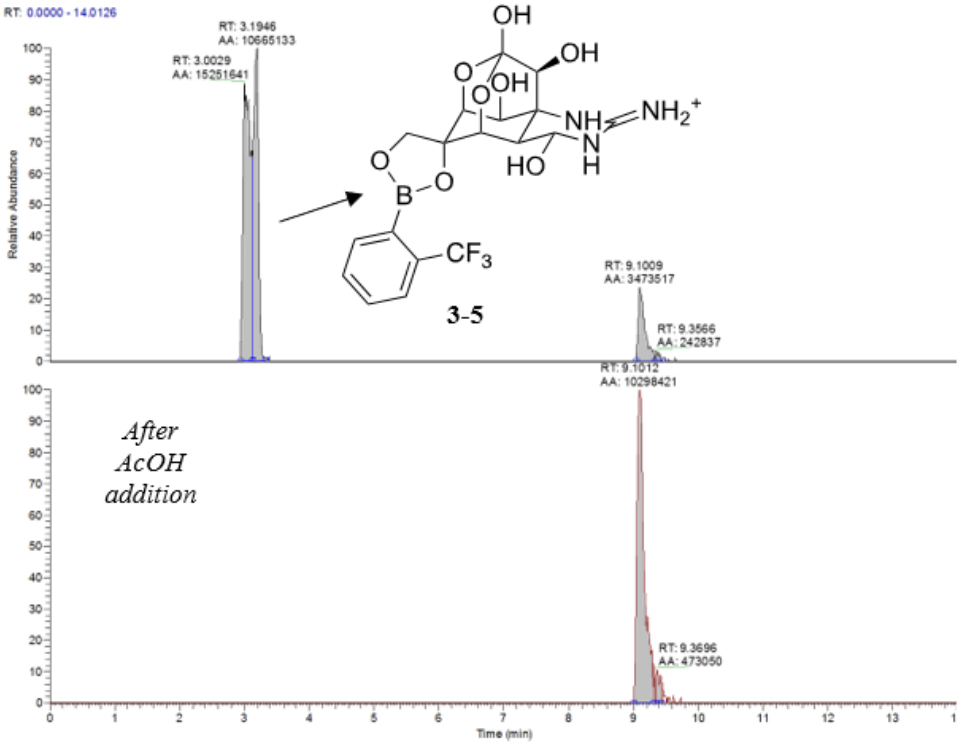
RT: 0.0000 - 14.0126
RT: 3.1946
AA: 10665133
RT: 3.0029
AA: 15251641
RT: 9.1009
AA: 3473517
RT: 9.3566
AA: 242837
RT: 9.1012
AA: 10298421
RT: 9.3696
AA: 473050
Relative Abundance
Time (min)
After
AcOH
addition
3-5

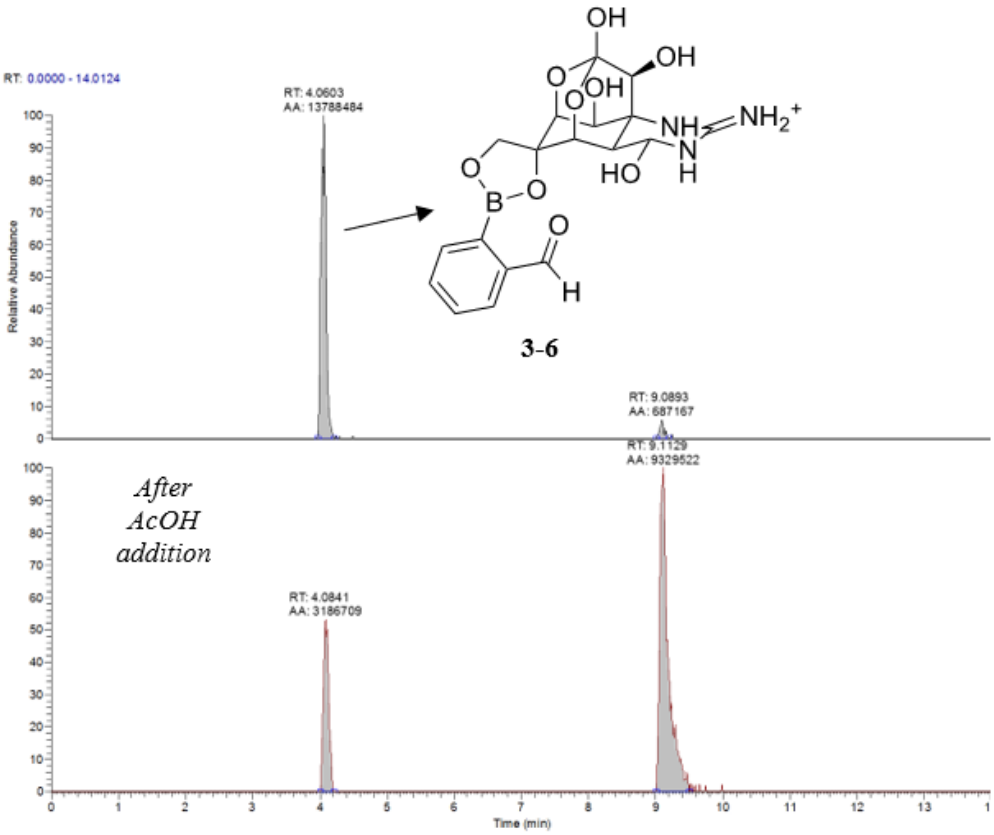
RT: 0.0000 - 14.0124
RT: 4.0603
AA: 13788484
Relative Abundance
3-6
RT: 9.0893
AA: 687167
RT: 9.1129
AA: 9329522
After
AcOH
addition
RT: 4.0841
AA: 3186709
Time (min)

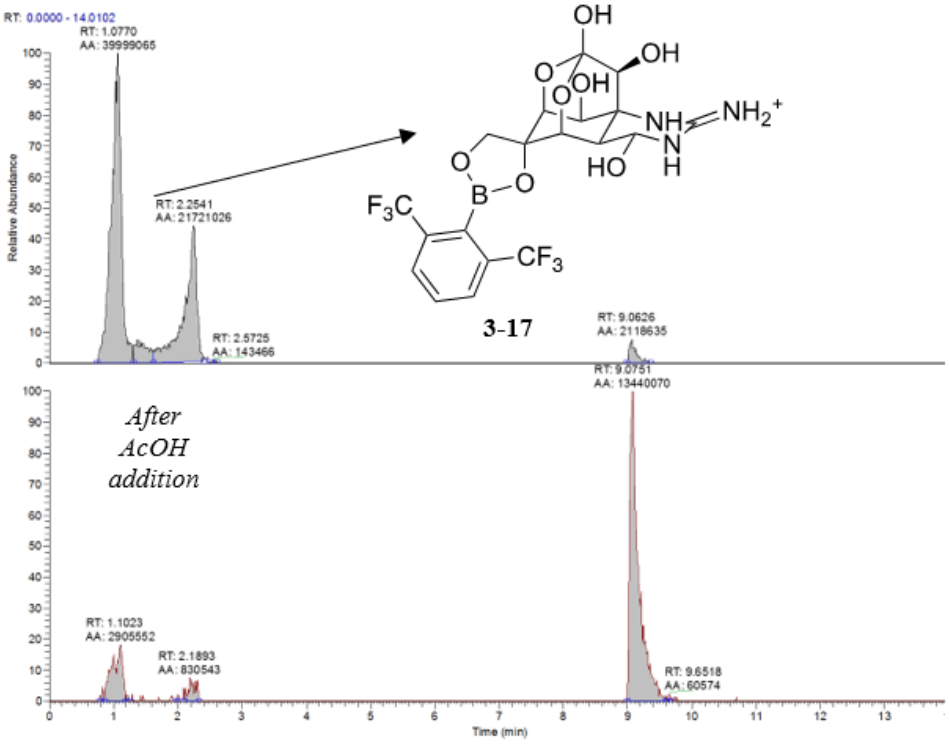
RT: 0.0000 - 14.0102
RT: 1.0770
AA: 39999065
Relative Abundance
RT: 2.2541
AA: 21721026
RT: 2.5725
AA: 143466
3-17
RT: 9.0626
AA: 2118635
RT: 9.0751
AA: 13440070
After
AcOH
addition
RT: 1.1023
AA: 2905552
RT: 2.1893
AA: 830543
RT: 9.6518
AA: 60574
Time (min)

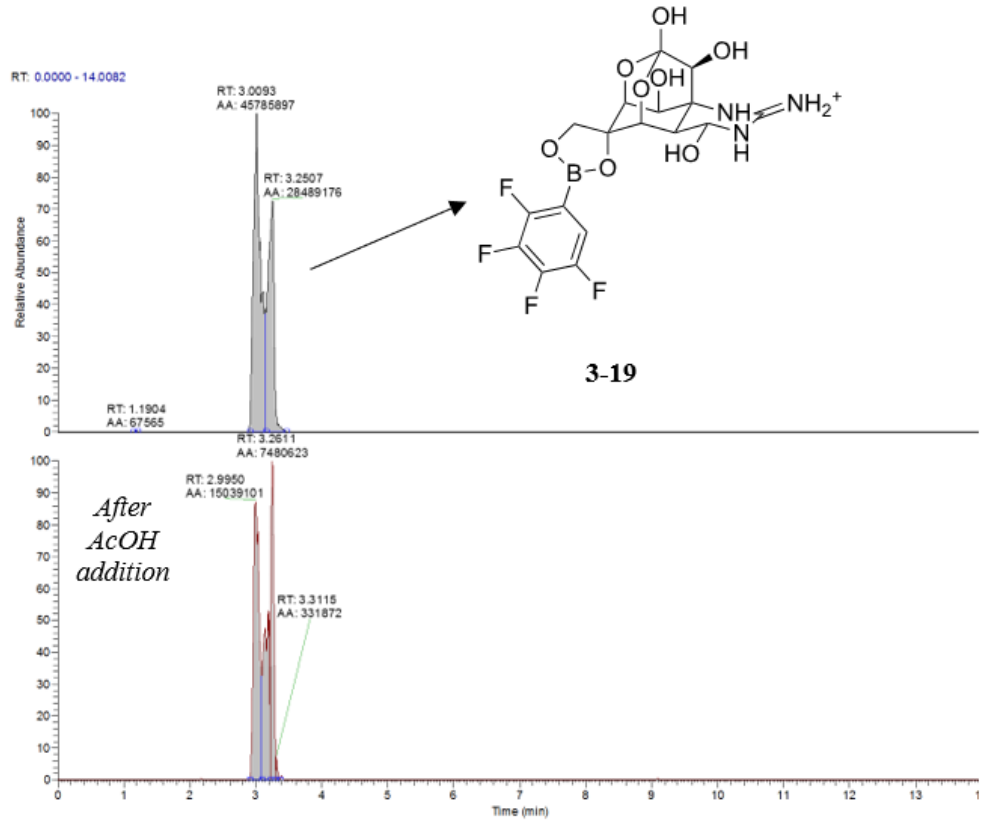
RT: 0.0000 - 14.0082
RT: 3.0093
AA: 45785897
RT: 3.2507
AA: 28489176
RT: 1.1904
AA: 67565
RT: 3.2611
AA: 7480623
Relative Abundance
Time (min)
After AcOH addition
RT: 2.9950
AA: 15039101
RT: 3.3115
AA: 331872
3-19

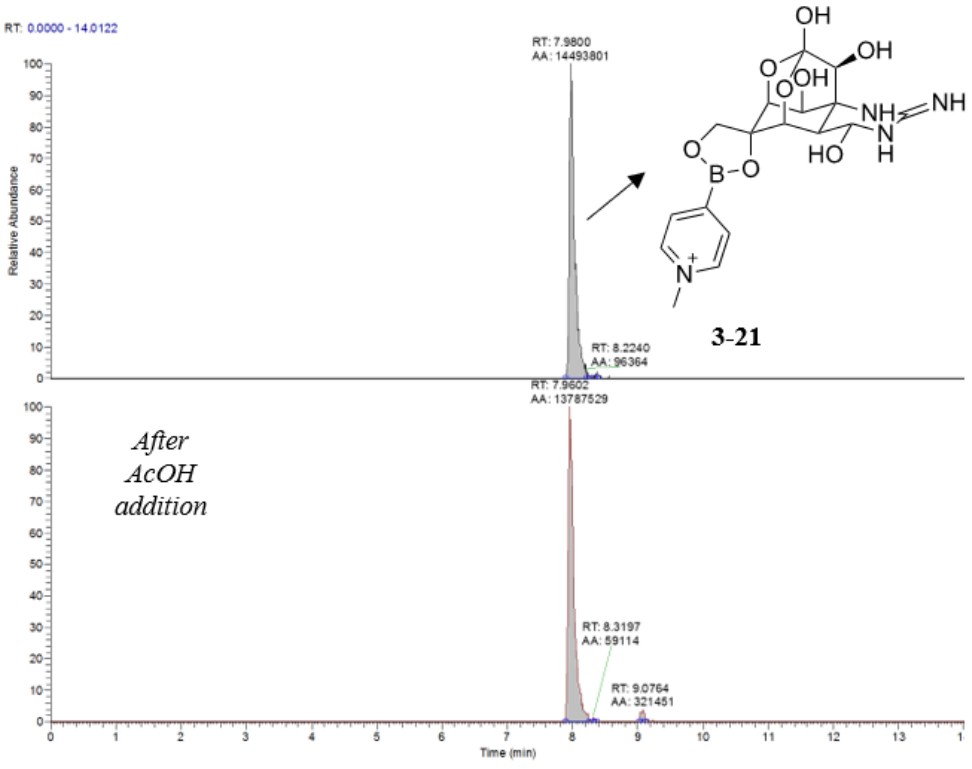
RT: 0.0000 - 14.0122
RT: 7.9800
AA: 14493801
RT: 8.2240
AA: 96364
RT: 7.9602
AA: 13787529
Relative Abundance
Time (min)
After AcOH addition
RT: 8.3197
AA: 59114
RT: 9.0764
AA: 321451
3-21

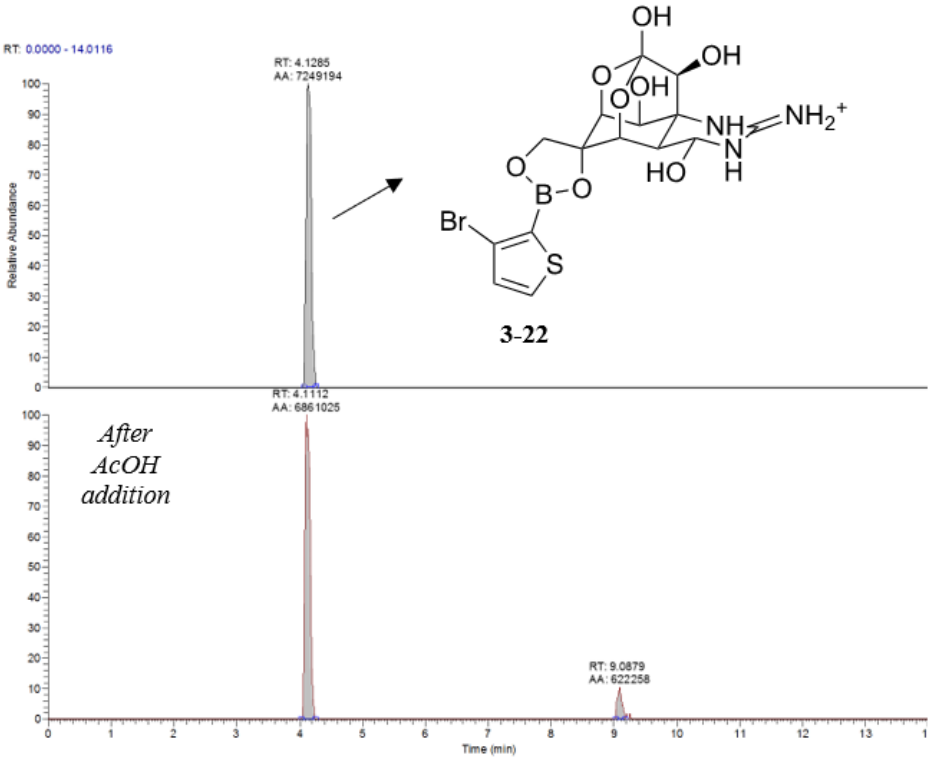

Figure 3–9. TTX boronate conjugation and free TTX peak before (top half of each spectrum) and after addition of 0.1 M AcOH (bottom half of each spectrum).

Figure 3–9 shows that the TTX boronate conjugate with PBA does not fully hydrolyze, which is consistent with the original finding that TTX does not release from BAG very efficiently at all. However, conjugates with compounds **3-3**, **3-19**, **3-21** and **3-22** show an even greater resistance to acid hydrolysis than PBA, with the conjugate peak intact and little to no increase in free TTX. Notably, the compounds that are resistant to hydrolysis also have lower than average pKa, between 4.5 to 6, resulting in stronger binding. TTX boronate conjugates of compounds **3-1**, **3-2**, **3-4**, **3-5** and **3-17** all show the desired outcome, with near complete hydrolysis. To narrow down the compounds further in terms of efficiency, the rate of hydrolysis for each conjugate was monitored over time (Figure 3–10). From Figure 3-10, it can be seen that the peaks of TTX conjugates of compounds **3-1**, **3-4** and **3-17** are still visible after eight hours. In contrast, the conjugate peak of

compounds **3-2** and **3-5** are completely hydrolyzed in the shortest amount of time at six and four hours respectively. Consequently, both boronic acids **3-2** and **3-5** are the ideal candidates for installation onto a polymer gel (cf. Figure 3–4) for their efficient binding and facile acid hydrolysis.

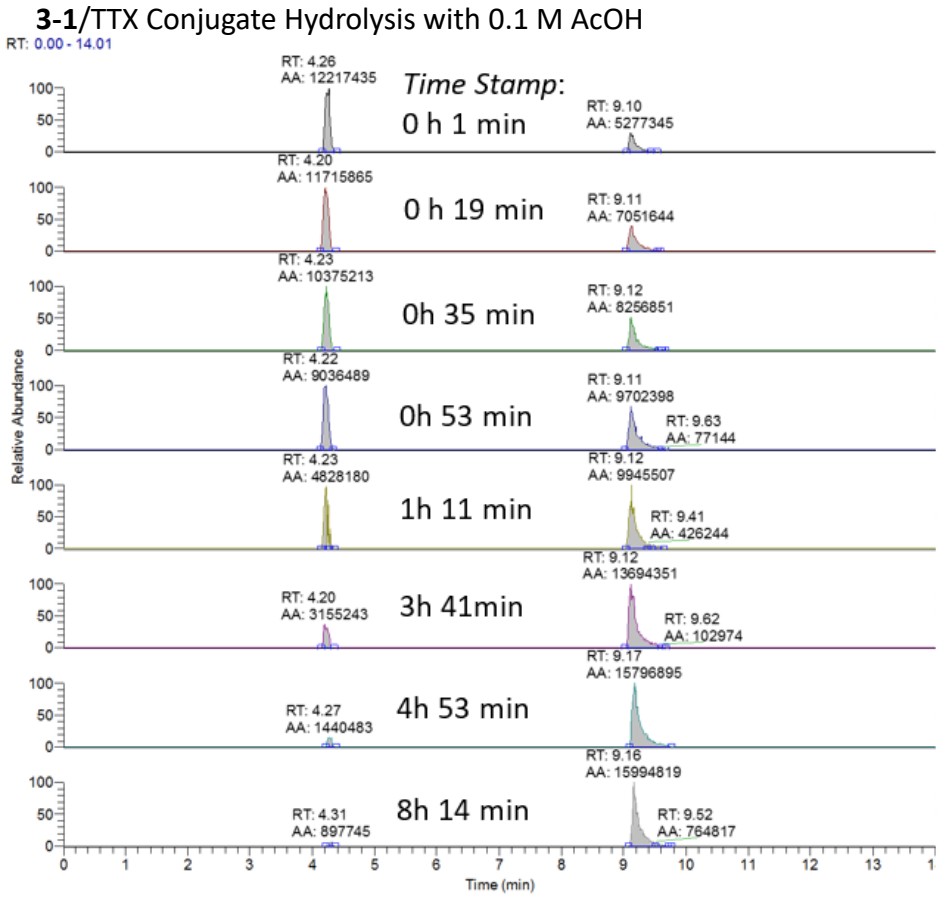

3-2/TTX Conjugate Hydrolysis with 0.1 M AcOH

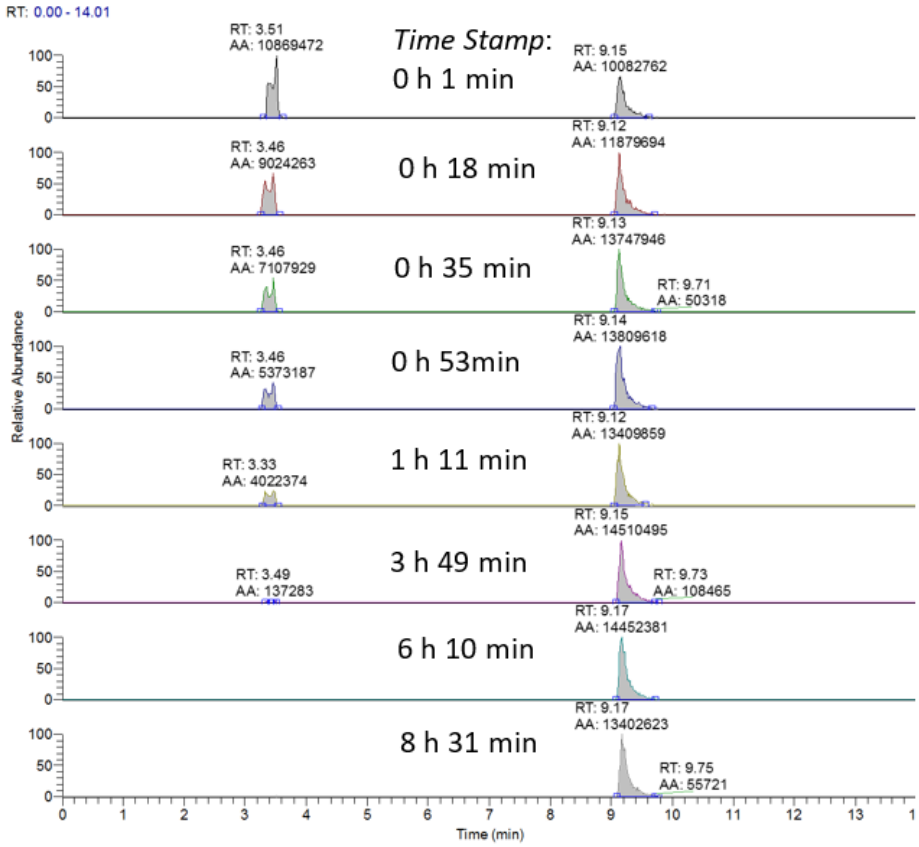

3-4/TTX Conjugate Hydrolysis with 0.1 M AcOH

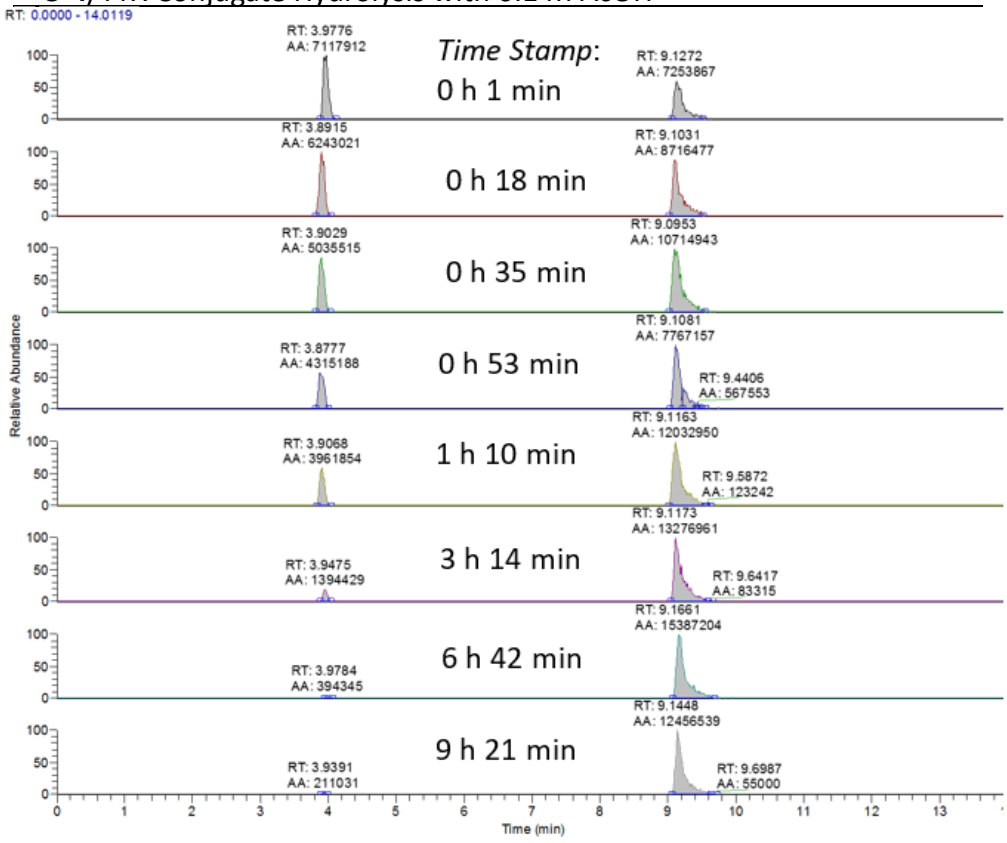

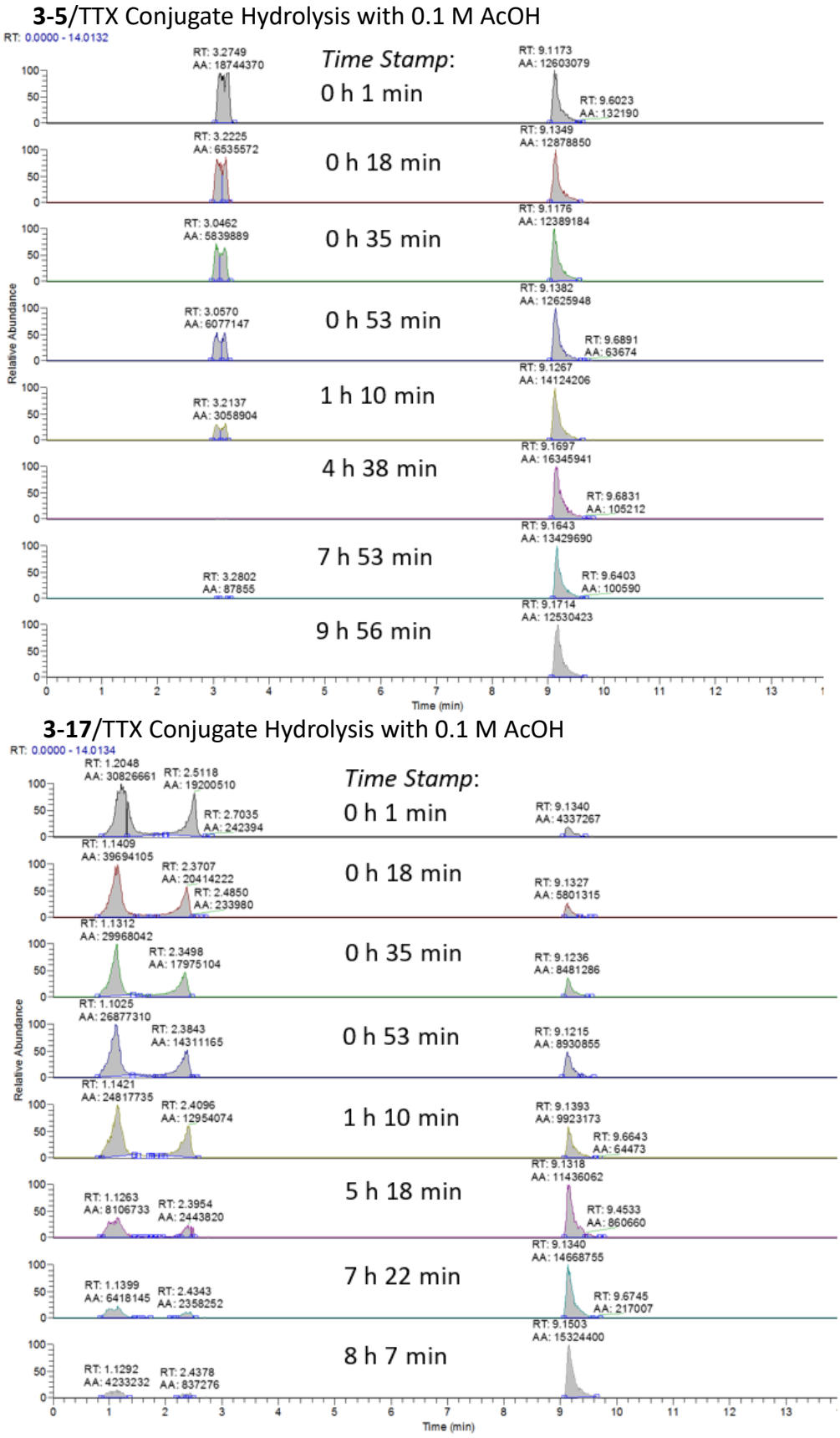

Figure 3–10. The hydrolysis of TTX boronate complexes of compounds **3-1**, **3-2**, **3-4**, **3-5** and **3-17** over time with aqueous 0.1 M AcOH.

For coupling into a polymer gel, either compound **3-2** or **3-5** was needed to be redesigned and synthesized with a handle on the aryl group for polymer coupling. After much literature searching, it was decided to install a carboxylic acid to compound **3-5**, in the meta position to the boronic acid, for a simple amidation reaction on a polymer gel containing amino functionality. To this end, commercially available 3-bromo-4-(trifluoromethyl)benzoic acid successfully underwent Molander borylation to provide compound **3-23** in a moderate yield (Figure 3–11).[18] Plans to couple to an amine containing polymer via an amide bond are underway.

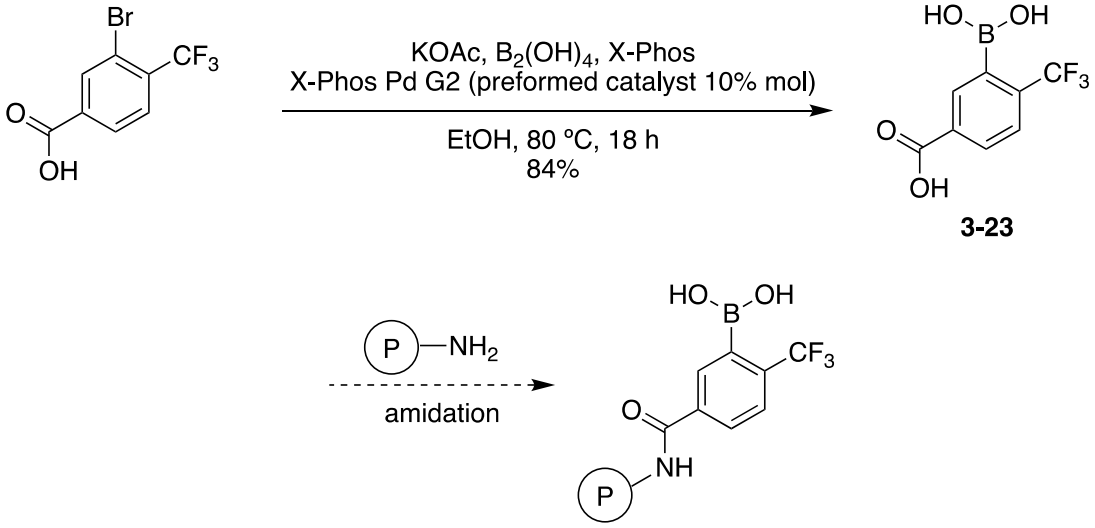

Scheme 3–1. Synthesis of compound **3-23** and plans for the eventual coupling onto a polymer gel.

3.2.2 Bond Strength and Fragmentation Studies of TTX Boronate Conjugates

To study bond strength in TTX boronate conjugates, the fragmentation patterns of two conjugates at increasing electron voltage (eV) were studied by LC-MS/MS. Initially the TTX conjugate of PBA was analyzed (Figure 3–11).

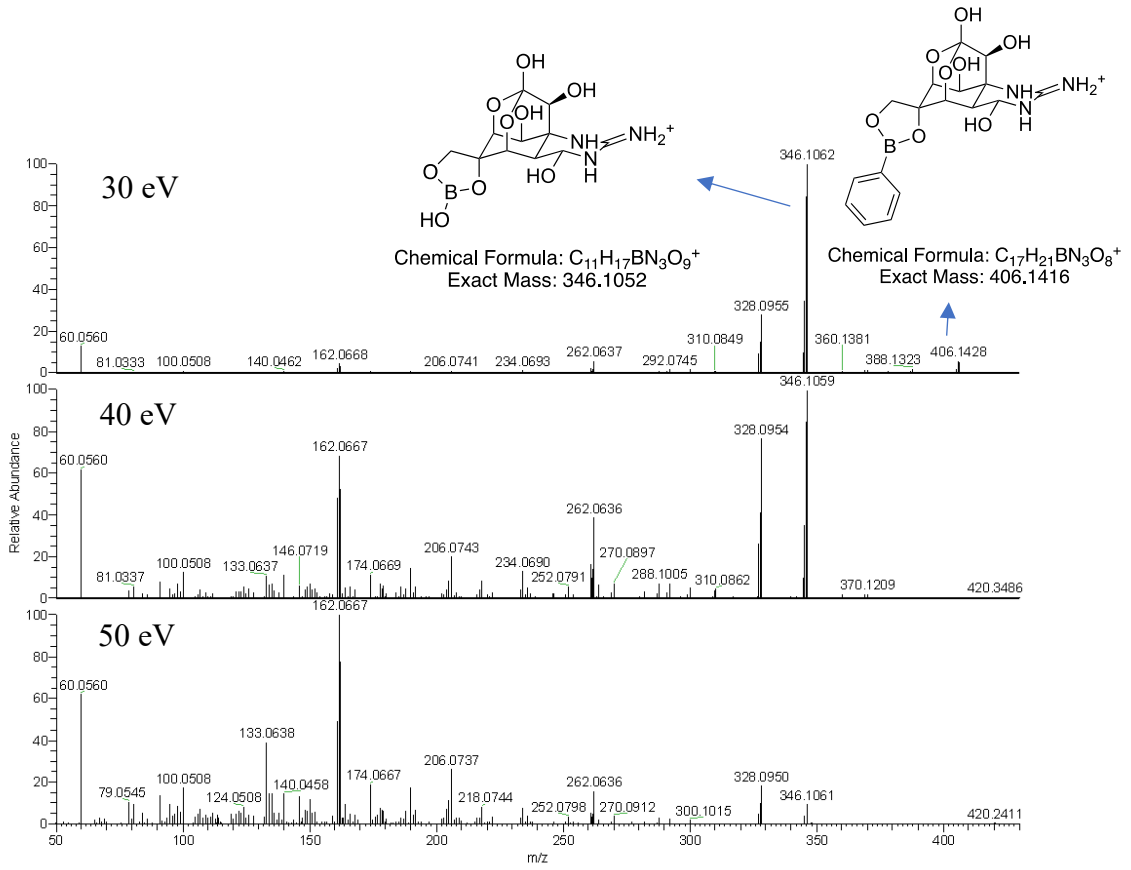

Figure 3–11. Fragmentation pattern by LC-MS/MS of the TTX boronate conjugate with PBA.

In Figure 3–11 it can clearly be seen that the B–C bond on PBA is fairly weak, as it oxidizes easily to produce the most significant fragment of a boric acid bound TTX. The molecular ion peak for the TTX boronate conjugate, is clearly visible at 30 eV, although small, but completely fragments at stronger voltages. In contrast, with tighter binding boronic acids, such as compound **3-4**, the molecular ion peak for the TTX boronate conjugate is much stronger, and is even intact with 40 eV (Figure 3-12). There is also a much smaller peak seen 346.1 *m/z* for B–C cleavage to boric acid bound TTX, indicating the B–C bond here is significantly stronger.

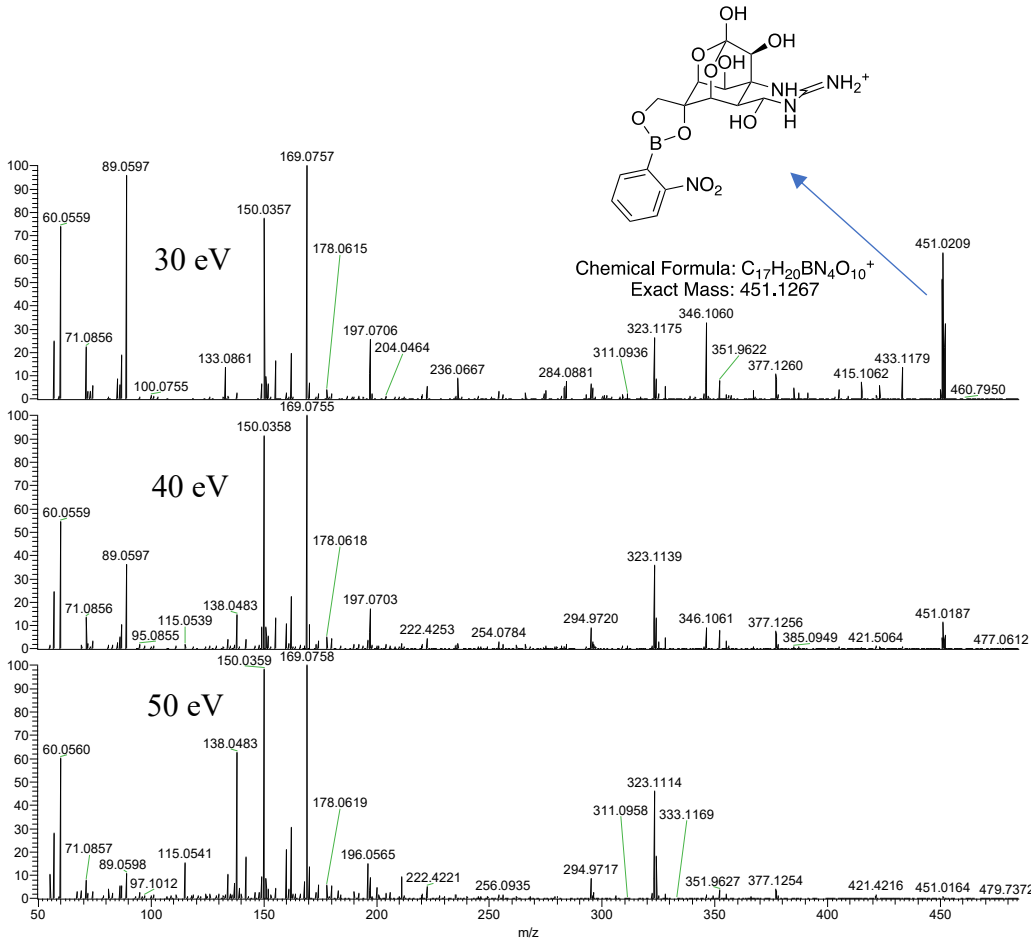

Figure 3–12. Fragmentation pattern by LC-MS-MS of the TTX boronate conjugate with boronic acid **3-4**.

Unfortunately, the LC-MS/MS experiment with the TTX boronate conjugate of compound **3-5** provided little information (Figure 3–13). There is no molecular ion peak visible, and the fragments were not identifiable to any structures.

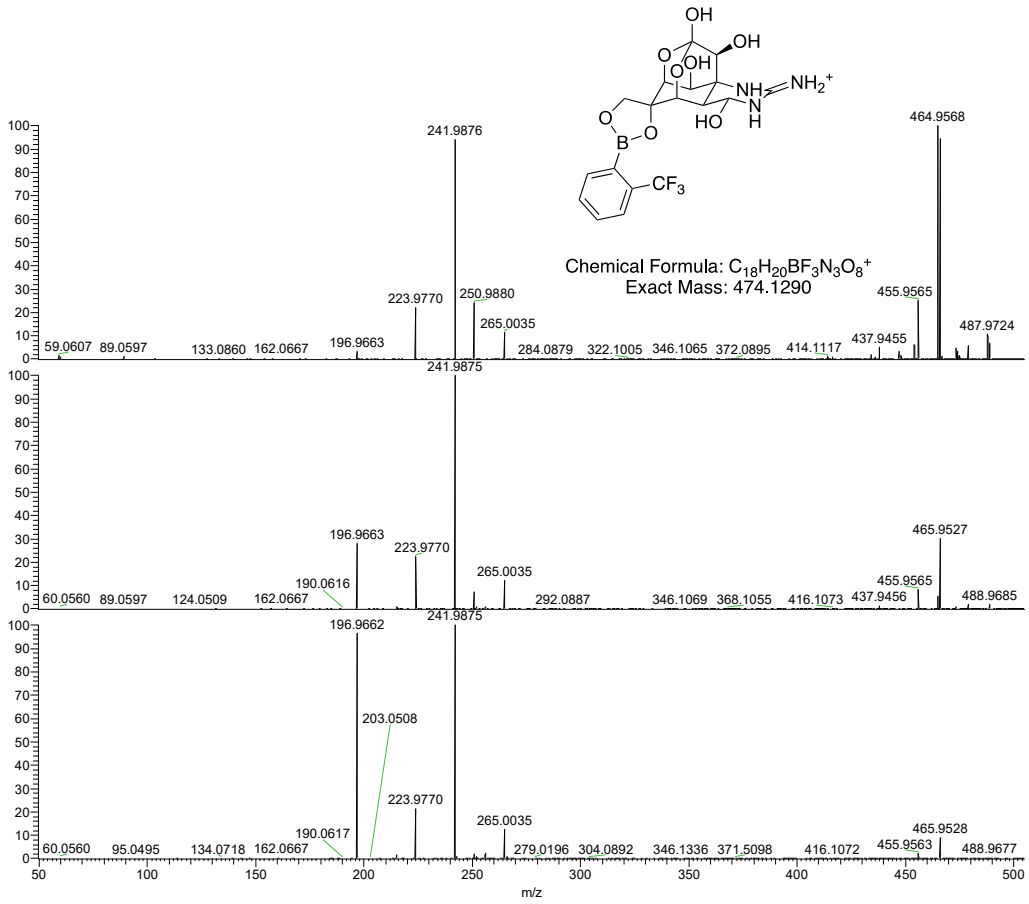

Figure 3–13. Fragmentation pattern by LC-MS-MS of the TTX boronate conjugate with **3-5**.

3.3 Conclusions

Chapter 3 describes the efforts made towards an efficient catch and release system of diol containing marine neurotoxins. Tetrodotoxin, a known strong binder of boronic acid gel, was chosen as a model neurotoxin for the development of an efficient SPE boronic ester purification method with boronic acids. A set of 22 boronic acids with varying pKa and electronic properties were chosen to study for TTX binding via LC-HRMS. Of these 22 boronic acids, 2-isopropylphenylboronic acid **3-2** and 2-(trifluoromethyl)phenylboronic acid **3-5** showed excellent TTX boronate conjugate peaks with minimal free TTX remaining in solution. Furthermore, the complete hydrolysis of the TTX boronate conjugates of **3-2** and **3-5** with aqueous AcOH took six and four hours respectively. This was significantly faster than the control study with PBA, the core

structure on BAG, which only hydrolyzed by 50% after six hours. Boronic acid **3-5** was chosen to be redesigned and synthesized with a carboxylic acid handle for the coupling onto an amide containing polymer gel. This new method of SPE with compound **3-23** could potentially bind and cleave diol containing toxins more efficiently than the current BAG that is commercially available, and lead to more reliable analytical detection methods.

3.4 Experimental

3.4.1 General Information

Unless otherwise indicated, all reactions were performed under air using glassware that was washed thoroughly prior to use. All reagents were purchased from Sigma-Aldrich used as received except tetrodotoxin, which was from a certified reference material calibration solution (CRM-TTX) from the National Research Council of Canada (Halifax, Canada). The buffer used was 0.1 M ammonium acetate at pH 6.8 and adjusted to pH 5.7 and 8.2 with aqueous solutions of acetic acid and ammonium hydroxide respectively. HPLC grade ACN used purchased from Sigma-Aldrich. LC-HRMS analyses were carried out using 2 μL injections on an Agilent 1200 series HPLC (Palo Alto, CA, USA) coupled to a Thermo Scientific Q Exactive HF. A combined full scan and MS/MS method using the 60000-resolution setting, a full scan range of m/z 100 to 800 and a spray voltage of 3 kV were used. Separations were performed with a Waters ACQUITY UPLC BEH Amide Column (1.7 μm, 2.1 × 100 mm) at 40 °C, with mobile phases of 50 mM ammonium formate in H_2O (pH 7) (A) and 95% ACN–H_2O (B). Elution (0.3 mL/min) was with a linear gradient from 0 to 60% A in 8 min, 60% A for 4 min, and post-run equilibration at 0% A for 2 min.

3.4.2 TTX Boronate Conjugation and Hydrolysis

All boronate TTX conjugation reactions were prepared by the following procedure:

To 125 µL of ammonium acetate buffer at a certain pH was added 25 µL TTX solution from a 35 µM concentration stock CRM-TTX and 50 µL of respective boronic acid solution from a stock solution of 1:1 H_2O:ACN at 5 mM concentration. The final volume of each reaction totalled 200 µL in volume with concentration of 1.25 mM boronic acid and 4.38 µM TTX in a buffered solution of 12.5% ACN in water. Immediately after mixing, each reaction was transferred via micropipette to HPLC vials with plastic inserts and stored in a 4 ºC fridge overnight to reach equilibrium before being ran on LC-HRMS. To check for hydrolysis, 50 µL was removed from each equilibrated reaction and mixed with 30 µL of 0.1 M aqueous acetic acid in another vial with a plastic insert then allowed to sit at room temperature for six hours before being ran on LC-HRMS. For rate of hydrolysis studies, the same solution of boronic acid, TTX and acetic acid was mixed then immediately ran on LC-HRMS, then at various time intervals until a span of eight hours was reached.

3.4.3 Analytical Data of TTX Boronate Conjugates

The numbers correspond to the boronic acid compound used to conjugate TTX at a pH of 6.8. The boron isotope pattern is seen for all conjugates except with boronic acid **3-11** as the signal was too weak.

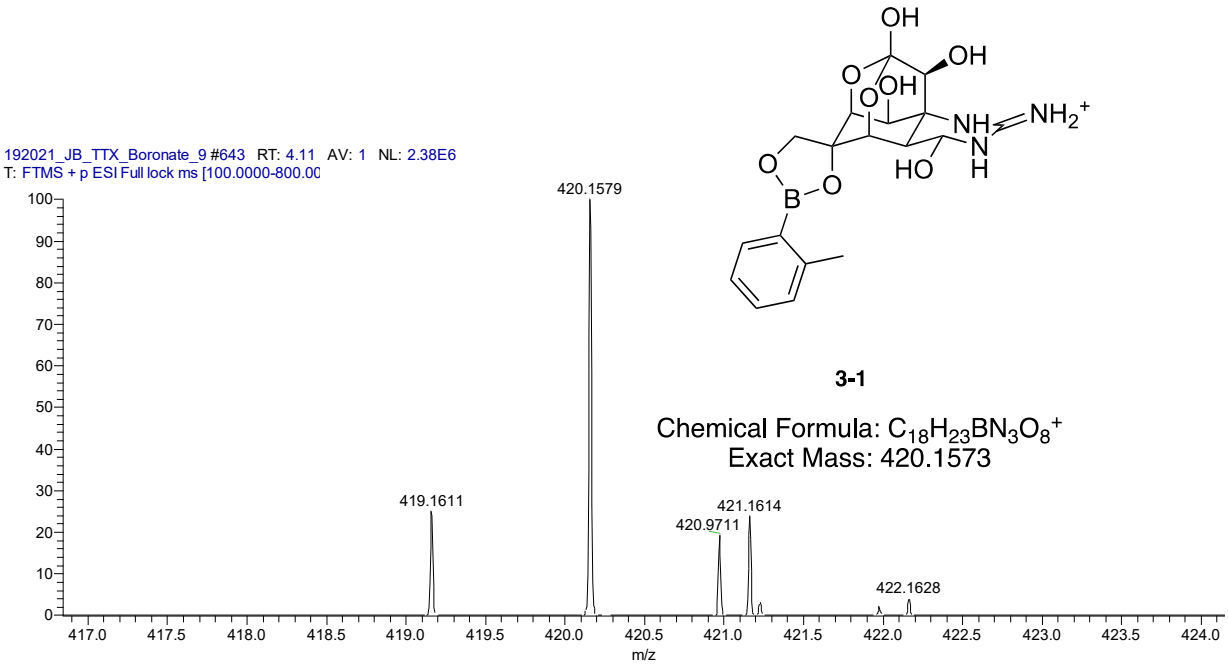

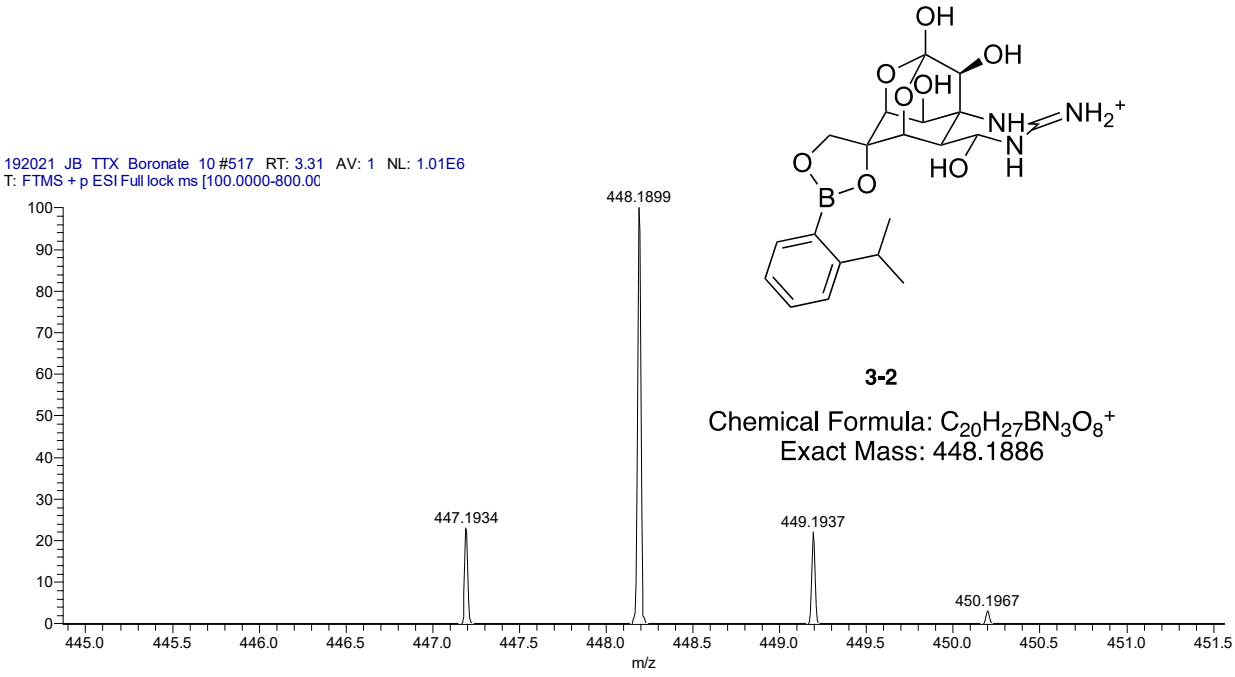

3-2

Chemical Formula: $C_{20}H_{27}BN_3O_8^+$
Exact Mass: 448.1886

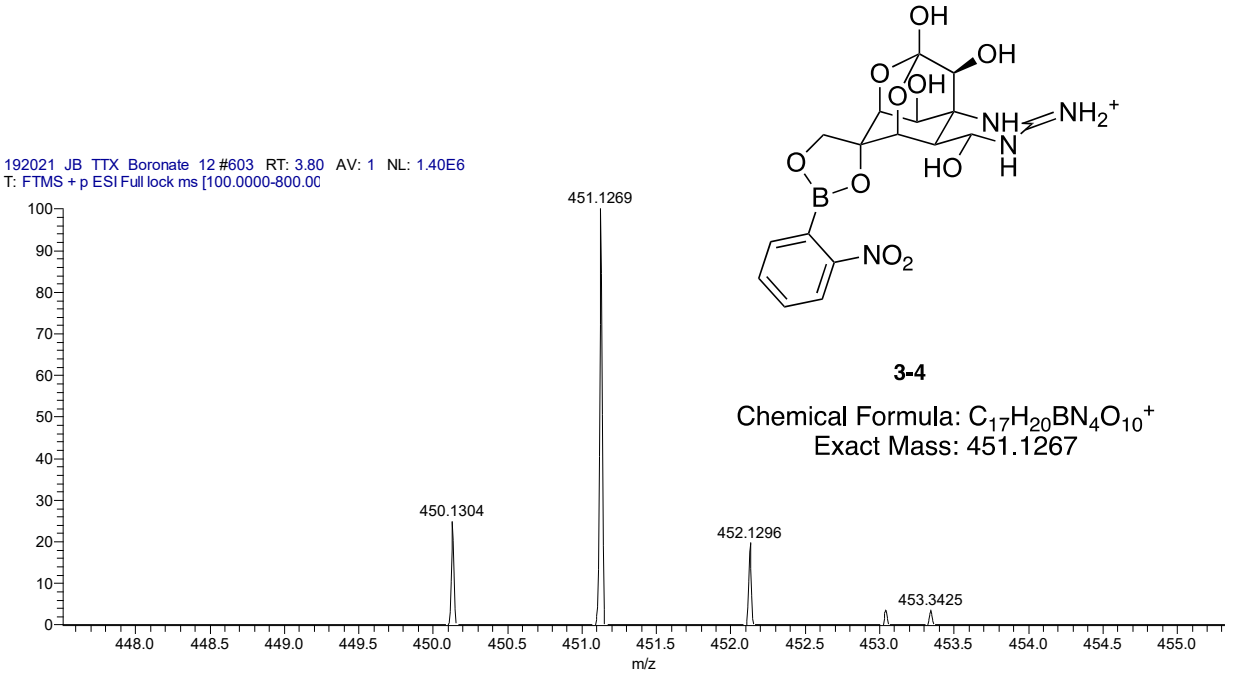

3-4

Chemical Formula: $C_{17}H_{20}BN_4O_{10}^+$
Exact Mass: 451.1267

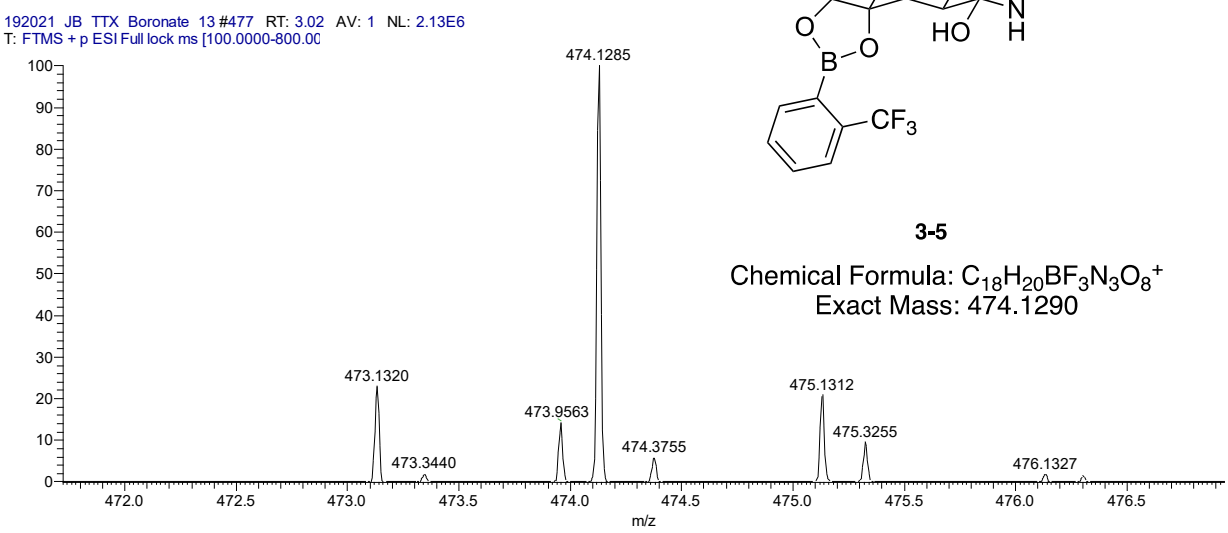

3-5

Chemical Formula: $C_{18}H_{20}BF_3N_3O_8^+$
Exact Mass: 474.1290

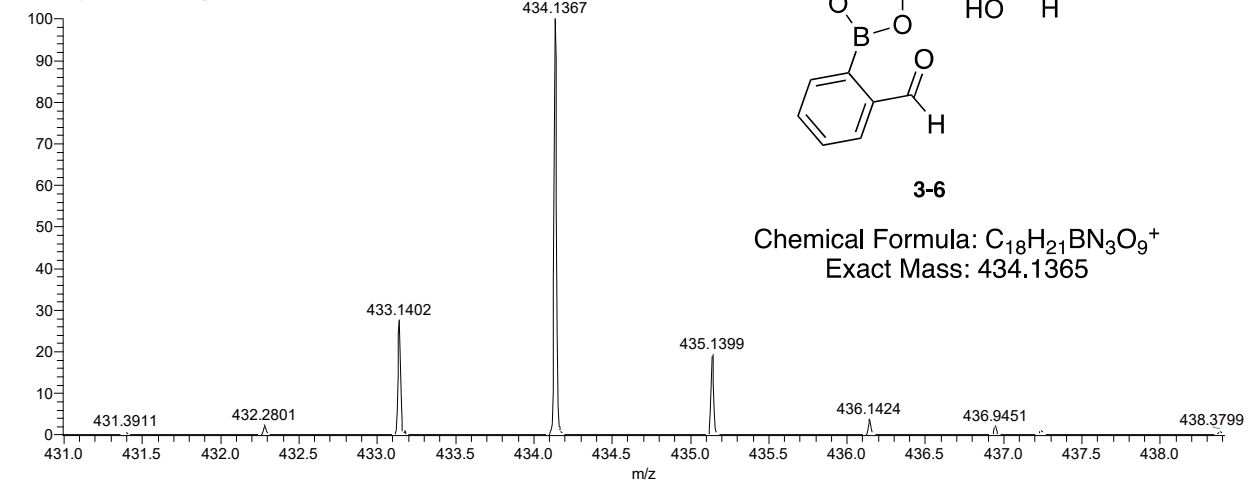

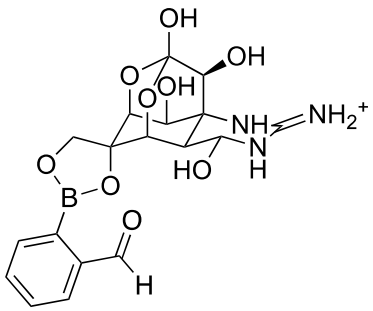

3-6

Chemical Formula: $C_{18}H_{21}BN_3O_9^+$
Exact Mass: 434.1365

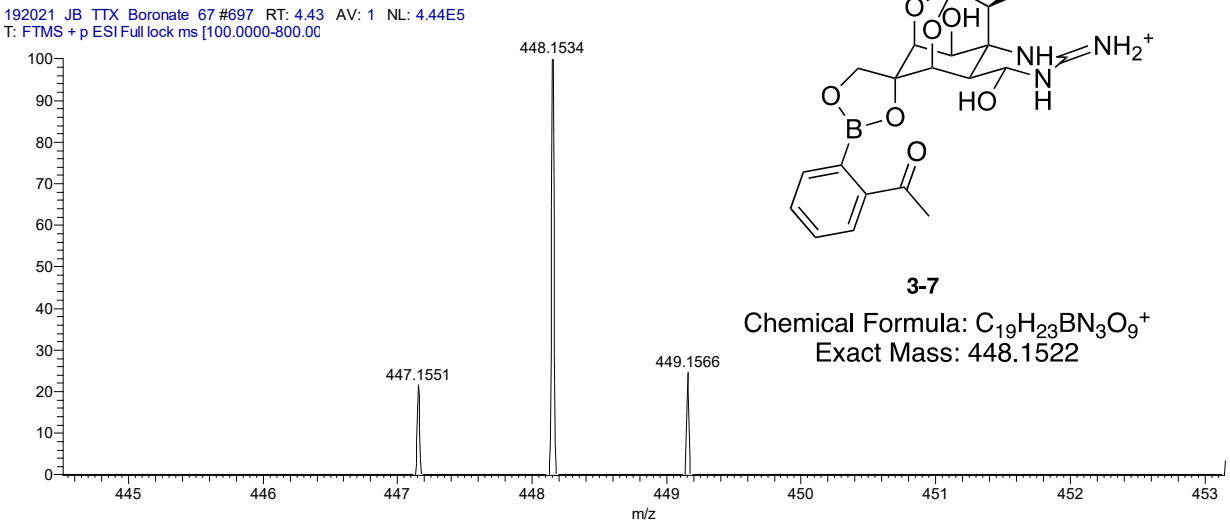

3-7

Chemical Formula: $C_{19}H_{23}BN_3O_9^+$
Exact Mass: 448.1522

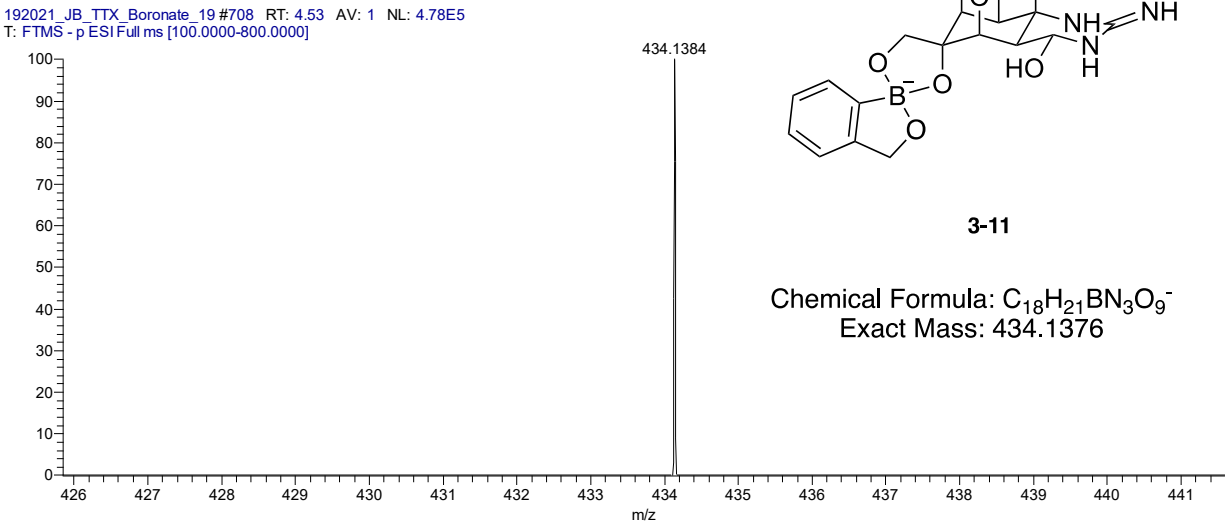

3-11

Chemical Formula: $C_{18}H_{21}BN_3O_9^-$
Exact Mass: 434.1376

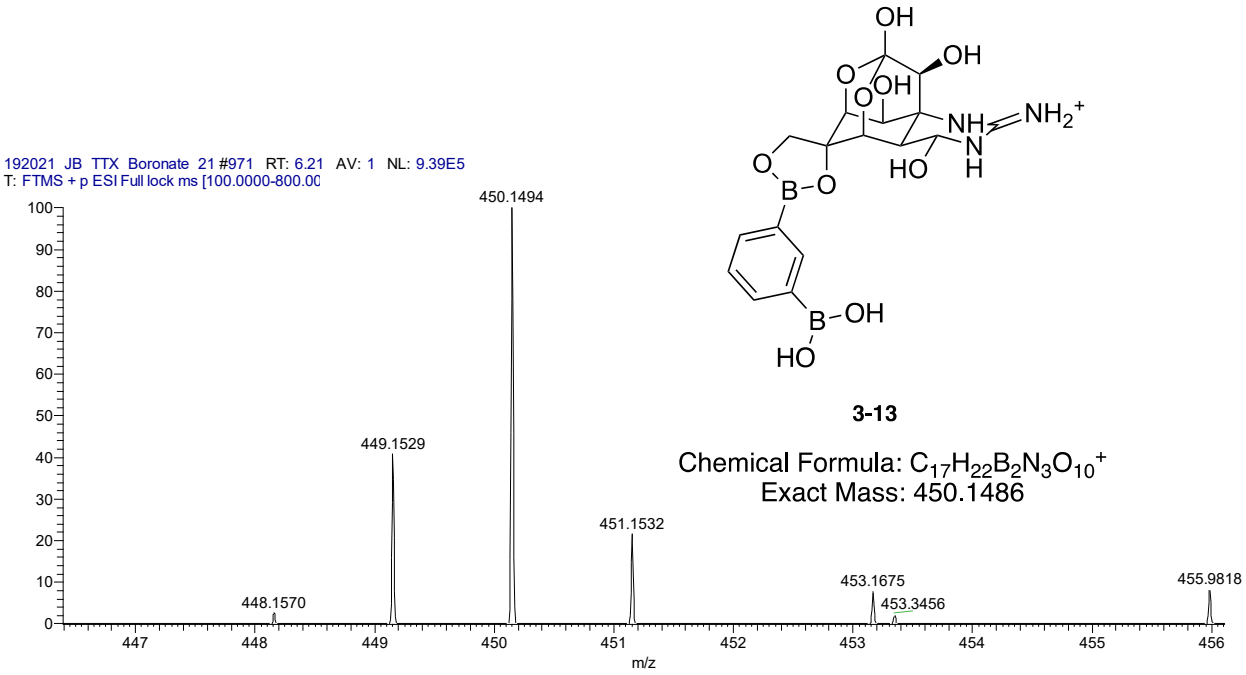

3-13

Chemical Formula: $C_{17}H_{22}B_2N_3O_{10}^+$
Exact Mass: 450.1486

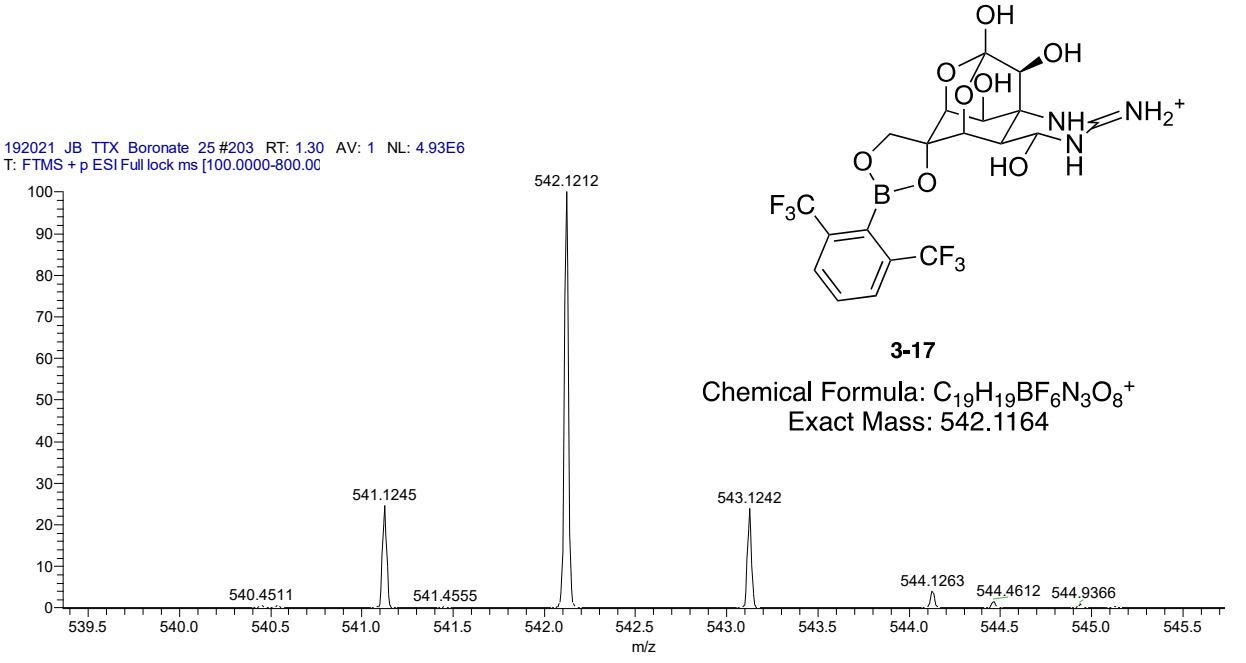

3-17

Chemical Formula: $C_{19}H_{19}BF_6N_3O_8^+$
Exact Mass: 542.1164

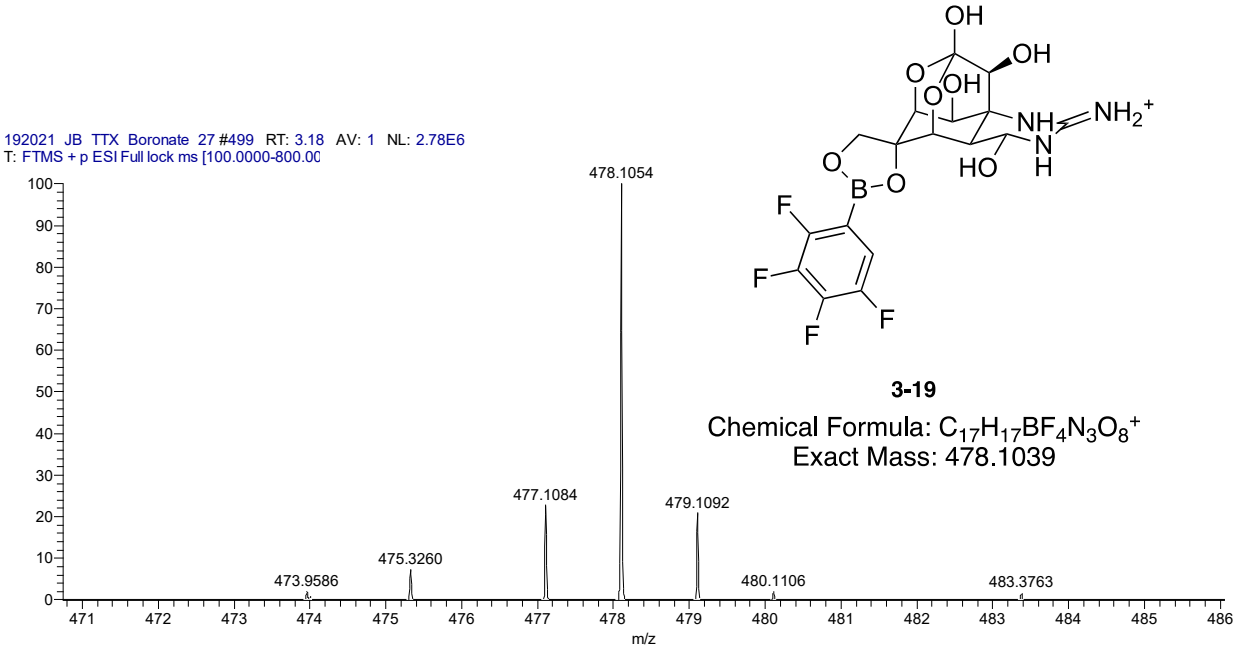

3-19

Chemical Formula: $C_{17}H_{17}BF_4N_3O_8^+$
Exact Mass: 478.1039

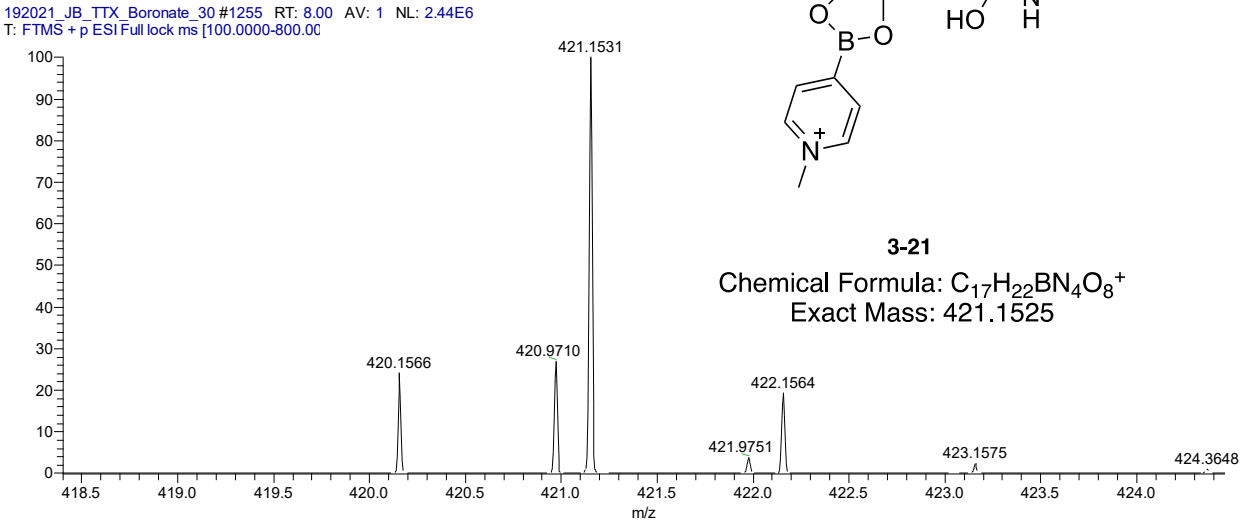

3-21

Chemical Formula: $C_{17}H_{22}BN_4O_8^+$
Exact Mass: 421.1525

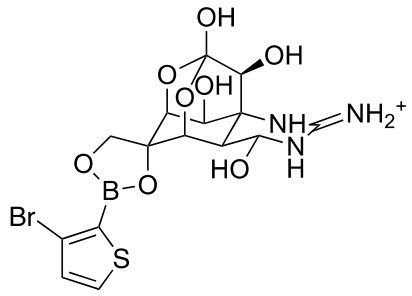

3-22

Chemical Formula: $C_{15}H_{18}BBrN_3O_8S^+$
Exact Mass: 490.0086

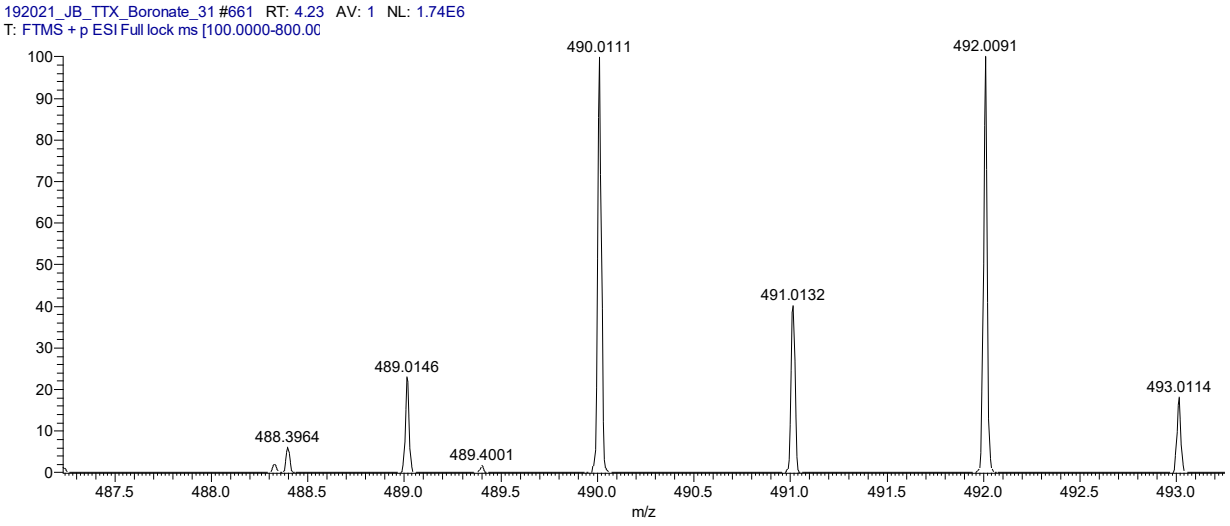

3.4.3 Chemical Synthesis and Analytical Data

Synthesis of compound **3-23** (Scheme 3–1)

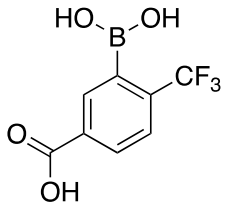

3-23

3-borono-4-(trifluoromethyl)benzoic acid (3-23): To a flame-dried 100 mL round bottom flask under nitrogen was added **3-5** (400 mg, 1.40 mmol), X-Phos palladium(II) biphenyl preformed catalyst (11.8 mg, 15 µmol), X-Phos (14.3 mg, 30 µmol), $B_2(OH)_4$ (405 mg, 4.5 mmol) and KOAc (441 mg, 4.5 mmol). The reaction was sealed then evacuated and purged with nitrogen three times. EtOH (15 mL, degassed) was added and the reaction heated to 80 ºC and stirred for 16 h then brought to room temperature. The reaction was concentrated *in vacuo* then diluted with EtOAc and acidified with aqueous 1 M HCl and the phases separated. The aqueous phase was extracted with EtOAc (3 × 15 mL) and the combined organic extracted were washed with water (15 mL) and brine (15 mL), dried over Na_2SO_4, filtered and concentrated *in vacuo*. The crude residue was triturated with hexanes and filtered to afford the title compound as a grey solid (293 mg, 84 %).

^{1}H NMR (498 MHz, DMSO-d_6) δ 8.08 – 7.92 (m, 2H), 7.77 (d, J = 8.2 Hz, 1H).

^{13}C NMR (126 MHz, DMSO-d_6) δ 164.85, 135.8, 135.0, 128.8, 125.8, 123.60, 121.42, 119.1.

^{11}B (160 MHz, DMSO-d_6) δ 29.634.

3.5 References

(1) Dowlut, M.; Hall, D. G. *J. Am. Chem. Soc.* **2006**, *128* (13), 4226.

(2) Andersen, K. A.; Smith, T. P.; Lomax, J. E.; Raines, R. T. *ACS Chem. Biol.* **2016**, *11* (2), 319.

(3) Halo, T. L.; Appelbaum, J.; Hobert, E. M.; Balkin, D. M.; Schepartz, A. *J. Am. Chem. Soc.* **2009**, *131* (2), 438.

(4) Akgun, B.; Hall, D. G. *Angew. Chem. Int. Ed.* **2016**, *55* (12), 3909.

(5) Akgun, B.; Li, C.; Hao, Y.; Lambkin, G.; Derda, R.; Hall, D. G. *J. Am. Chem. Soc.* **2017**, *139* (40), 14285.

(6) Meadows, M. K.; Roesner, E. K.; Lynch, V. M.; James, T. D.; Anslyn, E. V. *Org. Lett.* **2017**, *19* (12), 3179.

(7) Chapin, B. M.; Metola, P.; Lynch, V. M.; Stanton, J. F.; James, T. D.; Anslyn, E. V. *J. Org. Chem.* **2016**, *81* (18), 8319.

(8) Cusick, K.; Sayler, G. *Marine Drugs* **2013**, *11* (12), 991.

(9) Gerssen, A.; Pol-Hofstad, I. E.; Poelman, M.; Mulder, P. P. J.; Van den Top, H. J.; De Boer, J. *Toxins* **2010**, *2* (4), 878.

(10) Bane, V.; Lehane, M.; Dikshit, M.; O'Riordan, A.; Furey, A. *Toxins* **2014**, *6* (2), 693.

(11) Boundy, M. J.; Selwood, A. I.; Harwood, D. T.; McNabb, P. S.; Turner, A. D. *J. Chromatogr. A* **2015**, *1387*, 1.

(12) Zhuo, L.; Yin, Y.; Fu, W.; Qiu, B.; Lin, Z.; Yang, Y.; Zheng, L.; Li, J.; Chen, G. *Food Chem.* **2013**, *137* (1–4), 115.

(13) Miles, C. O.; Kilcoyne, J.; McCarron, P.; Giddings, S. D.; Waaler, T.; Rundberget, T.; Samdal, I. A.; Løvberg, K. E. *J. Agric. Food Chem.* **2018**, *66* (11), 2962.

(14) Turner, A.; Dhanji-Rapkova, M.; Coates, L.; Bickerstaff, L.; Milligan, S.; O'Neill, A.; Faulkner, D.; McEneny, H.; Baker-Austin, C.; Lees, D. N.; Algoet, M. *Marine Drugs* **2017**, *15* (9), 277.

(15) Shen, H.; Li, Z.; Jiang, Y.; Pan, X.; Wu, J.; Cristofori-Armstrong, B.; Smith, J. J.; Chin, Y. K. Y.; Lei, J.; Zhou, Q.; King, G. F.; Yan, N. *Science* **2018**, *362* (6412), eaau2596.

(16) Hall, D. G. *Boronic Acids. Preparation and Applications in Organic Synthesis, Medicine and Materials*, 2nd Completely Revised ed.; Hall, D. G., Ed.; Wiley-VCH: Weinheim, Germany, 2011.

(17) Lorand, J. P.; Edwards, J. O. *J. Org. Chem.* **1959**, *24* (6), 769.

(18) Molander, G. A.; Trice, S. L. J.; Kennedy, S. M.; Dreher, S. D.; Tudge, M. T. *J. Am. Chem. Soc.* **2012**, *134* (28), 11667.

Chapter Four

Improved Synthesis of a Boronate/Thiosemicarbazone System for Live Imaging

4.1 Introduction

As mentioned in Section 1.2.3 (Chapter 1) Hall and coworkers developed a fast and tight "click" boronate formation system with a fluorophore conjugated nopoldiol and boronic acid tagged cells.[1] This system allowed for fast ligation (k_{ON} 340 $_{M}^{-1}s^{-1}$) in live cell labelling that is stable to competing biological polyols such as glucose, fructose and catecholamines. This boronate bioconjugation strategy was then modified to become irreversible by utilizing a dual binding boronate/thiosemicarbazone system.[2] Specifically, an *ortho*-acetylboronic acid is installed onto a cell using a SNAP-tag approach, followed by incubation with a thiosemicarbazide-functionalized nopoldiol with a fluorescent probe for visualization by fluorescence microscopy. This work caught the attention of the Brudno group at the University of North Carolina (UNC) that specialise in chemical prodrug therapy and controlled drug delivery. Prof. Brudno recently worked on *in vivo* imaging using traditional click chemistry fluorescent labelling techniques.[3,4] Brudno and coworkers were able to functionalize hydrogels with either azide or tetrazine functionalities, inject them into live mice then inject the mice with a fluorescent click partner, namely dibenzocyclooctyne and trans-cyclooctene respectively, and observe site specific labelling (Figure 4–1).[3] This work was later optimized to make replenishable click-modified hydrogel depots, based on bioconjugation click chemistry.[4] In this system, circulating dibenzocyclooctyne with attached

prodrugs are captured by azide functionalized hydrogels placed intramuscularly at the site of administration and the prodrug is cleaved to release the active drug locally. This ability to target specific tissues can allow for refills of hydrogel depots in a non-invasive manner; however, the bioconjugation techniques used for these *in vivo* systems don't come without disadvantages. Azide/alkyne cycloaddition conjugation has low kinetics and the synthesis of the alkyne can be challenging.[5] Although tetrazine/trans-cyclooctene conjugation is extremely fast, isomerization of cyclooctene to the unreactive *cis* isomer is possible, along with the hydrolysis of tetrazine.[6] Further exploration of suitable bioorthonal click chemistry systems are needed for expansion of this drug delivery work.

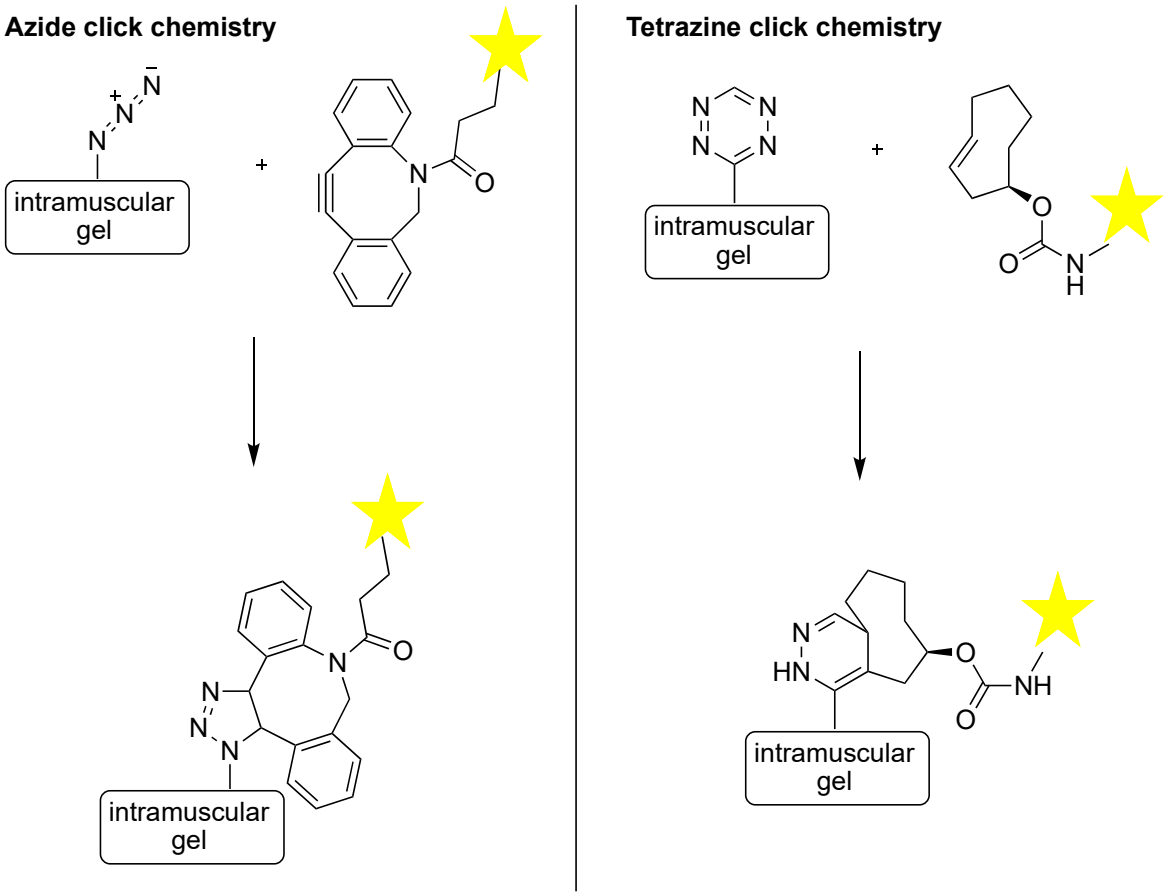

Figure 4–1. Azide-dibenzocyclooctyne (left) and tetrazine- trans-cyclooctene (right) bioconjugational click chemistry.

4.2 Objective

The irreversible boronate/thiosemicarbazone system created by Hall and coworkers was envisioned to be applicable in the *in vivo* delivery systems developed by Prof. Brudno. However, in order for the Brudno group to be able to best visualize the labeling with their microscope, the fluorophore on the thiosemicarbazide-functionalized nopoldiol had to be changed to emit at the desired wavelength. In this regard, NIR-797 isothiocyanate was chosen as the fluorophore as it can be installed onto nopol diol using the same chemistry as the original publication, and it is suitable for visualization by the microscope (Figure 4–2a).[2] The boronic acid was also required to be altered to include an *N*-hydroxysulfosuccinimide sodium salt (*sulfo*-NHS) activated carboxylic acid functionality for aqueous solubility and attachment onto amino groups in the hydrogels (Figure 4–2b). The main goal of this project was to resynthesize both components of the boronate/thiosemicarbazone system on a large enough scale and make the required changes to produce compounds **4-1** and **4-2** shown in Figure 4–2 and deliver to the Brudno lab for *in vivo* imaging.

a) NIR-797 isothiocyanate functionalized nopoldiol **b) *sulfo*-NHS activated boronate acid tag**

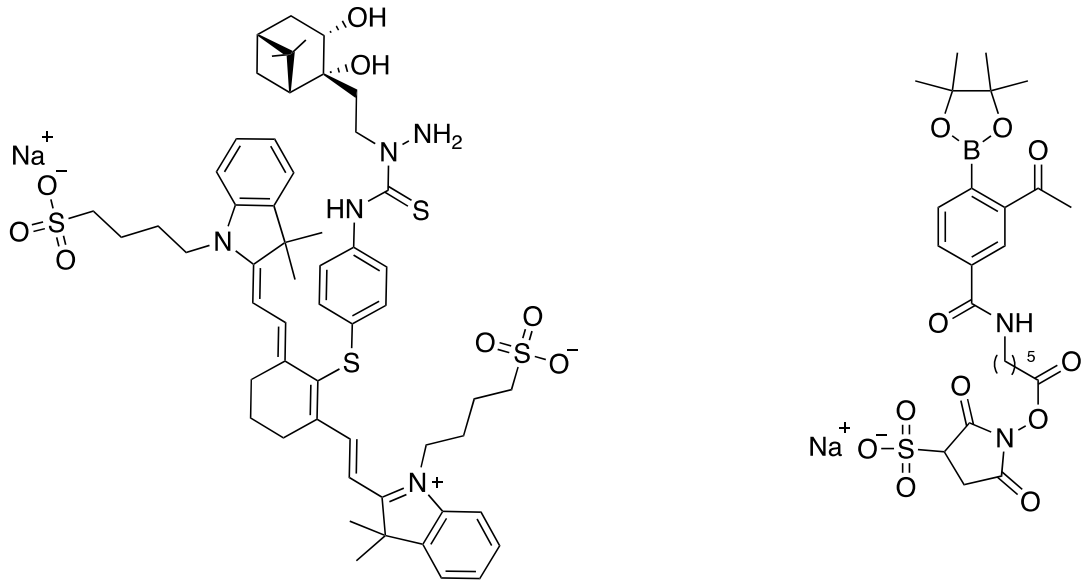

4-1 **4-2**

Figure 4–2. New designed fluorescent nopol diol **4-1** (a) and boronic acid tag **4-2** (b).

4.3 Results and Discussion

4.3.1 Synthesis of Boronic Acid Tag

The first step in the reported synthesis of the boronic acid tag **4-2** was a Friedel-Crafts acylation on compound **4-3** with a low yield of 27% (Figure 4–3a).[2] This reaction was attempted twice, resulting in about 20% yield which afforded compound **4-4** as a messy dark purple clay that was difficult to work with. A literature search into alternatives for making compound **4-4** identified a promising report where Zhang and coworkers achieved a Fries rearrangement on compound **4-5**, which contains an *O*-acetyl group that will migrate, to give desired compound **4-4** (Figure 4–3b).[7]

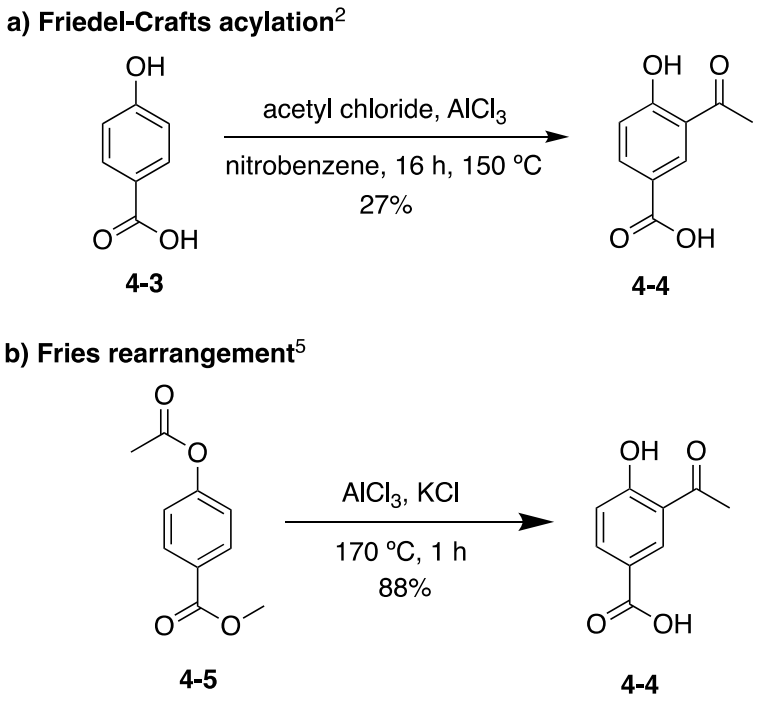

Figure 4–3. Reported Friedel-Crafts acylation (a) and Fries rearrangement (b) towards the synthesis of **4-4**.

The reported Fries rearrangement was performed without solvent. It was hypothesized that the methyl ester **4-5** has a melting point somewhere below 150 ºC and acts as a solvent-type of medium for the reaction to occur. Unfortunately, the Hall Group inventory only had the carboxylic acid **4-6**, which upon esterification lost the acetyl group to give alcohol **4-7** (Scheme 4–1). This acetyl group was easily reinstalled by deprotonation of the alcohol with an amine base, followed by nucleophilic attack on acetyl chloride. Compound **4-5** then underwent the reported Fries rearrangement to produce compound **4-4** as a solid beige crystalline solid. Although this new procedure requires three steps instead of the one step required for Friedel-Crafts acylation, it is a 40% increase in yield and produces a significantly more pure material.

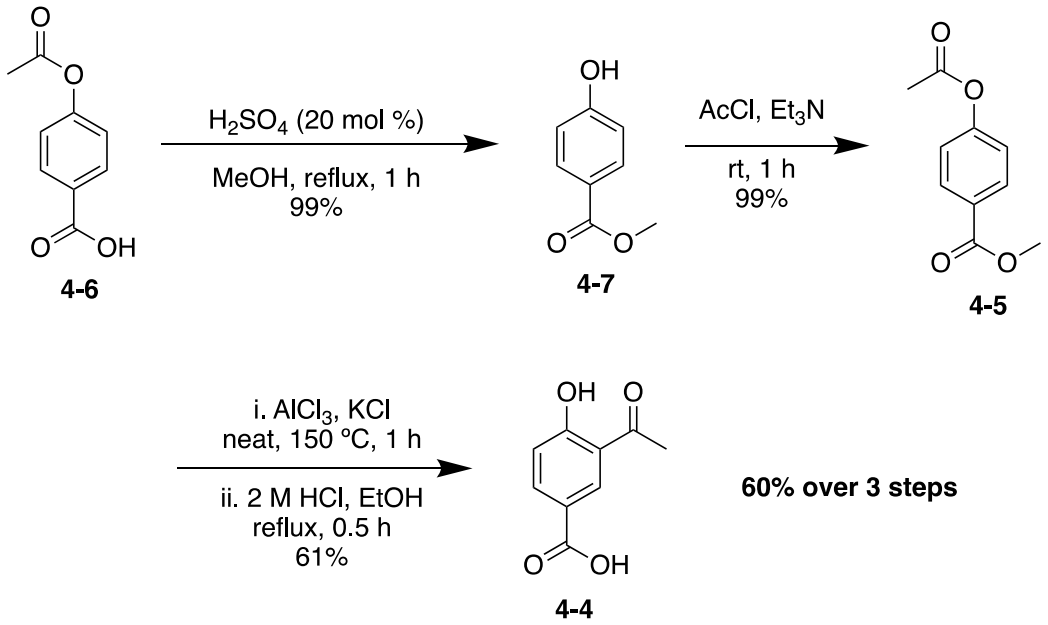

Scheme 4–1. Synthesis of compound **4-4**.

The next two steps, triflate installation and amide coupling, went according to the procedure (Scheme 4–2).a[2] The reported yields of the subsequent borylation and acid catalyzed ester deprotection could not be reproduced, after multiple attempts, in accordance to the original publication (Scheme 4–2).[2] Miyaura borylation is traditionally performed with potassium acetate, and the decision to use sodium acetate by the author could not be rationalized.[8] Furthermore, it is well known in the literature that ester cleavage is far more effective with a base as the reaction can go to completion to form a carboxylate salt, whereas under acid catalysis it is reversible and thus cannot go to completion.

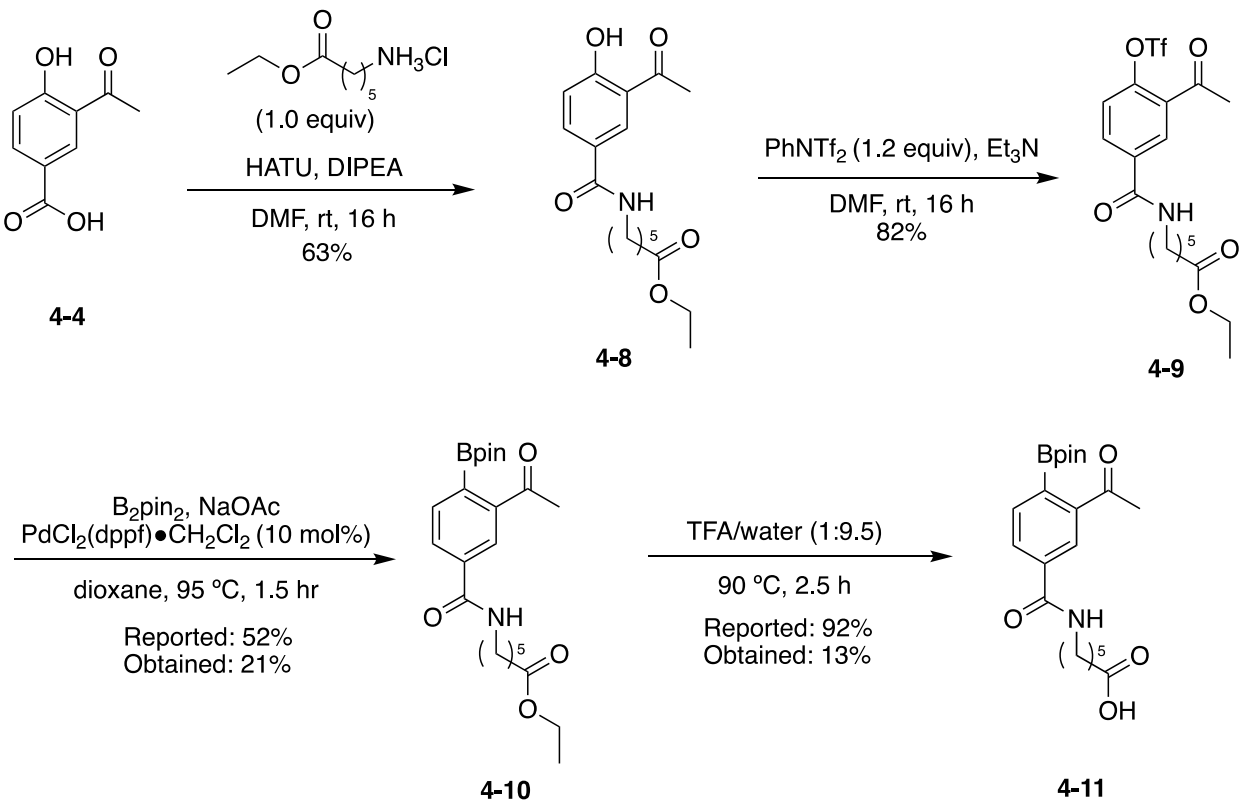

Scheme 4–2. First attempted synthesis of compound **4-11**.

In Scheme 4–3, it can be seen that after switching to potassium acetate as the base in the Miyaura borylation reaction, the yield matched that reported by Hall and coworkers.[2] It is thought that the original author may have confused the salts they used. Likewise, the deprotection of the ethyl ester to carboxylic acid proved to be significantly more effective in the present of base instead of acid, as the reaction was seen to have gone to completion via TLC after 30 mins at room temperature. The improved synthesis of compounds **4-10** and **4-11** were repeated at least once to ensure reproducibility and accuracy within ±5% yield.

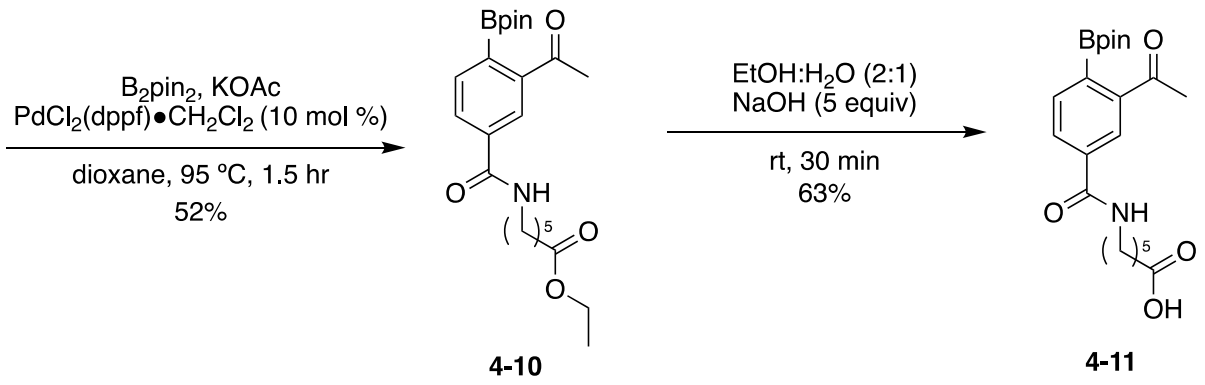

Scheme 4–3. Improved synthesis of compounds **4-10** and **4-11**.

The final functionalization required for the boronic acid tag was to activate the carboxylic acid with *sulfo*-NHS. This was achieved using DCC as a coupling agent (Scheme 4-4). The removal of the urea by-product DCU was significantly challenging. The precipitation of DCU is not immediate, after dissolving the crude material **4-2** in EtOAc, DCU would crash out then is removed by filtration, and the filtrate concentration. However, trying to dissolve the crude material in EtOAc would once again result in more DCU crashing out, which again had to be filtered off. This precipitation and filtration of DCU was done a total of four times until the LC-MS showed no DCU remaining in solution.

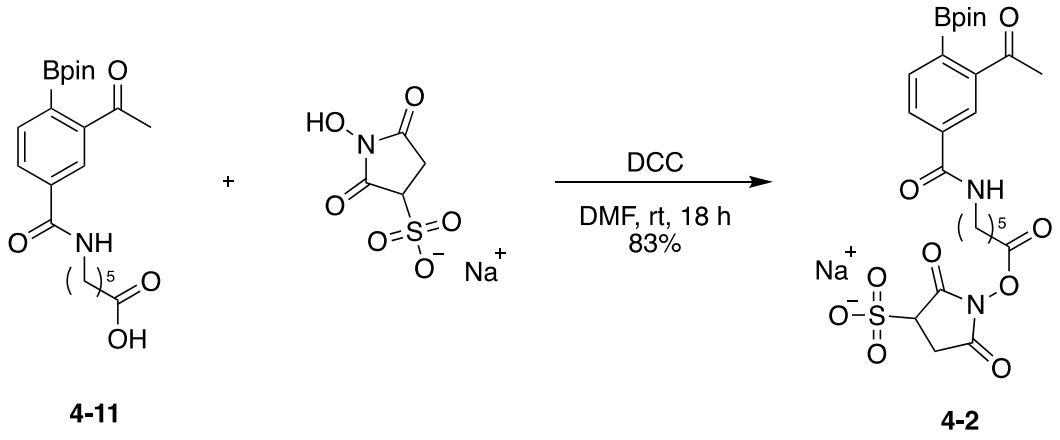

Scheme 4–4. Synthesis of activated *N*-hydroxysulfosuccinimide compound **4-2**.

4.3.2 Synthesis of Fluorescent Nopol Diol Reagent

The synthesis towards fluorescent diol **4-1** started with the *cis*-diol formation from commercially available (–)-nopol and the subsequent bromination to give bromide derivative **4-15**.[2] Compound **4-15** was first functionalized with hydrazine, then reacted with commercial fluorophore NIR-797 isothiocyanate to give compound **4-1** (Scheme 4–5). The purification of **4-1** by HPLC initially proved to be difficult, as the addition of any acid in a C8 HPLC column to give good peak separation ultimately resulted in degradation of the final compound. Attempts at HPLC purification without acid was inferior as adequate peak separation could not be obtained. Eventually, the substitution of acid for ammonium acetate gratifying gave compound **4-1** in 94% purity.

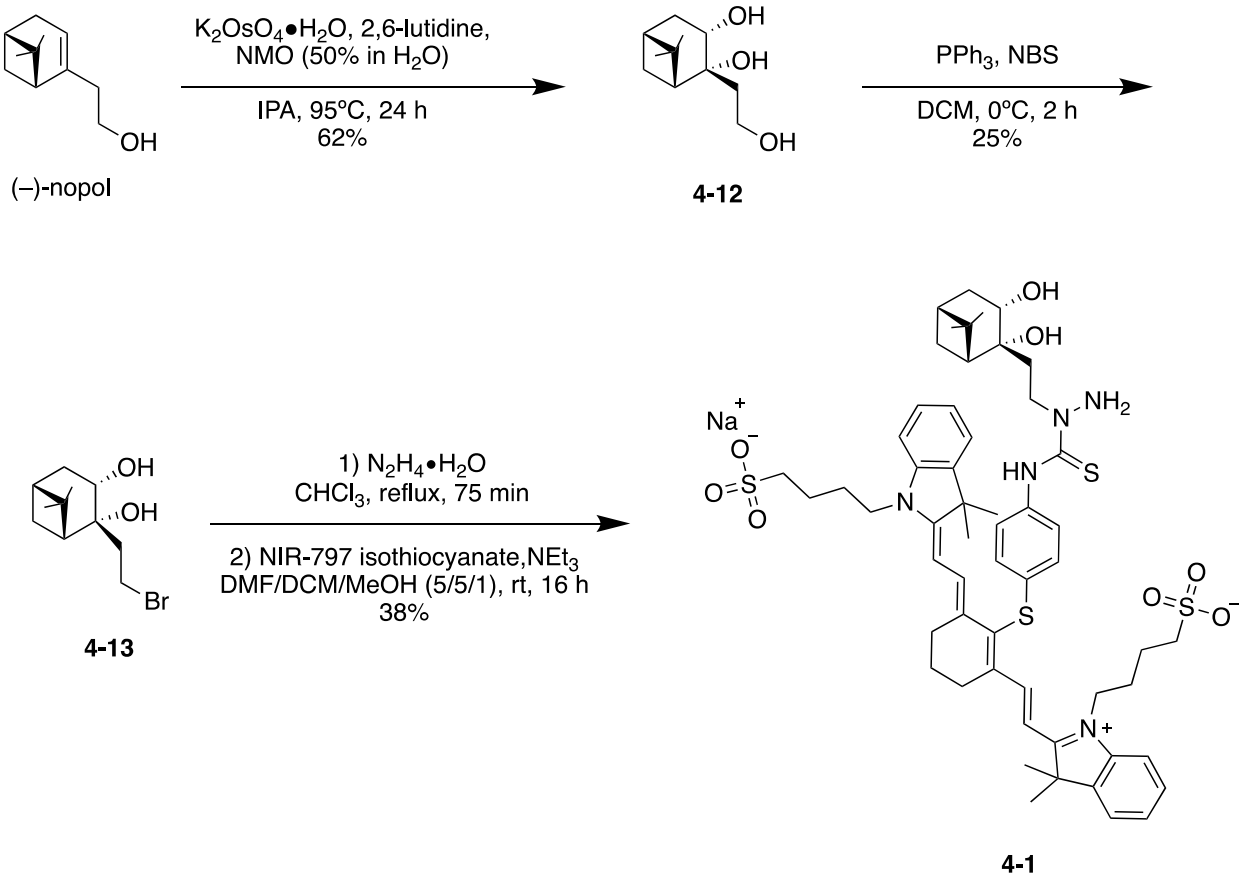

Scheme 4–5. Synthesis of **4-1**.

4.3.3 In Vivo Studies Conducted by the Brudno Lab

Compounds **4-1** and **4-2** were shipped to the Brudno lab at UNC for in vivo imaging testing. Amine group functionalized hydrogel deposits in healthy live mice were injected via syringe with 100 µL of boronic acid **4-2** in water at a concentration of 25 µM. After 24 hours, they were injected with 100 µL of nopol diol fluorophore **4-1** in water at a concentration of 50 µg/mL (Figure 4–4). On the second and seventh week, refills of the fluorophore of the same amount and concentration were administered again.

Figure 4–4. Pictures of mice after being injected with boronic acid **4-2** and fluorophore **4-1** on second week (top row), third week (middle row) and fourth week (bottom row).

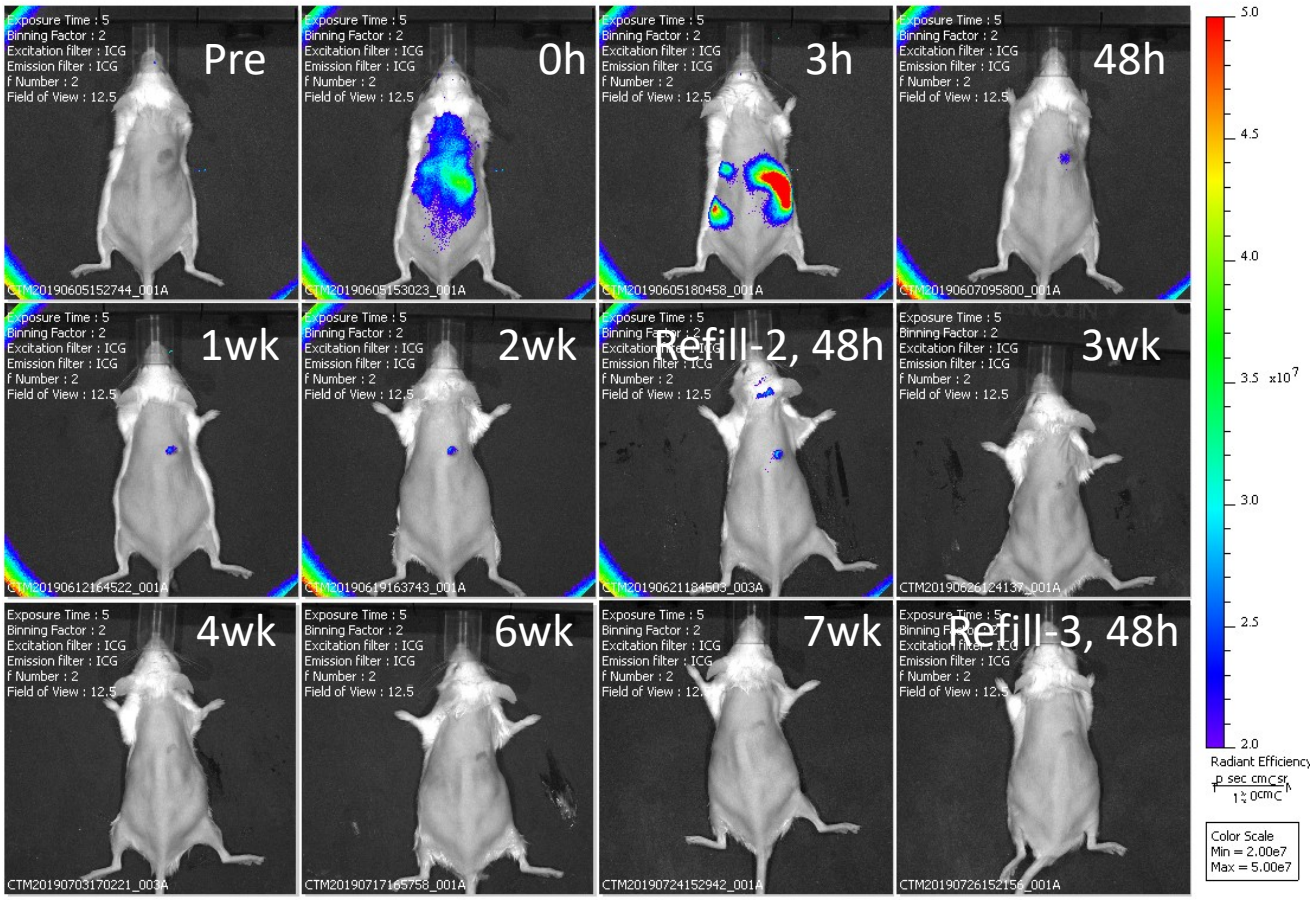

Figure 4–5. Emission captured of fluorescence in live mice by fluorescence microscopy.

The goal was to see increasing concentration of fluorescence at the site of boronic acid functionalized hydrogels in the live mice, and little to no fluorescence anywhere else. The results of emission captured by their fluorescence microscope are shown in Figure 4–5 and the values are graphically plotted and compared to control mice with no fluorescence compound injected in Figure 4–6.

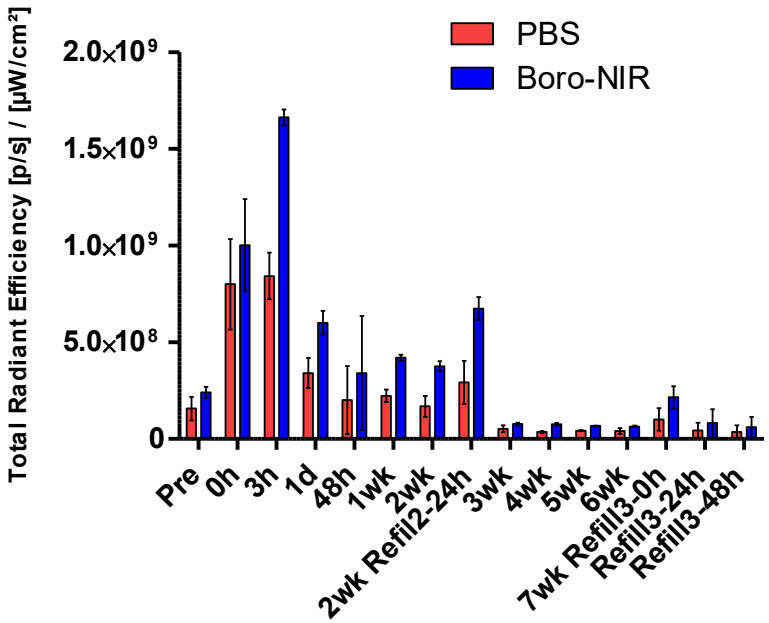

Three Refills Total Averaged Radiant Efficiencies

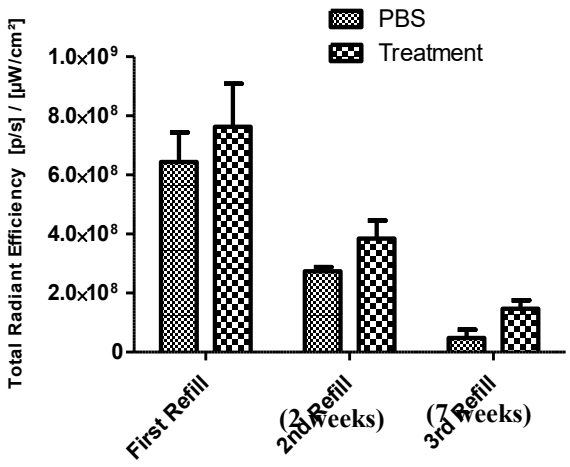

1. First Refill (First Refill Total Radiant Efficiency-Pre) P value = 0.13
2. Second Refill (Second refill After - Before) P value = 0.13
3. Third Refill (Third Refill After – Before) P value = 0.033

Figure 4–6. Graph comparing the total radiant efficiency of boronic acid tag **4-2** injected mice after being injected with a control phosphate-buffered saline solution and fluorophore compound **4-1**.

A notable observation in Figure 4–4 is that the mice have significant ulcerations once injected with the boron reagent **4-2** and these ulcerations cause an unwanted increase in emission detected by the microscope, as shown in Figures 4–5 and 4–6. The ulcerations are thought to have occurred from minor amounts of leftover DCU from the DCC coupling reaction (cf. Scheme 4–5). Despite this, the ulcerations clear up after about three weeks, and a statistically significant increase in fluorescence from a refill of compound **4-1** is seen in the mice compared to the PBS control mice (Figure 4–6).

4.4 Conclusions

Several synthetic steps of the boronic acid and nopol diol components of a boronate/thiosemicarbazone system were largely improved for use in bioconjugation imaging. The first step in the synthesis of the boronic acid tag, making compound **4-4**, was largely improved by employing a Fries rearrangement instead of a Friedel-Crafts acylation (cf. Scheme 4–1). This change resulted in an overall increase in yield of 40% and improved purity than previously reported. Although the alterations of the borylation and ester deprotection steps towards the synthesis of compound **4-2** did not lead to an overall increase in yield, they provided a reproducible procedure by consistently producing similar product yields; a feature missing in the original publication. The successful installation of a NIR-797 fluorophore to the nopol diol allowed the Brudno Group at the UNC to image this system *in vivo* with live mice. The Brudno Group observed some ulceration in the mice after injection with boronic acid tag **4-2**, which was thought to be due to minor amounts of leftover DCU from the DCC coupling (cf. Scheme 4–5). After three weeks, the ulcerations were largely gone, and re-administration of fluorophore **4-1** produced statistically significant results of emission compared to control mice injected with PBS only. The results

obtained by the Brudno Group show promising leads towards the use of the boronate/thiosemicarbazone system for *in vivo* imaging.

4.5 Experimental

4.5.1 General Information

Unless otherwise indicated, all reactions were performed under a nitrogen atmosphere using glassware that was washed thoroughly prior to use. All reagents were purchased from Sigma-Aldrich, Combi-Blocks or Alfa Aesar and used as received. DMF, DCM and THF were used directly from an MBraun Solvent Purification System. Thin layer chromatography (TLC) was performed on Merck Silica Gel 60 F254 plates, and visualized with UV light and curcumin stain. Flash chromatography was performed on ultra-pure silica gel 230-400 mesh. Nuclear magnetic resonance (NMR) spectra were recorded on Agilent/Varian INOVA-400 and INOVA-500 MHz instruments. The residual solvent protons (^{1}H) of $CDCl_3$ (7.26 ppm), acetone-d_6 (2.05 ppm), DMSO-d_6 (2.50 ppm), and D_2O (4.79 ppm) were used as internal standards, and the carbons signal (^{13}C) of $CDCl_3$ (77.06 ppm), DMSO-d_6 (39.51) and acetone-d_6 (29.84 and 206.26 ppm) were used as an internal standard. MestReNova software was used to analyze all of the NMR data. The following abbreviations are used in reporting NMR data: s, singlet; d, doublet; t, triplet; app t, apparent triplet; q, quartet; dd, doublet of doublets; ddd, doublet of doublet of doublets; dddd, doublet of doublet of doublet of doublets; dhept, doublet of heptlet; td, triplet of doublet; m, multiplet; comp m, complex multiplet. In ^{13}C NMR spectroscopy, the quaternary carbon bound to the boron atom is often missing due to the quadrupolar relaxation of boron. This effect was observed in each boronic acid or boronate ester compound. High-resolution mass spectra were recorded by the University of Alberta mass spectrometry services laboratory using either electron

impact (EI) or electrospray ionization (ESI) techniques. High-resolution mass spectra (HRMS) using electrospray ionization (ESI), and LC-MS mass spectra were recorded by the University of Alberta Mass Spectrometry Services Laboratory.

4.5.2 Chemical Synthesis and Analytical Data

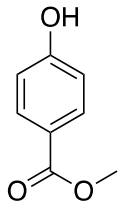

4-7

Methyl 4-hydroxybenzoate (4-7): To a 100 mL round bottom flask was added 4-acetoxybenzoic acid **4-6** and MeOH (32.0 mL). Concentrated sulfuric acid (8.00 mL) was added dropwise and the reaction refluxed for 2 h then brought to room temperature. The solution was concentrated in vacuo until 5-10 mL MeOH remained then diluted with 40 mL EtOAc. The phases were separated and the aqueous phase extracted with EtOAc (2 × 15 mL) and the combined organic extracts were washed with brine, dried over Na_2SO_4, filtered and concentrated *in vacuo* to afford the title compound as a pale-yellow solid (3.34 g, 99%) without any further purification. All spectral data matched the literature.[9]

^{1}H NMR (498 MHz, $CDCl_3$) δ 7.96 (dd, J = 4.2, 2.7 Hz, 2H), 6.89 (dt, J = 3.7, 1.7 Hz, 2H), 6.20 (s, 1H), 3.90 (s, 3H).

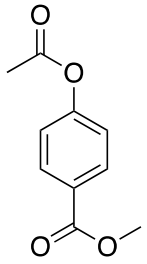

4-5

Methyl-(4-acetyl)benzoate (4-5): To a 100 mL round bottom flask was added **4-7** (3.28 g, 21.6 mmol) and dry DCM (50.0 mL) and cooled to 0 ºC. Triethylamine (4.52 mL, 32.4 mmol) was added dropwise and the reaction stirred for 1 h followed by the addition of acetyl chloride (1.70 mL, 23.8 mmol) via syringe. The solution was brought to room temperature and stirred for 2 h and diluted with water (20 mL). The phases were separated and the aqueous phase extracted with EtOAc (2 × 15 mL) and the combined organic extracts were washed with brine, dried over Na_2SO_4, filtered and concentrated *in vacuo* to afford the title compound as an off-white solid (4.14 g, 99%) without any further purification. All spectral data matched the literature.[10]

^{1}H NMR (400 MHz, DMSO-d_6) δ 8.00 (d, J = 8.7 Hz, 2H), 7.28 (d, J = 8.7 Hz, 2H), 3.85 (s, 3H), 2.29 (s, 3H).

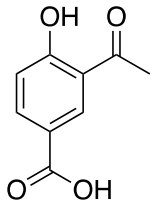

4-4

3-Acetyl-4-hydroxybenzoic acid (4-4): To a 250 mL round bottom flask was added **4-5** (4.05 g, 20.9 mmol), $AlCl_3$ (8.36 g, 62.7 mmol), and KCl (1.63 g, 21.9 mmol) equipped with an adapter under vacuum. The mixture was heated at 120 °C for 30 min and then heated at 150 °C for 1 h. After cooling to room temperature, a mixed solvent of 2 N HCl (100 mL) and EtOH (20 mL) was added to the reaction mixture. The resulting suspension was refluxed for 0.5 h. The crude product

was filtered using Büchner funnel to afford the title compound as a yellow solid (2.30 g, 61% yield). All spectral data matched the literature.[7]

^{1}H NMR (498 MHz, DMSO-d_6) δ 12.88 (s, 2H), 12.20 (s, 1H), 8.37 (d, *J* = 2.2 Hz, 1H), 8.02 (dd, *J* = 8.6, 2.2 Hz, 1H), 7.04 (d, *J* = 8.7 Hz, 1H), 2.67 (s, 3H).

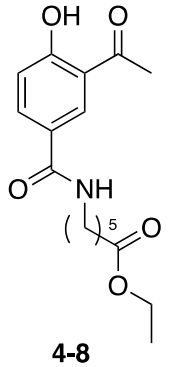

4-8

Ethyl 6-(3-acetyl-4-hydroxybenzamido)hexanoate (**4-8**): Ethyl 6-aminocaproate hydrochloride was prepared according to Sinyakov and coworkers.[11] To a 100 mL round bottom flask was added **4-4** (890 mg , 4.94 mmol) and HATU coupling reagent (1.88 g, 4.94) were dissolved in dry DMF (20 ml) at room temperature under nitrogen. Ethyl 6-aminocaproate hydrochloride (967 mg, 4.94 mmol) and N,N-diisopropylethylamine (2.75 mL, 15.8 mmol) were added. The reaction mixture was stirred for 16 h at room temperature, concentrated *in vacuo* and the crude residue dissolved in DCM (50 mL). The solution was washed with 1 M HCl (1 × 10 mL) and brine (1 × 10 ml). The organic phase was dried over Na_2SO_4, filtered and concentrated *in vacuo*. The crude material was purified by flash chromatography (1:9 to 5:5 EtOAc:hexanes) to afford the title compound was a yellow solid (1.00 g, 63% yield). All spectral data matched the literature.[2]

^{1}H NMR (498 MHz, $CDCl_3$) δ 8.34 (d, *J* = 2.2 Hz, 1H), 7.84 (dd, *J* = 8.7, 2.2 Hz, 1H), 6.94 (d, *J* = 8.7 Hz, 1H), 6.72 (s, 1H), 4.14 – 4.02 (m, 3H), 3.43 (td, *J* = 7.0, 5.5 Hz, 2H), 2.66 (s, 3H), 2.29

(t, *J* = 7.3 Hz, 2H), 1.62 (dt, *J* = 14.3, 7.4 Hz, 4H), 1.39 (t, *J* = 7.7 Hz, 2H), 1.22 (td, *J* = 7.1, 5.5 Hz, 4H).

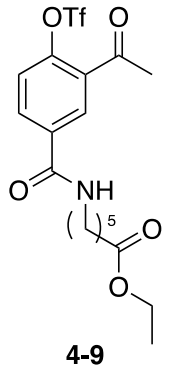

4-9

Ethyl 6-(3-acetyl-4-(((trifluoromethyl)sulfonyl)oxy)benzamido)hexanoate (**4-9**): *N*-Phenyl-bis(trifluoromethanesulfonimide) (3.05 g, 8.54 mmol) was added portion wise to a solution of **4-8** (2.11 g, 6.57 mmol) and NEt_3 (3.67 mL, 26.3 mmol) in dry DMF (20 ml) at room temperature under argon, and the reaction mixture was stirred for 16 h. The solution was concentrated *in vacuo* and purified by flash chromatography (1:3 to 1:1 EtOAc:hexanes) to afford the title compound as a beige solid (2.44 g, 82% yield). All spectral data matched the literature.[2]

^{1}H NMR (500 MHz, $CDCl_3$) δ 8.23 (d, *J* = 2.3 Hz, 1H), 8.01 (dd, *J* = 8.6, 2.3 Hz, 1H), 7.39 (d, *J* = 8.5 Hz, 1H), 6.58 (s, 1H), 4.10 (q, *J* = 7.1 Hz, 2H), 3.48 (td, *J* = 7.0, 5.8 Hz, 2H), 2.66 (s, 3H), 2.32 (t, *J* = 7.2 Hz, 2H), 1.65 (qd, *J* = 7.6, 2.1 Hz, 4H), 1.42 (dd, *J* = 8.8, 6.6 Hz, 2H), 1.23 (t, *J* = 7.1 Hz, 3H).

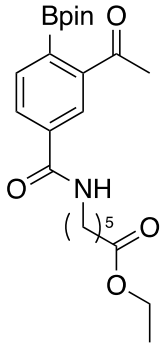

4-10

Ethyl-6-(3-acetyl-4-(4,4,5,5-tetramethyl-1,3,2-dioxaborolan-2-yl)benzamido)hexanoate (**4-10**): To a flame-dried round bottom flask flushed with argon was added **4-9** (1.12 g, 4.323 mmol), bis(pinacolato)diboron (2.20 g, 8.64 mmol), KOAc (1.27 g, 13.0 mmol), $PdCl_2$(dppf) (353 mg, 0.43 mmol) and freshly distilled dioxane (45 mL). The reaction mixture was stirred and heated at 80 °C for 90 min then concentrated *in vacuo*. The crude material was purified by flash chromatography (3:7 EtOAc:DCM) to afford the title compound as a colorless oil (688 mg, 52% yield). All spectral data matched the literature.[2]

^{1}H NMR (498 MHz, $CDCl_3$) δ 8.35 – 8.29 (m, 1H), 7.83 (dd, *J* = 7.6, 1.4 Hz, 1H), 7.55 (d, *J* = 7.5 Hz, 1H), 6.37 (s, 1H), 4.11 (q, *J* = 7.2 Hz, 2H), 3.48 (q, *J* = 6.6 Hz, 2H), 2.66 (s, 3H), 2.32 (t, *J* = 7.2 Hz, 2H), 1.67 (m, *J* = 10.0, 7.3 Hz, 5H), 1.44 (s, 12H), 1.24 (t, *J* = 7.1 Hz, 3H).

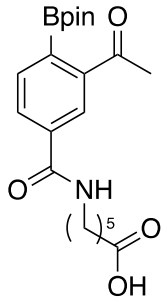

4-11

6-(3-Acetyl-4-(4,4,5,5-tetramethyl-1,3,2-dioxaborolan-2-yl)benzamido)hexanoic acid (4-11): To a solution of **4-10** (66 mg, 0.153 mmol) in EtOH (500 µL) and water (250 µL) was added NaOH (30.6 mg, 0.765 mmol) and the solution stirred for 30 min at room temperature. The solution was acidified with 1 M HCl (2 mL) and diluted with EtOAc (10 mL). The phases were separated and the aqueous phase extracted with EtOAc (2 × 5 mL) and the organic extracts dried over Na_2SO_4, filtered and concentrated *in vacuo*. The crude material was purified by flash chromatography (8% MeOH in EtOAc) to afford the title compound was an off-white solid (38.8 mg, 63% yield). All spectral data matched the literature.[2]

^{1}H NMR (498 MHz, $CDCl_3$) δ 8.29 (d, *J* = 1.7 Hz, 1H), 7.83 (dd, *J* = 7.6, 1.6 Hz, 1H), 7.51 (d, *J* = 7.6 Hz, 1H), 6.63 (t, *J* = 5.8 Hz, 1H), 3.43 (q, *J* = 6.9 Hz, 2H), 2.63 (s, 3H), 2.33 (t, *J* = 7.2 Hz, 2H), 1.73 – 1.55 (m, 4H), 1.43 (s, 14H).

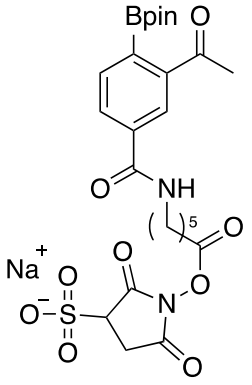

4-2

Reagent 4-2: To a flame-dried 10 mL round bottom flask was added **4-11** (53.0 mg, 0.131 mmol), sulfo-NHS (25.7 mg, 0.118 mmol), DCC (30.0 mg, 0.144 mmol) and dry DMF (1 mL). The mixture was stirred at room temperature for 18 h and concentrated in vacuo. The urea by-product DCU was precipitated with EtOAc and filtered using a Büchner funnel three times to provide the title compound as a white solid (58.3 mg, 83%). The Bpin and free boronic acid compounds were observed in LC-MS, as well as some protodeboronated product at a retention time of 4.3 min.

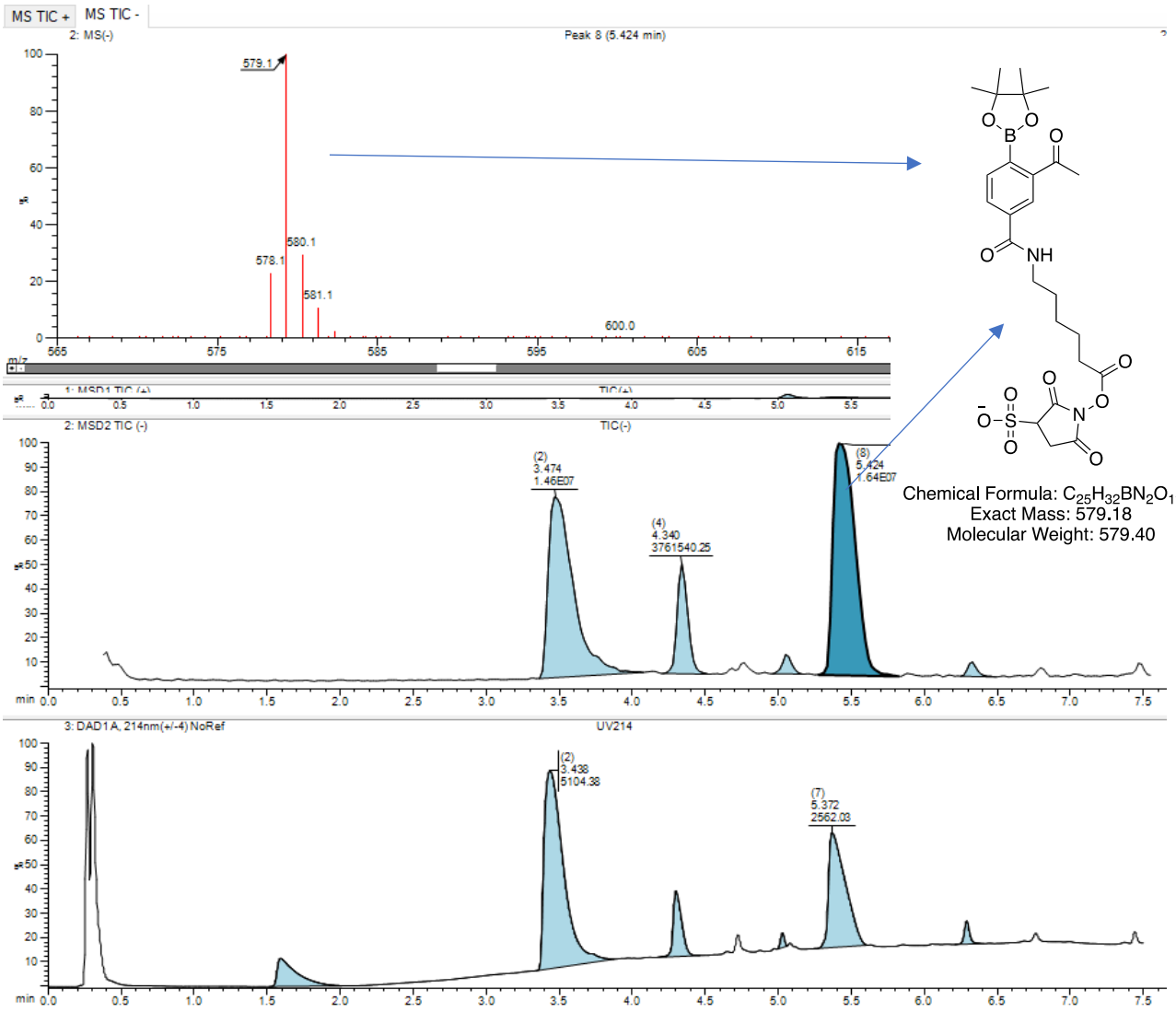
MS TIC +
MS TIC -
2: MS(-)
Peak 8 (5.424 min)
579.1
580.1
578.1
581.1
600.0
2: MSD2 TIC (-)
TIC(-)
(2)
3.474
1.46E07
(4)
4.340
3761540.25
(8)
5.424
1.64E07
3: DAD1A, 214nm(+/-4) NoRef
UV214
(2)
3.438
5104.38
(7)
5.372
2562.03
Chemical Formula: C25H32BN2O11S-
Exact Mass: 579.18
Molecular Weight: 579.40

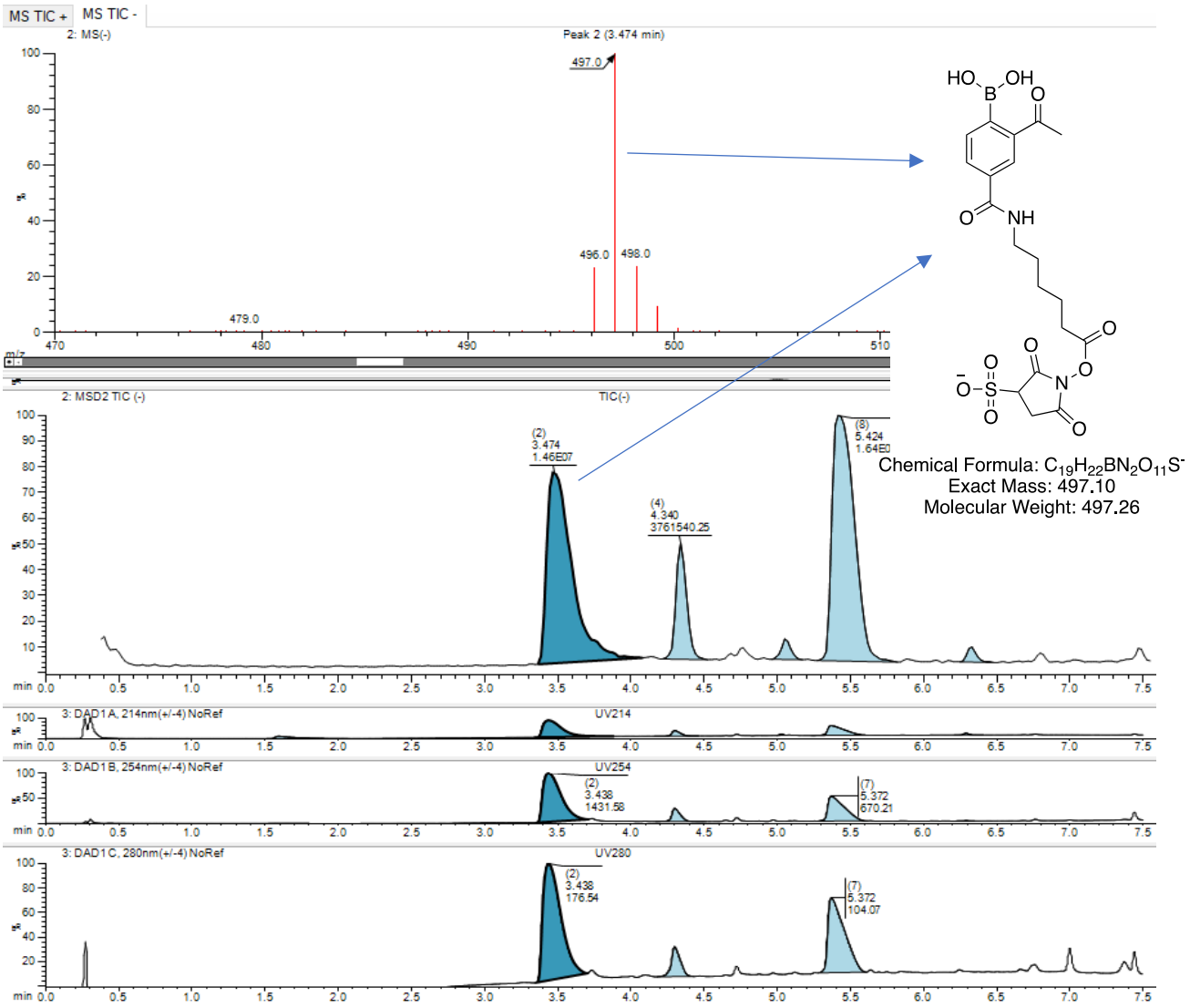

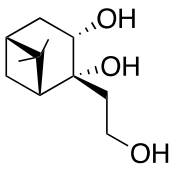

4-12

(1R,2R,3S,5R)-2-(2-Hydroxyethyl)-6,6-dimethylbicyclo[3.1.1]heptane-2,3-diol (4-12): NMO (50%) (1.3 equiv, 2.4 ml, 12 mmol) and 2,6-lutidine (1.2 equiv, 1.2 ml, 11 mmol) were added to commercially available (–)-nopol (1.0 equiv, 1.5 g, 8.9 mmol) in isopropanol (20 ml). $K_2OsO_4•H_2O$ purchased from Strem chemicals (1.7 mol%, 55 mg, 0.15 mmol) was added to the

reaction mixture, which was then stirred and heated to reflux at 95 °C for 24 h under ambient atmosphere. The resulting mixture was concentrated *in vacuo* and diluted with EtOAc (100 ml). The organic phase was washed with distilled water (1 × 10 ml), 1 M HCl (1 × 10 ml), and brine (1 × 10 ml), dried over Na_2SO_4, filtered and concentrated *in vacuo*. The crude residue was purified by flash chromatography (1:3 acetone:hexanes) to afford the title compound **4-12** as a colourless oil (1.14 g, 62% yield). All spectral data matched the literature.[2]

^{1}H NMR (498 MHz, Chloroform-d) δ 4.11 (dd, *J* = 9.4, 5.6 Hz, 1H), 3.95 (dd, *J* = 8.2, 3.1 Hz, 1H), 3.92 – 3.82 (m, 1H), 3.51 (s, 3H), 2.51 – 2.36 (m, 1H), 2.25 – 2.15 (m, 1H), 2.11 (t, *J* = 5.8 Hz, 1H), 1.98 – 1.80 (m, 2H), 1.75 – 1.60 (m, 2H), 1.42 (d, *J* = 10.3 Hz, 1H), 1.27 (s, 3H), 0.92 (s, 3H).

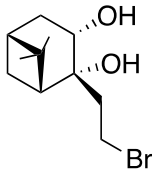

4-13

(1R,2R,3S,5R)-2-(2-Bromoethyl)-6,6-dimethylbicyclo[3.1.1]heptane-2,3-diol (4-13): To a mixture of compound 4-12 (300 mg, 1.50 mmol) and triphenylphosphine (433 mg, 1.65 mmol) in DCM (10 ml) at 0 ºC was added NBS (293 mg, 1.65 mmol) at once (to get improved yield, NBS needs to be added portion-wise to the reaction mixture). The reaction mixture was then brought to room temperature and stirred for 2 h after which time it was concentrated in vacuo. The crude residue was purified by flash chromatography (15:85 acetone:hexanes) to provide compound **4-13** as white solid (98.5 mg, 25% yield). All spectral data matched the literature.[2]

^{1}H NMR δ/ppm: (500 MHz, $CDCl_3$) 4.10 (ddd, *J* = 9.4, 6.0, 5.1 Hz, 1H), 3.63 – 3.57 (m, 1H), 3.57 – 3.51 (m, 1H), 2.97 (s, 1H), 2.54 (d, *J* = 6.0 Hz, 1H), 2.53 – 2.47 (m, 1H), 2.28 – 2.20 (m, 2H),

2.13 – 2.06 (m, 2H), 1.97 – 1.91 (m, 1H), 1.65 (ddd, *J* = 14.0, 5.1, 2.5 Hz, 1H), 1.36 (d, *J* = 10.5 Hz, 1H), 1.28 (s, 3H), 0.96 (s, 3H).

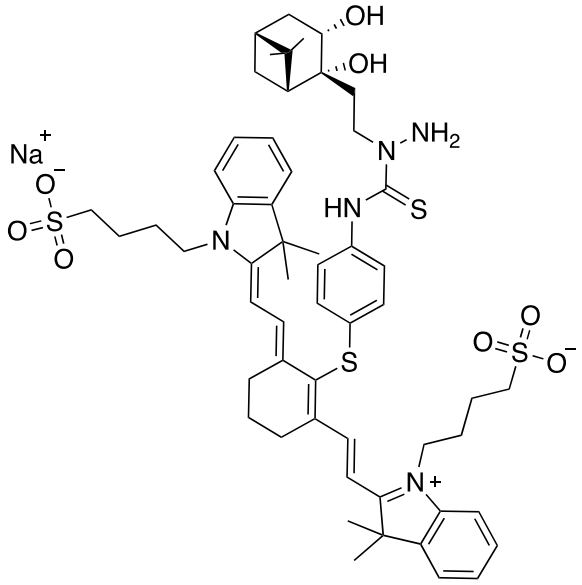

4-1

Reagent 4-1: To a solution of compound **4-13** (3.00 mg, 0.011 mmol) in chloroform (1.0 ml) was added $NH_2NH_2•H_2O$ (11.0 µl, 0.228 mmol) under inert atmosphere at room temperature. The reaction mixture was stirred under reflux for 75 min at 75 °C and then concentrated in vacuo. The crude residue was kept under vacuum for 2 h and used in the next step without further purification. To the crude residue was added NIR-797 isothiocyanate (10.0 mg, 0.011 mmol) and the reagents dissolved in DMF/DCM/MeOH (0.45 ml/0.45 ml/0.050 ml) at room temperature under inert atmosphere. NEt_3 (1.2 equiv, 21 µl, 0.15 mmol) was added via syringe and the reaction was stirred for 16 h at room temperature. The reaction mixture was concentrated in vacuo and purified using reverse phase HPLC using a Agilent Eclipse XDB-C18, 5um, 9.4X250 mm column with 10 mM ammonium acetate in both water (A) and acetonitrile (B). Elution (3 mL/min) was with a linear gradient from 0 to 20% B in 2 min, 20% to 95% B for 12 min and a post run elution

from 95% to 20% B over 2 mins to provide the title compound **4-1** as a greenish blue powder (4.2 mg, 38% yield).

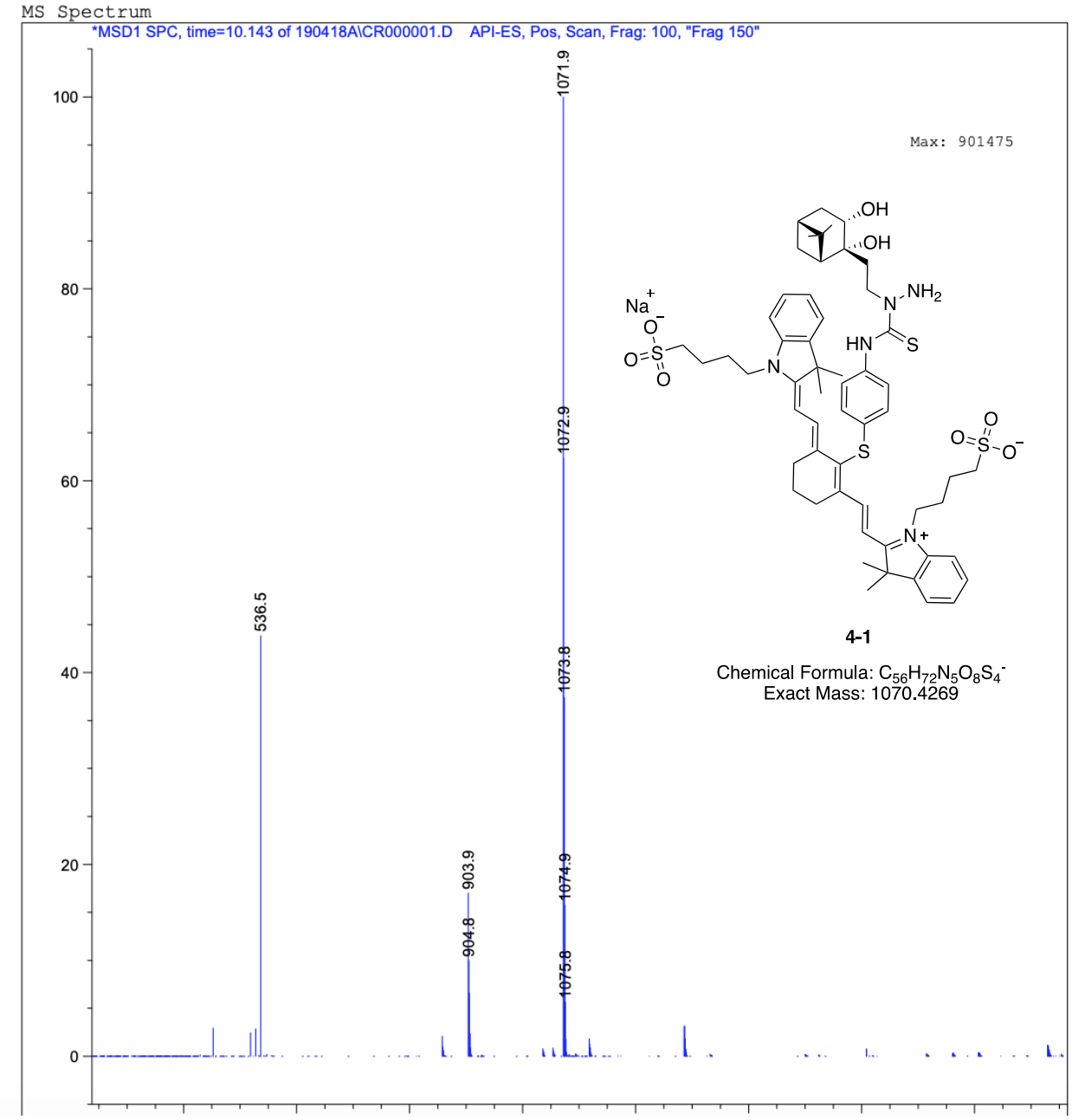

4.6 References

(1) Akgun, B.; Hall, D. G. *Angew. Chem. Int. Ed.* **2016**, *55* (12), 3909.

(2) Akgun, B.; Li, C.; Hao, Y.; Lambkin, G.; Derda, R.; Hall, D. G. *J. Am. Chem. Soc.* **2017**, *139* (40), 14285.

(3) Brudno, Y.; Desai, R. M.; Kwee, B. J.; Joshi, N. S.; Aizenberg, M.; Mooney, D. J. *ChemMedChem* **2015**, *10* (4), 617.

(4) Brudno, Y.; Pezone, M. J.; Snyder, T. K.; Uzun, O.; Moody, C. T.; Aizenberg, M.; Mooney, D. J. *Biomaterials* **2018**, *178*, 373.

(5) Conte, M. L.; Staderini, S.; Marra, A.; Sanchez-Navarro, M.; Davis, B. G.; Dondoni, A. *Chem. Commun.* **2011**, *47* (39), 11086.

(6) Patterson, D. M.; Nazarova, L. A.; Prescher, J. A. *ACS Chem. Biol.* **2014**, *9* (3), 592.

(7) Zhang, M.; Zhang, Y.; Song, M.; Xue, X.; Wang, J.; Wang, C.; Zhang, C.; Li, C.; Xiang, Q.; Zou, L.; Wu, X.; Wu, C.; Dong, B.; Xue, W.; Zhou, Y.; Chen, H.; Wu, D.; Ding, K.; Xu, Y. *J. Med. Chem.* **2018**, *61* (7), 3037.

(8) Miyaura, N.; Suzuki, A. *Chem. Rev.* **1995**, *95* (7), 2457.

(9) Wei, P.-F.; Qi, M.-Z.; Wang, Z.-P.; Ding, S.-Y.; Yu, W.; Liu, Q.; Wang, L.-K.; Wang, H.-Z.; An, W.-K.; Wang, W. *J. Am. Chem. Soc.* **2018**, *140* (13), 4623.

(10) Chakraborti, A. K.; Gulhane, R. *Chem. Commun.* **2003**, No. 15, 1896.

(11) Ryabinin, V. A.; Zakharova, O. D.; Yurchenko, E. Y.; Timofeeva, O. A.; Martyanov, I. V.; Tokarev, A. A.; Belanov, E. F.; Bormotov, N. I.; Tarrago-Litvak, L.; Andreola, M. L.; Litvak, S.; Nevinsky, G. A.; Sinyakov, A. N. *Bioorganic & Medicinal Chemistry* **2000**, *8* (5), 985.

Chapter Five

Thesis Conclusions and Future Perspectives

5.1 Thesis Conclusions

Boron containing compounds have a great potential to be applicable in many aspects of chemistry and biology due to their versatile nature in terms of reactivity and physical properties. The synthesis of new types of boron compounds will open doors for application not yet seen, and can improve applications that currently exist in the areas of materials, pharmaceuticals and biology. In this regard, Chapter 2 describes the efforts made in the development and synthesis of a novel, water soluble, "frustrated" benzoxaborole, which to the best of my knowledge, is the first ever reported permanently open-benzoxaborole. The synthesis of this novel frustrated benzoxaborole was efficiently completed in seven high yielding steps that utilize the polarity of the compound for simple purification without the need of chromatography. This novel compound was shown to exist in a permanent open ortho-hemiacetal phenylboronic acid structure through various NMR and mass spectroscopic methods. The unique properties of this novel compound were also explored, such as its binding behavior, which is distinctive from both traditional boronic acids and benzoxaboroles, and its low pKa in aqueous systems allowing for high solubility in water. Furthermore, the bioconjugation of this compound with amines, cysteine and lysozyme was shown to be effective and comparable to known methods that currently exist in literature.

Chapter 3 highlights the work executed during collaboration between the Hall Group and the National Research Council (NRC) in Halifax towards the identification of a boronic acid for the optimal "catch-and-release" system of diol containing marine neurotoxins. A large survey of

mostly ortho substituted boronic acids were examined for the binding of a potent neurotoxin called tetrodotoxin (TTX). The importance of pKa and Lewis acidity of these boronic acids were highlighted in these assays as the binding affinity of most boronic acids to TTX was more favorable with low pKa boronic acids and in high pH solutions. The kinetics for the hydrolysis of boronic acid/TTX conjugates were also examined and analyzed by LC-MS. These assays revealed 2-(trifluoromethyl)phenylboronic acid to give the fastest and most efficient conjugation with TTX, as well as rapid and near complete hydrolysis with acid.

Finally, Chapter 4 is on the collaboration efforts with Prof. Brudno's group at the University of Northern Carolina (UNC). Here, the "click" boronate/thiosemicarbazone conjugation system developed by Hall and coworkers was to be tested for imaging in live mice. Several synthetic steps towards the synthesis of the boronic acid tag were improved, and the nopoldiol derivatized with a varied fluorophore to meet the needs of the fluorescence microscope in the Brudno Group. The Brudno group reported statistically significant fluorescence detection in the boronic acid tagged mice injected with fluorescent nopoldiol, compared to a control group injected with phosphate saline buffered (PBS) solution.

5.2 Future Perspectives

5.2.1 Derivatized "Frustrated" Benzoxaborole for Improved Conjugation

The novel "frustrated" benzoxaborole compound proved to be suitable for conjugation of small amine compounds and amino residues on lysozyme, but the dual binding of amino and thiol containing *N*-terminal cysteine proved not to give the desired conjugate. Unfortunately, the attack of the nucleophilic thiol group occurred on the hemiacetal functionality to release the hydroxy arm, instead of on the boronic acid functionality which would have possibly provided a very stable

3-fused membered ring system (Figure 5–1a). It is postulated that the hydroxy group is not nucleophilic enough group to remain cyclized during attack by a more nucleophilic group such as thiol. Alternatively, the five membered hemiacetal may not be thermodynamically favored enough, and therefore is reversible and opens during conjugation. To transform this hemiacetal to a more stable ring, installing a more nucleophilic thiol group could potentially keep the ring closed, or alternatively, a 6-membered hemiacetal ring could provide superior thermodynamic stability which is less likely to be reversible (Figure 5–1b). The derivatives in Figure 5–1b would not only induce stronger binding with *N*-terminal cysteines, but also be two new "frustrated" benzoxaborole type structures, provided they remain as ortho-hydroxy boronic acid structures.

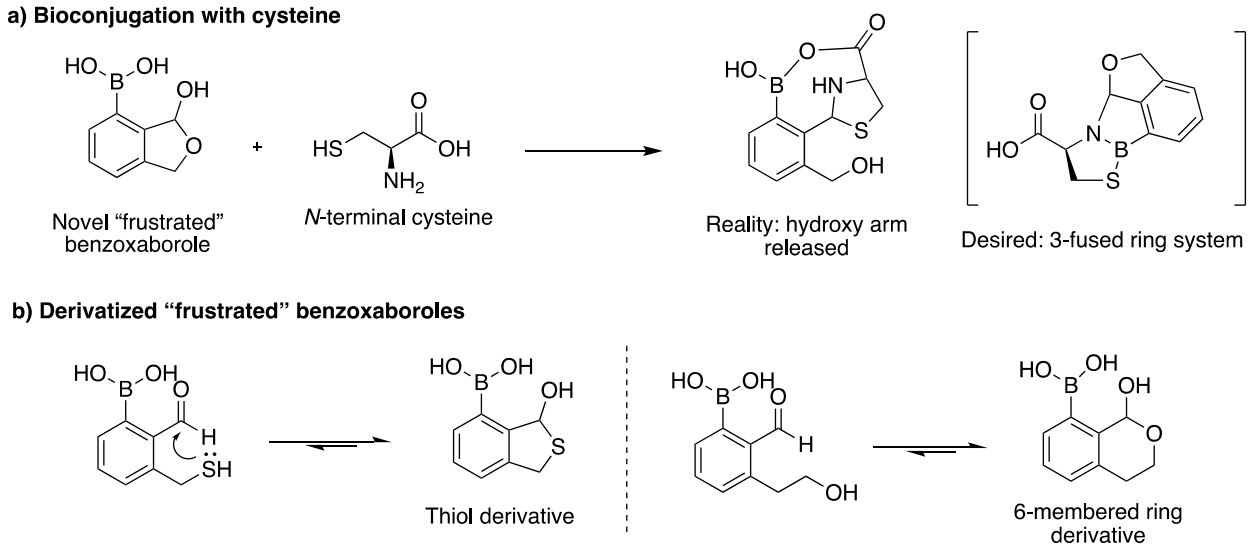

Figure 5–1. Original "frustrated" benzoxaborole conjugation result with *N*-terminal cysteine (a) and potential derivatives (b).

5.2.2 Other Boronic Acid Polymer Gels for Purification of Toxins

2-(Trifluoromethyl)phenylboronic acid proved to be the ideal candidate for a "catch-and-release" system of diol containing neurotoxins in the survey conducted. A carboxylic acid

functionality was introduced for conjugation onto an amine functionalized polymer, however, a longer linker between the boronic acid and polymer may be required instead to avoid sterics of the binding toxins. The NRC in Halifax will explore conjugation of carboxylated 2-(trifluoromethyl)phenylboronic onto a polymer and then purification of the toxin and hopefully observe better binding and release than current commercially available boronic acid polymer gels. Furthermore, the results in Chapter 3 revealed that 2-isopropylphenylboronic acid was also great at toxin conjugation and acid release, and this may also be a suitable compound to consider derivatizing for polymer attachment.

5.2.3 Further Modifications for *in vivo* Imaging of the Boronate Thiosemicarbazone Conjugation

The Brudno group provided valuable information about *in vivo* labelling of the boronate/thiosemicarbazone system developed by Hall and coworkers, although modifications still need to be addressed. Firstly, the boronic acid tag needs to be re-synthesized and purified by HPLC prior to injection into mice to avoid ulcerations. The ulcerations transmitted signals that interfere with the signals emitted from the fluorophore injected into the mice. Secondly, Prof. Brudno highlighted that a different fluorophore would need to be examined for better compatibility with their microscope. The NIR-797 isothiocyanate fluorophore proved to not emit fluorescence exactly at the reported wavelength after conjugation onto nopol diol.

Bibliography

(1) Hall, D. G. *Boronic Acids. Preparation and Applications in Organic Synthesis, Medicine and Materials*, 2nd Completely Revised ed.; Hall, D. G., Ed.; Wiley-VCH: Weinheim, Germany, 2011.

(2) Baker, S. J.; Zhang, Y.-K.; Akama, T.; Lau, A.; Zhou, H.; Hernandez, V.; Mao, W.; Alley, M. R. K.; Sanders, V.; Plattner, J. J. *J. Med. Chem.* **2006**, *49* (15), 4447.

(3) Field-Smith, A.; Morgan, G. J.; Davies, F. E. *Ther. Clin. Risk Manag.* **2006**, *2* (3), 271.

(4) Lomovskaya, O.; Sun, D.; Rubio-Aparicio, D.; Nelson, K.; Tsivkovski, R.; Griffith, D. C.; Dudley, M. N. *Antimicrob. Agents Chemother.* **2017**, *61* (11), e01443.

(5) Akama, T.; Baker, S. J.; Zhang, Y.-K.; Hernandez, V.; Zhou, H.; Sanders, V.; Freund, Y.; Kimura, R.; Maples, K. R.; Plattner, J. J. *Bioorg. Med. Chem. Lett.* **2009**, *19* (8), 2129.

(6) Adamczyk-Woźniak, A.; Borys, K. M.; Sporzyński, A. *Chem. Rev.* **2015**, *115* (11), 5224.

(7) Adamczyk-Woźniak, A.; Cyrański, M. K.; Żubrowska, A.; Sporzyński, A. *J. Organomet. Chem.* **2009**, *694* (22), 3533.

(8) Torssell, K. *Ark. Kemi.* **1957**, *10*, 507.

(9) Settepani, J. A.; Stokes, J. B.; Borkovec, A. B. *J. Med. Chem.* **1970**, *13* (1), 128.

(10) Torssell, K.; McClendon, J. H.; Somers, G. F. *Acta Chem. Scand.* **1958**, *12* (7), 1373.

(11) Wiskur, S. L.; Lavigne, J. J.; Ait-Haddou, H.; Lynch, V.; Chiu, Y. H.; Canary, J. W.; Anslyn, E. V. *Org. Lett.* **2001**, *3* (9), 1311.

(12) Ni, W.; Kaur, G.; Springsteen, G.; Wang, B.; Franzen, S. *Bioorganic Chem.* **2004**, *32* (6), 571.

(13) Zhu, L.; Shabbir, S. H.; Gray, M.; Lynch, V. M.; Sorey, S.; Anslyn, E. V. *J. Am. Chem. Soc.* **2006**, *128* (4), 1222.

(14) Collins, B. E.; Sorey, S.; Hargrove, A. E.; Shabbir, S. H.; Lynch, V. M.; Anslyn, E. V. *J. Org. Chem.* **2009**, *74* (11), 4055.

(15) Dewar, M. J. S.; Jones, Richard. *J. Am. Chem. Soc.* **1967**, *89* (10), 2408.

(16) Allen, F. H. *Acta Crystallogr. Sect. B* **2002**, *58* (3 Part 1), 380.

(17) Cyrański, M. K.; Jezierska, A.; Klimentowska, P.; Panek, J. J.; Sporzyński, A. *J. Phys. Org. Chem.* **2008**, *21* (6), 472.

(18) Korich, A. L.; Iovine, P. M. *Dalton Trans.* **2010**, *39* (6), 1423.

(19) Bhat, K. L.; Markham, G. D.; Larkin, J. D.; Bock, C. W. *J. Phys. Chem. A* **2011**, *115* (26), 7785.

(20) Adamczyk-Woźniak, A.; Kaczorowska, E.; Kredátusova, J.; Madura, I.; Marek, P. H.; Matuszewska, A.; Sporzyński, A.; Uchman, M. *Eur. J. Inorg. Chem.* **2018**, *2018* (13), 1492.

(21) Frankland, E.; Duppa, B. F. *Ann. Chem. Pharm.* **1860**, *115* (3), 319.

(22) Frankland, E.; Duppa, B. F. *Proc. R. Soc. Lond.* **1860**, *10*, 568.

(23) Miyaura, N.; Suzuki, A. *Chem. Rev.* **1995**, *95* (7), 2457.

(24) Gilman, H.; Santucci, L.; Swayampati, D. R.; Ranck, R. O. *J. Am. Chem. Soc.* **1957**, *79* (12), 3077.

(25) Evans, D. A.; Katz, J. L.; Peterson, G. S.; Hintermann, T. *J. Am. Chem. Soc.* **2001**, *123* (49), 12411.

(26) Ishiyama, T.; Takagi, J.; Ishida, K.; Miyaura, N.; Anastasi, N. R.; Hartwig, J. F. *J. Am. Chem. Soc.* **2002**, *124* (3), 390.

(27) Chotana, G. A.; Rak, M. A.; Smith, M. R. *J. Am. Chem. Soc.* **2005**, *127* (30), 10539.

(28) Tomsho, J. W.; Pal, A.; Hall, D. G.; Benkovic, S. J. *ACS Med. Chem. Lett.* **2012**, *3* (1), 48.

(29) Nocentini, A.; Supuran, C. T.; Winum, J.-Y. *Expert Opin. Ther. Pat.* **2018**, *28* (6), 493.

(30) Zhang, J.; Zhu, M.; Lin, Y.; Zhou, H. *Sci. China Chem.* **2013**, *56* (10), 1372.

(31) Fernandes, G. F. S.; Denny, W. A.; Dos Santos, J. L. *Eur. J. Med. Chem.* **2019**, *179*, 791.

(32) Sletten, E. M.; Bertozzi, C. R. *Angew. Chem. Int. Ed.* **2009**, *48* (38), 6974.

(33) Ramil, C. P.; Lin, Q. *Chem. Commun.* **2013**, *49* (94), 11007.

(34) Akgun, B.; Hall, D. G. *Angew. Chem. Int. Ed.* **2018**, *57* (40), 13028.

(35) Cal, P. M. S. D.; Vicente, J. B.; Pires, E.; Coelho, A. V.; Veiros, L. F.; Cordeiro, C.; Gois, P. M. P. *J. Am. Chem. Soc.* **2012**, *134* (24), 10299.

(36) Cal, P. M. S. D.; Frade, R. F. M.; Cordeiro, C.; Gois, P. M. P. *Chem. - Eur. J.* **2015**, *21* (22), 8182.

(37) Cal, P. M. S. D.; Frade, R. F. M.; Chudasama, V.; Cordeiro, C.; Caddick, S.; Gois, P. M. P. *Chem. Commun.* **2014**, *50* (40), 5261.

(38) Gutiérrez-Moreno, N. J.; Medrano, F.; Yatsimirsky, A. K. *Org. Biomol. Chem.* **2012**, *10* (34), 6960.

(39) Schmidt, P.; Stress, C.; Gillingham, D. *Chem. Sci.* **2015**, *6* (6), 3329.
(40) Bandyopadhyay, A.; Gao, J. *Chem. - Eur. J.* **2015**, *21* (42), 14748.
(41) Gillingham, D. *Org. Biomol. Chem.* **2016**, *14* (32), 7606.
(42) Dilek, O.; Lei, Z.; Mukherjee, K.; Bane, S. *Chem. Commun.* **2015**, *51* (95), 16992.
(43) Gu, H.; Chio, T. I.; Lei, Z.; Staples, R. J.; Hirschi, J. S.; Bane, S. *Org. Biomol. Chem.* **2017**, *15* (36), 7543.
(44) Bandyopadhyay, A.; Cambray, S.; Gao, J. *J. Am. Chem. Soc.* **2017**, *139* (2), 871.
(45) Bandyopadhyay, A.; Cambray, S.; Gao, J. *Chem. Sci.* **2016**, *7* (7), 4589.
(46) Faustino, H.; Silva, M. J. S. A.; Veiros, L. F.; Bernardes, G. J. L.; Gois, P. M. P. *Chem. Sci.* **2016**, *7* (8), 5052.
(47) Botti, P.; Pallin, T. D.; Tam, J. P. *J. Am. Chem. Soc.* **1996**, *118* (42), 10018.
(48) Dowlut, M.; Hall, D. G. *J. Am. Chem. Soc.* **2006**, *128* (13), 4226.
(49) Ellis, G. A.; Palte, M. J.; Raines, R. T. *J. Am. Chem. Soc.* **2012**, *134* (8), 3631.
(50) Andersen, K. A.; Smith, T. P.; Lomax, J. E.; Raines, R. T. *ACS Chem. Biol.* **2016**, *11* (2), 319.
(51) Wulff, G. *Pure Appl. Chem.* **1982**, *54* (11), 2093.
(52) Yang, W.; Fan, H.; Gao, X.; Gao, S.; Karnati, V. V. R.; Ni, W.; Hooks, W. B.; Carson, J.; Weston, B.; Wang, B. *Chem. Biol.* **2004**, *11* (4), 439.
(53) Hoeg-Jensen, T. *QSAR Comb. Sci.* **2004**, *23* (5), 344.
(54) Akgun, B.; Hall, D. G. *Angew. Chem. Int. Ed.* **2016**, *55* (12), 3909.
(55) Akgun, B.; Li, C.; Hao, Y.; Lambkin, G.; Derda, R.; Hall, D. G. *J. Am. Chem. Soc.* **2017**, *139* (40), 14285.
(56) Halo, T. L.; Appelbaum, J.; Hobert, E. M.; Balkin, D. M.; Schepartz, A. *J. Am. Chem. Soc.* **2009**, *131* (2), 438.
(57) Meadows, M. K.; Roesner, E. K.; Lynch, V. M.; James, T. D.; Anslyn, E. V. *Org. Lett.* **2017**, *19* (12), 3179.
(58) Chapin, B. M.; Metola, P.; Lynch, V. M.; Stanton, J. F.; James, T. D.; Anslyn, E. V. *J. Org. Chem.* **2016**, *81* (18), 8319.
(59) Vshyvenko, S.; Clapson, M. L.; Suzuki, I.; Hall, D. G. *ACS Med. Chem. Lett.* **2016**, *7* (12), 1097.
(60) Luliński, S.; Serwatowski, J. *J. Organomet. Chem.* **2007**, *692* (14), 2924.

(61) Li, X.; Zhang, Y.-K.; Liu, Y.; Ding, C. Z.; Zhou, Y.; Li, Q.; Plattner, J. J.; Baker, S. J.; Zhang, S.; Kazmierski, W. M.; Wright, L. L.; Smith, G. K.; Grimes, R. M.; Crosby, R. M.; Creech, K. L.; Carballo, L. H.; Slater, M. J.; Jarvest, R. L.; Thommes, P.; Hubbard, J. A.; Convery, M. A.; Nassau, P. M.; McDowell, W.; Skarzynski, T. J.; Qian, X.; Fan, D.; Liao, L.; Ni, Z.-J.; Pennicott, L. E.; Zou, W.; Wright, J. *Bioorg. Med. Chem. Lett.* **2010**, *20* (19), 5695.

(62) Molander, G. A.; Trice, S. L. J.; Kennedy, S. M.; Dreher, S. D.; Tudge, M. T. *J. Am. Chem. Soc.* **2012**, *134* (28), 11667.

(63) Yuen, A. K. L.; Hutton, C. A. *Tetrahedron Lett.* **2005**, *46* (46), 7899.

(64) Molander, G. A.; Cavalcanti, L. N.; Canturk, B.; Pan, P.-S.; Kennedy, L. E. *J. Org. Chem.* **2009**, *74* (19), 7364.

(65) Ricardo, C. L.; Mo, X.; McCubbin, J. A.; Hall, D. G. *Chem. Eur. J.* **2015**, *21* (11), 4218.

(66) Roughley, S. D.; Jordan, A. M. *J. Med. Chem.* **2011**, *54* (10), 3451.

(67) Valeur, E.; Bradley, M. *Chem. Soc. Rev.* **2009**, *38* (2), 606.

(68) Montalbetti, C. A. G. N.; Falque, V. *Tetrahedron* **2005**, *61* (46), 10827.

(69) Ishihara, K.; Ohara, S.; Yamamoto, H. *J. Org. Chem.* **1996**, *61* (13), 4196.

(70) Arnold, K.; Batsanov, A. S.; Davies, B.; Whiting, A. *Green Chem.* **2008**, *10* (1), 124.

(71) Starkov, P.; Sheppard, T. D. *Org. Biomol. Chem.* **2011**, *9* (5), 1320.

(72) Gernigon, N.; Al-Zoubi, R. M.; Hall, D. G. *J. Org. Chem.* **2012**, *77* (19), 8386.

(73) Cusick, K.; Sayler, G. *Marine Drugs* **2013**, *11* (12), 991.

(74) Gerssen, A.; Pol-Hofstad, I. E.; Poelman, M.; Mulder, P. P. J.; Van den Top, H. J.; De Boer, J. *Toxins* **2010**, *2* (4), 878.

(75) Bane, V.; Lehane, M.; Dikshit, M.; O'Riordan, A.; Furey, A. *Toxins* **2014**, *6* (2), 693.

(76) Boundy, M. J.; Selwood, A. I.; Harwood, D. T.; McNabb, P. S.; Turner, A. D. *Journal of Chromatography A* **2015**, *1387*, 1.

(77) Zhuo, L.; Yin, Y.; Fu, W.; Qiu, B.; Lin, Z.; Yang, Y.; Zheng, L.; Li, J.; Chen, G. *Food Chemistry* **2013**, *137* (1–4), 115.

(78) Miles, C. O.; Kilcoyne, J.; McCarron, P.; Giddings, S. D.; Waaler, T.; Rundberget, T.; Samdal, I. A.; Løvberg, K. E. *J. Agric. Food Chem.* **2018**, *66* (11), 2962.

(79) Turner, A.; Dhanji-Rapkova, M.; Coates, L.; Bickerstaff, L.; Milligan, S.; O'Neill, A.; Faulkner, D.; McEneny, H.; Baker-Austin, C.; Lees, D. N.; Algoet, M. *Marine Drugs* **2017**, *15* (9), 277.

(80) Shen, H.; Li, Z.; Jiang, Y.; Pan, X.; Wu, J.; Cristofori-Armstrong, B.; Smith, J. J.; Chin, Y. K. Y.; Lei, J.; Zhou, Q.; King, G. F.; Yan, N. *Science* **2018**, *362* (6412), eaau2596.

(81) Lorand, J. P.; Edwards, J. O. *J. Org. Chem.* **1959**, *24* (6), 769.

(82) Brudno, Y.; Desai, R. M.; Kwee, B. J.; Joshi, N. S.; Aizenberg, M.; Mooney, D. J. *ChemMedChem* **2015**, *10* (4), 617.

(83) Brudno, Y.; Pezone, M. J.; Snyder, T. K.; Uzun, O.; Moody, C. T.; Aizenberg, M.; Mooney, D. J. *Biomaterials* **2018**, *178*, 373.

(84) Conte, M. L.; Staderini, S.; Marra, A.; Sanchez-Navarro, M.; Davis, B. G.; Dondoni, A. *Chem. Commun.* **2011**, *47* (39), 11086.

(85) Patterson, D. M.; Nazarova, L. A.; Prescher, J. A. *ACS Chem. Biol.* **2014**, *9* (3), 592.

(86) Zhang, M.; Zhang, Y.; Song, M.; Xue, X.; Wang, J.; Wang, C.; Zhang, C.; Li, C.; Xiang, Q.; Zou, L.; Wu, X.; Wu, C.; Dong, B.; Xue, W.; Zhou, Y.; Chen, H.; Wu, D.; Ding, K.; Xu, Y. *J. Med. Chem.* **2018**, *61* (7), 3037.

(87) Wei, P.-F.; Qi, M.-Z.; Wang, Z.-P.; Ding, S.-Y.; Yu, W.; Liu, Q.; Wang, L.-K.; Wang, H.-Z.; An, W.-K.; Wang, W. *J. Am. Chem. Soc.* **2018**, *140* (13), 4623.

(88) Chakraborti, A. K.; Gulhane, R. *Chem. Commun.* **2003**, No. 15, 1896.

(89) Ryabinin, V. A.; Zakharova, O. D.; Yurchenko, E. Y.; Timofeeva, O. A.; Martyanov, I. V.; Tokarev, A. A.; Belanov, E. F.; Bormotov, N. I.; Tarrago-Litvak, L.; Andreola, M. L.; Litvak, S.; Nevinsky, G. A.; Sinyakov, A. N. *Bioorganic & Medicinal Chemistry* **2000**, *8* (5), 985.

Appendices

Appendix 1: Selected copies of NMR spectra of compounds studies found in Chapter 2.

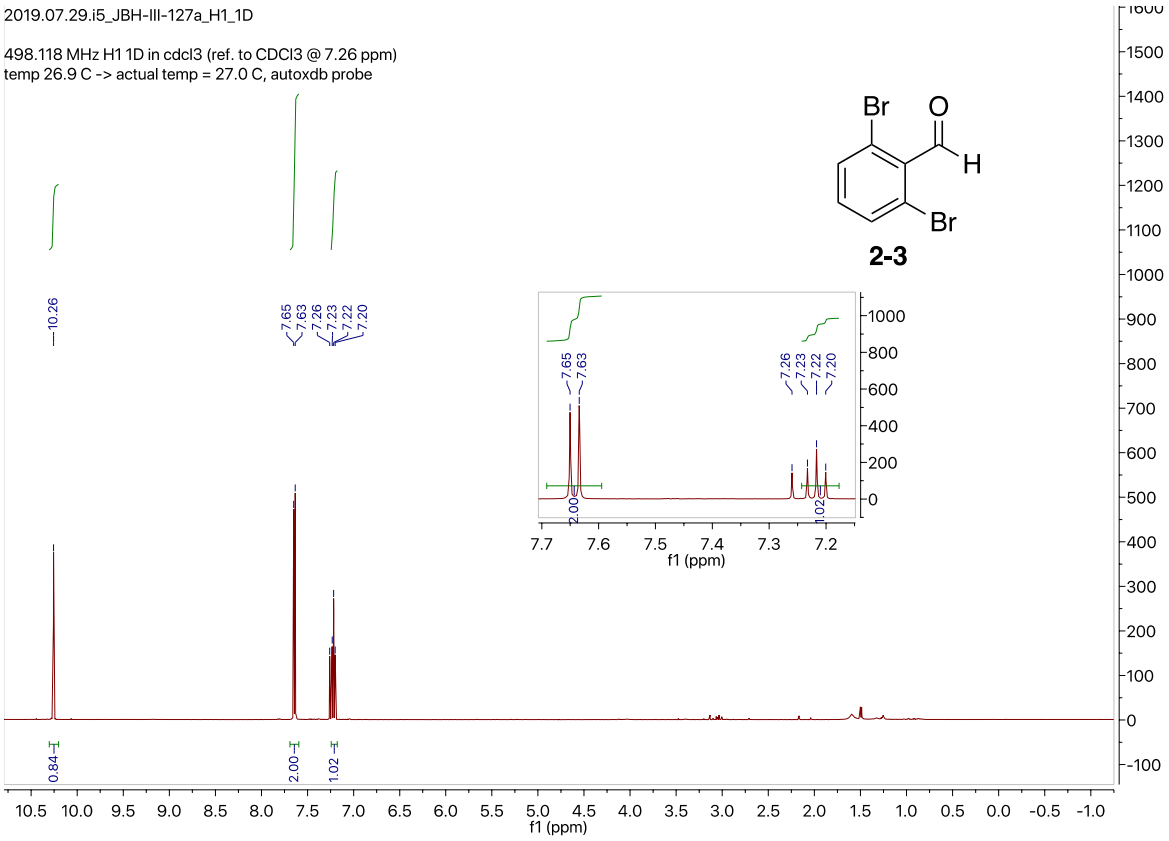

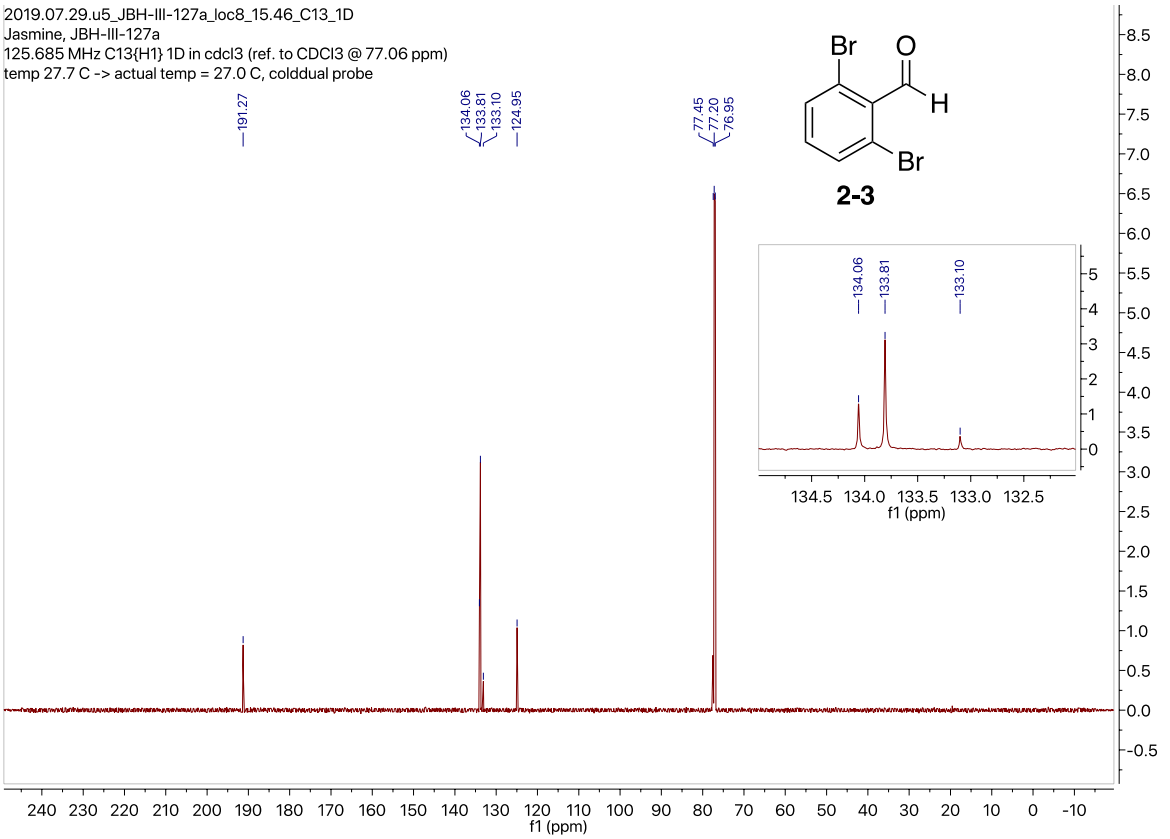
2019.07.29.u5_JBH-III-127a_loc8_15.46_C13_1D
Jasmine, JBH-III-127a
125.685 MHz C13{H1} 1D in cdcl3 (ref. to CDCl3 @ 77.06 ppm)
temp 27.7 C -> actual temp = 27.0 C, colddual probe
191.27
134.06
133.81
133.10
124.95
77.45
77.20
76.95
Br
O
H
Br
2-3
f1 (ppm)

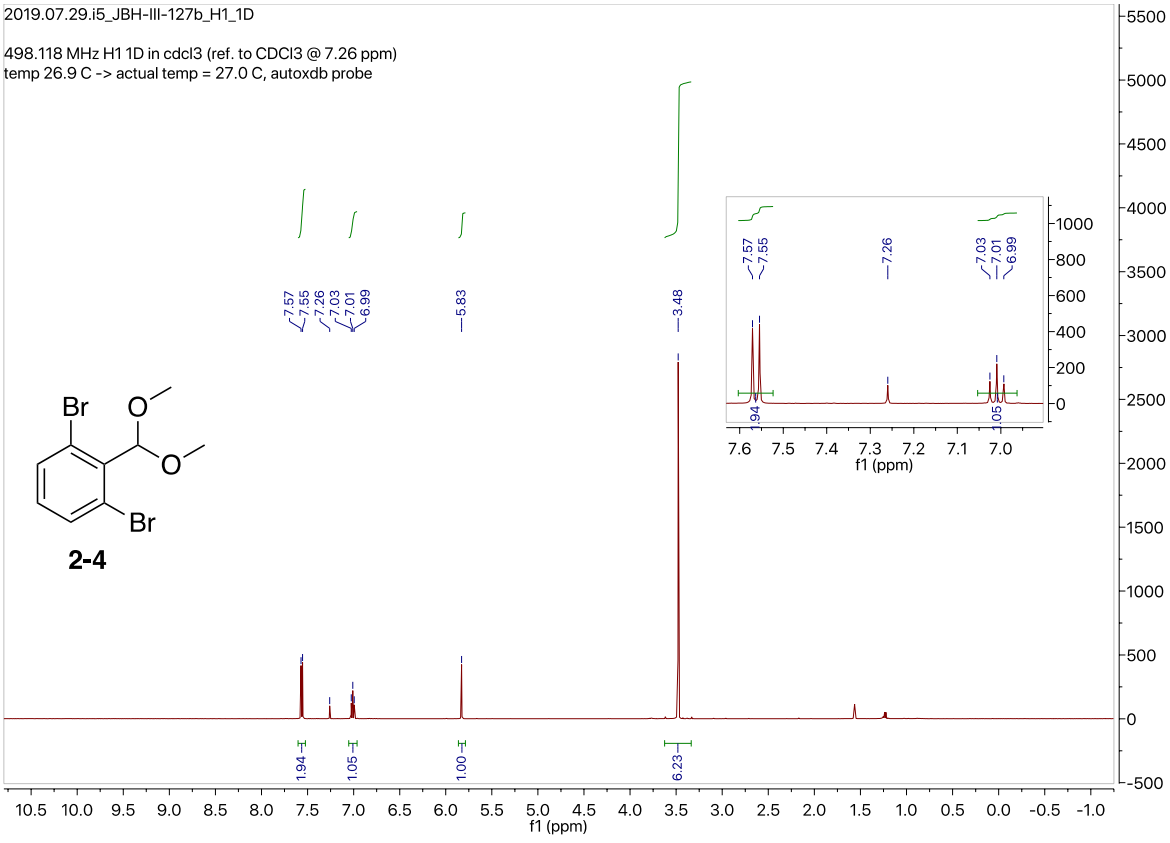
2019.07.29.i5_JBH-III-127b_H1_1D
498.118 MHz H1 1D in cdcl3 (ref. to CDCl3 @ 7.26 ppm)
temp 26.9 C -> actual temp = 27.0 C, autoxdb probe
7.57
7.55
7.26
7.03
7.01
6.99
5.83
3.48
1.94
1.05
1.00
6.23
Br
O
O
Br
2-4
f1 (ppm)

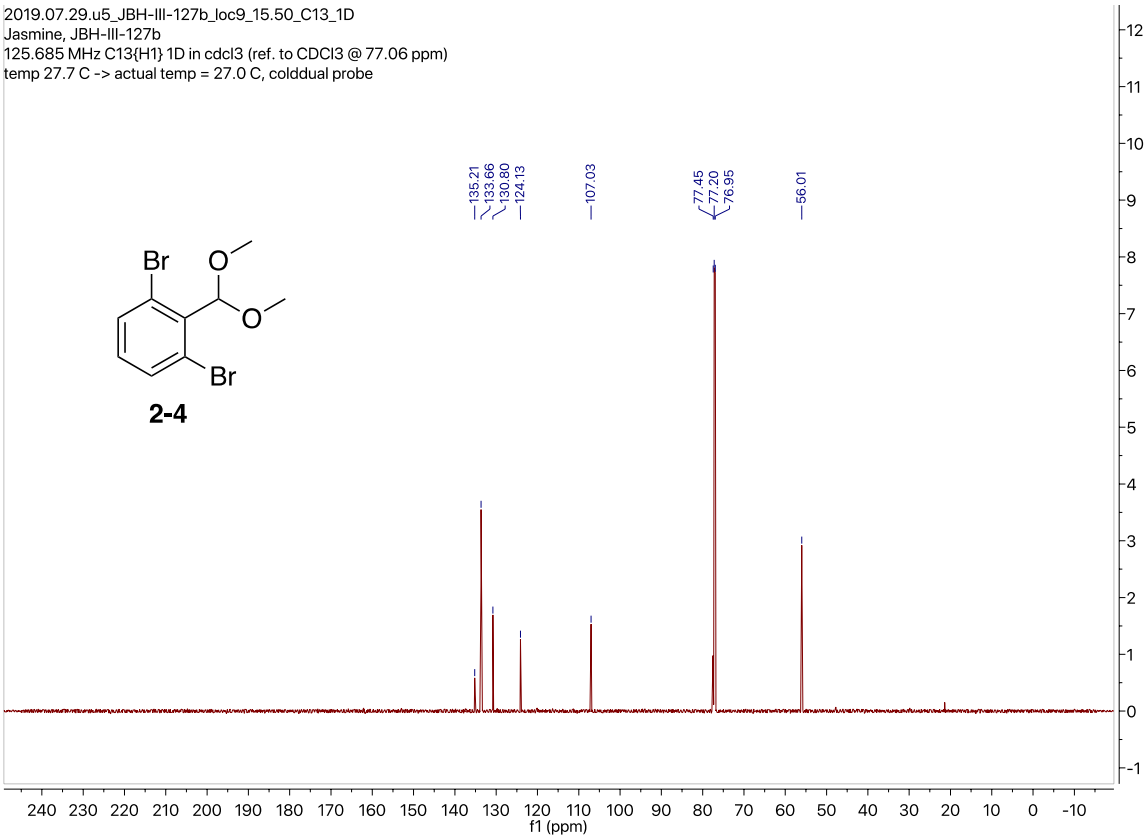
2019.07.29.u5_JBH-III-127b_loc9_15.50_C13_1D
Jasmine, JBH-III-127b
125.685 MHz C13{H1} 1D in cdcl3 (ref. to CDCl3 @ 77.06 ppm)
temp 27.7 C -> actual temp = 27.0 C, colddual probe
135.21
133.66
130.80
124.13
107.03
77.45
77.20
76.95
56.01
Br
O
O
Br
2-4
f1 (ppm)

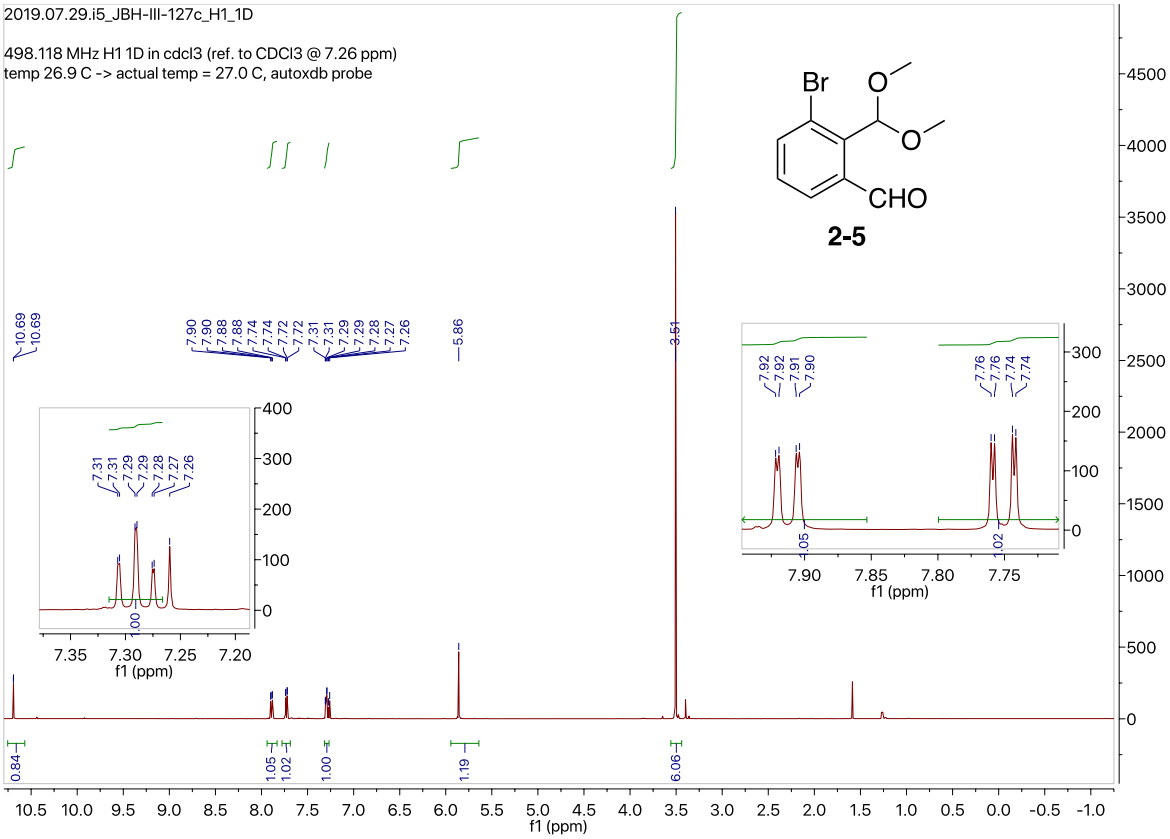
2019.07.29.i5_JBH-III-127c_H1_1D
498.118 MHz H1 1D in cdcl3 (ref. to CDCl3 @ 7.26 ppm)
temp 26.9 C -> actual temp = 27.0 C, autoxdb probe
Br
O
O
CHO
2-5
10.69
10.69
7.90
7.90
7.88
7.88
7.74
7.74
7.72
7.72
7.31
7.31
7.29
7.29
7.28
7.27
7.26
5.86
3.51
0.84
1.05
1.02
1.00
1.19
6.06
f1 (ppm)

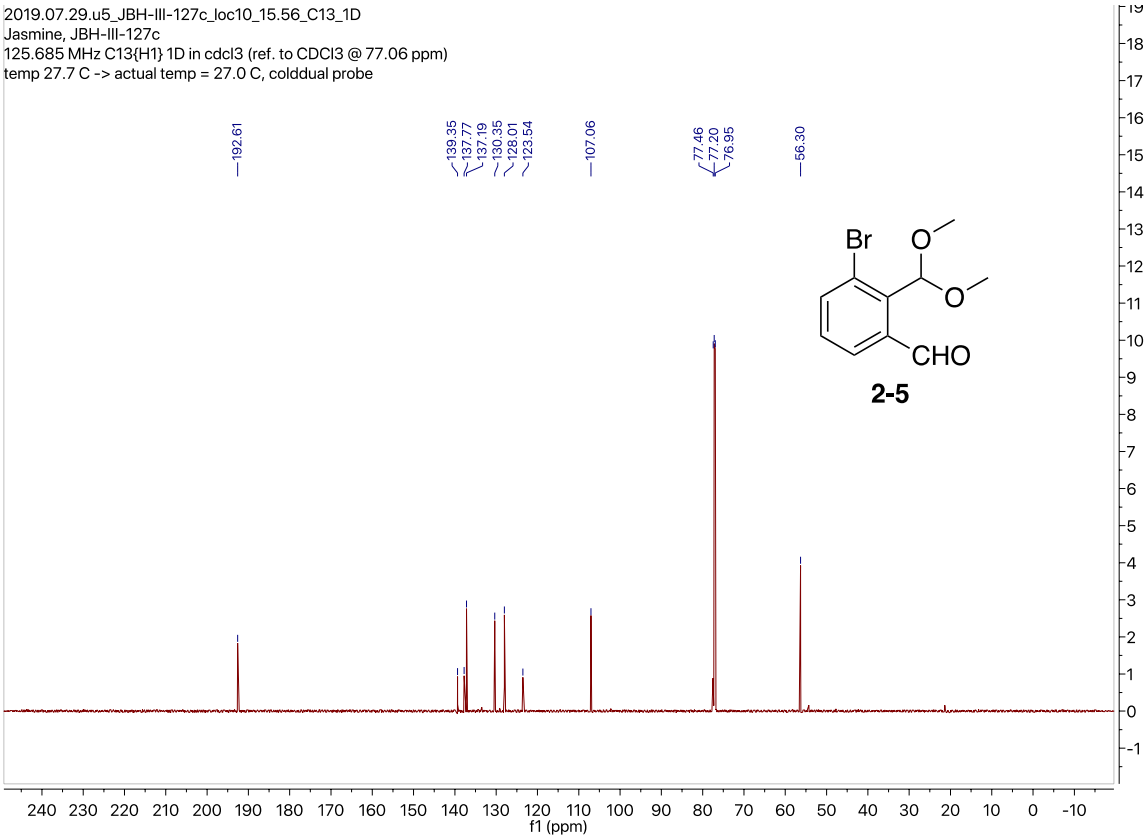
2019.07.29.u5_JBH-III-127c_loc10_15.56_C13_1D
Jasmine, JBH-III-127c
125.685 MHz C13{H1} 1D in cdcl3 (ref. to CDCl3 @ 77.06 ppm)
temp 27.7 C -> actual temp = 27.0 C, colddual probe
192.61
139.35
137.77
137.19
130.35
128.01
123.54
107.06
77.46
77.20
76.95
56.30
Br
O
O
CHO
2-5
f1 (ppm)

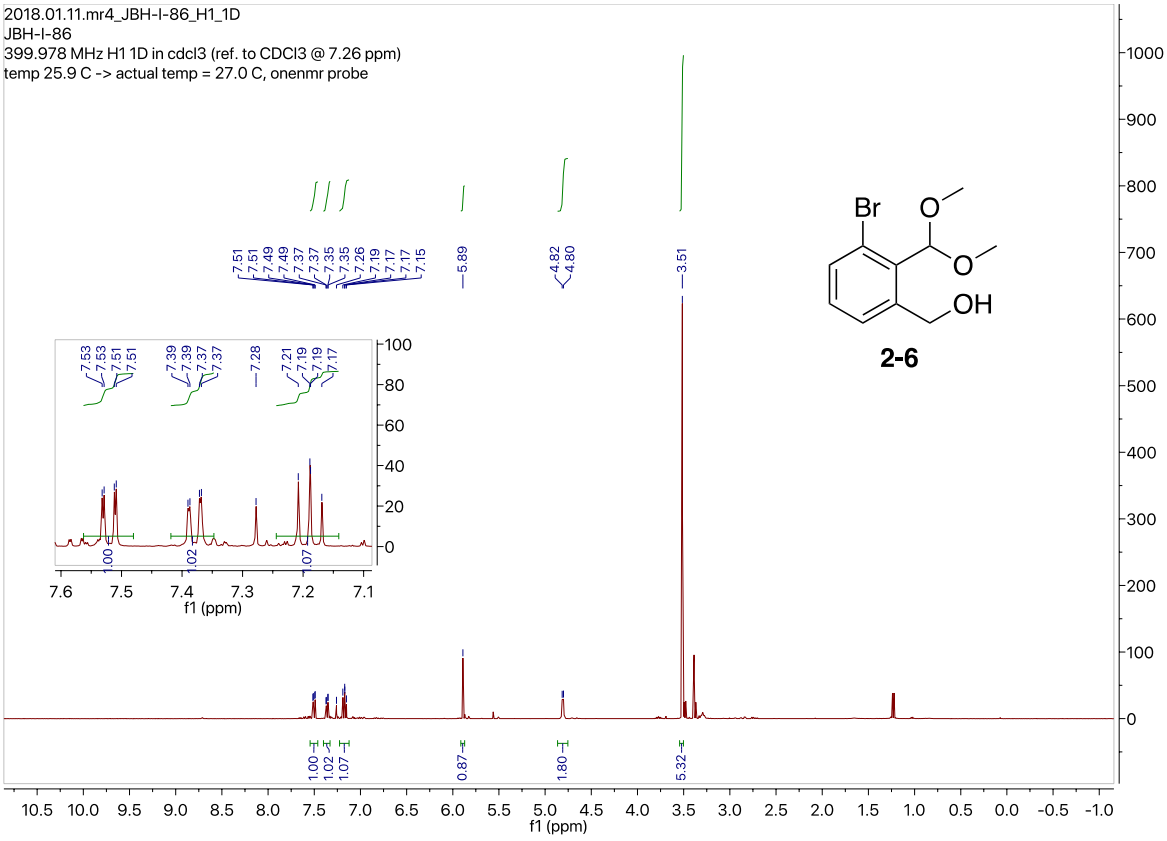
2018.01.11.mr4_JBH-I-86_H1_1D
JBH-I-86
399.978 MHz H1 1D in cdcl3 (ref. to CDCl3 @ 7.26 ppm)
temp 25.9 C -> actual temp = 27.0 C, onenmr probe
7.51
7.51
7.49
7.49
7.37
7.37
7.35
7.35
7.26
7.19
7.17
7.17
7.15
5.89
4.82
4.80
3.51
Br
O
O
OH
2-6
f1 (ppm)

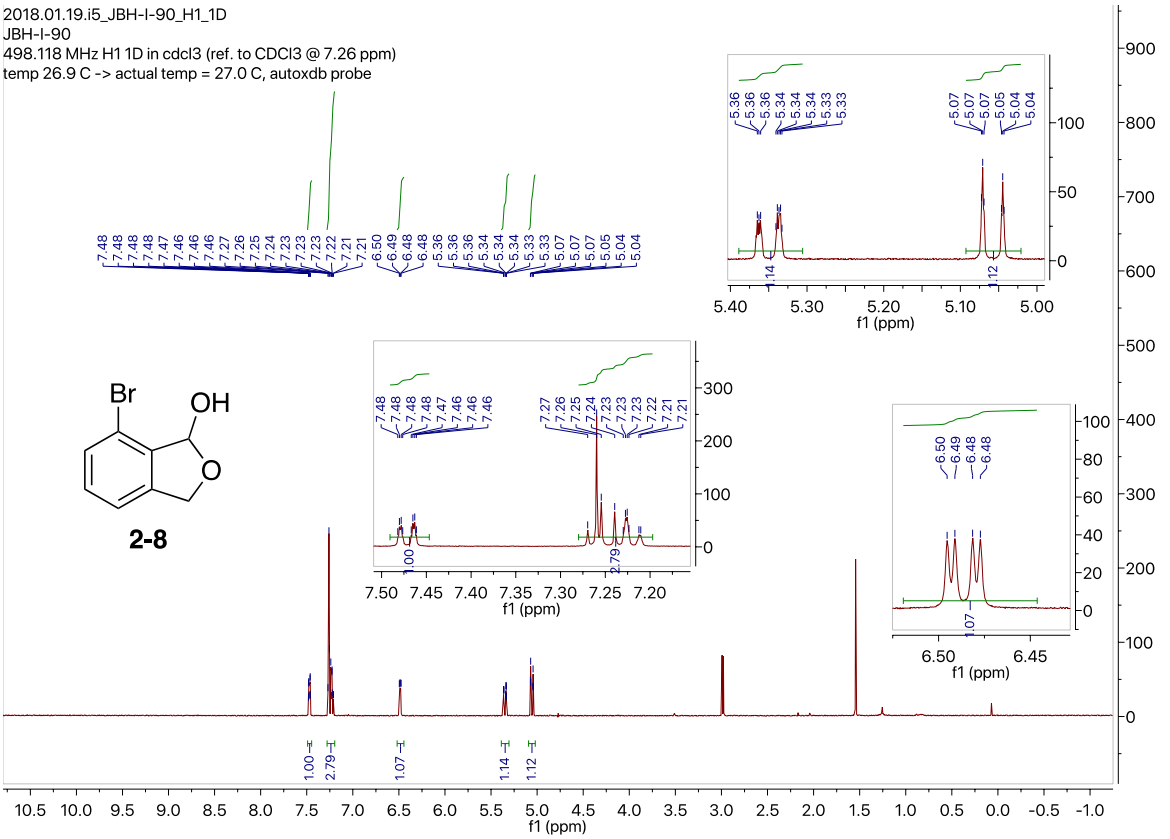
2018.01.19.i5_JBH-I-90_H1_1D
JBH-I-90
498.118 MHz H1 1D in cdcl3 (ref. to CDCl3 @ 7.26 ppm)
temp 26.9 C -> actual temp = 27.0 C, autoxdb probe
Br
OH
O
2-8
f1 (ppm)

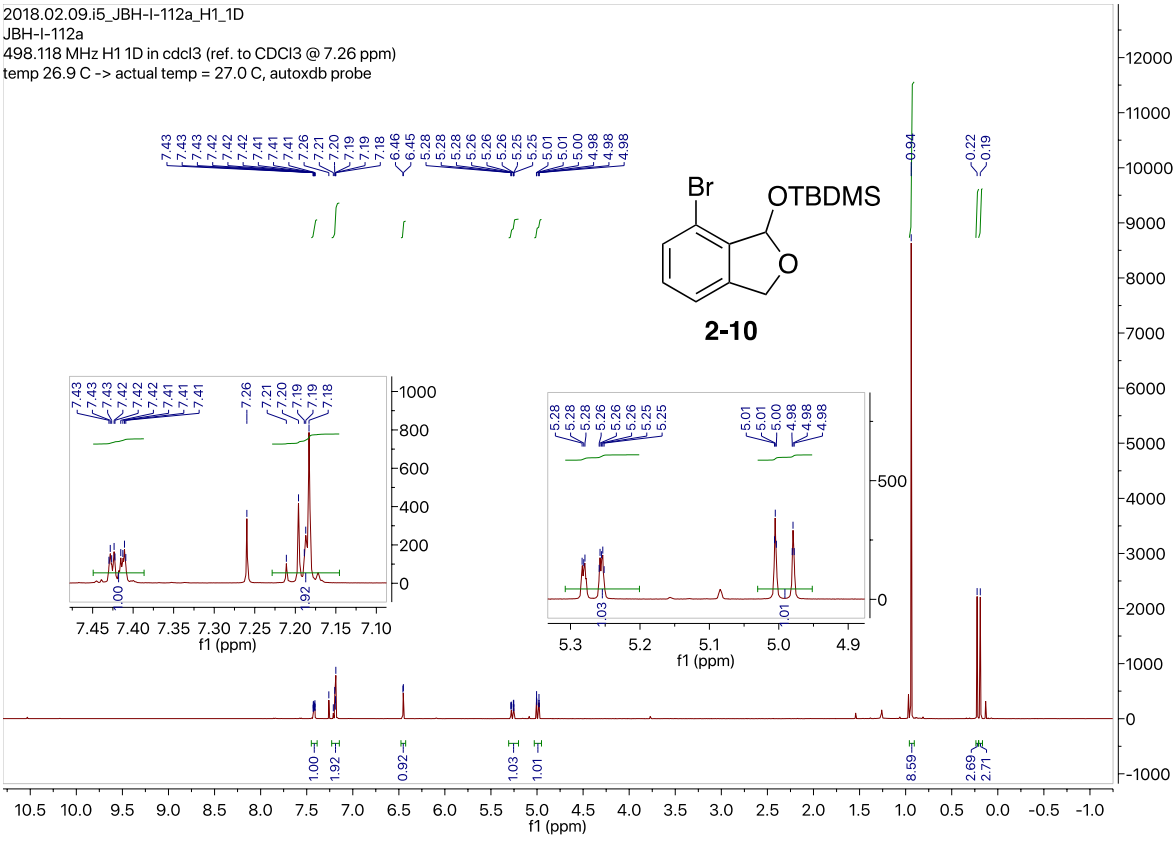
2018.02.09.i5_JBH-I-112a_H1_1D
JBH-I-112a
498.118 MHz H1 1D in cdcl3 (ref. to CDCl3 @ 7.26 ppm)
temp 26.9 C -> actual temp = 27.0 C, autoxdb probe
Br
OTBDMS
O
2-10
f1 (ppm)

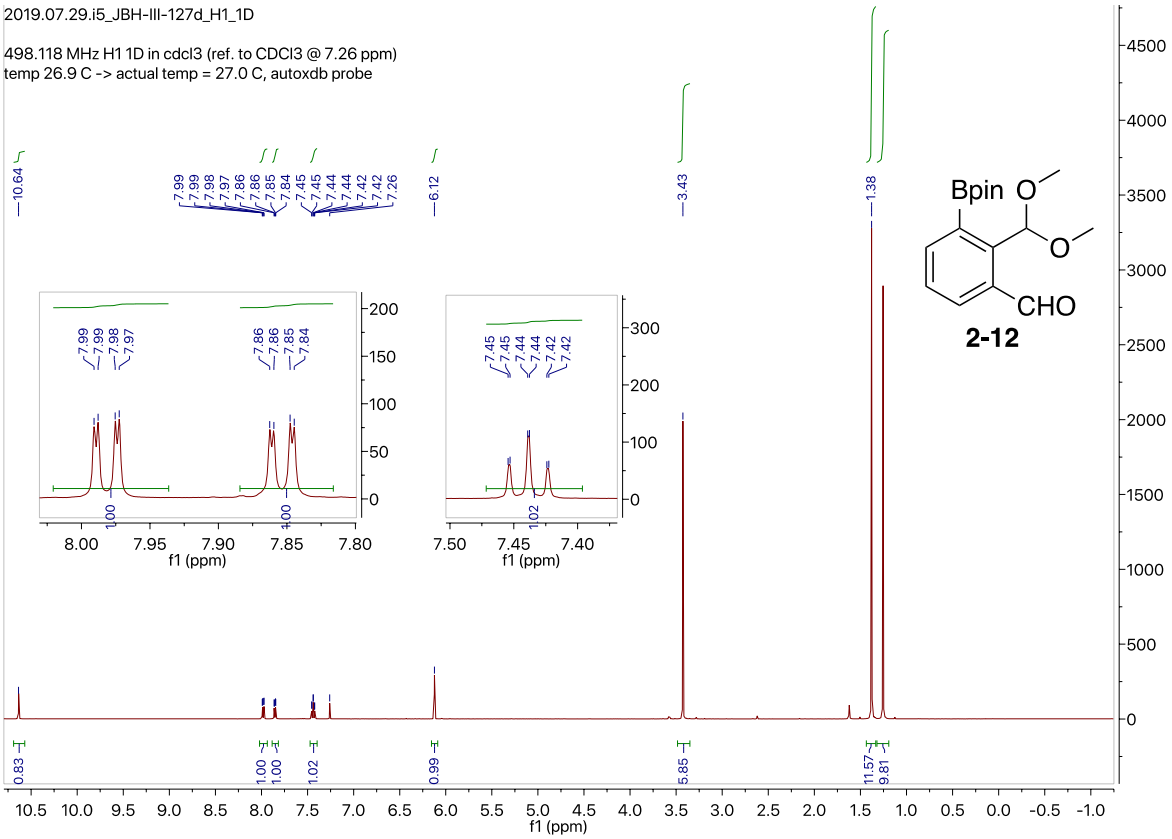
2019.07.29.i5_JBH-III-127d_H1_1D
498.118 MHz H1 1D in cdcl3 (ref. to CDCl3 @ 7.26 ppm)
temp 26.9 C -> actual temp = 27.0 C, autoxdb probe
Bpin
O
O
CHO
2-12
f1 (ppm)

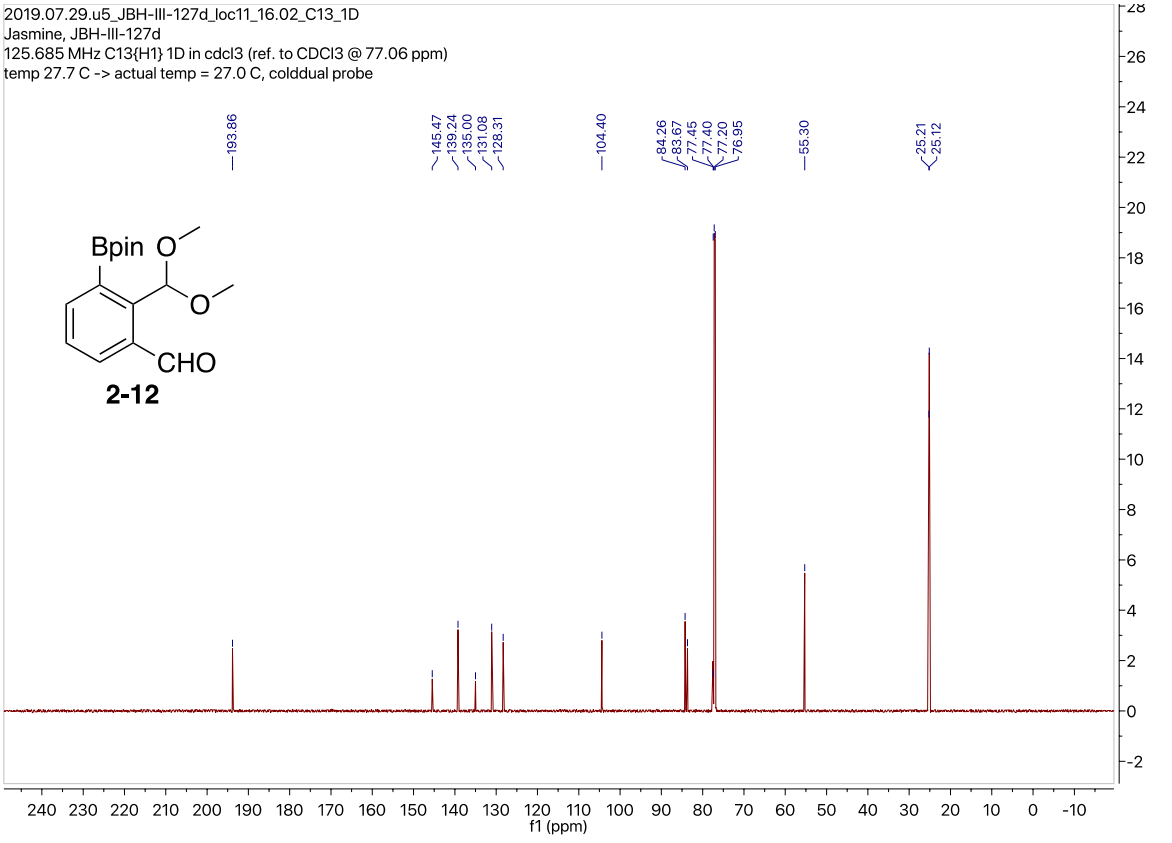
2019.07.29.u5_JBH-III-127d_loc11_16.02_C13_1D
Jasmine, JBH-III-127d
125.685 MHz C13{H1} 1D in cdcl3 (ref. to CDCl3 @ 77.06 ppm)
temp 27.7 C -> actual temp = 27.0 C, colddual probe
Bpin
O
O
CHO
2-12
f1 (ppm)

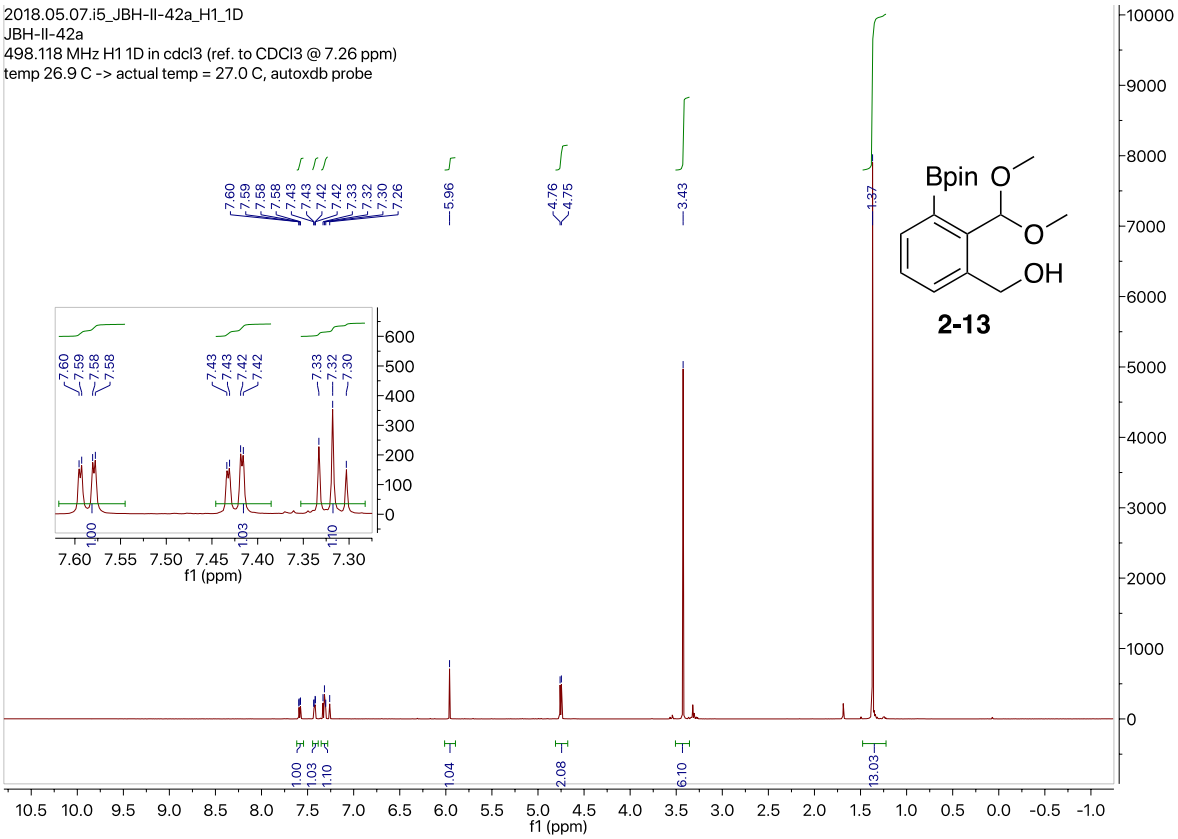
2018.05.07.i5_JBH-II-42a_H1_1D
JBH-II-42a
498.118 MHz H1 1D in cdcl3 (ref. to CDCl3 @ 7.26 ppm)
temp 26.9 C -> actual temp = 27.0 C, autoxdb probe
7.60
7.59
7.58
7.58
7.43
7.43
7.42
7.42
7.33
7.32
7.30
7.26
5.96
4.76
4.75
3.43
1.37
Bpin
O
O
OH
2-13
1.00
1.03
1.10
1.04
2.08
6.10
13.03
f1 (ppm)

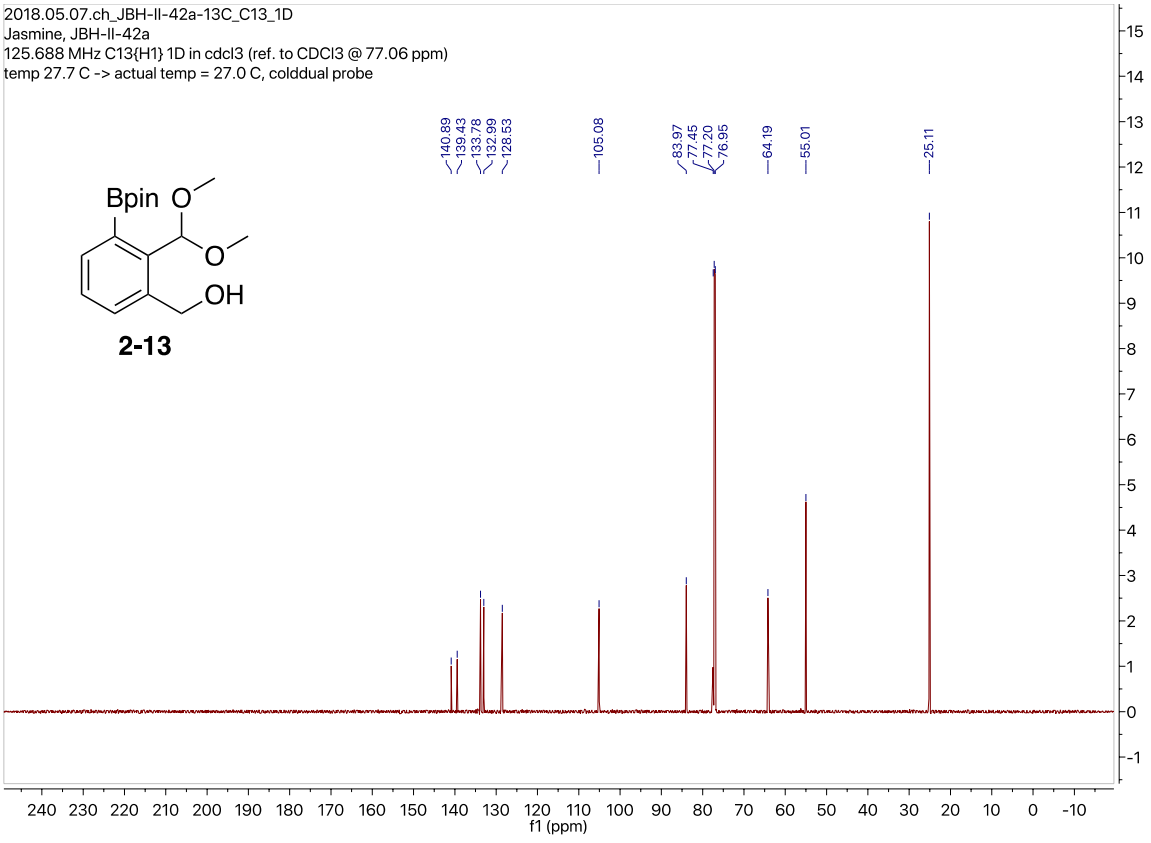
2018.05.07.ch_JBH-II-42a-13C_C13_1D
Jasmine, JBH-II-42a
125.688 MHz C13{H1} 1D in cdcl3 (ref. to CDCl3 @ 77.06 ppm)
temp 27.7 C -> actual temp = 27.0 C, colddual probe
140.89
139.43
133.78
132.99
128.53
105.08
83.97
77.45
77.20
76.95
64.19
55.01
25.11
Bpin
O
O
OH
2-13
f1 (ppm)

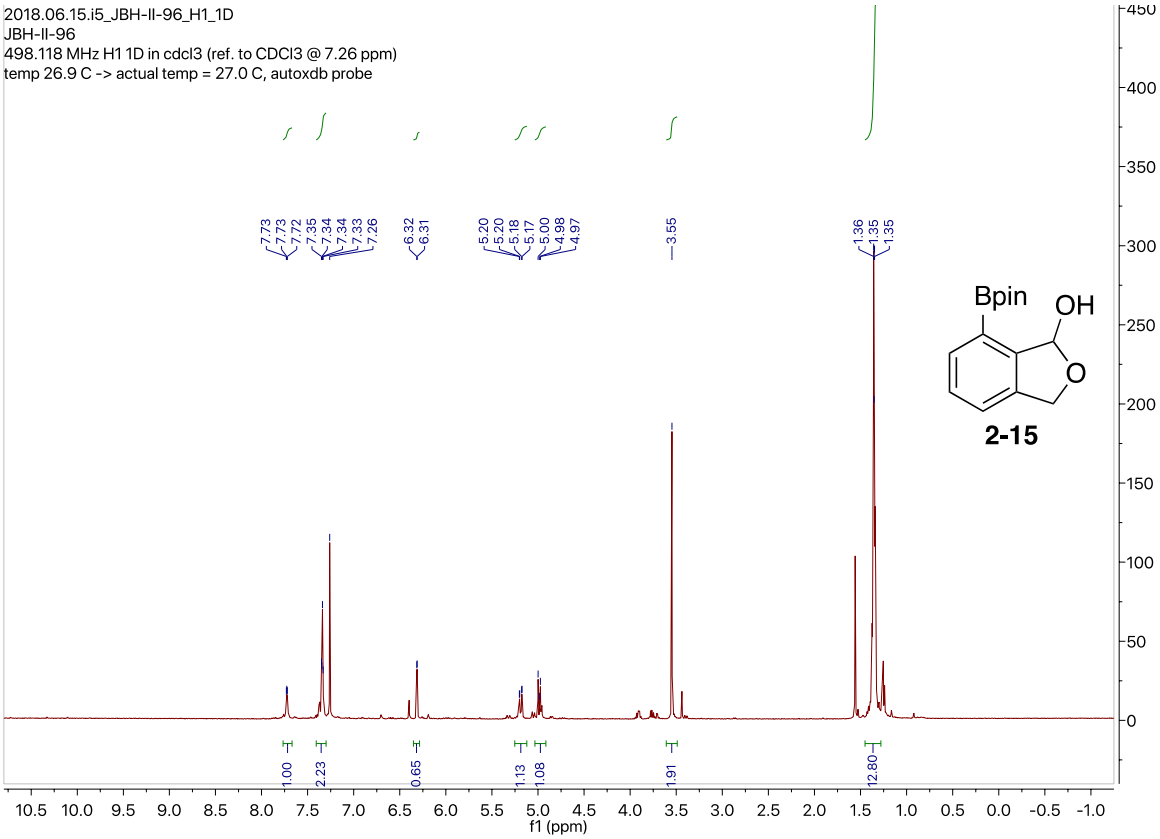
2018.06.15.i5_JBH-II-96_H1_1D
JBH-II-96
498.118 MHz H1 1D in cdcl3 (ref. to CDCl3 @ 7.26 ppm)
temp 26.9 C -> actual temp = 27.0 C, autoxdb probe
Bpin
OH
O
2-15
f1 (ppm)

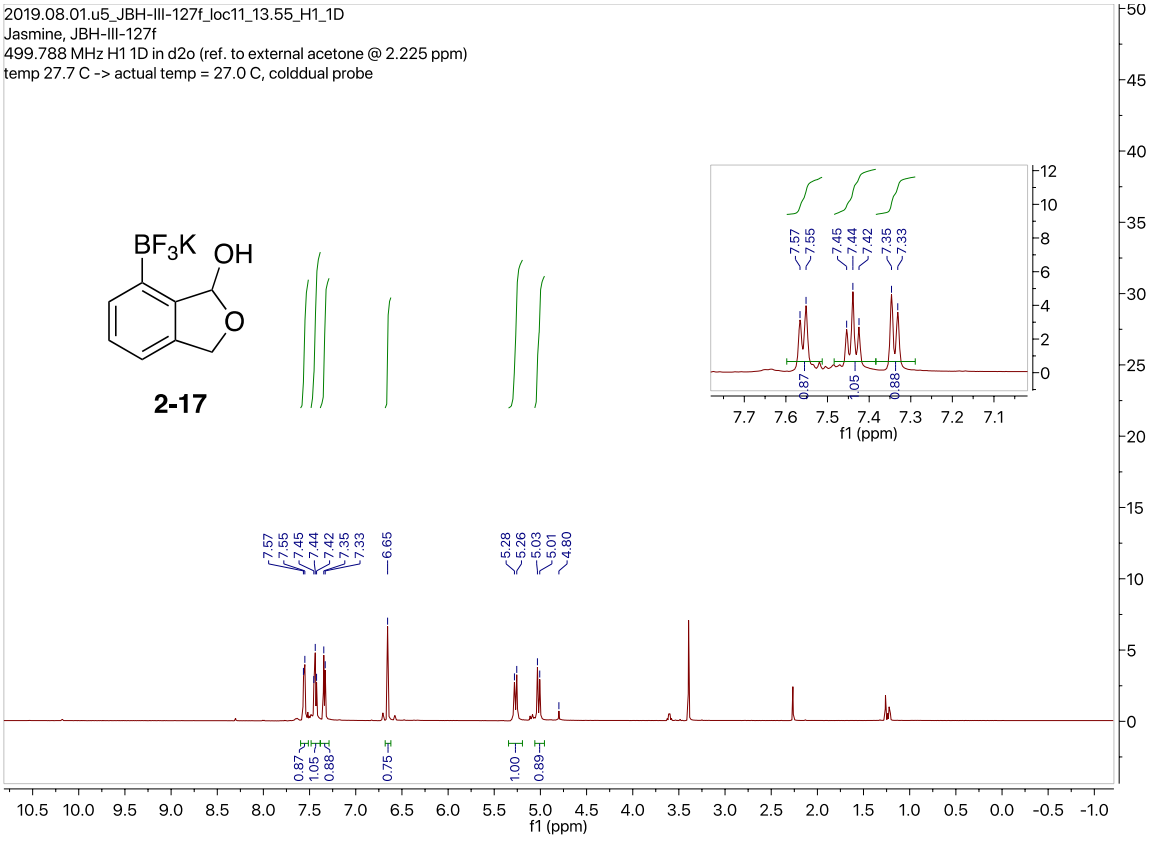
2019.08.01.u5_JBH-III-127f_loc11_13.55_H1_1D
Jasmine, JBH-III-127f
499.788 MHz H1 1D in d2o (ref. to external acetone @ 2.225 ppm)
temp 27.7 C -> actual temp = 27.0 C, colddual probe
BF3K
OH
O
2-17
f1 (ppm)

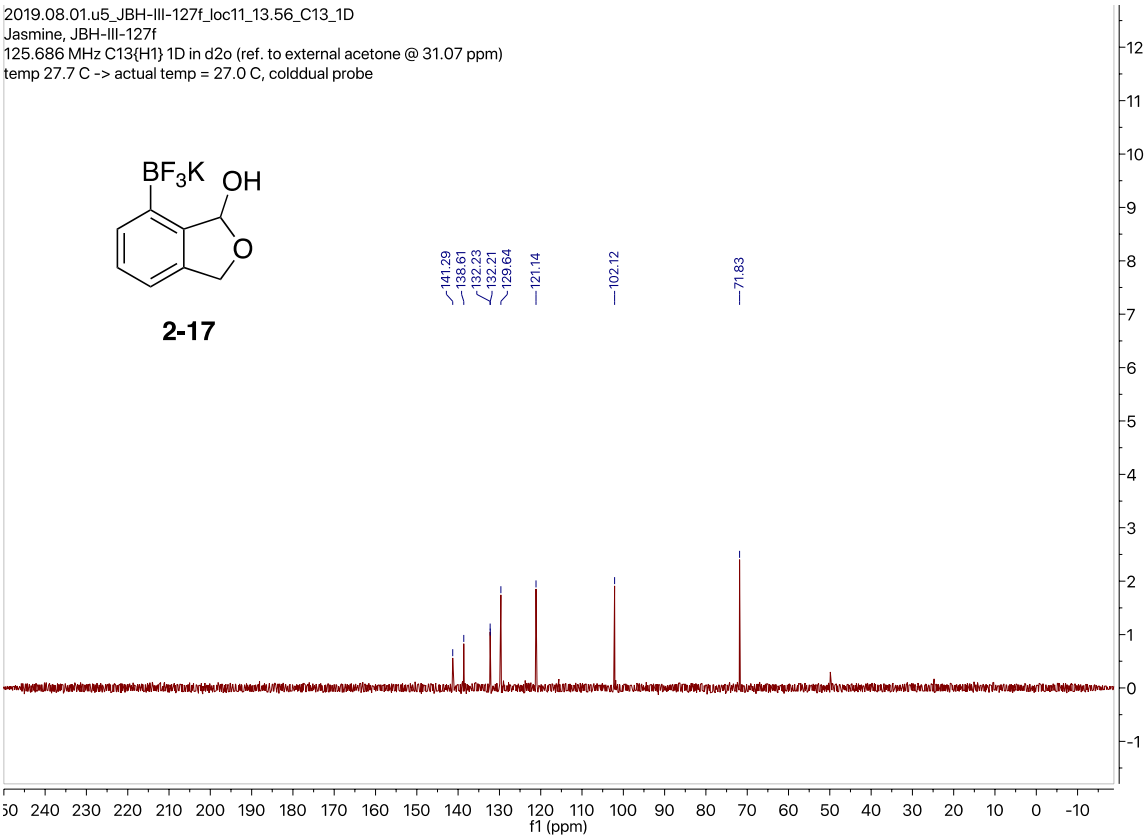
2019.08.01.u5_JBH-III-127f_loc11_13.56_C13_1D
Jasmine, JBH-III-127f
125.686 MHz C13{H1} 1D in d2o (ref. to external acetone @ 31.07 ppm)
temp 27.7 C -> actual temp = 27.0 C, colddual probe
BF3K
OH
O
2-17
141.29
138.61
132.23
132.21
129.64
121.14
102.12
71.83
f1 (ppm)

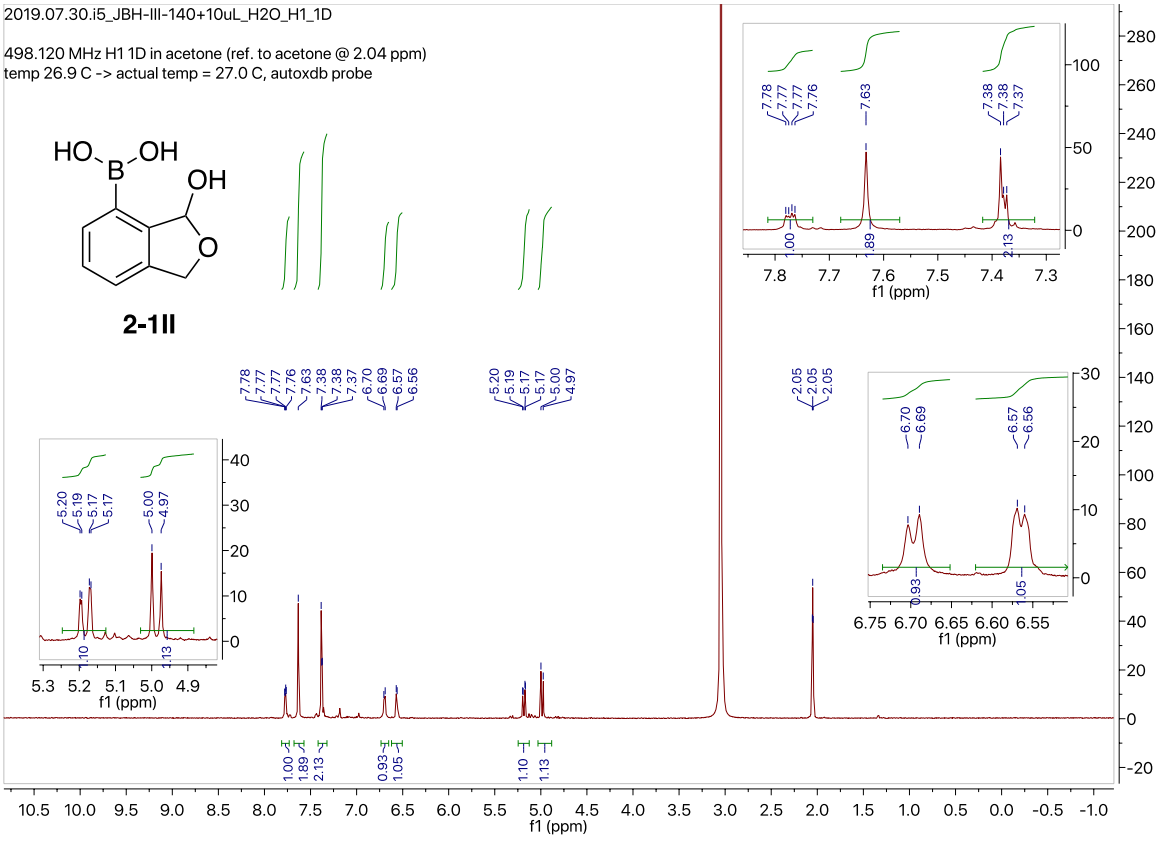
2019.07.30.i5_JBH-III-140+10uL_H2O_H1_1D
498.120 MHz H1 1D in acetone (ref. to acetone @ 2.04 ppm)
temp 26.9 C -> actual temp = 27.0 C, autoxdb probe
HO
B
OH
OH
O
2-1II
7.78
7.77
7.77
7.76
7.63
7.38
7.38
7.37
6.70
6.69
6.57
6.56
5.20
5.19
5.17
5.17
5.00
4.97
2.05
2.05
2.05
1.00
1.89
2.13
0.93
1.05
1.10
1.13
f1 (ppm)

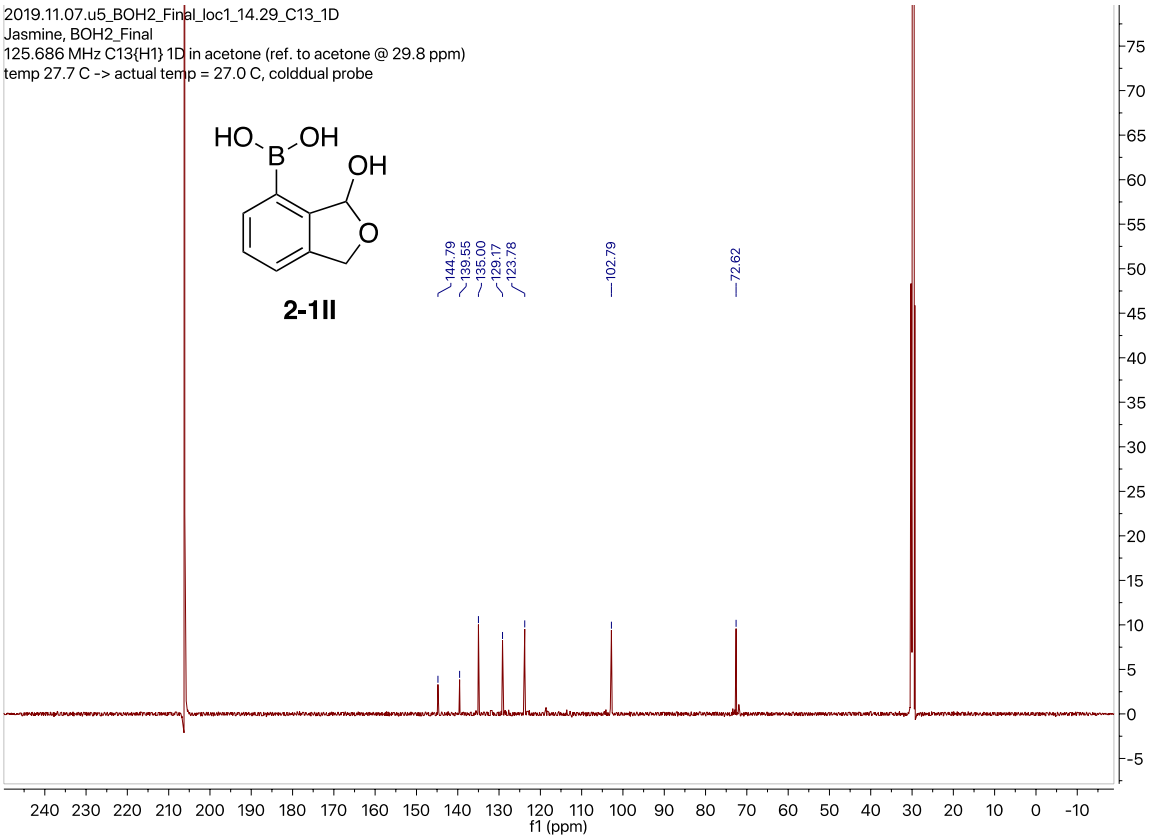
2019.11.07.u5_BOH2_Final_loc1_14.29_C13_1D
Jasmine, BOH2_Final
125.686 MHz C13{H1} 1D in acetone (ref. to acetone @ 29.8 ppm)
temp 27.7 C -> actual temp = 27.0 C, colddual probe
HO
B
OH
OH
O
2-1II
144.79
139.55
135.00
129.17
123.78
102.79
72.62
f1 (ppm)

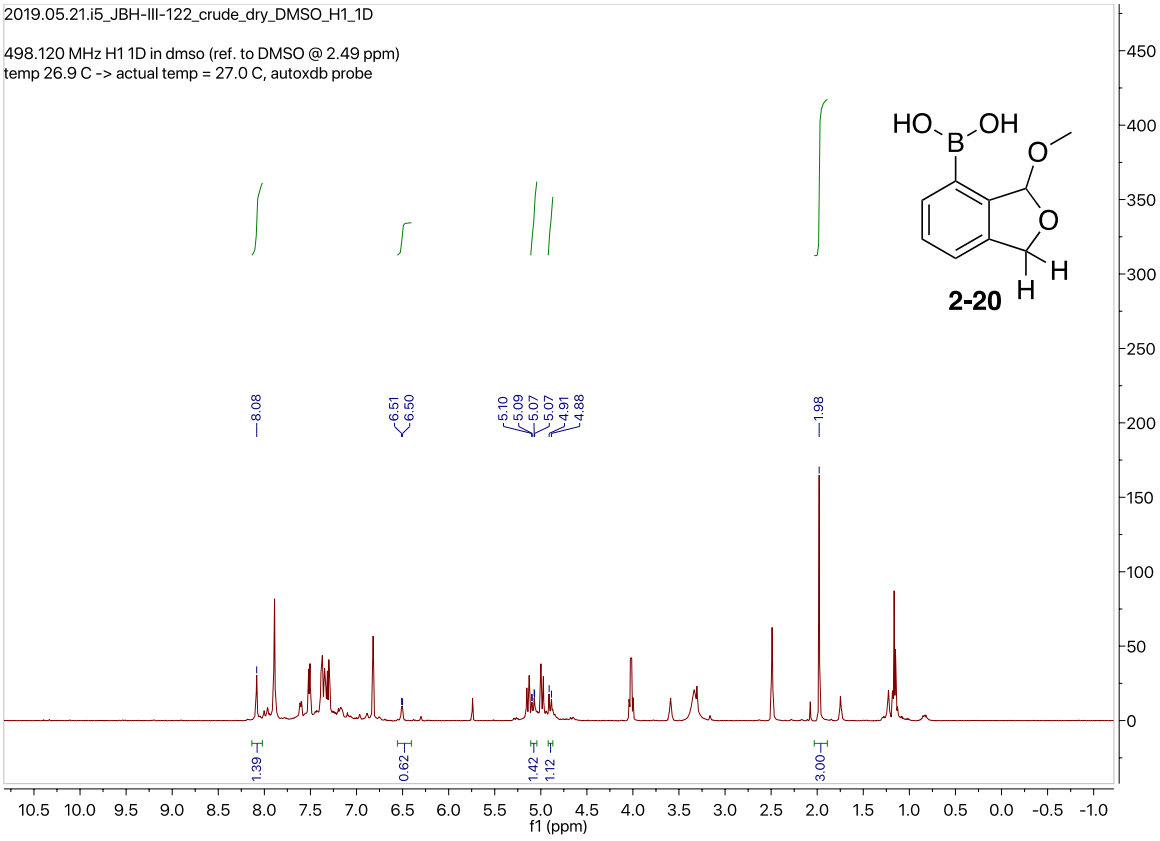
2019.05.21.i5_JBH-III-122_crude_dry_DMSO_H1_1D
498.120 MHz H1 1D in dmso (ref. to DMSO @ 2.49 ppm)
temp 26.9 C -> actual temp = 27.0 C, autoxdb probe
HO
B
OH
O
O
H
H
2-20
8.08
6.51
6.50
5.10
5.09
5.07
5.07
4.91
4.88
1.98
1.39
0.62
1.42
1.12
3.00
f1 (ppm)

Appendix 2: Selected copies of NMR spectra of compounds studies found in Chapter 3.

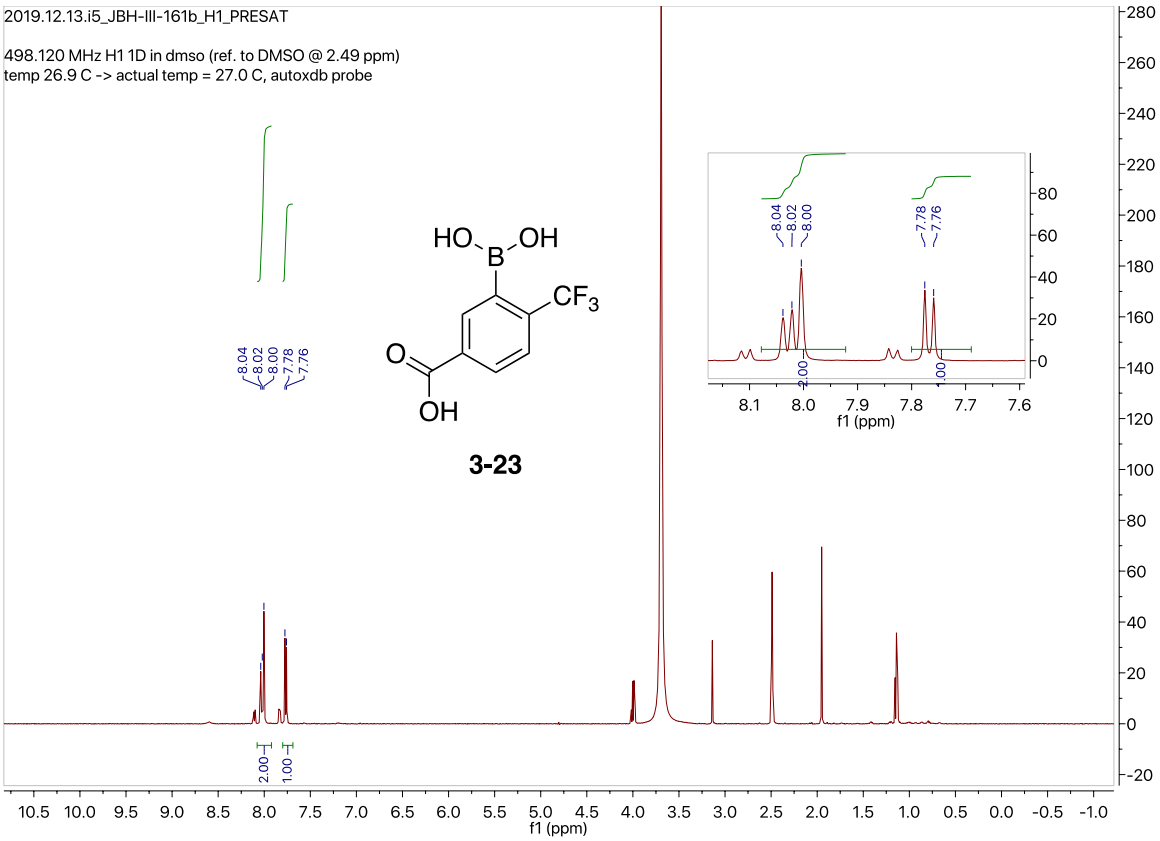

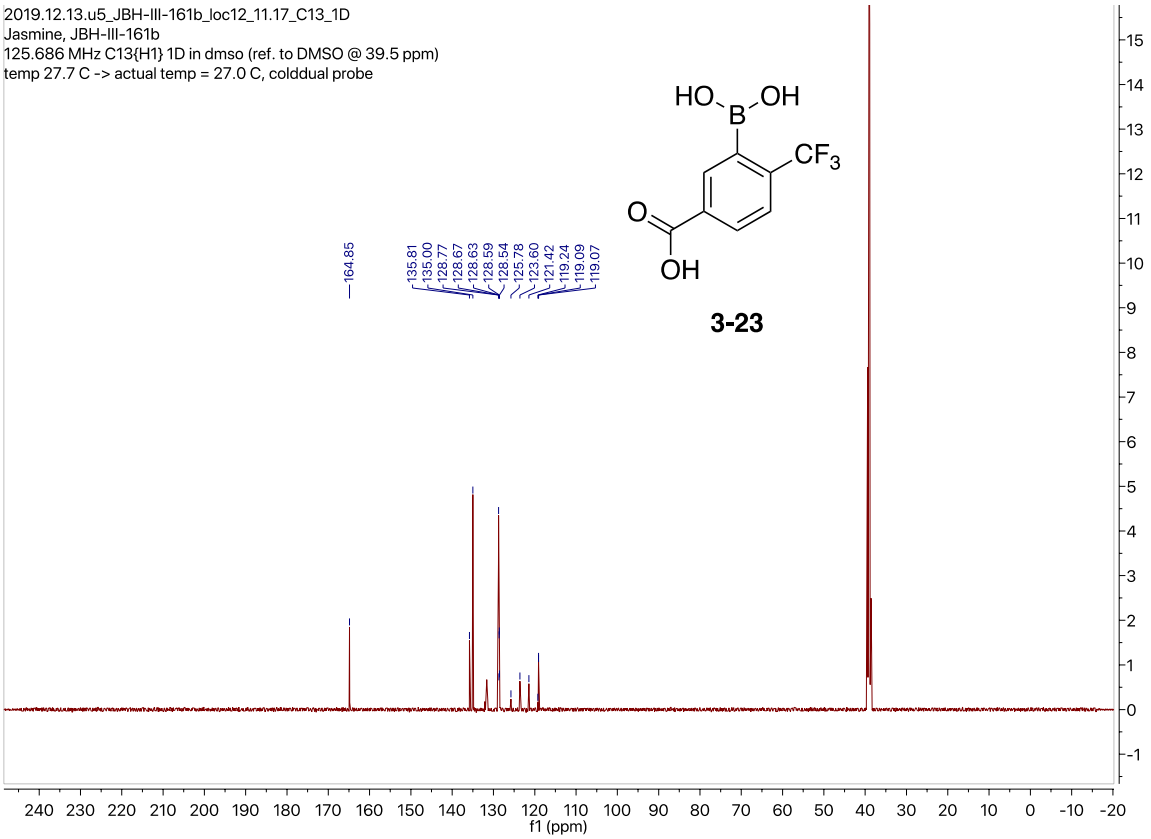
2019.12.13.u5_JBH-III-161b_loc12_11.17_C13_1D
Jasmine, JBH-III-161b
125.686 MHz C13{H1} 1D in dmso (ref. to DMSO @ 39.5 ppm)
temp 27.7 C -> actual temp = 27.0 C, colddual probe
HO
B
OH
CF3
O
OH
3-23
164.85
135.81
135.00
128.77
128.67
128.63
128.59
128.54
125.78
123.60
121.42
119.24
119.09
119.07
f1 (ppm)

Appendix 3: Selected copies of NMR spectra of compounds studies found in Chapter 4.

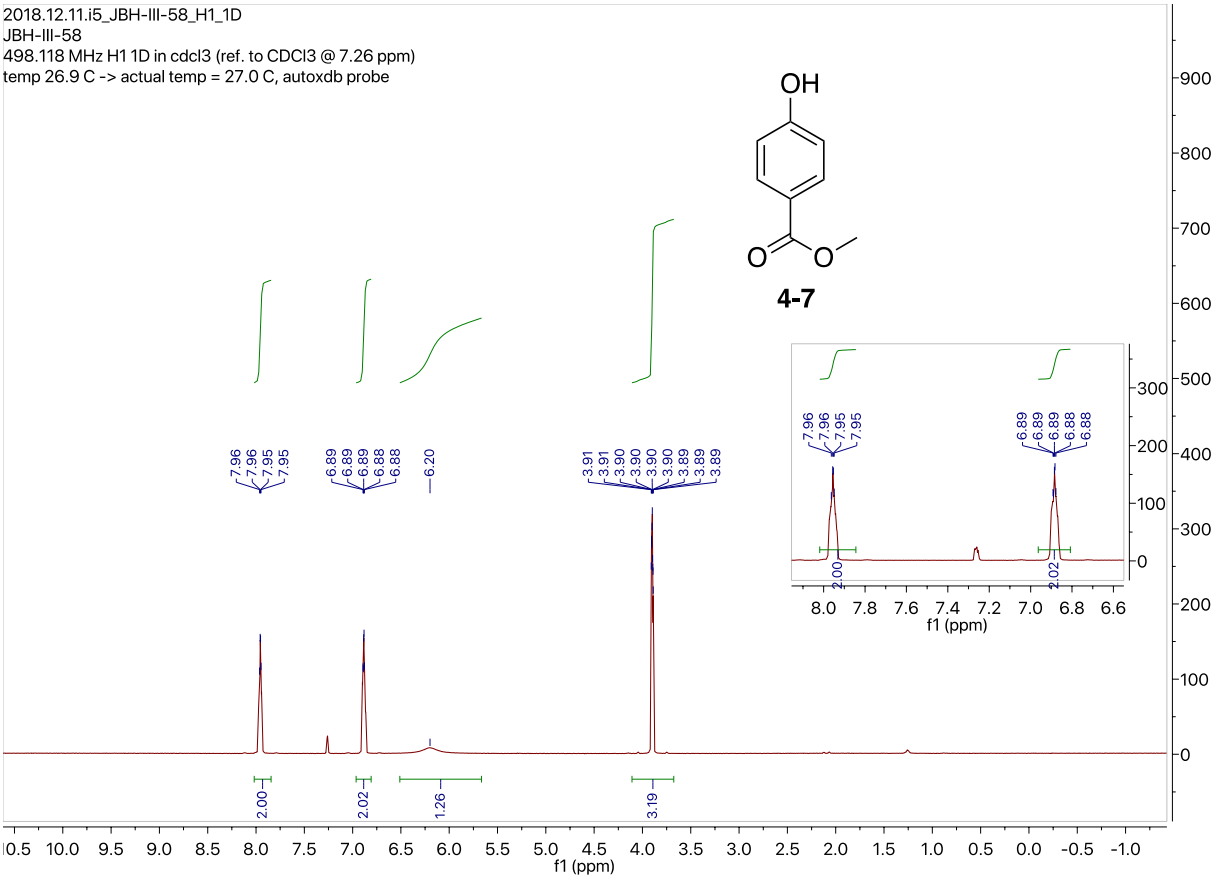

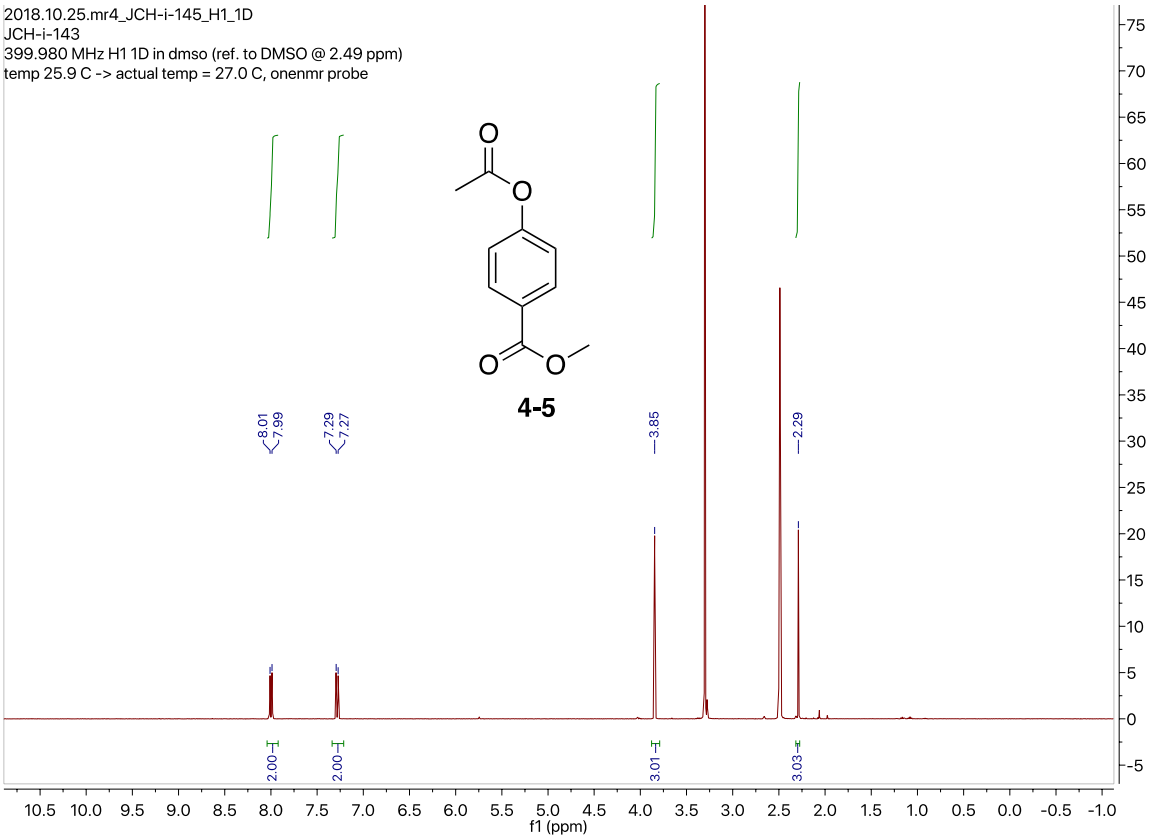
2018.10.25.mr4_JCH-i-145_H1_1D
JCH-i-143
399.980 MHz H1 1D in dmso (ref. to DMSO @ 2.49 ppm)
temp 25.9 C -> actual temp = 27.0 C, onenmr probe
4-5
8.01
7.99
7.29
7.27
3.85
2.29
2.00
2.00
3.01
3.03
f1 (ppm)

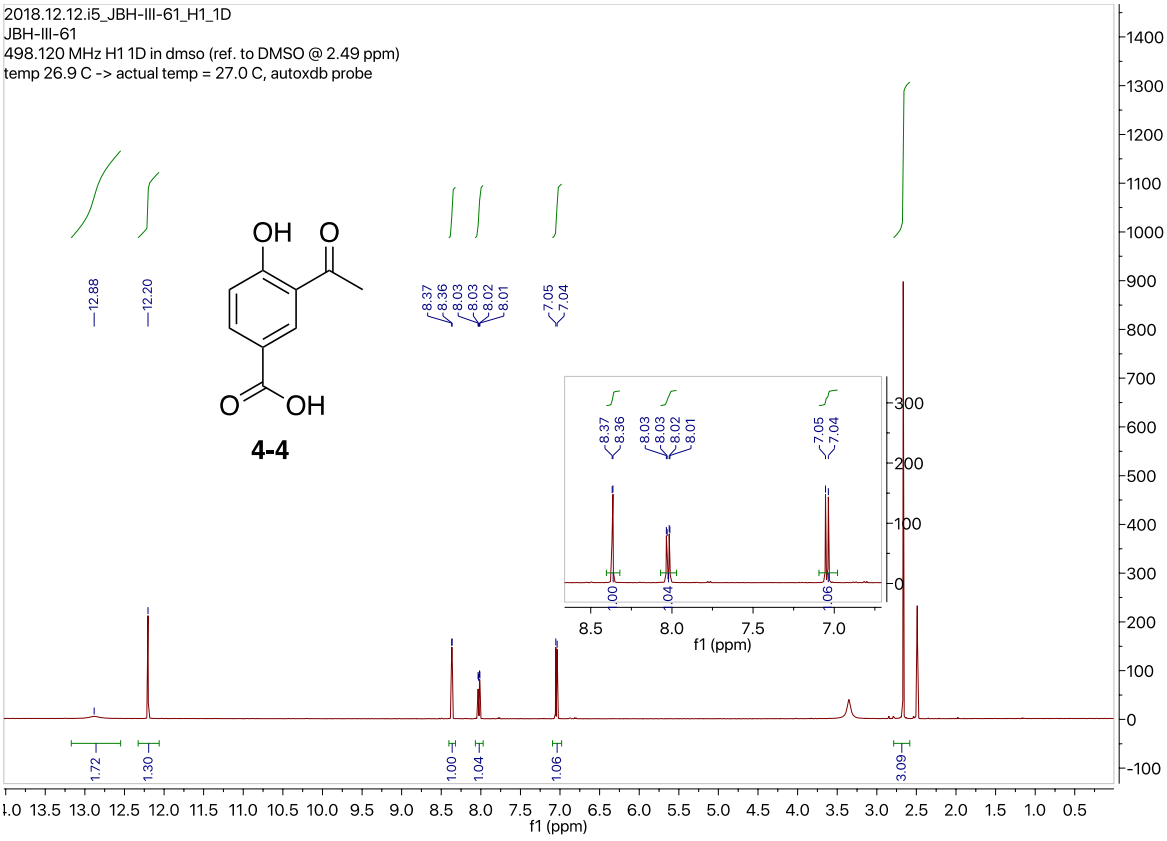
2018.12.12.i5_JBH-III-61_H1_1D
JBH-III-61
498.120 MHz H1 1D in dmso (ref. to DMSO @ 2.49 ppm)
temp 26.9 C -> actual temp = 27.0 C, autoxdb probe
4-4
12.88
12.20
8.37
8.36
8.03
8.03
8.02
8.01
7.05
7.04
1.72
1.30
1.00
1.04
1.06
3.09
f1 (ppm)

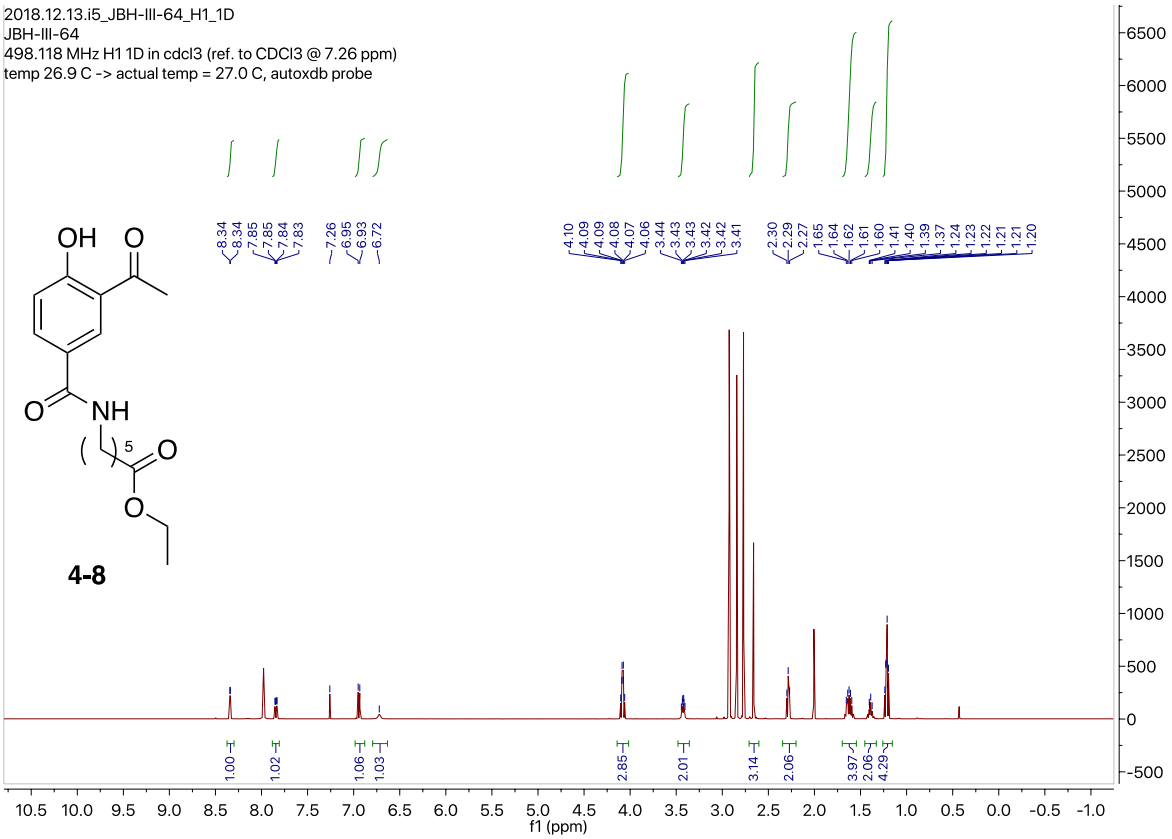
2018.12.13.i5_JBH-III-64_H1_1D
JBH-III-64
498.118 MHz H1 1D in cdcl3 (ref. to CDCl3 @ 7.26 ppm)
temp 26.9 C -> actual temp = 27.0 C, autoxdb probe
OH
O
NH
5
O
O
4-8
f1 (ppm)

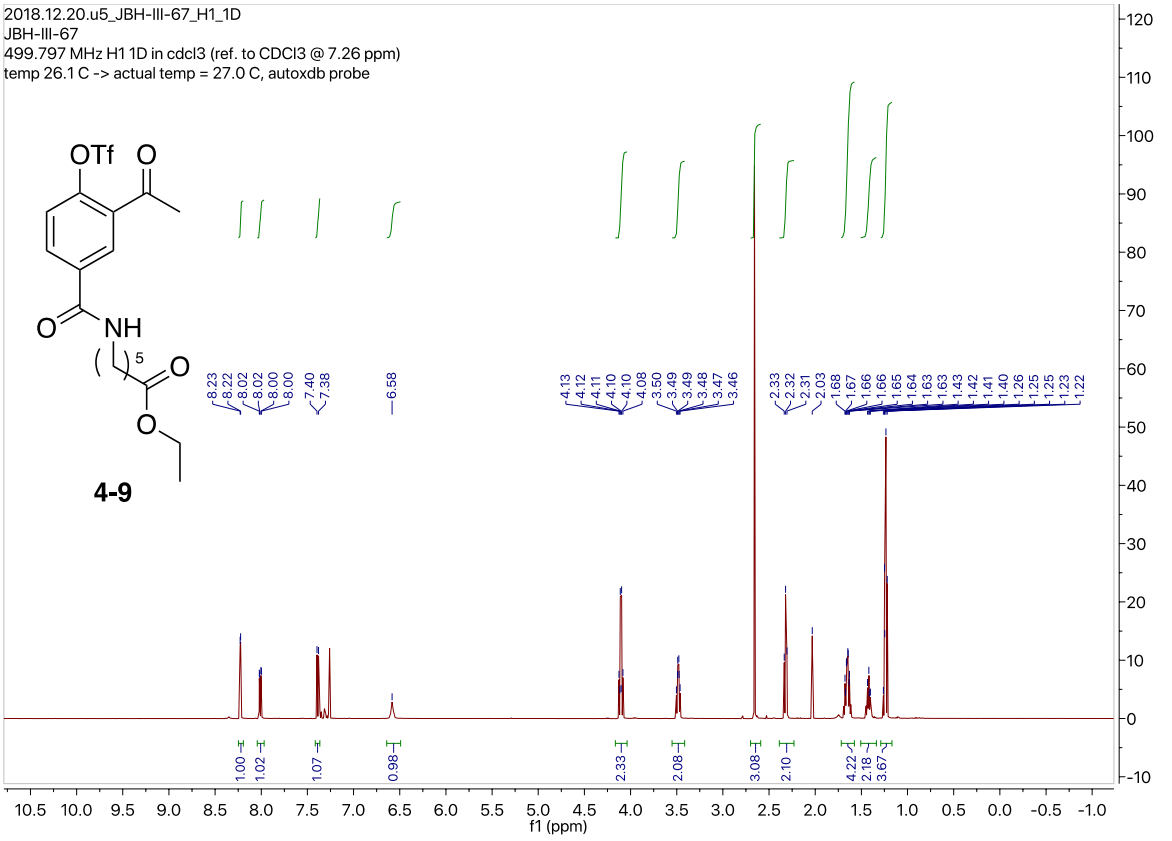
2018.12.20.u5_JBH-III-67_H1_1D
JBH-III-67
499.797 MHz H1 1D in cdcl3 (ref. to CDCl3 @ 7.26 ppm)
temp 26.1 C -> actual temp = 27.0 C, autoxdb probe
OTf
O
NH
5
O
O
4-9
f1 (ppm)

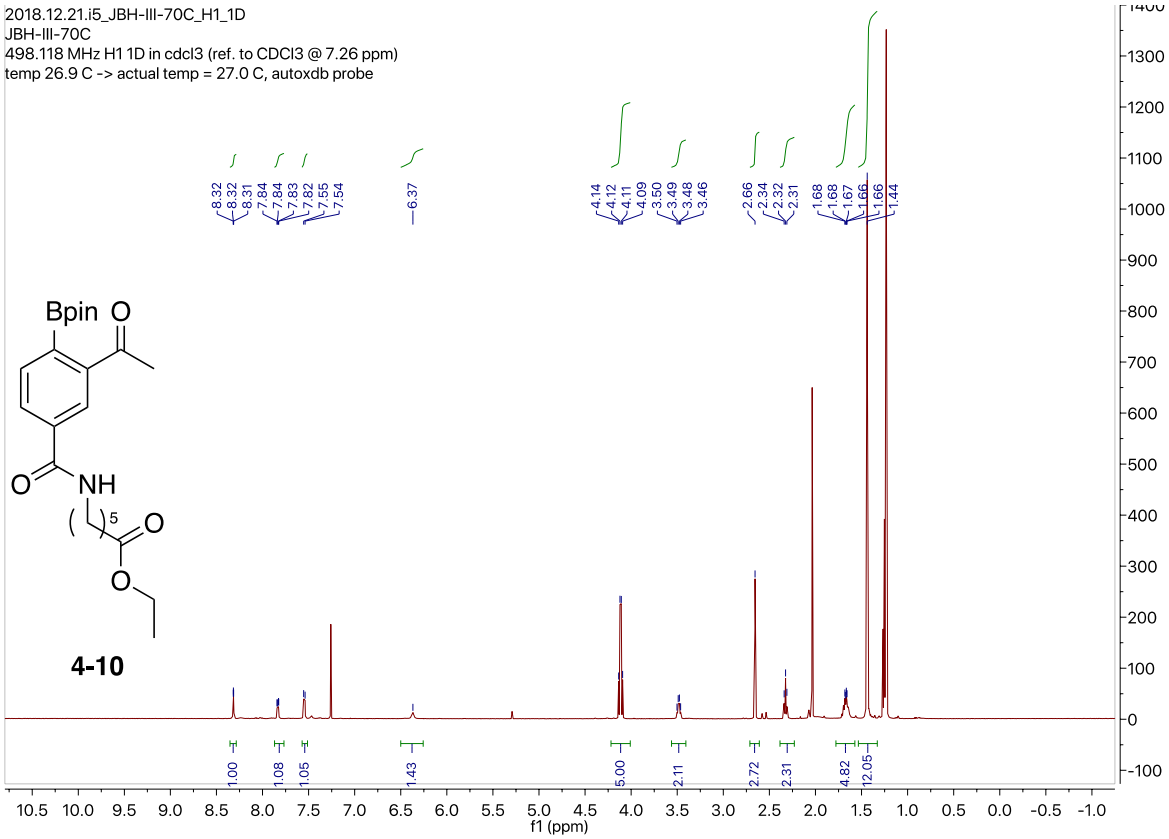
2018.12.21.i5_JBH-III-70C_H1_1D
JBH-III-70C
498.118 MHz H1 1D in cdcl3 (ref. to CDCl3 @ 7.26 ppm)
temp 26.9 C -> actual temp = 27.0 C, autoxdb probe
Bpin
O
NH
5
O
O
4-10
f1 (ppm)

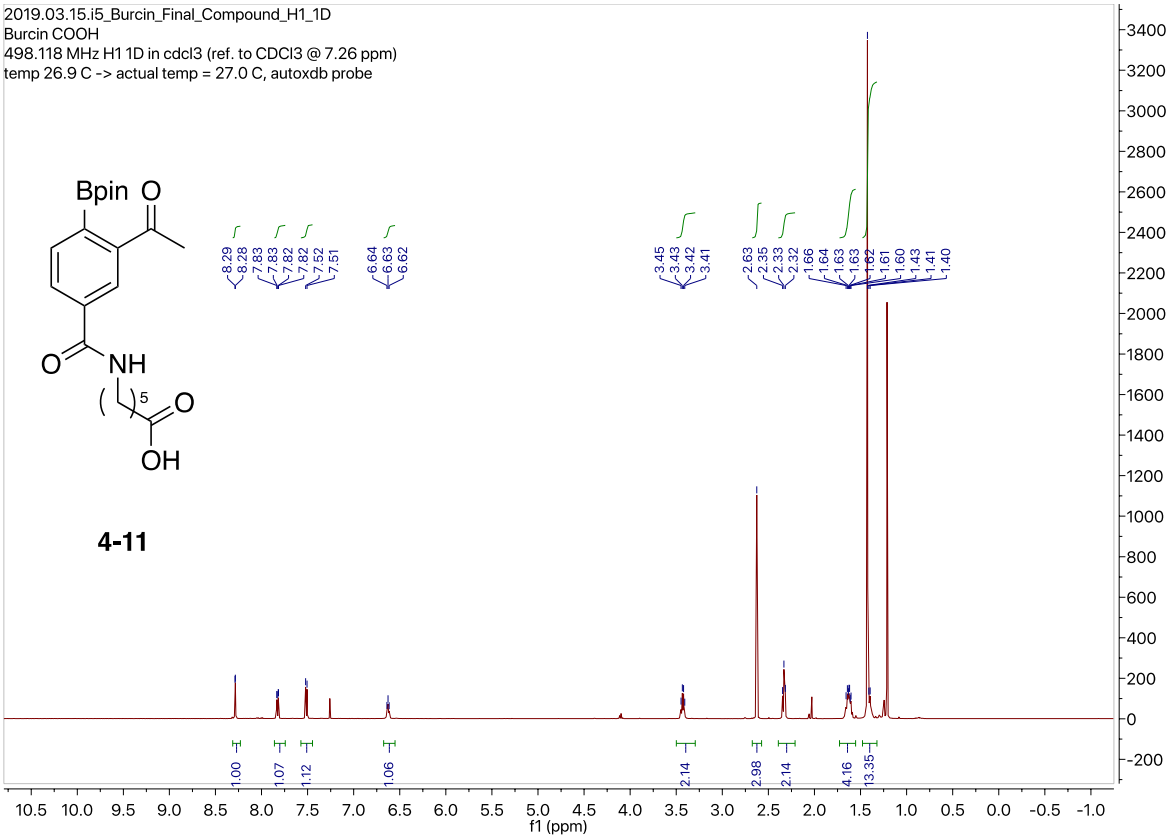
2019.03.15.i5_Burcin_Final_Compound_H1_1D
Burcin COOH
498.118 MHz H1 1D in cdcl3 (ref. to CDCl3 @ 7.26 ppm)
temp 26.9 C -> actual temp = 27.0 C, autoxdb probe
Bpin
O
NH
5
O
OH
4-11
f1 (ppm)

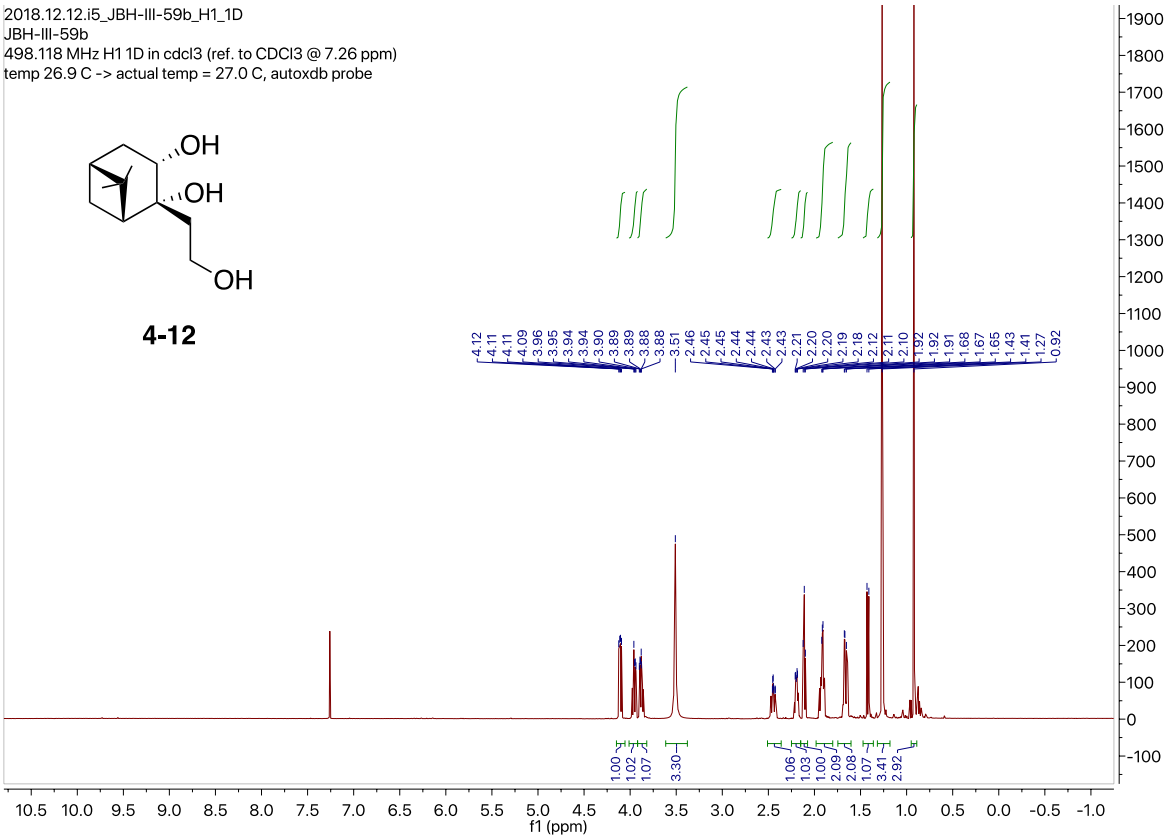
2018.12.12.i5_JBH-III-59b_H1_1D
JBH-III-59b
498.118 MHz H1 1D in cdcl3 (ref. to CDCl3 @ 7.26 ppm)
temp 26.9 C -> actual temp = 27.0 C, autoxdb probe
OH
OH
OH
4-12
f1 (ppm)